



Terms and Conditions of Use of Digitised Theses from Trinity College Library Dublin

Copyright statement

All material supplied by Trinity College Library is protected by copyright (under the Copyright and Related Rights Act, 2000 as amended) and other relevant Intellectual Property Rights. By accessing and using a Digitised Thesis from Trinity College Library you acknowledge that all Intellectual Property Rights in any Works supplied are the sole and exclusive property of the copyright and/or other IPR holder. Specific copyright holders may not be explicitly identified. Use of materials from other sources within a thesis should not be construed as a claim over them.

A non-exclusive, non-transferable licence is hereby granted to those using or reproducing, in whole or in part, the material for valid purposes, providing the copyright owners are acknowledged using the normal conventions. Where specific permission to use material is required, this is identified and such permission must be sought from the copyright holder or agency cited.

Liability statement

By using a Digitised Thesis, I accept that Trinity College Dublin bears no legal responsibility for the accuracy, legality or comprehensiveness of materials contained within the thesis, and that Trinity College Dublin accepts no liability for indirect, consequential, or incidental, damages or losses arising from use of the thesis for whatever reason. Information located in a thesis may be subject to specific use constraints, details of which may not be explicitly described. It is the responsibility of potential and actual users to be aware of such constraints and to abide by them. By making use of material from a digitised thesis, you accept these copyright and disclaimer provisions. Where it is brought to the attention of Trinity College Library that there may be a breach of copyright or other restraint, it is the policy to withdraw or take down access to a thesis while the issue is being resolved.

Access Agreement

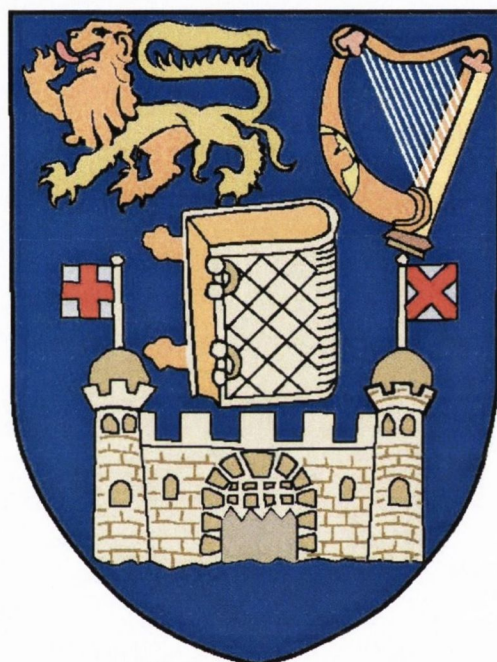
By using a Digitised Thesis from Trinity College Library you are bound by the following Terms & Conditions. Please read them carefully.

I have read and I understand the following statement: All material supplied via a Digitised Thesis from Trinity College Library is protected by copyright and other intellectual property rights, and duplication or sale of all or part of any of a thesis is not permitted, except that material may be duplicated by you for your research use or for educational purposes in electronic or print form providing the copyright owners are acknowledged using the normal conventions. You must obtain permission for any other use. Electronic or print copies may not be offered, whether for sale or otherwise to anyone. This copy has been supplied on the understanding that it is copyright material and that no quotation from the thesis may be published without proper acknowledgement.

**Pharmaceutical stability and
prodrug studies on the antidepressant bupropion**

Paul Matthew O'Byrne B.Sc., M.Sc.

A thesis presented to the University of Dublin
For the degree of
Doctor of Philosophy in Pharmaceutical Chemistry

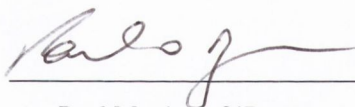


Based on research carried out under the supervision of
John Gilmer B.A. (Mod.), Ph.D
And
John Walsh B.A (Mod.), Ph.D
At the
School of Pharmacy and Pharmaceutical Sciences,
Trinity College Dublin.

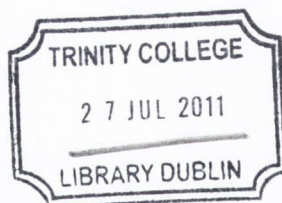
2010

This thesis has not been presented as an exercise for a degree at any other university.
The work described, except where duly acknowledged, was carried out by me entirely.

I agree that the library may lend or copy this thesis upon request.



Paul Matthew O'Byrne



THESIS
9276

Abstract

This thesis describes the work carried out at the School of Pharmacy and Pharmaceutical Sciences, Trinity College on the pharmaceutical stability and prodrug studies on the antidepressant bupropion.

Chapter 1 gives an overview of bupropion, discussing its therapeutic uses, pharmacokinetics, adverse effects and pharmacology. The prodrug concept is introduced with particular reference to central nervous system brain delivery and prodrug options relating to these types. Prodrugs of bupropion would be advantageous to improve its stability and side-effect profile.

Chapter 2 addresses the aqueous stability of bupropion with particular emphasis on the kinetics of degradation. The pH rate profile of bupropion shows instability above pH 5 and this problem can be addressed by prodrug design.

Chapter 3 describes the chemistry, synthesis and characterization of potential prodrugs of bupropion. A number of potential single step prodrugs, namely the *N*-methyl, *N*-benzyl and hydroxyimine were synthesized. Potential multistep prodrugs such as the di-acetylated, di-alkylated and cyclic derivatives such as the cyclic carbamate, oxadiazinone, oxazolone and oxadiazine were also synthesized.

In Chapter 4 a prodrug screening tool was developed and used to evaluate the potential prodrugs for their activation *in vitro*. The screening tool put each potential prodrug through hydrolytic and metabolic events that mimic the oral route of delivery. A number of analogue candidates emerged as potential prodrugs of bupropion. All the potential prodrugs were *N*- or *O*-dealkylated in human liver and intestinal microsomes suggesting that these functional groups are particularly susceptible to oxidative de-alkylation in bupropion. *N*-methyl bupropion was further characterized by enzyme kinetics, pH stability, pharmacology and CACO-2 cell permeability. This potential prodrug was selected as a candidate for a proof-of-concept animal study.

Chapter 5 describes the method development, validation and execution of the determination of *N*-methyl bupropion, bupropion and metabolites in guinea-pig plasma and brain pharmacokinetic study. *N*-methyl bupropion was demonstrated to be successfully transformed to bupropion *in vivo* when dosed by intraperitoneal injection and by oral gavage. A number of metabolites were identified with potential pharmacological activity.

The chapter and thesis conclude with some proposed future work and recommendations for application of these findings. Bupropion is particularly susceptible to oxidative *N*-dealkylation by human liver and intestinal microsomes and this can be used to develop potential prodrugs of bupropion to address the inherent instability of bupropion and its therapeutic efficacy.

Acknowledgements

I would like to express my sincerest gratitude to Dr. John Gilmer for his guidance, supervision and enthusiasm on this project. I am especially thankful to Dr. John Walsh for his supervision during the initial years of the project, his use of the pharmacognosy laboratories and training on the LTQ-Orbitrap. I would like to thank Dr. Robert Williams formerly of Biovail Technologies Ireland for his collaboration and consultancy; his advice was instrumental to the development of this project. I look forward to working with you guys again in the future. I would like to thank Biovail Corporation for their funding of the project for the last number of years.

I would like to thank Dr. John O'Brien and Dr. Manuel Ruether for their assistance in the NMR department. I would like to thank Dr. Martin Feeney for use of his mass spectrometer and for all the samples he identified. I would like to thank Prof. Mary Meegan for allowing me use of the microwave synthesis reactor. I would like to thank Dr. Michael Jones and Dr. Shona Harmon for their help with the CACO-2 cell experiments. I would like to thank Dr. Pierce Kavanagh of James Street hospital for his advice and help.

I would like to thank all the technical staff in the School of Pharmacy for their help especially Ray, Rhona, Brian and Joe. I would like to thank all the administrative staff at the School of Pharmacy who have been very kind over the years.

I would like to thank all the staff at the Drug laboratory of the Drug Treatment Centre Board, Pearse Street especially Siobhan, Jean, Maura, Louise, Jenny, Áine, Orlagh, Nicola, Gráinne, Emma and Seibh.

A special thank you to all my friends, fellow post-grads, post-docs and those involved in the 5-aside leagues at Trinity College from Pharmacy, Physics, Neuroscience, Chemistry, Biochemistry and of course all the lads from Kennedys!

I would especially like to thank my great mates, Allan, Darragh, Ciaran, Derek, Paddy, Paul and Stephen. I would also like to thank Tammy and Karen. Thanks to my housemates, Justine and Justyna for putting up with my whining over the last few months!

Thank you Gary and Shannon for making life sweet. Keep up the good work. I love you guys. And finally, thank you mother dearest. Your love and support has pulled me through the toughest of times. I couldn't have done it without you.

Dedicated to the memory of my father
Matthew O'Byrne
(6th June 1951 – 13th January 1999)

Abbreviations

3-CBA	3-chlorobenzoic acid
AA	aminoacetone
ABL	aqueous boundary layer
ACN	acetonitrile
ACTH	adrenocorticotrophic hormone
ADH	alcohol dehydrogenase
ADHD	attention deficit/hyperactivity disorder
ADME	absorption distribution metabolism elimination
AGE	Advanced Glycation End product
AKA	also known as
AKR	aldo-keto reductase
ALA	5-aminolevulinic acid
ALDH	aldehyde dehydrogenase
amu	atomic mass units
AP	apical side
APCI	atmospheric pressure chemical ionization
APPI	atmospheric pressure photo-ionization
AUC	area under the curve
BBB	blood brain barrier
BDI	Beck Depression Inventory
BDNF	brain derived neurotrophic factor
bk	beta-keto
BL	basolateral side
Bup	bupropion
BupOH	hydroxybupropion
CACO	epithelial colorectal adenocarcinoma cells
cAMP	cyclic adenosine monophosphate
CE	carboxylesterase
CNS	central nervous system
CRF	corticotropin releasing hormone
CYP	cytochrome P450 enzyme
DAT	dopamine transporter
DCM	dichloromethane
DDI	drug-drug interaction
DEPT	distortionless enhancement polarisation transfer
DIPEA	diisopropylethylamine
DMAP	dimethylaminopyridine
DMF	dimethylformamide
DMSO	dimethylsulphoxide
DSM	diagnostic and statistical manual for mental disorders
ESI	electrospray ionization
FDA	food and drug administration
FGF	fibroblast growth factor
FMO	flavin containing monooxygenase
FTIR	fourier transform infrared spectroscopy

GABA	γ -aminobutyric acid
GST	glutathione S-transferase
hCE	human carboxylesterase
HIM	human intestinal microsomes
HLM	human liver microsomes
HMPA	hexamethylphosphoramide
HPA	hypothalamic-pituitary-adrenal
HPLC-UV	high performance liquid chromatography -ultraviolet detection
HRMS	high resolution mass spectrum
HTS	high throughput screening
HVA	homovanillic acid
ICHQ	international conference on harmonisation quality guidelines
IDO	indoleamine-2,3-dioxygenase
IL	interluekin
INF	interferon
IP	intraperitoneal administration
IR	immediate release
LC-MS	liquid chromatography - mass spectrometry
LDA	lithium diisopropylamide
LOD	limit of detection
LOQ	limit of quantitation
LPS	lipopolysaccharide
mAChRs	muscarinic acetylcholine receptors
MAO	monoamine oxidase
MAOI	monoamine oxidase inhibitor
MeOH	methanol
MRM	multiple reaction monitoring
nAChRs	nicotinic acetylcholine receptors
NADP	nicotinamide adenine dinucleotide phosphate
NaH	sodium hydride
NAT	N-acetyltransferase
NCAM	neural cell adhesion molecule
NCE	new chemical entity
NDA	new drug application
NET	norepinephrine transporter
N-MeBup	N-methyl bupropion
N-MeTHB	N-methyl threohydrobupropion
NMR	nuclear magnetic resonance
NO	nitric oxide
O&NS	oxidative and nitrosative stress
PEA	phenethylamine
pH	minus log of hydronium ion concentration
PHP	pooled human plasma
PK	pharmacokinetics
pKa	minus log of the acid dissociation constant
PO	oral administration

PTFE	teflon
PUFA	polyunsaturated fatty acid
Q-TOF	quadrupole time of flight
RLS	restless legs syndrome
RP	reversed phase
RT	room temperature
SAD	seasonal affective disorder
SD	sexual dysfunction
SERT	serotonin transporter
SGF	simulated gastric fluid
SIF	simulated intestinal fluid
SIM	selected ion monitoring
SR	sustained release
SRM	selected reaction monitoring
SSQMS	single-stage quadrupole mass spectrometers
SSRI	selective serotonin reuptake inhibitor
ST	sulfotransferase
STAR*D	Sequenced Treatment Alternatives to Relieve Depression
TCA	tricyclic antidepressant
TEA	triethylamine
TEER	transepithelial electrical resistance
TFAA	trifluoroacetic acid anhydride
THB	threo-hydrobupropion
THF	tetrahydrofuran
TIC	total ion chromatogram
TLC	thin layer chromatography
TMPT	thiopurine methyltransferase
TNF	tumour necrosis factor
TOF	time of flight
TQD	target quit date
TRI	triple reuptake inhibitor
TRYCAT	tryptophan catabolites
TSQMS	triple-stage quadrupole mass spectrometers
UDPGT	uridine diphosphate-glucuronosyltransferase
UPLC	ultra high performance liquid chromatography
WIPO	World intellectual property organization

Table of contents

Abstract.....	iii
Acknowledgements.....	iv
Abbreviations.....	vi
Table of contents.....	ix
Table of tables.....	xiv
Table of figures.....	xv
Table of schemes.....	xviii
Chapter 1 - Introduction to bupropion and the prodrug concept.....	1
1 Introduction.....	2
1.1 Bupropion.....	2
1.1.1 The synthesis of bupropion	4
1.1.2 Formulations.....	5
1.1.3 Pharmacokinetics	5
1.1.4 Pharmacology.....	8
1.1.5 Adverse effects.....	9
1.1.6 Drug-drug interactions	11
1.1.7 Therapeutic uses.....	13
1.2 Prodrugs	28
1.2.1 Introduction	28
1.2.2 Central nervous system type prodrugs	30
1.2.3 Prodrugs and bioprecursors of CNS type compounds.....	31
1.2.4 Carbamate type prodrugs.....	32
1.2.5 Amide prodrugs.....	33
1.2.6 <i>N</i> -alkylated prodrugs	34
1.2.7 Imine prodrugs	35
1.2.8 Oxime prodrugs.....	35
1.2.9 <i>O</i> -alkylated prodrugs.....	36
1.2.10 Prodrugs of hydroxybupropion	36
1.2.11 Potential codrugs of bupropion/metabolites.....	37
1.2.12 Prodrugs of compounds relating to bupropion.....	37
1.2.13 Bupropion analogues	38
1.2.14 Potential prodrugs of bupropion	38
Chapter 2 - The aqueous stability of bupropion.....	39
2 The aqueous stability of bupropion.....	40
2.1 Introduction.....	40

2.1.1	Tautomerism of bupropion	41
2.1.2	Thermal rearrangement of aminoketones	42
2.2	Results & Discussion.....	42
2.2.1	pH-rate profile of bupropion.....	42
2.2.2	Mechanistic interpretation of pH-rate profile	44
2.2.3	Effects of temperature and buffer on the stability of bupropion.....	47
2.2.4	Identification of bupropion degradants and mechanistic proposal	49
2.2.5	Bupropion as a pro-oxidant	53
2.2.6	Hydroxyketones as inhibitors of urease.....	55
2.2.7	Known pharmacological effects of the degradants of bupropion.....	55
2.2.8	Addressing stability with a prodrug.....	56
2.3	Conclusion.....	58
2.4	Experimental	59
2.4.1	Chemicals	59
2.4.2	Instrumentation.....	59
Chapter 3 - The synthesis of potential prodrugs of bupropion.....		61
3	The synthesis of potential prodrugs of bupropion.....	62
3.1	Brief overview of the commercial synthesis of bupropion.....	62
3.2	Overview of the chemistry of bupropion.....	64
3.3	Prodrugs of bupropion.....	65
3.3.1	Prodrug formation at the amine site on bupropion	65
3.3.2	Prodrug formation at the keto site on bupropion	66
3.3.3	Double prodrug forms of bupropion.....	66
3.3.4	Carbamate type prodrugs of bupropion	67
3.3.5	Preparation of a double prodrug by acylation of bupropion	74
3.3.6	N-alkylation of bupropion	77
3.3.7	Oxime type prodrugs of bupropion.....	78
3.3.8	Imine prodrugs of bupropion	84
3.3.9	O-alkylated prodrugs of bupropion	84
3.4	Conclusion.....	94
3.5	Experimental	96
3.5.1	Reagents and chemicals.....	96
3.5.2	Instrumentation.....	96
3.5.3	Synthesis of 2-bromo-1-(3-chlorophenyl) propan-1-one (3.4).....	97
3.5.4	Synthesis of bupropion hydrochloride (3.6).....	97
3.5.5	Synthesis of a dioxolane of bupropion (3.8).....	97
3.5.6	Synthesis of a 8-membered ring cyclic carbamate of bupropion (3.10).....	98

3.5.7	Synthesis of the dioxolane brominated starting material (3.15).....	99
3.5.8	Synthesis of the oxazolone of bupropion (3.17).....	99
3.5.9	Synthesis of the (E/Z)- <i>N,O</i> -diacetylated bupropion (3.18)	100
3.5.10	Synthesis of <i>N</i> -methyl bupropion (3.19).....	100
3.5.11	Synthesis of bupropion hydroxyimine (3.21).....	100
3.5.12	Synthesis of the benzyl oximine of bupropion (3.22).....	101
3.5.13	Synthesis of an oxadiazine of bupropion (3.23).....	101
3.5.14	Synthesis of an oxadiazinone of bupropion (3.24).....	102
3.5.15	Synthesis of <i>N,O</i> -dimethylated bupropion (3.27)	102
3.5.16	Synthesis of <i>N</i> -benzyl bupropion (3.31)	103
3.5.17	Synthesis of (E/Z)- <i>O</i> -methyl <i>N</i> -benzyl bupropion (3.32).....	103
Chapter 4 - The screening and evaluation of potential prodrugs of bupropion.....		104
4	The screening and evaluation of potential prodrugs of bupropion.....	105
4.1	Introduction.....	105
4.1.1	Biochemical barriers to oral drug delivery	106
4.1.2	Physiological barriers to oral drug delivery	110
4.1.3	Chemical barriers to oral drug delivery.....	111
4.1.4	Development of a screening tool to evaluate drug metabolic stability.....	112
4.2	Screening results	122
4.2.1	Cyclic carbamate derivative of bupropion (3.10).....	124
4.2.2	Oxazolone of bupropion (3.17)	124
4.2.3	<i>N,O</i> -diacetylated bupropion (3.18).....	125
4.2.4	<i>N</i> -methyl bupropion (3.19).....	125
4.2.5	Hydroxyimine of bupropion (3.21)	141
4.2.6	Oxadiazine of bupropion (3.23)	142
4.2.7	Oxadiazinone of bupropion (3.24)	145
4.2.8	<i>N,O</i> -dimethyl bupropion (3.27).....	145
4.2.9	<i>N</i> -benzyl bupropion.....	147
4.2.10	<i>N</i> -benzyl <i>O</i> -methyl bupropion (3.32).....	151
4.3	Conclusion	152
4.4	Experimental	153
4.4.1	Materials.....	153
4.4.2	Chromatographic method for screening potential prodrugs.....	153
4.4.3	Mass Spectrometer conditions for detection of potential prodrugs.....	153
4.4.4	Metworks software.....	154
4.4.5	Human liver microsome stock solution preparation.....	154
4.4.6	Human intestinal microsome stock solution preparation	154

4.4.7	NADPH regenerating solution A stock solution preparation	154
4.4.8	NADPH regenerating solution B stock solution preparation.....	154
4.4.9	Pooled human plasma solution preparation.....	155
4.4.10	USP simulated gastric fluid preparation.....	155
4.4.11	USP simulated intestinal fluid preparation.....	155
4.4.12	Determination of microsomal metabolic stability	155
4.4.13	Synthesis of <i>N</i> -methyl amino alcohol of bupropion (4.1).....	155
4.4.14	Determination of Michaelis-Menten kinetic parameters.....	156
4.4.15	Pharmacological screening of <i>N</i> -methyl bupropion.....	156
4.4.16	CACO-2 cell transport experiment.....	157
Chapter 5 - <i>In vivo</i> evaluation of N-methyl bupropion		158
5	<i>In-vivo</i> evaluation of N-methyl bupropion.....	159
5.1	Introduction	159
5.1.1	LC-MS methods already known.....	160
5.1.2	Choice of chromatographic conditions.....	163
5.1.3	Method development	164
5.1.4	Optimization of protein precipitation	166
5.2	Guinea pig enzyme kinetics	166
5.2.1	Method validation.....	168
5.3	<i>In vivo</i> study results & discussion.....	172
5.3.1	Guinea pig pharmacokinetics via IP injection	172
5.3.2	Guinea pig pharmacokinetics via oral administration (PO).....	178
5.4	Identification of new <i>in vivo</i> metabolites of N-methyl bupropion.....	182
5.5	Conclusion.....	184
5.6	Proposed future work	185
5.6.1	Identification of CYP450 enzymes responsible for metabolism	185
5.6.2	<i>In vivo</i> efficacy and toxicology	186
5.6.3	Evaluation of <i>N</i> -benzyl bupropion <i>in vivo</i> pharmacokinetics.....	187
5.6.4	Stereo-selective pharmacological and pharmacokinetic analysis.....	187
5.6.5	Evaluation of pharmacological activity of hydroxyimine of bupropion.....	187
5.6.6	Dialkylated prodrugs of bupropion.....	188
5.6.7	Evaluation of SAR of <i>N</i> -alkylated analogues of bupropion	189
5.6.8	Identification of new metabolites of <i>N</i> -alkylated analogues of bupropion.....	189
5.6.9	Co-drugs for depression.....	190
5.6.10	Prodrugs and co-drugs for Nicotine replacement therapy.....	192
5.6.11	Co-drug for Crohn's disease (inflammatory bowel disease).....	193
5.6.12	Pharmacotherapies for treating drugs of abuse addiction.....	193

5.6.13	Headshop type substituted cathinones	194
5.7	Experimental	195
5.7.1	Reagents and chemicals.....	195
5.7.2	Instrumentation.....	195
5.7.3	Chromatographic conditions	195
5.7.4	Mass spectrometer conditions	195
5.7.5	Guinea pig enzyme kinetics (Michaelis-Menten).....	196
5.7.6	Standard preparation.....	196
5.7.7	System suitability	196
5.7.8	Analytical method validation	197
5.7.9	Pharmacokinetic study	198
6	Bibliography.....	200
7	Appendices.....	213
7.1	The aqueous stability of bupropion (Publication).....	213
7.2	Isosorbide-based aspirin prodrugs (Publication).....	213
7.3	Bupropion pharmacology.....	213
7.4	N-methyl bupropion pharmacology	213
7.5	Bupropion and N-methyl bupropion pharmacology (nAChR subtypes).....	213

Table of tables

Table 1.1 A selection of some of the substituted cathinones.....	3
Table 1.2 Blockade of DA and NE transporters.....	6
Table 1.3 In vitro, inhibition of biogenic amine uptake in rat brain by bupropion	6
Table 1.4 Biochemical pharmacological mechanisms and their possible side effects.	9
Table 1.5 Substrates, inhibitors and inducers of the enzyme that metabolize bupropion.	12
Table 1.6 Classification of prodrugs.	29
Table 2.1 Dilutions of stock buffers to give constant ionic strength with varying pH.....	42
Table 2.2 First-order rate constants determined for the degradation of bupropion.....	44
Table 2.3 The macro reaction constants determined by non-linear regression analysis	47
Table 3.1 Deprotection strategies for N-TFA O-Me analogue of bupropion 3.30.....	93
Table 4.1 The testing matrix of potential prodrugs and hydrolysis/metabolism results.....	123
Table 4.2 Pharmacological screen of N-methyl bupropion and bupropion.....	131
Table 4.3 CACO-2 cell permeability values for N-methyl bupropion.....	140
Table 5.1 Shows correlation levels for bupropion and its principal human metabolites.....	168
Table 5.2 Signal to noise ratios (S/N) at the nominal LOD levels.	169
Table 5.3 Accuracy/precision results.	170
Table 5.4 Plasma LOQ accuracy and precision results.	171
Table 5.5 Brain LOQ/accuracy and precision results.....	171
Table 5.6 The pharmacokinetic parameters for N-methyl bupropion, bupropion and	175
Table 5.7 The brain/plasma ratio of bupropion and metabolites.....	175
Table 5.8 The brain/plasma ratio of N-methyl bupropion and metabolites.....	175
Table 5.9 Estimated pharmacokinetic parameters for N-methyl bupropion	179
Table 5.10 The brain/plasma ratio of bupropion and metabolites.....	179
Table 5.11 The brain/plasma ratio of N-methyl bupropion and metabolites.....	179

Table of figures

Figure 1.1 The structure of bupropion and some related compounds	2
Figure 1.2 The β_2 adrenergic receptor agonist, albuterol	3
Figure 1.3 The structures of important active metabolites of bupropion	7
Figure 1.4 The pharmacological targets of bupropion and its related therapeutic uses.	13
Figure 1.5 The inflammatory and neurodegenerative (I&ND) pathways in depression.	16
Figure 1.6 A representative illustration of the prodrug concept.....	28
Figure 1.7 Examples of some bioprecursor prodrugs of some CNS compounds.....	32
Figure 1.8 The common catalytic mechanism of hydrolases in ester and amide hydrolysis.	34
Figure 2.1 Keto-enol/enamine-imine tautomerism of bupropion.....	41
Figure 2.2 Thermal rearrangement of α -hydroxy imines and α -hydroxyketones	42
Figure 2.3 First-order plots showing the degradation of bupropion at 333 K.....	44
Figure 2.4 The six empirical reactions that contribute to the stability of bupropion.	46
Figure 2.5 pH degradation profile of bupropion at 40, 50 and 60°C, I = 0.055	47
Figure 2.6 The effect of different buffer systems on the rate of degradation of bupropion.....	48
Figure 2.7 Shows the pH degradation profile of bupropion at 60°C, I = 0.055.	49
Figure 2.8 Shows the time course profile for degradation of bupropion.	51
Figure 2.9 Shows actual data pH 8.7, 50°C, I = 0.12	53
Figure 2.10 Non-enzymatic aerobic oxidation of α -aminoketones.....	54
Figure 2.11 An example of Fe(II) catalysed aerobic oxidation of the aminoketone.....	54
Figure 2.12 Base-catalyzed hydrolysis of bupropion.....	56
Figure 2.13 Removing the liability of imine formation by alkylation at the amine.....	56
Figure 2.14 Degradation of bupropion, showing oxidation pathways..	57
Figure 2.15 Removing the liability of enol formation by oxime conversion	57
Figure 2.16 A typical LCUV chromatogram of bupropion hydrolysis at pH 8.7.	59
Figure 3.1 ^1H NMR and ^{13}C NMR spectra of bupropion hydrochloride.....	63
Figure 3.2 A high resolution LC-MS chromatogram/spectrum of bupropion	64
Figure 3.3 The multistep prodrug ximelagatran.....	66
Figure 3.4 The carbamate prodrug loratadine	68
Figure 3.5 ^1H NMR, ^{13}C NMR and DEPT 135 spectrum of the ketal of bupropion.....	69
Figure 3.6 ^1H NMR, ^{13}C NMR and DEPT135 spectra of the cyclic carbamate.....	71
Figure 3.7 ^1H NMR and ^{13}C NMR of the cyclic carbamate oxazolone	74
Figure 3.8 ^1H NMR of 3.18 shows the two isomers incompletely resolved.	75
Figure 3.9 Shows an LC-MS chromatogram of 3.18.	76
Figure 3.10 ^1H NMR and ^{13}C NMR of N-methylated bupropion	78
Figure 3.11 ^1H NMR of the hydroxyimine potential prodrug of bupropion	79

Figure 3.12 ¹³ CNMR of the hydroxyimine potential prodrug of bupropion	80
Figure 3.13 ¹ HNMR and ¹³ CNMR spectra of the potential oxadiazine double prodrug.	81
Figure 3.14 ¹ HNMR and ¹³ CNMR of the potential oxadiazinone double prodrug	82
Figure 3.15 ¹ HNMR of the benzyl oxime derivative of bupropion.....	83
Figure 3.16 ¹ HNMR and ¹³ CNMR spectra of N-methyl O-methyl bupropion.....	86
Figure 3.17 An LC-MS chromatogram of dimethyl bupropion	87
Figure 3.18 The ¹ HNMR and ¹³ CNMR of N-benzyl bupropion.	88
Figure 3.19 ¹ HNMR and ¹³ CNMR spectra of N-benzyl protected methyl enol ether	89
Figure 3.20 ¹ HNMR spectrum of 3.30	91
Figure 3.21 ¹³ CNMR and ¹⁹ FNMR spectra of 3.30.....	92
Figure 4.1 The generalized P450 catalytic cycle.....	108
Figure 4.2 A schematic is shown of how compounds can permeate the intestine.....	111
Figure 4.3 The prodrug assessment scheme used to develop potential prodrugs.....	113
Figure 4.4 A typical LC-MS chromatogram of N-methyl bupropion	126
Figure 4.5 Substrate saturation study in pooled human liver microsomes.	130
Figure 4.6 Dose response curve for N-methyl bupropion in the DAT assay	132
Figure 4.7 Dose response curve for N-methyl bupropion in the NET assay.....	134
Figure 4.8 Dose response curves for N-methyl bupropion in the muscarinic assay.....	134
Figure 4.9 Dose response curves for N-methyl bupropion in the nAChR assay.....	135
Figure 4.10 The pH stability profile of N-methyl bupropion.....	138
Figure 4.11 A schematic of the CACO-2 cell permeability	139
Figure 4.12 Stability of the hydroxyimine of bupropion.....	141
Figure 4.13 A +ESI LC-MS spectrum of the hydroxyimine of bupropion	142
Figure 4.14 An LC-MS chromatogram of the oxadiazine prodrug	143
Figure 4.15 A typical LC-MS chromatogram of the oxadiazine of bupropion.	144
Figure 4.16 A typical HRLC-MS chromatogram of the metabolism of dimethyl bupropion ...	147
Figure 4.17 A typical HRLC-MS chromatogram of N-benzyl bupropion	149
Figure 4.18 Substrate saturation study in pooled human liver microsomes.	150
Figure 4.19 Metabolism of N-benzyl bupropion during a 60 minute incubation in HLM.....	150
Figure 5.1 LC-FTMS chromatogram.	165
Figure 5.2 A substrate saturation curve for N-methyl bupropion in guinea pig S9.....	167
Figure 5.3 The least squares linear – regression curve for bupropion.....	169
Figure 5.4 The mean plasma levels of bupropion and metabolites	176
Figure 5.5 The mean plasma concentrations of N-methyl bupropion and metabolites	176
Figure 5.6 The mean brain concentrations of bupropion and metabolites	177
Figure 5.7 The mean brain concentrations of N-methyl bupropion and metabolites	177
Figure 5.8 The mean plasma concentrations of bupropion and metabolites	180

Figure 5.9 The mean plasma concentrations of N-methyl bupropion and metabolites.....	180
Figure 5.10 Mean brain concentrations of bupropion and metabolites.....	181
Figure 5.11 Mean brain concentrations of N-methyl bupropion and metabolites.....	181
Figure 5.12 Proposed four new metabolites.....	183
Figure 5.13 LC-MS chromatogram of guinea-pig plasma	183
Figure 5.14 Potential multistep hydroxyimine-N-alkylated prodrugs of bupropion.....	188
Figure 5.15 Potential O-alkylated double prodrugs and co-drugs of bupropion.....	188
Figure 5.16 Alkylation and metabolism of an acidic co-drug (Niacin) to bupropion	189
Figure 5.17 Potential triple reuptake inhibitor co-drugs of bupropion and SSRI's.	191
Figure 5.18 Potential co-drugs for Nicotine replacement therapy and smoking cessation	192
Figure 5.19 N-alkylated prodrugs of 2x.....	193
Figure 5.20 Potential co-drug of bupropion and 5-aminosalicylic acid.....	193
Figure 5.21 Potential N-alkylated analogue of bupropion for drugs of abuse addiction	194
Figure 5.22 Substituted cathinones used as designer drugs	194

Table of schemes

Scheme 1.1 Synthesis of bupropion via the method described by Mehta.....	4
Scheme 1.2 The mechanism of hydrolysis of carbamates.....	32
Scheme 1.3 The hydrolysis of imines	35
Scheme 1.4 The hydrolysis of hydroxyimines	35
Scheme 2.1 Proposed pathway for base catalyzed degradation of bupropion.....	50
Scheme 3.1 Synthesis of bupropion via the method described by Mehta.....	62
Scheme 3.2 Synthesis of the hydrochloride salt of bupropion.....	62
Scheme 3.3 Keto-enol/enamine-imine tautomerism of bupropion.....	65
Scheme 3.4 Prodrugs associated with the enolization of bupropion.....	66
Scheme 3.5 Potential double prodrugs of bupropion	67
Scheme 3.6 Attempted synthesis of a carbamate type potential prodrug of bupropion.....	68
Scheme 3.7 Synthesis of 3.10.....	70
Scheme 3.8 Synthesis of benzyl tert butyl carbamate	72
Scheme 3.9 Attempted synthesis of a benzyl carbamate prodrug of bupropion	72
Scheme 3.10 Attempted synthesis of ketal protected benzyl carbamate prodrug of bupropion..	72
Scheme 3.11 Synthesis of an oxazolone type potential prodrug of bupropion.....	73
Scheme 3.12 The synthesis of a potential amide prodrug of bupropion.....	75
Scheme 3.13 Synthesis of the N-alkylated potential prodrug of bupropion.....	77
Scheme 3.14 Synthesis of the potential hydroxyimine prodrug of bupropion.....	79
Scheme 3.15 Synthesis of the double prodrug oxadiazine of bupropion	80
Scheme 3.16 Synthesis of the double prodrug oxadiazinone of bupropion	81
Scheme 3.17 The synthesis of a benzyl oximine of bupropion.....	83
Scheme 3.18 Attempted synthesis of a potential imine prodrug of bupropion.....	84
Scheme 3.19 Protective group strategies for the amine of bupropion.....	85
Scheme 3.20 The synthesis of dimethylated bupropion.....	86
Scheme 3.21 The synthesis of O-methyl N-benzyl bupropion.....	87
Scheme 3.22 Synthesis of N-benzyl O-methyl bupropion	89
Scheme 3.23 Synthesis of TFA-protected bupropion.....	90
Scheme 3.24 Synthesis of N-TFA O-methyl bupropion	91
Scheme 3.25 Attempted removal of the trifluoroacetyl protecting group.....	93
Scheme 3.26 Summary of successful synthesis of potential prodrugs of bupropion.....	95
Scheme 4.1 Synthesis of N-methyl amino alcohol of bupropion.....	127
Scheme 4.2 Metabolism of N-methyl bupropion in human intestinal and liver microsomes ...	127
Scheme 4.3 The possible mechanisms of oxidative dealkylation of the oxadiazine.....	144
Scheme 4.4 Metabolism of dimethyl bupropion 3.27	146
Scheme 4.5 Metabolism of N-benzyl bupropion in human liver and intestinal microsomes....	148

Scheme 4.6 Metabolism of N-benzyl,O-methyl bupropion in human liver microsomes.....	151
Scheme 5.1 N-methyl bupropion, its metabolites	160

Chapter 1 - Introduction to bupropion and the prodrug concept

This chapter introduces the drug bupropion and the prodrug concept. Bupropion is an α -aminoketone that acts primarily at four therapeutic sites, increasing dopamine, increasing norepinephrine, as a nicotinic acetylcholine receptor antagonist and by modulating cytokine levels such as lowering tumour necrosis factor- α and interferon- γ . From these four pharmacological targets bupropion derives its many therapeutic uses ranging from CNS diseases to systemic inflammatory diseases. A literature survey of potential uses of bupropion is described referencing peer reviewed journals and the patent archives. The pharmacokinetics and pharmacology of bupropion is discussed. The prodrug concept is introduced with particular emphasis on central nervous system prodrugs and the reasons for applying the prodrug concept to bupropion are listed and discussed.

1 Introduction

1.1 Bupropion

Bupropion HCl (2-*tert*-butylamino-3'-chloropropiophenone hydrochloride) is a water soluble hydrochloride salt of the α -aminoketone [1]. The freebase form of this aminoketone is highly lipophilic, enabling the drug to enter many tissues, including the brain. Bupropion is a low molecular weight compound, which has been in therapeutic use as an antidepressant since 1989. Its chemical structure is similar to the endogenous monoamine neurotransmitters dopamine and norepinephrine. It contains a phenylethylamine backbone which is also found in other psychoactive compounds and abused stimulants. Despite sharing this structural similarity, bupropion does not appear to have significant abuse potential [2]. Bupropion is a non-selective inhibitor of the dopamine transporter (DAT) and the norepinephrine transporter (NET) and is also an antagonist at neuronal nicotinic acetylcholine receptors (nAChRs). It has recently been shown to have anti-inflammatory properties due to its lowering of cytokines such as tumour necrosis factor- α and interferon- γ . Clinically, bupropion is used as a treatment for two indications, as an antidepressant, the indication for which it was developed, and as a tobacco use cessation agent. More recently new therapeutic uses are emerging.

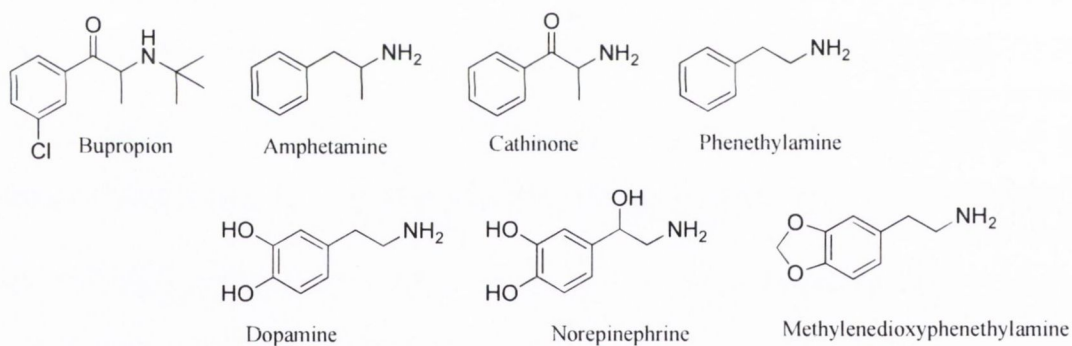
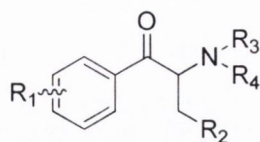


Figure 1.1 The structure of bupropion and some related compounds

Bupropion is chemically related to substituted cathinones, which are a chemical class of stimulants and entactogens. The substituted cathinones feature a phenethylamine core with an alkyl group attached to the α -carbon and a keto-group attached to the β -carbon, along with additional substitutions, Table 1.1. All α -aminoketones chemically related to bupropion have been scheduled under law due to their narcotic effect. These compounds, also known as 'headshop' or (beta-keto) bk-amphetamine compounds are chemically and biologically related to the phenethylamines, amphetamines and appetite suppressants such as diethylpropion and ethylpropion. They are used as designer drugs.



Compound	R1	R2	R3	R4
Cathinone	H	H	H	H
Methcathinone	H	H	H	Me
Ethcathinone	H	H	H	Et
Buphedrone	H	Me	H	Me
Pentedrone	H	Et	H	Me
Dimethylcathinone	H	H	Me	Me
Diethylpropion	H	H	Et	Et
Bupropion	3-Cl	H	H	<i>t</i> -Bu
Mephedrone	4-Me	H	H	Me
4-MEC	4-Me	H	H	Et
<i>N,N</i> -DMMC	4-Me	H	Me	Me
3,4-DMMC	3,4-dimethyl	H	H	Me
Methedrone	4-MeO	H	H	Me
3-FMC	3-F	H	H	Me
Flephedrone	4-F	H	H	Me
Brephedrone	4-Br	H	H	Me
Methylone	3,4-methylene dioxy	H	H	Me
MDPV	3,4-methylene dioxy	Et	Pyrrolidinyl	

Table 1.1 A selection of some of the substituted cathinones

One other group of structurally related compounds are the adrenergic receptor agonists. These compounds are α -aminoalcohols that contain a secondary *t*-butylated amine or other bulky substituents. β_2 -Adrenergic receptor agonists such as albuterol, terbutaline, pirbuterol, bitolterol, bambuterol and clenbuterol all contain a *t*-butylated secondary amine.

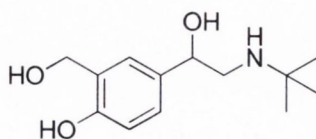
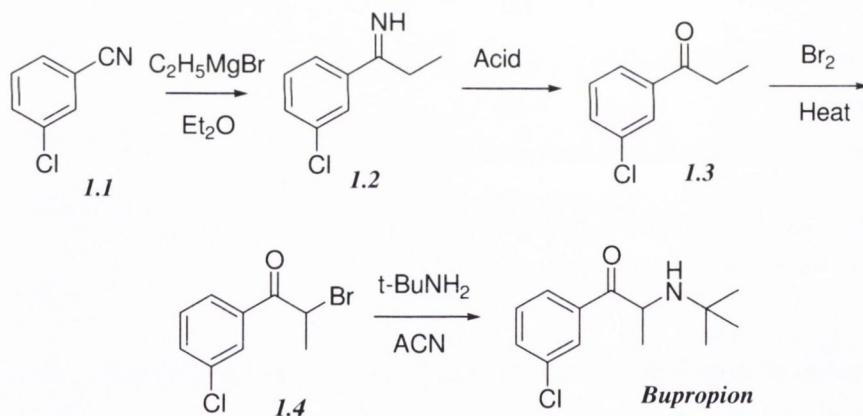


Figure 1.2 The β_2 adrenergic receptor agonist, albuterol

1.1.1 The synthesis of bupropion

The synthesis of bupropion was first described in 1975 by Mehta [3]. It was prepared in three steps starting with the meta-chloro substituted benzonitrile **1.1**, Scheme 1.1. The propiophenones were not commercially available at that time so they were prepared from the treatment of the benzonitrile with an ethyl Grignard reagent. Treatment of the resulting imine **1.2** with aqueous acid hydrolysed the imine to the ketone **1.3**. The bromination step according to Mehta was not rapid and required heating. It was unnecessary to isolate the brominated ketone as pure substance as long as the hydrogen bromide produced during this step was removed during workup. The final stage of the reaction was coupling of *t*-butylamine with the brominated ketone **1.4**. This was subject to hindrance and *t*-butylamine usually reacted slowly with α -bromopropiophenones. The addition of an organic solvent greatly increased the speed of the reaction and it was found that acetonitrile was the optimum choice. It offered a marked advantage over other solvents as it was a 'fast' solvent, unreactive under the conditions and was relatively low boiling. Other polar solvents, protic and aprotic were also used, for example lower aliphatic ketones or ethers, but the reaction was slow in these solvents. DMF, nitromethane, DMSO and hexamethylphosphoramide were also used. It was desirable to heat this step to reflux temperature.



Scheme 1.1 Synthesis of bupropion via the method described by Mehta.

1.1.2 Formulations

Bupropion is available in three oral formulations, immediate release (IR), sustained release (SR), and extended release (XL). Immediate release (IR) tablets are inexpensive and available worldwide from several generic manufacturers. Marketed in 75 and 100mg strengths, original recommendations were for three times daily dosing, although twice daily dosing is commonly used. Sustained release (SR) tablets, available generically and as proprietary Wellbutrin SR, are available in 100, 150 and 200mg and are easier for some patients to tolerate at twice daily dosing. The most recent formulation is an extended release (XL) tablet available only as proprietary Wellbutrin XL 150 and 300mg, designed for once daily administration. The maximum daily dose approved by the US FDA is 400mg for the SR and 450mg for the IR and XL formulations. Dose reduction should be undertaken in patients with mild to moderate hepatic impairment and avoidance should be considered for those with severe hepatic dysfunction. The total daily dose should remain the same when converting between the three formulations as these three products are considered bioequivalent [4].

1.1.3 Pharmacokinetics

Hepatic metabolism of bupropion produces three pharmacologically active metabolites, which may contribute to its clinical profile. Hepatic cytochrome P450 (CYP) 2B6 catalyzes hydroxylation of the side chain *tert*-butyl group of bupropion to form an active metabolite, hydroxybupropion. CYP2B6 contributes to approximately 90 % of hydroxybupropion formation [5] while CYP2C19 contributes to approximately 70-90 % formation of alternate hydroxylation pathways. CYP2B6 is a polymorphic drug metabolizing enzyme such that the metabolism and, hence, systemic exposure to parent drug and metabolites may vary widely depending on an individual's genotype. CYP2B6 is expressed in the brain at lower levels than the liver; however, the distribution in the brain is not homogenous, leaving the possibility of localized high expression in discrete brain regions where bupropion and hydroxybupropion may exert their pharmacologic action [6].

Enantioselective effects of the hydroxy metabolites of bupropion on behaviour and function of monoamine transporters and nicotinic receptors has been studied by Damaj *et al.* [7]. This study investigated the effects of hydroxybupropion enantiomers on monoamine transporters and nicotinic acetylcholine receptor (nAChR) subtypes (results Table 1.2). The effects of bupropion and enantiomers of hydroxybupropion on human nAChR subtypes indicates that the (2S,3S) isomer is more potent than the (2S,3R) isomer or racemic bupropion as an antagonist of $\alpha 4\beta 2$. In addition, (2S,3S)-hydroxybupropion and bupropion were considerably more potent than (2R, -3R)-hydroxybupropion in a mouse depression model (forced swimming test) and in antagonism of acute nicotine effects in mice. Together, the results suggest that clinical and behavioral

effects of bupropion arise from actions at nAChR as well as DA and NE transporters. Furthermore, the data suggest that the (2S,3S)-hydroxybupropion isomer may be a better drug candidate for smoking cessation than bupropion because of its higher potency at the relevant targets. The 2S,3S-isomer was filed as a new drug candidate by GlaxoSmithKline in 2007, called Radafaxine but development was discontinued due to 'poor test results'.

Drug	IC ₅₀	
	[3H] DA	[3H] NE
	nM	
Bupropion	550 ± 65	1900 ± 12
2RS, 3RS-hydroxybupropion	> 10,000	1700 ± 830
2S, 3S-hydroxybupropion	790 ± 11	520 ± 35
2R, 3R-hydroxybupropion	> 10,000	> 10,000

Table 1.2 Blockade of DA and NE transporters uptake in rat cortical synaptosomes by bupropion and its hydroxy metabolites. Values given are mean ± S.D, taken from Damaj et al [7].

Two less active metabolites, threohydrobupropion and erythrohydrobupropion, are formed through reduction of the side chain ketone group, likely by a xenobiotic carbonyl reductase enzymes. There is little known about the carbonyl reductase enzyme that reduces bupropion to its aminoalcohol metabolites but is likely reduced by Aldo-keto reductase (AKR) or Short-chain dehydrogenases/reductases (SDR). Both these enzymes systems take part in the oxidoreduction of endogenous and xenobiotic carbonyls, alcohols and C-C double bonds. The main cytosolic carbonyl reducing enzymes in mammals are carbonyl reductase (EC 1.1.1.184), aldehyde reductase (EC 1.1.1.2), aldose reductase (EC 1.1.1.21) and dihydrodiol dehydrogenases [8]. Less than 1% of bupropion is eliminated in the urine as unchanged drug. The majority of parent drug and metabolites are eliminated in the urine as glycine conjugates [4].

	Hydroxybupropion	Threohydrobupropion	Bupropion
	IC ₅₀ (µM)		
Serotonin uptake	105	67	58
Norepinephrine uptake	7	16	5
Dopamine uptake	23	47	2

Table 1.3 In vitro, inhibition of biogenic amine uptake in rat brain by bupropion and its major metabolites, hydroxybupropion and threohydrobupropion, taken from Horst et al.[9]

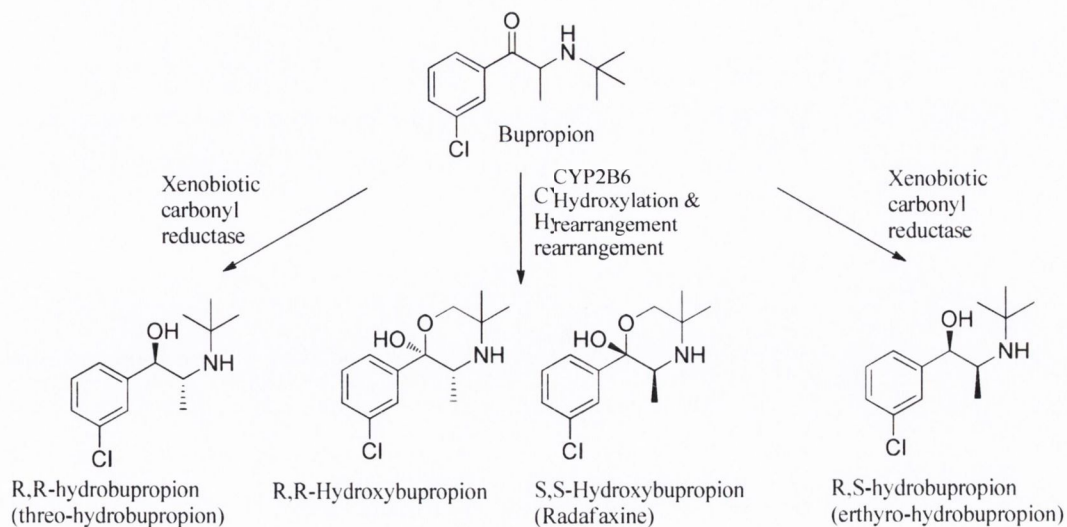


Figure 1.3 The structures of important active metabolites of bupropion

Intestinal absorption of bupropion is reported to be close to 100 % [4]. This is not surprising given bupropion's small mass and lipophilicity. However, absolute oral bioavailability (absorbed bupropion that does not undergo first pass metabolism in the liver) is unknown because no intravenous formulation has been tested. According to the manufacturer, studies in rats and dogs suggest absolute bioavailability may be 5-20 % [2].

Bupropion's pharmacokinetic profile is best fitted to a two-compartment model as evidenced by its biphasic plasma concentration-time curve. Steady state plasma levels of bupropion and its main metabolite hydroxybupropion will occur after 5-7 days of administration. Bupropion and its metabolites display linear pharmacokinetics at steady state within the 150-450 mg daily dose range [4]. The apparent oral clearance of bupropion following chronic dosage in adults is reported to be approximately 160 L/h. The fact that this experimental value exceeds hepatic blood flow indicates extensive first pass metabolism and low oral bioavailability.

1.1.4 Pharmacology

Bupropion is an aminopropiophenone with a chemical structure dissimilar to selective serotonin reuptake inhibitors (SSRIs) or tricyclic antidepressants (TCAs) but similar to the endogenous neurotransmitters dopamine and norepinephrine.

1.1.4.1 Neuropharmacology

Bupropion is a dopamine and norepinephrine reuptake inhibitor [10]. It is about twice as potent an inhibitor of dopamine reuptake than of norepinephrine reuptake. Bupropion enhances monoaminergic function by inhibiting reuptake of norepinephrine and dopamine to prolong their concentration and time in the synaptic cleft. As bupropion is rapidly converted in the body into several metabolites with differing activity, its action cannot be understood without reference to its metabolism. Reviews on the mechanism of action of bupropion are uncertain, but may be related to inhibition of presynaptic dopamine and norepinephrine reuptake transporters. The activity of vesicular monoamine transporter-2, the transporter pumping dopamine, norepinephrine and serotonin from the cytosol into presynaptic vesicles, is increased by bupropion and may be a component of its mechanism of action [11].

Bupropion is a nicotinic acetylcholine receptor antagonist [12]. Neuronal nicotinic receptors are ligand-gated ion channels of the central and peripheral central nervous system that regulate synaptic activity from both pre- and postsynaptic sites. Slemmer *et al.* established the acute interaction of bupropion with nicotine and nicotinic receptors using different *in vivo* and *in vitro* tests. Bupropion was found to block nicotine's antinociception (in two tests), motor effects, hypothermia, and convulsive effects with different potencies, suggesting that bupropion possesses selectivity for neuronal nicotinic receptors underlying the various nicotinic effects. In addition, bupropion blocks nicotine activation of $\alpha 3\beta 2$, $\alpha 4\beta 2$, and $\alpha 7$ neuronal acetylcholine nicotinic receptors (nAChRs) with selectivity. It was approximately 50 and 12 times more effective in blocking $\alpha 3\beta 2$ and $\alpha 4\beta 2$ than $\alpha 7$. Furthermore, bupropion at high concentration failed to displace brain [3H] nicotine binding sites, a site largely composed of $\alpha 4\beta 2$ subunit combination. Given the observation that bupropion inhibition of $\alpha 3\beta 2$ and $\alpha 4\beta 2$ receptors exhibits voltage-independence properties, bupropion may not be acting as an open channel blocker. The authors concluded that these effects may explain in part bupropion's efficacy in nicotine dependence. These findings suggest that functional blockade of neuronal nAChRs are useful in nicotine dependence treatment.

1.1.4.2 Cytokine modulation

Bupropion has been shown to modulate specific cytokine levels. Cytokines are signalling molecules secreted by the glial cells of the nervous system and by cells of the immune system. They are a category of signalling molecules used extensively in intercellular communication. The term 'cytokine' can refer to immunomodulating agents such as interleukins, interferons and

tumour necrosis factor. Cytokines circulate the system in picomolar concentrations and can increase 1000 fold during trauma or infection. Bupropion decreases levels of TNF- α , INF- γ , IL-1 β , and NO. Bupropion increases levels of IL-10 [13]. These cytokines are implicated in numerous inflammatory diseases. A graphical representation of the pharmacological activity and therapeutic uses of bupropion is presented in Figure 1.4.

1.1.5 Adverse effects

Bupropion is generally well tolerated. The most common adverse effects during initial treatment are dry mouth, constipation, headache, nausea, agitation, insomnia and weight loss [14]. These side effects are common for drugs that work on the noradrenergic and dopaminergic functions. The most common cause for stopping bupropion treatment is jitteriness or an unpleasant state. SSRI antidepressants are known to cause sexual dysfunction as a side effect. Bupropion is recognized as a better antidepressant than other antidepressants for sexual dysfunction side effects. Most adverse effects with bupropion occur in the initial weeks of therapy and become less apparent over time. There is evidence that the adverse effects associated with bupropion treatment are due to the metabolites of bupropion.

Mechanism	Possible side effect
Enhancement of noradrenergic function	Agitation
	Dry mouth
	Hypertension (peripheral effect)
Enhancement of dopaminergic function	Agitation
	Constipation
	Insomnia

Table 1.4 Biochemical pharmacological mechanisms and their possible side effects, adapted from Stahl [15].

1.1.5.1 Seizures

The most contentious side effect of bupropion treatment is due to seizures and in 1986 shortly after FDA approval, the drug was taken off the market. The drug was reintroduced in 1989 at a lower dose range and currently has contraindications for use in patients with seizure history, eating disorders or those undergoing ethanol or other CNS depressant withdrawal [9]. A study published in 1989 by Davidson examined the relationship between seizure occurrence and use of bupropion based on manufacturer's reports. The observed occurrence of seizures with bupropion doses of 450 mg/day or less ranged from 0.35%–0.44%. The cumulative 2-year risk

of seizures in patients receiving the maximum recommended dose of 450 mg/day or less was 0.48%. The risk of seizure appears to be higher with bupropion doses above the recommended maximum, and predisposing factors were noted in over half of the 37 reported cases [16].

The convulsive liability of bupropion metabolites were reported in Swiss Albino mice by Silverstone *et al.* [17]. They investigated the convulsive liability and dose-response of the three major bupropion metabolites following intraperitoneal administration of single doses in female Swiss albino mice, namely erythrohydrobupropion HCl, threo hydrobupropion HCl, and hydroxybupropion HCl. They compared these to bupropion HCl. The actual doses of the metabolites administered to mice were equimolar equivalents of bupropion HCl 25, 50 and 75 mg/kg. Post treatment, all animals were observed continuously for 2 h during which the number, time of onset, duration and intensity of convulsions were recorded. The primary outcome variable was the percentage of mice in each group who had a convulsion at each dose. All metabolites were associated with a greater percentage of seizures compared to bupropion, but the percentage of convulsions differed between metabolites. Hydroxybupropion HCl treatment induced the largest percentage of convulsing mice (100 % at both 50 and 75 mg/kg) followed by threo hydrobupropion HCl (50 % and 100 %), and then erythrohydrobupropion HCl (10 % and 90 %), compared to bupropion HCl (0 % and 10 %). Bupropion HCl, erythrohydrobupropion HCl, and threo hydrobupropion HCl were significantly less likely to induce convulsions within the 2-h post treatment observation period compared to hydroxybupropion HCl. The mean convulsions per mouse also showed the same dose-dependent and metabolite-dependent trends. This demonstration of the dose-dependent and metabolite-dependent convulsive effects of bupropion metabolites was significant as it was the first study of its kind but it also showed that the metabolites of bupropion particularly hydroxybupropion were primarily the cause of seizures. One drawback to this data was the absence of stereoselective effects. There are four isomers of hydroxybupropion and it would have been prudent to analyse the seizure effect of each of the isomers of hydroxybupropion. There would be significant differences in seizure liability between the stereo-isomers. This was studied briefly by Lukas *et al.* [18].

Lukas synthesized and evaluated 23 analogues of the 2S,3S-isomer of hydroxybupropion for their abilities to inhibit monoamine uptake and nAChR subtype activities in vitro and acute effects of nicotine in vivo. They found that the potency of 2S,3S-hydroxybupropion in their mouse testing model was close to 50-fold lower than the racemic hydroxybupropion metabolite active doses reported by Silverstone *et al.* They found no evidence for seizure or convulsive activities at any of the doses tested in their study. Therefore the seizures seen in Silverstone's study must have been caused by different isomers of hydroxybupropion and not the 2S,3S-isomer. This highlights the importance of stereoselective effects of metabolites of bupropion.

1.1.5.2 Metabolites of bupropion

It is believed that the effects of bupropion's major metabolites may be critical to its antidepressant activity, because bupropion is extensively metabolized. The concentrations of hydroxybupropion isomers present in cerebrospinal fluid are six times greater than those of the parent bupropion [19]. Although it has weak NE-uptake properties, the high levels of the metabolite in brain may be sufficient to produce clinically meaningful blockade of NE reuptake and thereby account for much of the drug's activity and side effect profile.

Studies on the metabolites of bupropion have also shown that the higher levels of metabolites in plasma and CSF than parent bupropion are associated with poor clinical outcome and can be responsible for the adverse effects associated with bupropion treatment. Golden *et al.* studied the steady-state pharmacokinetics of bupropion hydrochloride [20]. The metabolites hydroxybupropion, threohydrobupropion, and erythrohydrobupropion predominated over the parent compound in plasma and cerebrospinal fluid at steady state. Plasma concentrations of each metabolite correlated with cerebrospinal fluid concentrations. Higher plasma metabolite concentrations were associated with poor clinical outcome. This relationship was most striking with hydroxybupropion. Plasma hydroxybupropion levels correlated with post-treatment plasma homovanillic acid levels. HVA is a major catecholamine metabolite and its levels are used as a marker of metabolic stress in the brain. Golden concluded that high levels of bupropion metabolites may be associated with poor clinical outcome due to toxic effects involving dopaminergic systems.

1.1.6 Drug-drug interactions

The potential for pharmacological interactions with bupropion is important particularly in relation to co-administration of drugs which lower seizure threshold. The effect of either CYP2B6 inhibition or induction is potentially clinically significant. Co-administration of antiplatelet drugs clopidogrel and ticlopidine (potent inhibitors of CYP2B6) with bupropion caused up to 90 % decrease in hydroxybupropion: bupropion ratio. The majority of the ratio was due to a decrease in hydroxybupropion formation. Only a moderate increase in the AUC and C_{max} of bupropion occurred, indicating an alternative metabolic pathway occurred during inhibition of CYP2B6 [21]. Therefore, the clinician should monitor patients closely when co-administering a CYP2B6 inhibitor with bupropion.

Another concern regarding bupropion metabolism is the fact that CYP2B6 is an inducible enzyme. Cigarette smoking, alcohol, phenobarbital and carbamazepine are some examples of inducers and their concurrent use may lead to increased production of the hydroxybupropion metabolite [4].

Bupropion is an inhibitor of CYP2D6 despite not being a substrate for this enzyme and this may lead to clinically significant drug interactions with CYP2D6 substrates [22]. The inhibition is caused by the hydroxybupropion metabolite. At present it is recommended that patients requiring co-administration of CYP2D6 substrates, particularly highly extracted oral drugs with narrow therapeutic indexes and drugs that may lack alternative metabolic pathways are monitored closely. The manufacturer specifically cautions of potential interaction with various antidepressants, antipsychotics, β -blockers and type IC antiarrhythmics, and suggests initiating these drugs at lower end of the dose range in the presence of bupropion [2, 14]. Bupropion is contraindicated in conjunction with monoamine oxidase inhibitors (MAOIs). It is recommended to wait 14 days following MAOI discontinuation. The concern is an increase in monoamines (serotonin, dopamine and norepinephrine) owing to concurrent uptake blockade and inhibition of monoamine metabolism at neuronal synapses.

Substrates	Inhibitors	Inducers
	CYP2B6	
<i>Bupropion</i>	Orphenadrine	Carbamazepine
Cyclophosphamide	Paroxetine	Rifampicin
Efavirenz	Fluoxetine	
Ifosfamide	Sertraline	
Selegiline	Ticlopidine	
Nicotine		
Sertraline		
	CYP2D6	
Metoprolol	<i>Hydroxybupropion</i>	Piperidines
Carvedilol	SSRI's	Glutethimide
Imipramine		Carbamazepine
TCA's		
SSRI's		
Venlafaxine		

Table 1.5 Substrates, inhibitors and inducers of the enzyme that metabolize bupropion to hydroxybupropion (CYP2B6) and the enzyme to which hydroxybupropion is an inhibitor (CYP2D6). Adapted from the Indiana University website [23].

1.1.7 Therapeutic uses

There is an abundance of literature on therapeutic uses of bupropion in both peer reviewed journals and patent archives. As of October 2010, a PubMed search with bupropion in the title of the journal article retrieves 1065 hits. A similar search of the world patent literature on freepatentsonline.com which includes, US patents, US patent applications, EP documents, abstracts of Japan and WIPO retrieves 235 articles with bupropion in the title. The majority of patents are based around formulation technologies such as stabilized or controlled dosage forms but there are an increasing number of patents based around new therapeutic uses. The following are a summary list of the preclinical and clinical studies performed with bupropion, and the patented therapeutic areas of use. A graphical representation of the pharmacological activity and therapeutic uses of bupropion is presented in Figure 1.4.

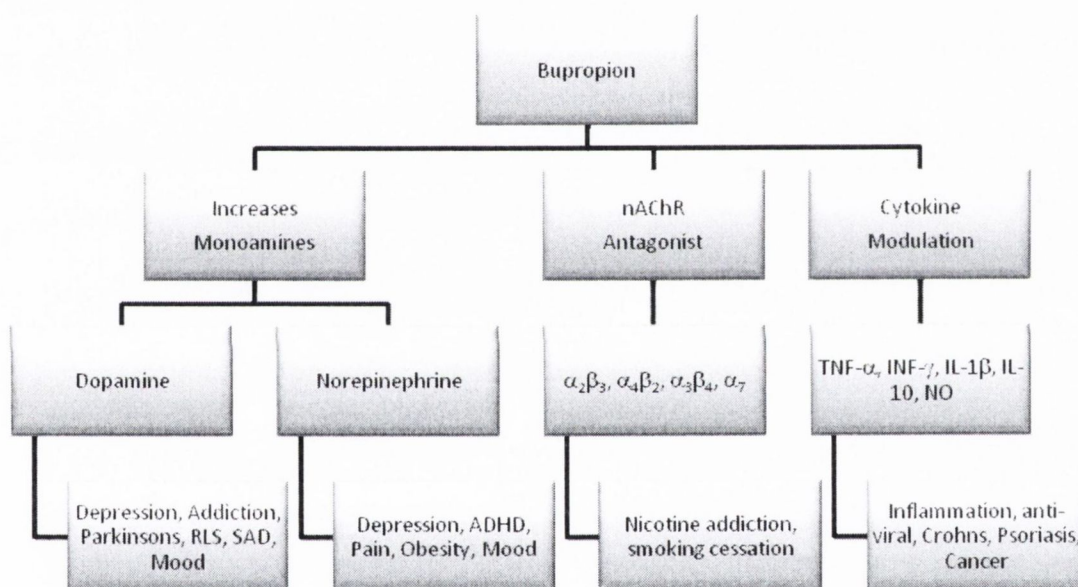


Figure 1.4 The pharmacological targets of bupropion and its related therapeutic uses. In the brain bupropion can increase levels of dopamine and norepinephrine, it antagonises the nicotinic acetylcholine receptor subtypes $\alpha_3\beta_2$, $\alpha_4\beta_2$, $\alpha_3\beta_4$ and α_7 . Systemically bupropion acts on the cytokines, particularly decreasing $TNF-\alpha$, $INF-\gamma$, $IL-1\beta$, NO and increasing $IL-10$.

1.1.7.1 Depression

Major depression is characterized by clinically significant depression of mood, feelings of intense sadness and despair, mental slowing, loss of concentration, anhedonia, self-deprecation, and an overall impairment of functioning. Furthermore, major depression is often associated with insomnia or hypersomnia, altered eating patterns, decreased energy, disruption of normal circadian rhythms of activity, body temperature, and endocrine function. Major depression is distinguished from normal grief, sadness, disappointment, and dysphoria often associated with medical illness. Recent clinical studies reveal a strong correlation between the incidence of mood disorders and tobacco smoking. Individuals with clinical depression are more likely to be tobacco smokers, to be dependent on nicotine and to have difficulty quitting, with greater withdrawal symptoms upon cessation. Smokers undergoing cessation experience symptoms of depression, which occur more frequently among those with a history of major depression. There are two hypotheses relating to the causal factors of depression, the monoamine hypothesis and cytokine hypothesis and both these hypotheses can be related to the pharmacological activity of bupropion. Bupropion fits the monoamine hypothesis by working on the dopaminergic and noradrenergic receptors, and fits the cytokine hypothesis by reducing cytokine levels such as TNF- α and IFN- γ .

1.1.7.1.1 Monoamine hypothesis of depression

The symptoms of depression can be improved by agents that act by various mechanisms to increase synaptic concentrations of monoamines. This finding led to the adoption of the monoamine hypothesis of depression, first put forward over 30 years ago, which proposes that the underlying biological or neuroanatomical basis for depression is a deficiency of central noradrenergic and/or serotonergic systems and that targeting this neuronal lesion with an antidepressant would tend to restore normal function in depressed patients. The hypothesis has enjoyed considerable support, since it attempts to provide a pathophysiologic explanation of the actions of antidepressants. However, in its original form it is inadequate, as it does not provide a complete explanation for the actions of antidepressants, and the pathophysiology of depression itself remains unknown. The hypothesis has evolved over the years to include, for example, adaptive changes in receptors to explain why there should be only a gradual clinical response to antidepressant treatment when the increase in availability of monoamines is rapid. Still, the monoamine hypothesis does not address key issues such as why antidepressants are also effective in other disorders such as panic disorder, obsessive-compulsive disorder, and bulimia, or why all drugs that enhance serotonergic or noradrenergic transmission are not necessarily effective in depression. Despite these limitations, however, it is clear that the development of the monoamine hypothesis has been of great importance in understanding depression and in the development of safe and effective pharmacologic agents for its treatment [24].

1.1.7.1.2 Cytokine hypothesis of depression

Developments in psychiatric research have led to the hypothesis that inflammatory processes and neural-immune interactions are involved in the pathogenesis of major depression and may underlie some of the frequently observed serotonergic and adrenocortical correlates. This hypothesis was termed the monocyte-T-lymphocyte or cytokine hypothesis of depression [25]. The first paper showing there was a connection between depression and T-cell activation was published in 1990 [26]. Since then there have been many findings over the years of increased levels of pro-inflammatory cytokines in patients with depression, e.g. interleukin-1 (IL-1), IL-2, IL-6, IL-8, IL-12, interferon- γ (IFN γ) and tumor necrosis factor- α (TNF α) [27]. Many other inflammatory biomarkers have been established in depression, such as increased acute phase proteins and lowered serum zinc [28]. Figure 1.5 shows the different inflammatory pathways occurring in depression.

Systemic exposure to inflammatory challenges, such as lipopolysaccharide (LPS), not only causes a systemic inflammation, but also induces a central neuro-inflammation, reflected by activation of brain microglia with a chronically elevated production of pro-inflammatory mediators, such as TNF α . It is well-known that LPS (either peripheral or central), brain neuroinflammation and the increased production of pro-inflammatory cytokines, such as IL-1 β , IL-6 and TNF α , may induce specific symptoms, labeled as the sickness behavior syndrome [29]. Symptoms of sickness behavior, such as anorexia, soporific effects, reduction of locomotor activity and exploration, anhedonia and cognitive disturbances, bear a strong similarity with those of depression. In depression, there is a strong correlation between those symptoms and the presence of inflammation. The above suggests that inflammatory reactions may have induced the symptoms of depression.

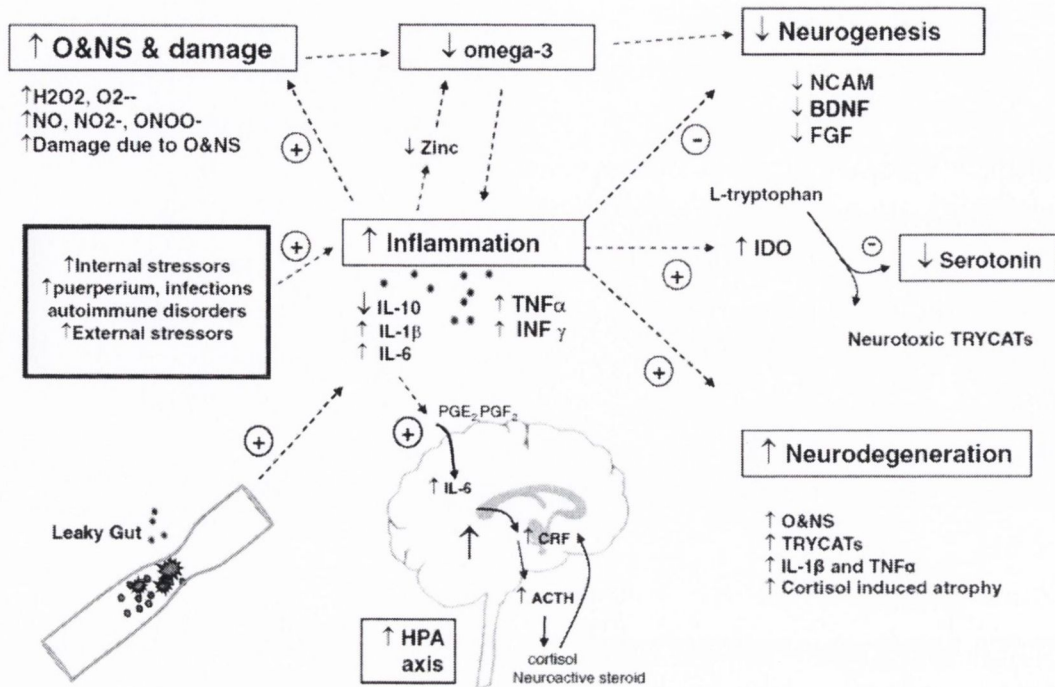


Figure 1.5 The inflammatory and neurodegenerative (I&ND) pathways in depression. Adapted from Maes [30].

Key findings in depression are the increased levels of pro-inflammatory cytokines, such as interleukin-1 β (IL-1 β), IL-6, interferon- γ (IFN γ) and tumor necrosis factor α (TNF α), with a relative shortage in the anti-inflammatory cytokine, IL-10. The pro-inflammatory response is induced by external and internal stressors and an increased translocation of the LPS from gram negative bacteria (leaky gut). The inflammatory response in depression is accompanied by lowered levels of zinc and a lowered ω 3 PUFA status; increased oxidative and nitrosative (O&NS) stress; induction of the hypothalamic-pituitary-adrenal (HPA)-axis via stimulated release/production of corticotropin releasing hormone (CRF), adrenocorticotrophic hormone (ACTH) and cortisol; the induction of indoleamine-2,3-dioxygenase (IDO) with decreased levels of tryptophan and serotonin and the consequent formation of tryptophan catabolites along the IDO-pathway (TRYCATs). Inflammation induces decreased neurogenesis in depression, which is characterized by decreased brain derived neurotrophic factor (BDNF); neural cell adhesion molecule (NCAM); and fibroblast growth factor (FGF). Inflammation may also induce neurodegeneration through increased levels of TRYCATs; O&NS; glucocorticoids; and some pro-inflammatory cytokines [30].

1.1.7.1.3 Bupropion and depression

The tricyclic antidepressants have been available since the early 1960s and are used widely to treat major depression. Compared to tricyclic antidepressants and selective serotonin reuptake inhibitors (SSRIs), bupropion is considered to be an atypical antidepressant with a mixed neuropharmacological profile. Placebo-controlled double-blind clinical studies have confirmed the efficacy of bupropion for clinical depression [31]. Comparative clinical studies demonstrated the equivalency of bupropion and sertraline (Zoloft), fluoxetine (Prozac), paroxetine (Paxil) [32] and escitalopram (Lexapro) [33] as antidepressants. A significantly higher remission rate with bupropion treatment than for venlafaxine (Effexor) was observed in a recent study [34]. Baldwin *et al.* have shown that bupropion is more effective than SSRIs at improving symptoms of hypersomnia and fatigue in depressed patients [35].

According to several surveys, the augmentation of a prescribed SSRI with bupropion is the preferred strategy among clinicians when the patient does not respond to the SSRI [36]. As recently as 2009, Jonas *et al.* were granted a patent for methods of treating central nervous system disorders with a low dose combination of escitalopram and bupropion [37] and there are currently patent applications for dual active formulations of bupropion with an SSRI [38].

For example, the combination of bupropion and citalopram (Celexa) was observed to be more effective than switching to another antidepressant. The addition of bupropion to an SSRI (primarily fluoxetine or sertraline) resulted in a significant improvement in 70–80 % of patients who had an incomplete response to the first-line antidepressant [39, 40]. Bupropion improved ratings of "energy", which had decreased under the influence of the SSRI; also noted were improvements of mood and motivation, and some improvement of cognitive and sexual functions. Sleep quality and anxiety ratings in most cases were unchanged [40]. In the STAR*D study, the patients who did not respond to citalopram (Celexa) were randomly assigned to augmentation by bupropion or buspirone (Buspar). Approximately 30 % of subjects in both groups achieved a remission. However, bupropion augmentation gave better results based on the patients' self-ratings and was much better tolerated. The authors observed that these findings reveal a consistently more favorable outcome with sustained-release bupropion than with buspirone augmentation of citalopram [41]. The same study indicated a possibility of higher remission rate when the non-responders to citalopram received bupropion augmentation rather than were switched to bupropion (30 % vs. 20 %) [42].

1.1.7.2 Smoking cessation

Nicotine is not itself a major cause of smoking-related disease. The major toxin in cigarette smoke is 'tar', a dark, viscous fluid formed from tobacco smoke. Tar contains as much as 4000 different chemicals, including > 50 known carcinogens and metabolic poison. Cigarette smoke contains carbon monoxide, nitrogen oxides and hydrogen cyanide [43]. Smoking-related illnesses are the leading cause of death in developed countries, accounting for approximately 20 % of deaths in the developed world. Currently, 3 million deaths per annum attributable to smoking occur worldwide, projected to increase to 10 million in 2030. Smoking has been identified as a causal factor in many diseases, including a wide range of malignancies and vascular diseases. There is a dose-response relationship between amount of pack years smoked and morbidity/ mortality. Half of long-term smokers can be expected to die of smoking-related illnesses, and half of these die prematurely in middle age [44].

Preclinical and clinical evidence indicate that bupropion has benefit as a tobacco use cessation agent [45, 46].

Data was drawn from a multicentre trial of bupropion for smoking cessation. Smokers received placebo or bupropion sustained-release at 100, 150, or 300 mg/day for six weeks after target quit date (TQD). The primary outcome was the point prevalence smoking abstinence at the end of treatment and at one year. The Beck Depression Inventory (BDI) was used to assess depressive symptoms. A significant dose-response effect of bupropion for smoking cessation was found. This was independent of history of major depression or alcoholism. Among those continuously abstinent from smoking for two weeks following TQD, an increase in BDI score was associated with a return to smoking at end of treatment. Bupropion is efficacious for smoking cessation independently of a former history of major depression or alcoholism. Increases in depressive symptoms during an initial period of abstinence are associated with a return to smoking [47].

1.1.7.3 Anti-inflammation (modulation of cytokine levels)

In 2001, Kast first reported the remission of a Crohn's disease case from use of bupropion and since then Kast, Brustolim and Altschuler have published numerous papers relating to the modulation of cytokines such as tumour necrosis factor- α (TNF) and interferon- γ (INF) by bupropion [13, 48-57].

In a wide range of human diseases of inflammatory nature like Crohn's disease, pathology is mediated in part by pro-inflammatory cytokines like TNF- α or interferon-gamma. Brustolim *et al.* published a paper in 2006 which showed that bupropion profoundly lowered levels of TNF- α , INF- γ , and interleukin-1 β in vivo, in a mouse lipopolysaccharide (LPS) induced inflammation model [13]. Mice challenged with an otherwise lethal dose of LPS were protected

by bupropion and levels of the anti-inflammatory cytokine interleukin-10 were increased. Previous data in rodents and humans indicate antidepressant effects of bupropion are mediated by its reuptake inhibition of norepinephrine and dopamine. Concordant with this, TNF suppression by bupropion in their mouse LPS model was largely abrogated by β -adrenergic or dopamine D1 receptor antagonists but not by a D2 antagonist. TNF synthesis is controlled by an inverse relationship with intracellular cyclic adenosine monophosphate (cAMP) and stimulation of either β -adrenoreceptors or D1 dopaminergic receptors result in increased cAMP but stimulation of D2 receptors lowers cAMP. They concluded that bupropion may suppress TNF synthesis by mediating increased signalling at β -adrenoreceptors and D1 receptors, resulting in increased cAMP that inhibits TNF synthesis. Bupropion is well tolerated also in non-psychiatric populations and has less risk with long term use than current anti-inflammatory, immunosuppressive or TNF suppressive treatments such as prednisone, azathioprine, infliximab, or methotrexate. Bupropion may therefore be good anti-inflammatory.

Altschuler and Kast have subsequently applied for a patent titled 'Methods for modulating TNF using bupropion' [58]. They have covered a series of illnesses that increase levels of TNF. This list is quite extensive but demonstrates the wide applicability of bupropion use in pro-inflammatory diseases. There are over one hundred diseases covered in the patent including viral and bacterial infections. Tumour necrosis factor plays a key role in many ailments.

1.1.7.4 Attention deficit hyperactivity disorder

In 1986 Simeon *et al.* published a study investigating the effects of bupropion on attention and conductivity disorders [59]. Seventeen male patients (age range 7 to 13.4 years; mean 10.4) participated in an open clinical trial consisting of a baseline placebo period (4 weeks), bupropion therapy (8 weeks), and post-drug placebo (2 weeks). Evaluations included clinical assessments, parents, teachers, and self-ratings; cognitive tests and blood level measurements of bupropion. Fifteen patients received a daily maximum of 150 mg, one received 100 mg and one 50 mg. Clinical global improvement with bupropion therapy was marked in 5 patients, moderate in 7, mild in 2, and none in 3. The Children's Psychiatric Rating Scale indicated improvements of hyperactivity, withdrawal, anxiety, hostility/uncooperativeness, sleep disorder, antisocial behaviour, neuroticism, depression and eating disturbance. Parents' Questionnaires indicated significant improvements of conduct disorder, anxiety, hyperactivity, muscle tension and psychosomaticism. While no single cognitive test showed significant improvement, all nine tests changed in the positive direction. Two weeks following bupropion discontinuation, clinical global improvement was maintained in 8 patients, 7 showed relapses, while 2 remained unimproved. Analyses of computerized EEG revealed that degree of clinical improvement was indexed by baseline EEG parameters and that there were significant bupropion effects on EEG measures. Their work concluded the recommendation of double-blind trials of bupropion in

children with psychiatry disorders. A number of years later Casat *et al.* published the results of a double-blind trial of bupropion in children with attention deficit hyperactivity disorder [60, 61]. Connors and Casat conducted a study to determine the safety and efficacy of bupropion in the treatment of children with attention deficit disorder with hyperactivity (ADDH) [62]. In a four-center, double-blind comparison of bupropion (n = 72) and placebo (n = 37), children aged 6 to 12 years meeting DSM-III criteria for ADDH were randomized to receive bupropion 3 to 6 mg/kg per day or placebo, administered twice daily, at 7 am and 7 pm. Measures of efficacy included the Conners Parent and Teacher Questionnaires (93-item, 39-item, and 10 item), Clinical Global Impressions Scales of Severity and Improvement, the Sternberg Short-Term Memory Task, and the Continuous Performance Test. Screen and post-treatment physical examinations, electrocardiograms, electroencephalograms, and clinical laboratory evaluations were performed. A significant treatment effect, apparent as early as day 3, was present for both conduct problems and hyperactivity on the Conners 10-item and 39-item teacher's checklist, and at day 28 for conduct problems and restless-impulsive behavior on the 93-item parent questionnaire. Significant treatment effects were present on both the Continuous Performance Test and memory retrieval test. Effect sizes of bupropion/placebo differences for teacher and parent ratings in this study were somewhat smaller than for standard stimulant drugs used to treat ADHD.

The positive ADHD clinical results have led to numerous patents being lodged for use of bupropion to treat this disorder. The most recent being granted in 2010 for the use of the hydrobromide salt of bupropion and its therapeutic uses [63].

1.1.7.5 Stimulant/substance abuse

In 2004, Tardieu *et al.* reported the case of an amphetamine-abusing patient who self-administered bupropion [64]. For 30 years, a 52-year-old woman used amphetamine derivatives. She explained her need for amphetamine use in order to perform daily activities. She then decided to experiment with bupropion. She abruptly stopped taking clobenzorex and simultaneously started taking bupropion (150 mg/day). The seventh day she reported a concomitant intake of clobenzorex; this induced adverse effects. Whilst taking bupropion, she described experiencing an euthymic state without any compulsion to take amphetamine drugs and was able to perform daily activities. After stopping it, no symptoms of withdrawal were reported by the patient. The conclusion of the study was that this observation supports suggestions that bupropion may be of help in weaning users from amphetamine and should be confirmed by clinical trials.

Bupropion has been considered as an alternative treatment for stimulant and substance abuse as it is an antidepressant with stimulant properties, which inhibits the reuptake of dopamine and norepinephrine. Bupropion is considered an appealing candidate medication for the treatment of

methamphetamine dependence. In 2006, Newton *et al.* conducted a study to assess the impact of bupropion treatment on the subjective effects produced by methamphetamine [65]. They assessed the effects of bupropion treatment on craving elicited by exposure to videotaped methamphetamine cues. A total of 26 participants were enrolled and 20 completed the entire study (n=10 placebo and n=10 bupropion, parallel groups design). Bupropion treatment was associated with reduced ratings of 'any drug effect' ($p < 0.02$), and 'high' ($p < 0.02$) following methamphetamine administration. There was also a significant bupropion-by-cue exposure interaction on General Craving Scale total score ($p < 0.002$), and on the Behavioral Intention subscale ($p < 0.001$). Overall, the data revealed that bupropion reduced acute methamphetamine-induced subjective effects and reduced cue-induced craving. Importantly, this data provided a rationale for the evaluation of bupropion in the treatment of methamphetamine dependence.

1.1.7.6 Pain treatment

Bupropion has been studied in the treatment of pain [66-68]. The first preliminary study of pain treatment by bupropion was by Semenchuk *et al.* They conducted an efficacy study of sustained release bupropion in neuropathic pain [69]. 68 % of patients in the study reported that their pain relief was improved or much improved with bupropion. Most patients were not depressed, and analgesia was observed to occur without change in depression ratings in most patients who responded. Side effects were rated as mild and consisted primarily of insomnia (8 patients), tremor (3 patients), and gastrointestinal upset (2 patients). These symptoms had a tendency to recede with continuation of therapy. They concluded that bupropion may be an effective and tolerated treatment for some patients with neuropathic pain. Blockade of norepinephrine reuptake may mediate this effect. The role of dopamine reuptake blockade was uncertain.

This result was confirmed again by Semenchuk when his team conducted a single-center, outpatient, randomized, double-blind, placebo-controlled, crossover study consisted of two phases [70].

McCullough *et al.* have recently been granted a patent for the use of bupropion in the treatment of pain and related disorders [71]. They have patented methods and compositions utilizing optically pure (+)-isomer of bupropion to assist in smoking cessation, for treating smoking and nicotine addiction, and for treating pain, including, chronic pain, neuropathetic pain and reflex sympathetic dystrophy, and other disorders such as narcolepsy, chronic fatigue syndrome, fibromyalgia, seasonal affective disorder and premenstrual syndrome, while avoiding adverse affects associated with racemic bupropion.

1.1.7.7 *Weight management*

The first study to describe effects of bupropion on body weight was published in 1983 by Harto-Traux *et al.* [72]. Patients' weights were assessed during placebo-controlled, amitriptyline-controlled, and uncontrolled bupropion trials. Low-moderate (50-450 mg/day) to moderate-high (300-750 mg/day) doses of bupropion were consistently associated with a lack of weight gain (average weight loss of 1-2 pounds); placebo was associated with an average weight gain of 1 lb and 75-225 mg/day of amitriptyline was associated with an increase of 3-9 lb.

A second study by Gadde *et al.* [73] was conducted to investigate the efficacy and tolerability of bupropion in 50 overweight and obese women. The core component of the study was a randomized, double-blind, placebo-controlled comparison for 8 weeks. Bupropion or placebo was started at 100 mg/d with gradual dose increase to a maximum of 200 mg twice daily. All subjects were prescribed a 1600 kcal/d balanced diet and compliance was monitored with food diaries. Responders continued the same treatment in a double-blind manner for an additional 16 weeks to a total of 24 weeks. There was additional single-blind follow-up treatment for a total of 2 years. They concluded that bupropion was more effective than placebo in achieving weight loss at 8 weeks in overweight and obese adult women.

The most recent double blind placebo controlled study was conducted by Anderson *et al.* [74] to examine the efficacy of bupropion SR for weight loss. A 24-week multi-centre, double-blind, placebo-controlled study randomized obese adults to placebo, bupropion SR 300, or 400 mg/d. Subjects were counselled on energy-restricted diets, meal replacements, and exercise. During a 24-week extension, placebo subjects were randomized to bupropion SR 300 or 400 mg/d in a double-blinded manner. Of 327 subjects enrolled, 227 completed 24 weeks; 192 completed 48 weeks. Percentage losses of initial body weight for subjects completing 24 weeks were 5.0 %, 7.2 %, and 10.1 % for placebo, bupropion SR 300, and 400 mg/d, respectively. Compared with placebo, net weight losses were 2.2 % ($p = 0.0468$) and 5.1 % ($p < 0.0001$) for bupropion SR 300 and 400 mg/d, respectively. The percentages of subjects who lost $\geq 5\%$ of initial body weight were 46 %, 59 %, and 83 % (p vs. placebo < 0.0001) for placebo, bupropion SR 300, and 400 mg/d, respectively; weight losses of $\geq 10\%$ were 20 %, 33 %, and 46 % (p vs. placebo = 0.0008) for placebo, bupropion SR 300, and 400 mg/d, respectively. Withdrawals, changes in pulse and blood pressure did not differ significantly from placebo at 24 weeks. Subjects who completed 48 weeks maintained mean losses of initial body weight of 7.5 % and 8.6 % for bupropion SR 300 and 400 mg/d, respectively. They concluded that Bupropion SR 300 and 400 mg/d were well-tolerated by obese adults and were associated with a 24-week weight loss of 7.2 % and 10.1 % and sustained weight losses at 48 weeks.

1.1.7.8 Parkinsons disease

In 1984 Goetz *et al.* described an efficacious study of bupropion on treating Parkinsons disease [75]. They evaluated this drug in 20 patients with idiopathic Parkinson's disease. Parkinsonism lessened by at least 30% (Northwestern University Disability Scale or Modified New York University Parkinson's Disease Scale) in half the patients. Depression, present in 12 of 20, was alleviated in only 5. They concluded that bupropion was mildly efficacious in Parkinson's disease.

Young *et al.* have since then patented the use of optically pure bupropion for Parkinsons disease [76]. They disclosed that (-)-bupropion is useful in the treatment of Parkinson's disease. In addition, it has been found that the optically pure (-)-isomer of bupropion is useful in the treatment of other disorders including but not limited to bipolar disorders, attention-deficit disorders, conduct disorders, psycho-sexual dysfunction, bulimia, eating disorders and specific food cravings.

1.1.7.9 Treatment of psychosexual dysfunction

SSRI induced sexual dysfunction for men and women can be treated by bupropion adjunct therapy. This has been studied extensively and most recently by Safarinejad *et al.* [77-79]. He has conducted two randomized double-blind placebo controlled studies on bupropion for treatment of SSRI induced sexual dysfunction. The first was to study the safety and efficacy of adjunctive bupropion sustained-release (SR) on male sexual dysfunction (SD) induced by a selective serotonin reuptake inhibitor (SSRI). The results showed that men who received bupropion had a significant increase in the total IIEF (the International Index of Erectile Function) score (54.4 % vs 1.2 %), and in the five different domains of the IIEF. They concluded that bupropion is an effective treatment for male SD induced by SSRIs.

The second trial examined the efficacy and safety of adjunctive bupropion in the treatment of SSRI-induced female sexual dysfunction. At the end of the trial the mean (SD) scores for desire, arousal, lubrication, orgasm, and satisfaction were significantly higher in the bupropion group. The highest improvement was observed in sexual desire, followed by lubrication. Compared with baseline, desire and lubrication domains increased by 86.4 % in the bupropion group. They concluded that adjunctive treatment with bupropion sustained release during a 12-week period significantly improved key aspects of sexual function in women with SSRI-induced sexual dysfunction.

Numerous patents have been granted for use of bupropion for treatment of sexual dysfunction. The first in 1985, Stern was granted a patent for treatment of psychosexual dysfunction using bupropion [80]. At the time of the patent granting there was no accepted pharmacological treatment of psychosexual dysfunction, the accepted treatment consisted of various forms of

psychotherapy and behavior therapy. The effectiveness of such treatment was quite variable, and since it tended to be both prolonged and expensive it was not accessible to many sufferers. The patent was granted for particular sexual dysfunctions such as, Inhibited Sexual Desire, Inhibited Sexual Excitement, Inhibited Female Orgasm, Inhibited Male Orgasm, Premature Ejaculation, Functional Dyspareunia, Functional Vaginismus and Atypical Psychosexual Dysfunction. Twenty five years later, that patent has now expired and other patents have been granted for use of the same [63].

1.1.7.10 Restless legs syndrome

Restless legs syndrome (RLS) is a common disorder for which agents that enhance dopaminergic activity, including dopamine agonists and levodopa, are the treatment of choice. However, long-term use of dopaminergic drugs can cause unwanted effects such as rebound, tolerance, and augmentation. Kim *et al.* reported three cases where bupropion may have improved the symptoms of restless legs syndrome [81]. The authors report that a low dose of bupropion rapidly and completely ameliorated RLS symptoms in 3 depressed patients within a few days of the initiation of treatment. To their knowledge, this was the first report to show that bupropion may be an effective alternative for treating RLS. Consequently, bupropion may be useful for the treatment of patients with both depression and RLS.

Lee *et al.* also described a study in 2009 where a case of RLS was successfully managed with bupropion [82]. A 45-year-old female presented to a Veterans Affairs primary care clinic with a history of chronic insomnia. Her complicated history of treatment failure to sedative-hypnotic agents, continued sleep disturbances, and complaints of intolerable leg sensations fostered collaboration between a psychiatrist and pharmacist to identify effective treatment. Further review of her medical history and subjective complaints led to a diagnosis of RLS. Based on this new diagnosis, she was prescribed several FDA-approved and alternative agents recommended for the management of RLS. Unfortunately, each medication resulted in a variety of intolerable adverse effects, limiting the list of treatment options. Although not widely used for RLS, bupropion XL (Wellbutrin XL) 150 mg daily was initiated, resulting in resolution of RLS within 3 days. This case supports findings from other cases suggesting a beneficial response with bupropion for the management of RLS.

This treatment has been patented by a number of different parties in one way or another. The most recent using the hydrobromide salt of bupropion [63].

1.1.7.11 Seasonal affective disorder

Seasonal affective disorder (SAD) is a form of depression with seasonal patterns or frequency. Wintertime depression is its most widely recognized form. In 2006, Bupropion was approved by the FDA for treatment of seasonal affective disorder [83, 84]. The first clinical study to show

that bupropion was an effective treatment for winter depression was by Dilsaver *et al.* [85]. Since then much larger studies have confirmed the efficacy of bupropion for treatment of SAD. Modell *et al.* conducted three prospective, randomized, placebo-controlled prevention trials on 1042 SAD patients, enrolled in autumn and treated while still well, across the northern US and Canada. Patients received either bupropion XL 150-300 mg or placebo daily by mouth from enrolment until spring and were then followed off medications for 8 additional weeks. Primary efficacy variables were end-of-treatment depression-free rates and survival distributions of depressive recurrence. Despite a reported average of 13 previous seasonal depressive episodes, almost 60% of patients had never previously been treated for depression. Major depression recurrence rates during the three studies for bupropion XL and placebo groups were 19% versus 30% ($p = 0.026$), 13% versus 21% ($p = 0.049$), and 16% versus 31%; yielding a relative risk reduction across the three studies of 44% for patients taking bupropion XL [86].

1.1.7.12 Bupropion as an anti-viral

Myles *et al.* have reported that bupropion can inhibit nicotine-induced viral reactivation in herpes simplex virus type 1 latent rabbits [87]. Their work was able to show that the incidence of herpes reactivation in rabbits was approximately four times less likely to recur when bupropion was administered.

Patent applications have been lodged for the use of bupropion as an antiviral. One such granted patent relates to a medical use for bupropion as an anti-viral, specifically the invention concerns the use of bupropion in treating infections caused by viruses of the Herpes family [88]. The inventor demonstrated that bupropion is useful for the prevention and treatment of viral infections. As indicated above, bupropion is of therapeutic and prophylactic benefit in the treatment of viral infections. In particular, bupropion is useful in the prevention and treatment of infectious diseases and conditions caused by viral infections. Such diseases include chicken pox (*Varicella zoster*), shingles (*Herpes zoster*), keratitis in rabbits, herpetic encephalitis in mice, cutaneous herpes in guinea pigs, cold sores (*herpes labialis*) and genital herpes (*herpes simplex virus*) in humans, retinitis, pneumonitis and keratitis in humans (*hCMV*), as well as diseases caused by Epstein Barr Virus (*EBV*), human herpes virus 6 (*HHV 6*), *HHV 7* and *HHV 8* and Human Immune deficiency Virus (*HIV*). Of particular mention are chicken pox, shingles, cold sores and genital herpes in humans; of special mention are cold sores and genital herpes in humans.

The authors have listed eight clinical examples where administration of bupropion led to complete remission of herpes after years of negative treatment. For example, the first case treated was a 50 year old businessman with recurrent genital Herpes Simplex viral infection. There were 5-6 recurrences per year. Acyclovir was partially effective in aborting the attacks as the severity of the attacks was reduced slightly the duration of the attacks was reduced from 2

weeks to 5-7 days. The subject took bupropion which resulted in an alteration of the course of the attack and within 2 days, the attack was aborted. Since that time, whenever the subject feels that an attack is about to commence, 4 doses of bupropion, each dose containing 150 mg of bupropion, are taken over 2 days and this either aborts the attack completely, or reduces it to a small crop of lesions which heal completely within 48 hours. There has not been a single significant recurrence of the sort that existed, since commencing this regime.

1.1.7.13 Cancer treatment (Multiple Myeloma)

Kast *et al.* have published two papers concluding the possibility of bupropion being used as adjuvant treatment for multiple myeloma [51, 54]. Multiple myeloma is a severe plasma dyscrasia with no known treatment or cure, even bone marrow transplantation. Cytokines such as tumor necrosis factor- α (TNF) and interleukin-6 (Il-6) are thought to be important trophic factors for the malignant plasma cells. In turn, histamine and nitric oxide are positive regulatory factors for Il-6. They noted the use of bupropion (Wellbutrin) as a respectively potent TNF, nitric oxide and histamine antagonist and thus might find some use in treatment of multiple myeloma. They possibly explained a mechanism for the action of bupropion in lowering tumour necrosis factor TNF.

Etanercept is a commercially available pharmaceutical protein approved for treatment of rheumatoid arthritis, RA. Given subcutaneously, etanercept binds and inactivates soluble tumor necrosis factor- α , TNF. Etanercept has a good safety record and is of benefit in lowering pain, inflammation, and joint destruction in RA. RA is mediated by many factors, TNF among them. Malignant myeloma, MM, is a malignant clonal expansion of a post-germinal center B lymphocyte. Since TNF is a necessary growth factor for expansion and maintenance of MM cells, and etanercept binds soluble TNF and is of clinical benefit in RA, etanercept was tried experimentally in MM. Contrary to expectations, etanercept resulted in increased levels of TNF and possibly shortened survival. Their paper presented a hypothesis of how this happened. There are two cognate receptors for TNF, termed R1 and R2 and two forms of TNF, soluble and transmembrane. Soluble TNF has greater affinity for TNF-R1 than for TNF-R2. Transmembrane TNF has equal affinity for the two receptors. Since TNF-R2 signaling tends to be more anti-apoptotic and activating of nuclear factor kappa B, NFkB, than is TNF-R1, and TNF-R1 tends to be more pro-apoptotic than is TNF-R2, by inactivating soluble TNF while leaving transmembrane TNF signaling relatively unchanged, etanercept changed the balance in TNF signaling from TNF-R1 towards TNF-R2 weighting. Anti-apoptosis and TNF synthesis would have been up-regulated by that shift. Early data indicated that bupropion may ameliorate Crohn's disease course by down regulating TNF synthesis, and it may slow the course of MM as well.

1.1.7.14 Psoriasis

A pilot study for the treatment of psoriasis with bupropion was carried out by Modell *et al.* [89]. The objective of the study was to determine whether bupropion may be useful in treating atopic dermatitis and psoriasis in non-depressed patients. Ten non-depressed subjects with atopic dermatitis and 10 with psoriasis completed a single-track, open-label treatment protocol with bupropion-SR in doses of 150 mg/day and 300 mg/day, administered sequentially for 3 weeks each, followed by a 3-week wash-out. Treatment response was assessed at the end of each 3-week period. The results showed that six out of ten subjects with atopic dermatitis showed a reduction in affected body surface area by the end of 6 weeks of bupropion treatment, with affected area increasing toward the pre-study baseline in all responders following bupropion discontinuation—a highly significant treatment effect ($p = 0.0003$). Of the 10 subjects having psoriasis, improvement over baseline after 6 weeks of treatment was seen in eight subjects, with coverage increasing toward the pre-study baseline in the responders following bupropion discontinuation ($p = 0.001$). Average reduction in affected area in the responders at week 6 of treatment was approximately 50% in both groups. Modell *et al.* concluded that the general good tolerability and relative safety of bupropion-SR makes a trial of this agent worthwhile in patients with atopic dermatitis or psoriasis who have failed treatment with more conventional medications.

1.1.7.15 Bupropion and effects from alcohol

Peck of Burroughs Wellcome Co. was granted a patent in 1983 for the use of bupropion in reversing the impaired mental alertness effects of ethanol in a human [90]. The patent discloses that the amount of bupropion required to substantially reverse the mental functional impairment depends on a number of factors such as the concentration of ethanol in the blood, weight and metabolism rate of the person receiving treatment and the presence of other drugs in the blood of the treated person which may interact with bupropion and/or ethanol. However, for an adult of approximately 70 kg who has consumed 16 to 32 mL of ethanol within 10 minutes and who has not taken any other drug within the past 24 hours the effective dose of bupropion will generally lie in the range of 50 mg to 300 mg and preferably from 75 mg to 200 mg. The authors performed a clinical study and were able to show that bupropion when administered to a human intoxicated with ethanol significantly restores impaired mental ability.

This patent would now have expired and there are no recent patents or literature data on this effect. It is unlikely that administration of an antidepressant with a depressant such as alcohol would be ethically or pharmacologically advantageous.

1.2 Prodrugs

1.2.1 Introduction

The term prodrug initially used by Albert [91], is a pharmacologically inactive compound that is converted into an active one by a metabolic transformation. The prodrug can also be activated by non-enzymatic processes such as chemical hydrolysis but in this case the compound maybe inherently unstable which will lead to later stability issues during formulation. The prodrug to drug conversion can occur before absorption, during absorption, after absorption or at a specific site in the body. In an ideal case a prodrug is converted to the drug as soon as the desired goal for designing the prodrug has been accomplished.

There are a number of reasons to rationalise the prodrug design. The prodrug design is an approach that is used to correct a flaw in a drug candidate. Prodrugs are designed to improve aqueous stability, absorption and distribution, site specificity, instability, prolong release, toxicity, poor patient acceptability, to address formulation issues or simply to expand on the intellectual property associated with a known compound [92].

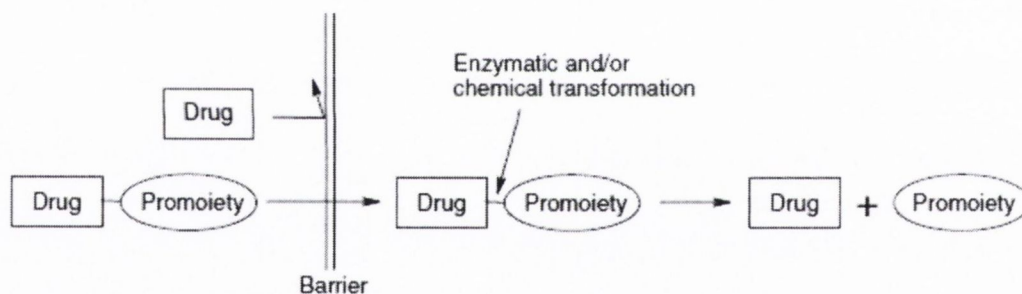


Figure 1.6 A representative illustration of the prodrug concept. The drug-promoiety indicates that part of the prodrug is pharmacologically inactive. The Barrier can be any limitation of a parent drug that prevents optimal performance, which must be overcome for the development of a marketable drug. Adapted from Rautio [93].

There are several classifications of prodrugs. Some prodrugs are not designed as such and it is only discovered after isolation and testing of the metabolites that activation of the drug had occurred. In most cases the modification in a drug has been made on the basis of known metabolic transformations. It is expected that after administration, the prodrug will be appropriately metabolized to the active form.

From a regulatory perspective, prodrugs are classified into two major types, based on their cellular sites of conversion into the final active drug form, with type 1 being those that are converted intracellularly (e.g., anti-viral nucleoside analogs, lipid lowering statins), and type 2 being those that are converted extracellularly, especially in digestive fluids or the systemic circulation [94, 95]. Both types can be further categorized into subtypes, type 1A, 1B, 2A, 2B, 2C, based on whether or not the intracellular converting location is also the site of therapeutic action, or the conversion occurs in the gastrointestinal fluids or systemic circulation (Table 1.6).

Type	Converting site	Subtype	Tissue location of conversion
1	Intracellular	1A	Therapeutic target tissue/cells
1	Intracellular	1B	Metabolic tissues (liver, GI mucosal cell, lung)
2	Extracellular	2A	GI fluids
2	Extracellular	2B	Systemic circulation and other extracellular fluid compartments
2	Extracellular	2C	Therapeutic target tissue/cells

Table 1.6 Classification of prodrugs, adapted from Wu [95].

Prodrugs can belong to multiple subtypes. A mixed type prodrug is one that is converted at multiple sites, either in parallel or sequential steps. From a chemical perspective, prodrugs can be classified into two types, carrier linked prodrugs and bioprecursors. Carrier linked prodrugs contain a group that can be easily removed enzymatically (such as an ester) to reveal the true drugs. Ideally the group removed is pharmacologically inactive and non-toxic while the connecting bond must be labile for efficient activation *in vivo*. Carrier linked prodrugs are the ones where the active drug is covalently linked to an inert carrier transport moiety. They are generally esters or amides. Such prodrugs have greatly modified lipophilicity due to the attached carrier and the active drug is released by hydrolytic cleavage, either chemically or enzymatically. It can be further subdivided into bipartite - composed of one carrier (group) attached to the drugs, tripartite - carrier group is attached via linker to drug and mutual prodrugs - two drugs linked together. Bioprecursor prodrugs are ones that are metabolized into a new compound that may itself be active or further metabolized to an active metabolite. They are obtained by chemical modification of the active drug and do not contain a carrier.

1.2.2 Central nervous system type prodrugs

Central nervous system (CNS) drug delivery remains a challenge, despite the efforts that have been made to develop novel strategies to overcome obstacles. The blood–brain barrier (BBB) presents an efficient structural and functional barrier for the delivery of agents to the central nervous system (CNS). Due to its unique properties, passage across the BBB often becomes the main limiting factor for the delivery of potential CNS drugs into the brain parenchyma. In fact, it is estimated that more than 98% of small-molecular weight drugs and practically 100% of large-molecular weight drugs developed for the CNS diseases do not readily cross the BBB. Many of the pharmacologically active drugs tend to fail early in their development phase because these molecules lack the structural features that are essential for passing the BBB. The BBB segregates the CNS from the systemic circulation, and its main physiological functions include maintaining homeostasis at the brain parenchyma and protecting the brain from potentially harmful chemicals. The BBB is primarily formed from capillary endothelial cells, which differ from the other tissues. The brain capillary endothelial cells are very closely joined together by tight intercellular junctions that efficiently restrict the paracellular diffusion of hydrophilic drugs. In addition, perivascular elements such as pericytes, which partially encircle the endothelium, astrocytic end-foot processes and neuronal cells, are important in the function of the BBB [93, 96].

In addition to being a selective structural diffusion barrier, the BBB constitutes an efficient functional barrier for solutes crossing the cell membrane. The high metabolic activity of brain capillary endothelial cells, as well as effective efflux systems that actively remove solutes from brain tissue and return them back to the blood stream, create a great challenge for potential neuro-therapeutics. Furthermore, the BBB expresses a number of specific carrier mediated inward transport mechanisms that ensure an adequate nutrient supply for the brain. Traditionally, various medicinal chemistry- (e.g. lipophilic drug analogs and prodrugs, or disruption of BBB) and physical neurosurgery-based invasive approaches (e.g., interstitial drug delivery) have been attempted to increase brain delivery of therapeutic agents. Novel CNS-targeted neuro-therapeutics should possess either the optimal physicochemical characteristics that allow for passive diffusion through the BBB via the transcellular route, or have the structural features necessary to serve as a substrate for one of the endogenous influx transport systems of the BBB. To be able to readily cross the BBB by passive diffusion in pharmacologically significant amounts, a drug should be relatively small (have a molecular weight of less than 500 Da), lipid soluble and, be either neutral or significantly uncharged at physiologically pH, and be capable of forming less than eight H-bonds with water. On the other hand, new knowledge of endogenous BBB transporters can be used in the rational reformulation

of drug molecules for active transport. However, it is important to recognize that the degree of BBB drug penetration and resultant CNS concentrations required for efficacy is related to the potency of the drug. Although a small amount of the drug may penetrate into the CNS, if it is potent, very small concentrations binding to the receptor will result in the desired effect. The human brain microvasculature consists of approximately 640 km of capillaries, with a surface area of about 20 m². Every neuron is essentially perfused by its own blood vessels, and these vessels are typically 40 µm apart from each other. A small molecule may diffuse through this 40 µm space in about 1 s, which indicates that after passage across the BBB the drug is almost instantly distributed within the whole cerebral tissue. These physiological facts indicate that the vascular route would be very promising in drug delivery for targeting the brain, if the CNS transport challenge could be solved. An attractive and rewarding chemistry-based strategy that has been successfully employed to increase the CNS transport of poorly penetrating therapeutic agents is their transient chemical modification by using the prodrug approach [96-98].

1.2.3 Prodrugs and bioprecursors of CNS type compounds

There are numerous examples of prodrugs for amines which directly relate to prodrugs for CNS agents and this has been reviewed extensively [99]. Some prodrugs of CNS compounds are shown in Figure 1.7.

Fenproporex is a stimulant and bioprecursor of amphetamine. Fenproporex is *N*-dealkylated to amphetamine *in vivo* [100]. L-threo-3,4-dihydroxyphenylserine (L-DOPS, droxydopa) is a synthetic catecholamino acid. When taken orally, L-DOPS is converted to the sympathetic neurotransmitter, norepinephrine (NE), via decarboxylation catalyzed by L-aromatic-amino-acid decarboxylase (LAAAD) [101]. Lisdexamphetamine is a prodrug of dextroamphetamine. Lisdexamphetamine is indicated for the treatment of attention deficit hyperactivity disorder (ADHD).

L-dopa is a dopamine prodrug. Dopamine is formed by decarboxylation of L-dopa. There are numerous dopamine prodrugs and this has been extensively described [102]. Aside from its natural and essential biological role, L-DOPA is also used in the clinical treatment of Parkinson's disease (PD) and dopamine-responsive dystonia (DRD).

Carbamate prodrugs of phenylethylamines have been used successfully in the past [103].

Prodrugs of ephedrine have been made successfully from oxazolidines [104].

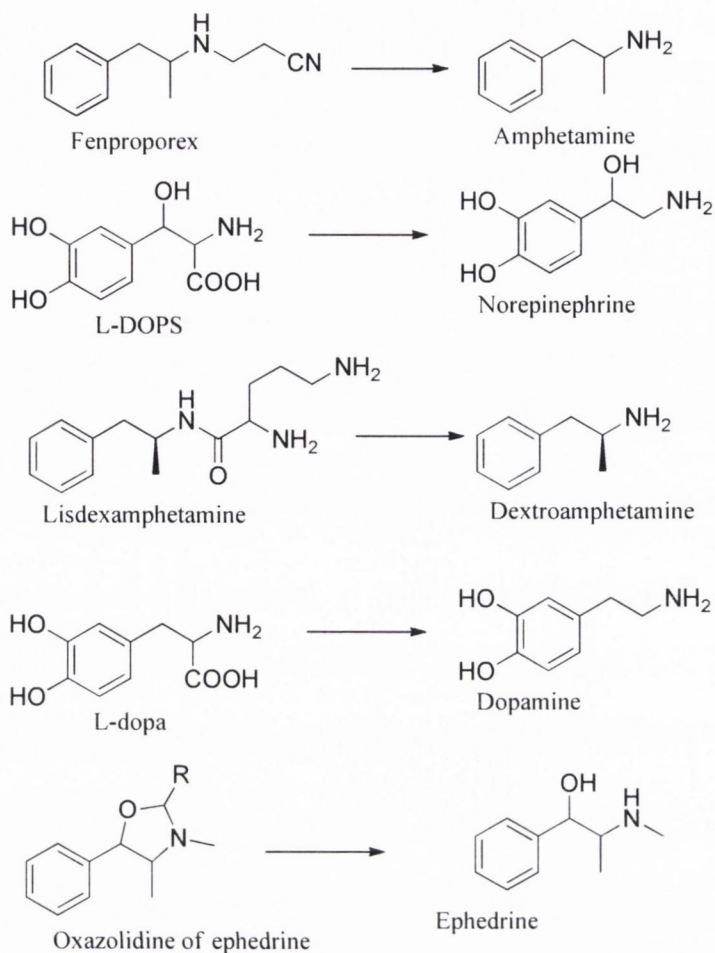
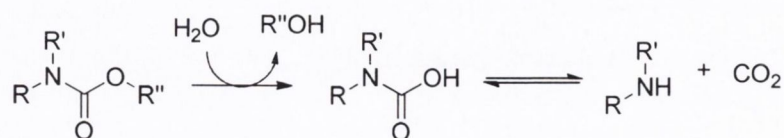


Figure 1.7 Examples of some bioprecursor prodrugs of some CNS compounds structurally related to bupropion

1.2.4 Carbamate type prodrugs

Carbamate type prodrugs have been used in drug design as releasing groups for amines and alcohols. The mechanisms of activation are namely enzymatic and non-enzymatic ones. The mechanism is as follows, Scheme 1.2; hydrolysis of the ester group liberates the alcohol which itself maybe a potential prodrug followed by spontaneous decarboxylation of the carbamic acid to liberate the active amine and carbon dioxide.



Scheme 1.2 The mechanism of hydrolysis of carbamates

Primary and secondary amino groups of different basicities have been derivatized to yield carbamate prodrugs, often of anti-tumour agents. For example, capecitabine is a recently marketed site selective multistep (triple) prodrug of the antitumour drug 5-fluorouracil [105]. The prodrug is well absorbed orally and is hydrolysed by liver carboxylesterase. The resulting metabolite is a carbamic acid, which spontaneously decarboxylates to 5'-deoxy-5-fluorouracytidine. The enzyme cytidine deaminase, which is present in the liver and tumours, transforms 5'-deoxy-5-fluorouracytidine to 5'-deoxy-5-fluorouridine. Transformation of 5-FU is catalyzed by thymidine phosphorylase and occurs selectively in tumor cells. In animal tumour models with human cancer xenografts, capecitidine proved much safer and more effective than 5-FU.

1.2.5 Amide prodrugs

Amides have been widely used in prodrug design as releasing groups for amines. Numerous endogenous enzymatic systems will hydrolyse the amide bond, ranging from amidases and esterases to peptidases for peptide prodrug conjugates. From a chemical point of view, amide and ester bonds have comparable structural and spectroscopic features and are hydrolysed by the same general mechanism, *i.e.*, a nucleophilic acyl substitution involving an addition-elimination sequence. However, in a given structure, the amide bond is more resistant than the ester bond to chemical hydrolysis. The reason for this is that the amide bond is less polarized than the ester bond due to the lower electronegativity of the *N*-atom compared to the corresponding *O*-atom. The amide bond also has partial double bond character due to delocalisation of electrons and resonance.

Both amides and esters are often hydrolysed by the same hydrolases. As a general rule, amides are hydrolysed more slowly than esters, due to stereoelectronic and catalytic properties of the enzymes. The greater stability of amides has, therefore, been used in the development of drugs that possess longer biological half-lives than their carboxylate analogues. For the same reason – *i.e.*, the relative stability of amides *in vivo* – *N*-acylation of amines to give amide prodrugs has been used to only a limited extent.

The mechanism of hydrolysis of esters and amides follows a similar pathway (Figure 1.8). The hydrolases include the following three catalytic features at the active site that enormously accelerate the rate of hydrolysis. First, each contains an electrophilic component, which increases the polarization of the carbonyl group in the substrate (Z^+). Second, each has a nucleophile ($Y:$) to attack the carbonyl C-atom, leading to the formation of a tetrahedral intermediate. And finally, each has a proton donor ($H-B$) to transform the $-OR'$ or $-NR'R''$ moiety into a better leaving group. These three catalytic functionalities are similar in practically all hydrolytic enzymes, but the actual functional groups performing these reactions differ among hydrolases.

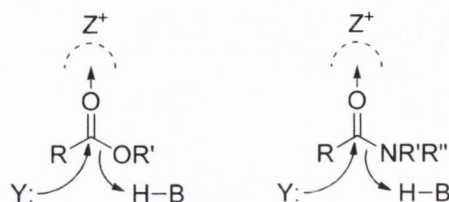


Figure 1.8 The common catalytic mechanism of hydrolases in ester and amide hydrolysis.

A systematic study on the metabolic hydrolysis of primary aliphatic amides was carried out in 1950 by Bray *et al.* [106]. The effect of chain length on the degree of hydrolysis of amides containing 1 to 18 C-atoms was shown in rabbit liver preparations. The extent of hydrolysis was very small for the first three homologues, then increased markedly to reach a maximum with hexanamide and heptanamide, then fell off rapidly. Branching of the side chain also reduced the extent of hydrolysis.

Secondary aliphatic have also been studied systematically. Chen and Dauterman [107] showed that an amidase isolated from sheep liver microsomes was unable to hydrolyse *N*-Me-substituted amides having fewer than four C-atoms in the acyl chain. Starting with *N*-methylvaleramide, the extent of hydrolysis increases with increasing chain length of the acyl chain; the maximum was reached with *N*-methylcaproamide and thereafter decreases with increasing chain length.

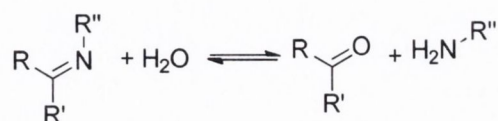
The last group of aliphatic amides are the tertiary amides and are most relevant to a potential amide prodrug of bupropion. Investigations of their chemical stability have disclosed a surprising difference between tertiary and secondary amides, since the rate of acid catalyzed hydrolysis of *N,N*-dimethyl amides is higher than that of *N*-methyl amides. If steric factors were predominant, tertiary amides would be less reactive. It has been proposed that this may result from a higher stability of the protonated intermediate. A comparable rule would appear to apply to enzymatic hydrolysis also. Investigation of the activity of amidase in sheep liver microsomes have shown that *N,N*-dimethylcaproamide was hydrolysed faster than the mono-methyl analogue [107].

1.2.6 *N*-alkylated prodrugs

N-dealkylation is a common metabolic transformation of xenobiotics. Many pharmaceutical compounds are transformed by the CYP450 group of enzymes to more active metabolites. Tamoxifen's *N*-demethylated metabolite is orders of magnitude more potent than the parent [108] and diethylcathinone is transformed to ethylcathinone and furthermore to cathinone *in vivo* which also account for most of diethylcathinone's activity [109].

1.2.7 Imine prodrugs

Imines are used as releasing groups for ketones. Imine type prodrugs, drugs, xenobiotics and metabolites are susceptible to hydrolysis. Their hydrolysis is essentially a nonenzymatic process, the rates depending not only on the biological context, but also on the structure and properties of the imine. Imines may undergo metabolic hydrolysis as described below, Scheme 1.3:



Scheme 1.3 The hydrolysis of imines

This reaction is reversible, since the condensation of a carbonyl compound and primary amine yields the imine under dehydrating conditions. In fact, acidic conditions usually tend to favour hydrolysis, whereas neutral or slightly alkaline conditions lead to deprotonation of the amine, which then behaves as a nucleophile toward the carbonyl.

Imines although usually too sensitive to hydrolysis and therefore too unstable for a prodrug approach, have nevertheless been used successfully in some cases. The anticonvulsant progabide was prepared as a prodrug form of γ -aminobutyric acid (GABA) since it crosses the blood brain barrier, while the free drug does not [110]. Metabolic studies in fish (ray) revealed two hydrolytic reactions, the major one being hydrolysis of the terminal amide group to form the corresponding carboxylic acid and a less important one being hydrolysis of the imine link to liberate GABA and gabamide (*i.e.* the amide of GABA). Detection of GABA and gabamide in the brain of rats dosed with progabide implies slow *in situ* generation of these active metabolites.

1.2.8 Oxime prodrugs

Oximes are used as releasing groups for ketones. Like imines, oximes are known to undergo metabolic hydrolysis by a nonenzymatic mechanism, Scheme 1.4.



Scheme 1.4 The hydrolysis of hydroxyimines

Cyclohexanone oxime is one example. Following administration to male rats by various routes, cyclohexanone oxime undergoes rapid metabolism and only trace amounts of the parent compound are found in the urine [111]. *In vitro* studies on rat liver preparations confirmed the metabolic pathway of nonenzymatic hydrolysis of the oxime to the ketone followed by

enzymatic reduction to the alcohol, hydroxylation to diols and then phase II conjugation by glucuronidation. The first step in this scheme is the nearly quantitative hydrolysis of the oxime to the ketone.

One complicating factor in the metabolism of oximes comes from the possibility that they may become reduced to the imine prior to hydrolysis thus releasing ammonia rather than hydroxylamine as a metabolite. Oximes are also known to undergo enzymatic hydrolysis. Buparvaquone hydroxyimine [112] and nabumetone hydroxyimine [113] are such examples both readily oxidized by CYP3A4 back to the parent ketone.

1.2.9 *O*-alkylated prodrugs

O-dealkylation is a common metabolic transformation for xenobiotics especially on aromatic rings or as ether functional groups. Enol ethers and enol esters have been shown to be hydrolysed by CYP450 enzymes in liver microsomes. Enol esters are distinct from other esters not because of a particular stability or lability towards hydrolases, but due to their hydrolysis releasing a 'ghost alcohol' (an enol), which generally will immediately tautomerize to the corresponding aldehyde or ketone. Therefore *O*-alkylation of enols can be used to mask ketones. A well studied example is that of vinyl acetate, a xenobiotic of great industrial importance that, upon hydrolysis liberates acetic acid and acetaldehyde, the stable tautomer of vinyl alcohol [114]. The results of two studies demonstrated that vinyl acetate is a very good substrate for carboxylesterase but not acetylcholinesterase or butyrylcholinesterase.

An example more suited to bupropion is that of α -acetoxystyrene which is an aromatic enol ester. Upon hydrolysis α -acetoxystyrene yields acetic acid and acetophenone. This compound is quite stable in physiological buffers but is readily hydrolysed in human and rat plasma [115, 116], such results suggest that enol esters may be of interest as potential prodrugs of enolizable aldehydes or ketones such as bupropion. Enol esters of polypeptide prodrugs of human neutrophil elastase inhibitors have also been demonstrated by Burkhart *et al.* [117].

1.2.10 Prodrugs of hydroxybupropion

The absence of literature data on a prodrug approach for bupropion is unusual for such a widely used drug, but some attempts have been made to develop prodrug approaches for its active metabolite hydroxybupropion. A transdermal prodrug delivery approach has been developed for percutaneous absorption of hydroxybupropion [118]. A carbamate prodrug of hydroxybupropion was evaluated *in vitro*. *In vitro* diffusion studies were conducted in a flow-through diffusion cell system. Bupropion freebase was also evaluated. Although bupropion traversed human skin at rates sufficient to achieve required plasma levels, it was chemically unstable and hygroscopic, and unsuitable for transdermal formulation. On the other hand, hydroxybupropion is stable but its transport across skin is much slower. Alternatively, the

prodrug butyl carbamate of hydroxybupropion was found to be stable, and also provided a 2.7-fold increase in the transdermal flux of hydroxybupropion across human skin *in vitro*. Thus, a prodrug of hydroxybupropion provides a viable option for the transdermal delivery of hydroxybupropion.

1.2.11 Potential codrugs of bupropion/metabolites

A codrug approach for delivery of hydroxybupropion has been developed [119]. A codrug is one that when metabolized forms two active compounds *in vivo*. This approach is similar to a prodrug approach as both require the body to metabolize the parent compound into the active/actives *in vivo*. A codrug approach for simultaneous treatment of alcohol abuse and tobacco dependence is considered as very desirable because of substantial evidence that smoking is increased significantly during drinking, and that smoking is regarded as a behavioural 'cue' for the urge to consume alcohol. The purpose of this study was to design and synthesize codrugs for simultaneous treatment of alcohol abuse and tobacco dependence. Two novel tripartate codrugs of naltrexone (NTX) and naltrexol (NTXOL) covalently linked to hydroxybupropion were synthesized and their hydrolytic cleavage to the parent drugs was determined. These codrugs were generally less crystalline when compared to NTX, or NTXOL, as indicated by their lower melting points, and were expected to be more lipid-soluble. Also, the calculated $c \log P$ values were found to be higher for the codrugs compared to those for NTX and NTXOL. The studies on the hydrolysis of the codrugs provided good evidence that they could be efficiently converted to the parent drugs in buffer at physiological pH. Thus, these codrugs are likely to be cleaved enzymatically *in vivo* to generate the parent drugs, and are considered to be potential candidates for simultaneous treatment of alcohol abuse and tobacco dependence.

1.2.12 Prodrugs of compounds relating to bupropion

Diethylpropion is an *N*-ethyl prodrug of ethylpropion. Ethylpropion is an α -aminoketone related to bupropion, used as an appetite suppressant to treat obesity. Diethylpropion is *N*-de-ethylated *in vivo* to ethcathinone which is a selective norepinephrine releasing agent [120]. The amino group is sensitive to oxidative *N*-de-ethylation in diethylpropion and this could possibly be used as a similar approach in bupropion.

Designer drugs such as mephedrone (4-methylmethcathinone) are also known to be *N*-dealkylated. These α -aminoketones are generally susceptible to oxidative *N*-dealkylation. Meher and Maurer have very recently published a review on the metabolism of designer drugs which includes the metabolic studies on mephedrone [121].

The urinary metabolites of methylone in humans and rats were investigated by analysing urine specimens from its abuser and after administrating to rats by Kamata *et al.* [122]. Methylone is the methylenedioxy analogue of methcathinone, it too is also an α -aminoketone. Two major metabolic pathways were revealed for both humans and rats as follows: (1) side-chain degradation by *N*-demethylation to the corresponding primary amine methylenedioxycathinone (MDC), partly conjugated; and (2) demethylenation followed by *O*-methylation of either a 3- or 4-OH group on the benzene ring to produce 4-hydroxy-3-methoxymethcathinone (HMMC) or 3-hydroxy-4-methoxymethcathinone (3-OH-4-MeO-MC), respectively, mostly conjugated. The *N*-dealkylation of these type compounds is a common theme and could be used a prodrug releasing strategy for bupropion.

1.2.13 Bupropion analogues

Carroll *et al.* have synthesized a number of bupropion analogues for the treatment of cocaine addiction [123] and as potential pharmacotherapies for smoking cessation [124]. There is no metabolic data or pharmacokinetic information reported as these are theoretically new drug candidates but there is a possibility that one of these analogues is a potential prodrug of bupropion. The *in vitro* and *in vivo* results are reported but their most promising candidates are unlikely prodrugs of bupropion as all the classical metabolic reactions that would occur on them would not release bupropion.

1.2.14 Potential prodrugs of bupropion

There are many reasons why a prodrug approach should be attempted for *in vivo* delivery of bupropion. Firstly there is an absence of literature on prodrugs of bupropion. The numerous therapeutic uses of bupropion and their methods of delivery may require different approaches to be successful. For example, a more stable prodrug would be required for transdermal delivery of bupropion, which would be more suitable for the treatment of a skin condition such as psoriasis or to deliver bupropion direct to the blood-stream by-passing the first-pass effect. A prodrug approach is a commercially good idea to extend patents and file NDAs. Another benefit to a prodrug approach for bupropion would be to improve the PK profile of bupropion perhaps lowering its therapeutic dose and side effects. Increasing the lipophilicity of the compound would improve its membrane permeability, possibly delivering higher levels of bupropion directly to its site of action *i.e.* the brain. The prodrug approach may reduce levels of metabolites of bupropion, which are known to contribute to its side effect profile and mitigate its clinical effects. Finally, since bupropion freebase has poor stability at physiological pH, any improvement in its stability profile would be advantageous as this would reduce the amount of degradants the toxicological effects of which are unknown. This is addressed in some detail in the aqueous stability study of bupropion in Chapter 2.

Chapter 2 - The aqueous stability of bupropion

This chapter describes the aqueous stability of bupropion. In this study the aqueous stability of bupropion was determined and the pH-degradation profile was obtained. The effects of hydrogen ion, solvent and hydroxide ion concentration are discussed with particular emphasis on the kinetics of degradation of bupropion. Kinetics and degradation of bupropion were determined by HPLC-UV and LC-MS analysis both utilising high pH chromatographic methods. Degradation of bupropion in aqueous solutions follows first-order reaction kinetics. The pH-degradation profile was determined using non-linear regression analysis. The micro- and macro-reaction constants for degradation are presented. Bupropion was most stable in aqueous solutions below pH 5. Hydrolytic degradation was catalyzed by water but mainly by hydroxide ion on the unionised form of bupropion. Bupropion is also susceptible to oxidation. The degradants of bupropion were positively identified and a mechanism of degradation is proposed. The inherent instability of bupropion above pH 5 has implications for its therapeutic use, formulation, pharmacokinetics and use during analysis and storage. Two prodrug concepts are presented to improve the stability of bupropion.

2 The aqueous stability of bupropion

2.1 Introduction

The purpose of stability testing is to provide evidence on how the quality of a drug substance or drug product varies with time under the influence of a variety of environmental factors such as temperature, humidity, and light, and to establish a re-test period for the drug substance or a shelf life for the drug product and recommended storage conditions. Stress testing of the drug substance can help identify the likely degradation products, which can in turn help establish the degradation pathways and the intrinsic stability of the molecule and validate the stability indicating power of the analytical procedures used. The nature of the stress testing will depend on the individual drug substance involved [125].

While there has been little published in peer reviewed journals, it is widely acknowledged that bupropion presents serious stability problems in manufacturing, formulation and use. This is partly reflected in the numerous patents directed at methods to improve the stability of bupropion formulations.

One method to improve the stability of bupropion in oral formulations involves addition of a stabilizer to the formulation, in this case cysteine or glycine hydrochloride. The hydrochloride salts of these weak bases have two functions. The first is to act to buffer the formulation at a pH between 0.9 and 4.0 [126]. The acidic environment keeps bupropion protonated, while compounds such as cysteine have antioxidant properties.

Other stabilizers used to improve the stability of bupropion in tablet formulations are organic acid [127], inorganic acids [128] and salts of organic bases [129]. Once again the acidic environment keeps bupropion in its protonated form where it is more stable so the common stabilising effect is by acidifying the formulations. Pharmaceutical compositions for transdermal administration containing fatty acid salts of bupropion free base and metabolites have also been developed [130]. Therefore from the patent literature it is can be inferred that the salt form of bupropion is more stable than the freebase. The levels of moisture are evidently critical in controlling degradation during processing. Chawla *et al.* developed a dry granulation process for tableting of bupropion, avoiding the use of stabilizers [131]. Indeed, an inclusion complex of bupropion hydrochloride with beta-cyclodextrin that stabilizes bupropion hydrochloride against degradation has been developed by Gidwani *et al.* [132]. Other physical methods have been developed to trap bupropion inside a moisture barrier within an oral tablet formulation. These usually involve polymer coatings around the tablet or sometimes polymer microspheres within the tablet. These formulations create dry micro-environments within the tablet matrix limiting access between bupropion and its outside environment. Stabilized bupropion hydrochloride pharmaceutical compositions are described that are free of acid additives and

provide for a sustained release of bupropion hydrochloride [133]. The particulate bupropion hydrochloride is coated with a polymer membrane coating.

From the limited amount of stability information published on bupropion, it can again be concluded that bupropion is stable under acidic conditions. Bupropion half-life in plasma stored at 22 and 37°C was 54.2 and 11.4 h, respectively. It was only shown to be stable at pH 2.5 [134]. Another study on the chemical stability of bupropion in isotonic pH 7.4 at 32°C over two weeks showed that its disappearance follows first-order kinetics [118]. The stability of bupropion in formalin has been studied and it was shown that at lower pH, bupropion is most stable; at higher pH, bupropion is converted into *N*-methyl bupropion [135]. Compounds with similar structure to bupropion, e.g. diethylpropion have shown similar degradation characteristics. Hydrolytic decomposition of diethylpropion in solution at 45°C occurred at a very slow and constant rate at pH 3.5 and below but increased rapidly as the pH was raised above 3.5 [136].

The formulation, stabilisation and use of bupropion is therefore an active area of pharmaceutical research. There is currently no injectable delivery vehicle for bupropion in clinical use and its absolute oral bioavailability in humans has not been reported for this reason.

Against this background and in the context of its expanding therapeutic uses this chapter reports on the kinetics of degradation of bupropion in aqueous solution including routes of degradation and influence of parameters such as ionic strength and buffer identity.

2.1.1 Tautomerism of bupropion

Bupropion like all α -aminoketones has the ability to tautomerize from the α -aminoketone to the amino-enol and to the α -hydroxyimine. Once bupropion is in its hydroxyimine form it is highly susceptible to hydrolysis with loss of the amino group, the product of which is an α -hydroxyketone.

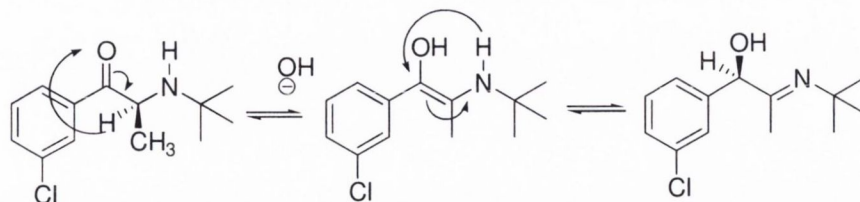


Figure 2.1 Keto-enol/enamine-imine tautomerism of bupropion

2.1.2 Thermal rearrangement of aminoketones

Thermal rearrangement is known to occur to α -aminoketones and their tautomers α -hydroxyimines by migration of alkyl groups. This has been studied extensively by Stevens *et al.* [137, 138]. This thermal rearrangement is known to occur at high temperatures and is not deemed a significant problem under even forced degradation conditions.

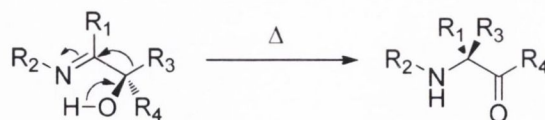


Figure 2.2 Thermal rearrangement of α -hydroxy imines and α -hydroxyketones. Adapted from [139].

2.2 Results & Discussion

2.2.1 pH-rate profile of bupropion

Bupropion solutions were prepared at a concentration of 250 ng/mL in aqueous buffers from a 1 mg/mL methanol stock solution. The final concentration of methanol in the buffered solutions was approximately 1 %. Buffers over the pH range of 2-13 were prepared by mixing two stock buffered solutions to give solutions of different pH but equal ionic strength. This buffer system was adapted from a previously described universal buffer system by Carmody (Table 2.1).

Stock buffer A: boric Acid 0.2 M, citric acid 0.05 M, NaCl 0.594 M, I = 0.6. Stock buffer B: tripotassium phosphate 0.1M, I = 0.6. For example, to prepare a solution of pH ~ 7.2 with an I = 0.055, add 0.5 mL solution A and 0.5 mL solution B to 10 mL deionised H₂O.

Vol. A (mL)	Vol. B (mL)	pH ₂₀ ^{°C}
1.0	0	3.0
0.9	0.1	3.5
0.8	0.2	4.2
0.7	0.3	5.1
0.6	0.4	6.3
0.5	0.5	7.4
0.4	0.6	8.3
0.3	0.7	9.4
0.2	0.8	10.7
0.1	0.9	12.1
0	1.0	12.5

Table 2.1 Dilutions of stock buffers to give constant ionic strength with varying pH. Stock buffer A: boric Acid 0.2 M, citric acid 0.05 M, NaCl 0.594 M, I = 0.6. Stock buffer B: tripotassium phosphate 0.1M, I = 0.6. Total Volume = 11 mL with deionised water.

Buffered solutions at the lowest and highest pH were prepared with 0.055 M HCl pH 2.0 and 0.055 M NaOH pH 13.1. Solution pH was measured at room temperature $20 \pm 1^\circ\text{C}$ using a Radiometer Copenhagen PHM61 laboratory pH meter. The pH meter was calibrated before use with standard buffers, 4.0, 7.0 and 10.0. Solutions were incubated either in a digital oven (for long term storage) or in the Accela LC system autosampler (for short term). Aliquots were taken at appropriate times depending on the decomposition rate and analyzed immediately for remaining bupropion. Buffer concentrations throughout the study were low. However the effect of buffer concentration on rate was evaluated at kinetically and mechanistically distinguishable phases of the resulting pH rate profile. Dilution did not affect degradation rate using the universal buffer system and therefore it was not necessary to extrapolate to zero buffer concentration.

The observed first-order degradation rate constants, k_{obs} , were calculated from the slopes of the natural-logarithmic plots of the drug fraction remaining versus time in accordance with Equation 2.1:

Equation 2.1

$$\ln\left(\frac{C_t}{C_0}\right) = -k_{obs} t$$

where C_0 was the initial concentration and C_t was the remaining concentration of bupropion at time t . Solutions were monitored for two weeks and stored protected from light.

The disappearance of bupropion in aqueous solution was monitored by HPLC-MS. The degradation in the pH range 2–13 followed apparent first-order rate kinetics. Rate constants from a matrix of different experiments are presented in Table 2.2, where the temperature, pH and ionic strength have been varied. Rate constants were estimated from the resulting slopes after a plot of $\ln [C_t/C_0]$ versus time (Figure 2.3) and the resulting k_{obs} values (Table 2.2) plotted against pH.

Temperature (K)	313	323	333
Ionic strength	0.055	0.12	0.055
pH _{RT}		k_{obs} (h ⁻¹)	
5.1	0.002	0.001	0.004
6.3	0.003	0.002	0.008
7.4	0.004	0.004	0.019
8.3	0.006	0.017	0.035
9.4	0.012	N/D	0.051
10.7	0.018	0.052	0.055
11.9	0.034	0.072	0.101
12.3	0.042	0.114	0.166
13.0	0.102	N/D	0.407

Table 2.2 First-order rate constants determined for the degradation of bupropion. N/D = not determined.

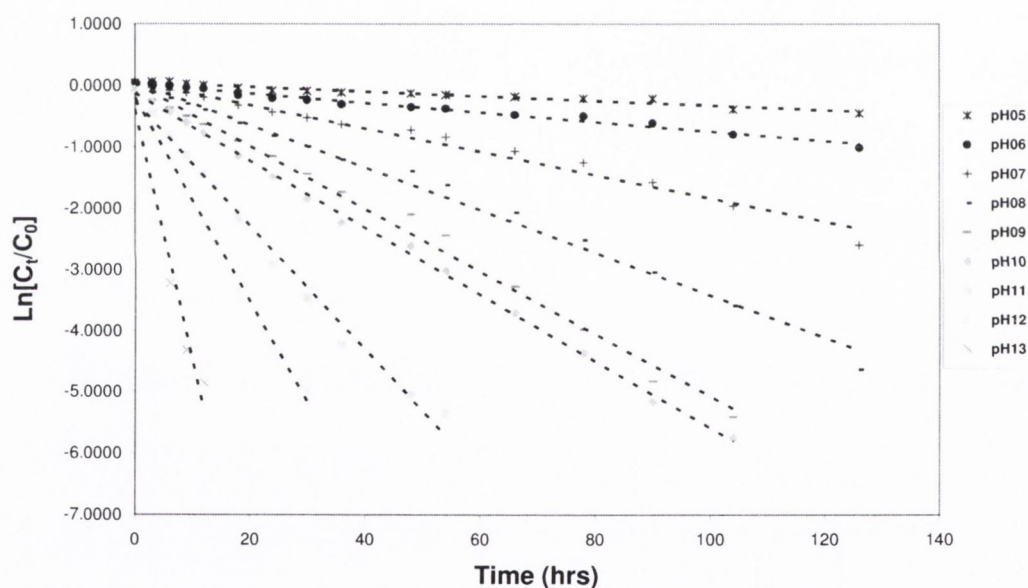


Figure 2.3 First-order plots showing the degradation of bupropion at 333 K in aqueous solution in the pH range 5–13.

2.2.2 Mechanistic interpretation of pH-rate profile

The pH rate profile was fitted using a mechanistic interpretation of pH-rate profiles suggested by Loudon [140]. Before the pH rate profile was mechanistically described a number of assumptions were made.

Only catalysis by protons and hydroxide ions, and not general acid-base catalysis, were considered because the sorts of dependencies of rate on the concentrations of general acids and

bases that one sees are no different in principle from those described for protons and hydroxide ions. Only pseudo-first order reactions were considered, which constitutes the majority of cases. The measure of rate is the observed pseudo first-order rate constant, k_{obs} . The standard way to present pH-rate data is by plotting of k_{obs} or $\log k_{obs}$ vs. pH, which we shall refer to as the pH-rate profile. With these assumptions and conditions in mind the process for understanding the pH-rate behavior of bupropion in aqueous solution breaks down the pH-rate profile into fundamental curves, and analyze these in terms of rate laws and mechanisms. This was done in three steps. Firstly, the pH rate data was obtained, Table 2.2. An empirical rate law was deduced that accurately fitted the data, Equation 2.2.

Equation 2.2 The pH rate equation for bupropion in aqueous solution

$$k_{obs} = c_1[H^+] + \frac{c_2[H^+]}{K_a + [H^+]} + \frac{c_3K_a}{K_a + [H^+]} + \frac{c_4K_w}{[H^+]}$$

where, K_a and K_w are the acid dissociation constant for bupropion and water respectively and $c1$, $c2$, $c3$ and $c4$ are the macro reaction rate constants of the pH rate profile. The macro reaction rate constants are derived from the six empirical reactions that can happen to bupropion in solution, these are visualized in Figure 2.4.

Constants $c1$ and $c4$ are kinetically distinguishable and are equal to the specific hydronium catalysed degradation on the protonated form (A) and hydroxide catalysed degradation on the deprotonated (F) form of bupropion respectively. Constants $c2$ and $c3$ contain contributions from kinetically indistinguishable micro reaction rate constants. The macro reaction rate constant $c2$ combines two micro reaction rate constants that are kinetically indistinguishable. Empirically these are the contribution of hydronium catalysed degradation on the deprotonated form of bupropion (B) and solvent catalysed degradation on the protonated form of bupropion (C). The macro reaction rate constant $c3$ combines two micro reaction rate constants that are also kinetically indistinguishable. These are the contribution of solvent catalysed degradation on the deprotonated form of bupropion (D) and hydroxide ion catalysis on the protonated form of bupropion (E). The magnitude of rate constants at 40, 50 and 60 °C follows $c4 > c3 > c2 > c1$, showing the rate of degradation is strongly influenced not only by hydroxide ion concentration but also from solvent catalysed degradation on the deprotonated form of bupropion. Bupropion degradation was not observed at $\text{pH} \leq 5.0$ at 60°C when it is principally in its protonated form. ($\text{p}K_a_{25^\circ\text{C}} = 7.9$)

The macro reaction rate constants were determined by fitting the k_{obs} values with the model and solving the rate equation using non-linear regression analysis. These rate constants are described in

Table 2.3. Bupropion was shown to be stable over the course of the degradation study below pH 5, and therefore the specific hydronium catalysis rate constant c_1 is many orders of magnitude lower than c_2 , c_3 and c_4 . Therefore c_1 can be assumed to be zero and Equation 2.2 simplifies to Equation 2.3:

Equation 2.3 The simplified pH rate equation for bupropion

$$k_{obs} = \frac{c_2[H^+]}{K_a + [H^+]} + \frac{c_3K_a}{K_a + [H^+]} + \frac{c_4K_w}{[H^+]}$$

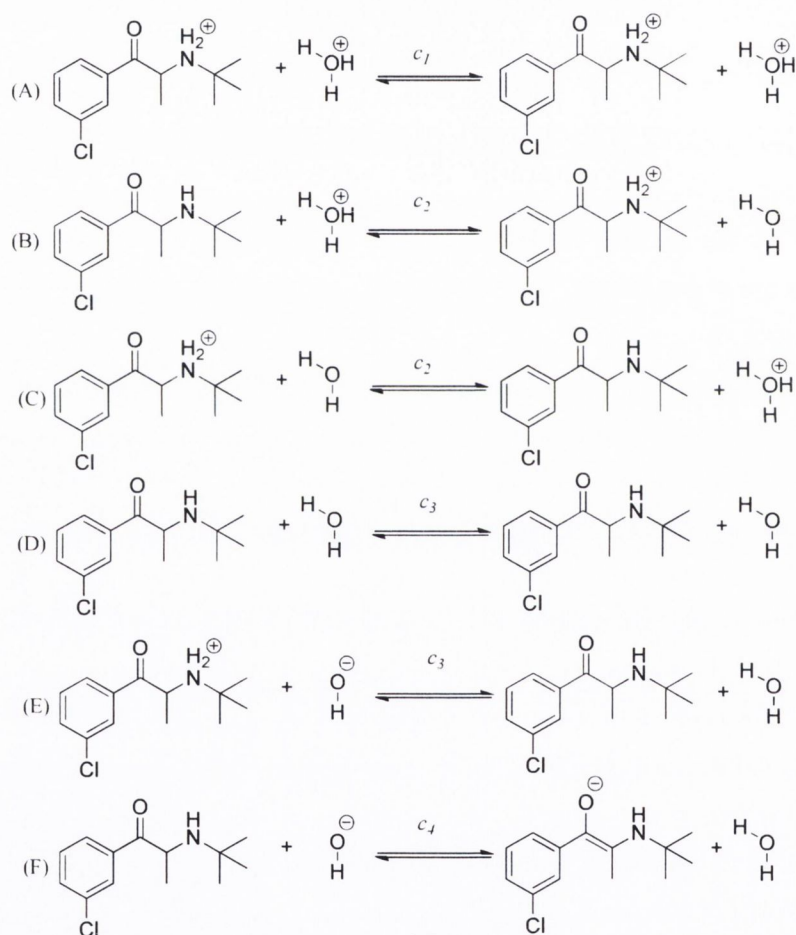


Figure 2.4 The six empirical reactions that contribute to the stability of bupropion in aqueous solution. The first two are the reactions of hydronium ion on the protonated (A) and deprotonated (B) forms of bupropion, followed by the effect of solvent (water) on the protonated (C) and deprotonated (D) forms, followed by the effect of hydroxide ion on the protonated (E) and deprotonated (F) forms.

	40°C	60°C
<i>c1</i>	0.0000	0.0000
<i>c2</i>	0.0000	0.0041
<i>c3</i>	0.0187	0.0596
<i>c4</i>	0.2914	0.2224
<i>K_a</i>	1.26×10^{-8}	1.26×10^{-8}
<i>K_w</i>	2.92×10^{-14}	1.26×10^{-13}

Table 2.3 The macro reaction constants determined by non-linear regression analysis

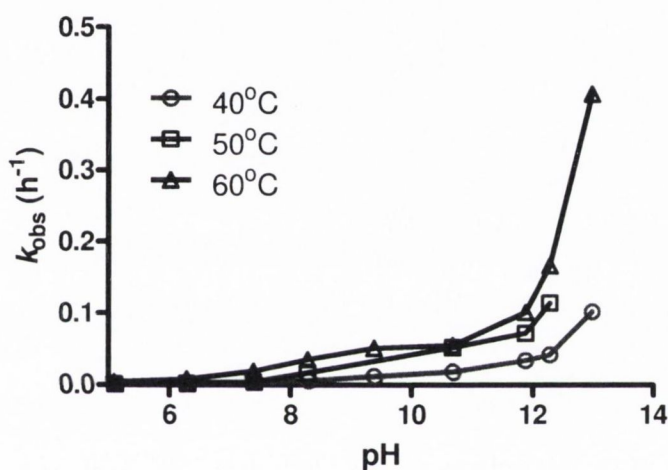


Figure 2.5 pH degradation profile of bupropion at 40, 50 and 60°C, *I* = 0.055

Figure 2.5 presents the pH degradation rate profile of bupropion at 40, 50 and 60°C, ionic strength 0.055. The degradation rate exhibited a marked pH dependence. An inflection point at pH 7.9 corresponds to the bupropion pK_a . At $pH \geq 11$ there was a significant increase in the rate of disappearance. Degradation of bupropion was markedly hydroxide ion dependent. Non-linear regression analysis of the pH degradation profile of bupropion is shown in Figure 2.7.

2.2.3 Effects of temperature and buffer on the stability of bupropion

The effect of temperature on the rate of bupropion degradation was determined at pH 10.7. Bupropion solutions were prepared in the appropriate buffers as described in section 2.4, and incubated at 40, 46, 54 and 60°C. Aliquots were taken at appropriate times depending on the decomposition rate and analyzed immediately for bupropion. The observed first-order degradation rate constants k_{obs} were calculated using Equation 2.1. The Arrhenius factor *A*,

and activation energy E_a for bupropion degradation were determined from a plot of $\ln(k_{obs})$ against $1/T$ (K) according to Equation 2.4 using least squares regression:

Equation 2.4

$$\ln k_{obs} = \ln A - \frac{E_a}{RT}$$

where R is the universal gas constant and T the absolute temperature (K).

Buffer catalysis was investigated by monitoring the amount of bupropion degradation in three different buffers pH 7.4 at 60°C, ionic strength 0.055, 0.275 and 0.55 using the universal buffer system described in Table 1. From the slope of plots of $\ln [C_t/C_0]$ versus time, the rate constant was calculated. A plot of rate constants versus buffer concentration gave a straight line of which extrapolation back to zero gave the buffer-free rate constant.

The effects of different buffers were determined by monitoring the disappearance of bupropion at pH 7.4 at 60°C in different buffer types with fixed ionic strength, 0.055. Four buffer systems were studied; citrate, phosphate, borate and a TRIS buffer system (Figure 2.6). Ionic strength was adjusted with NaCl. The slopes of plots of $\ln [C_t/C_0]$ versus time were determined to establish the effect of buffer anion on degradation of bupropion.

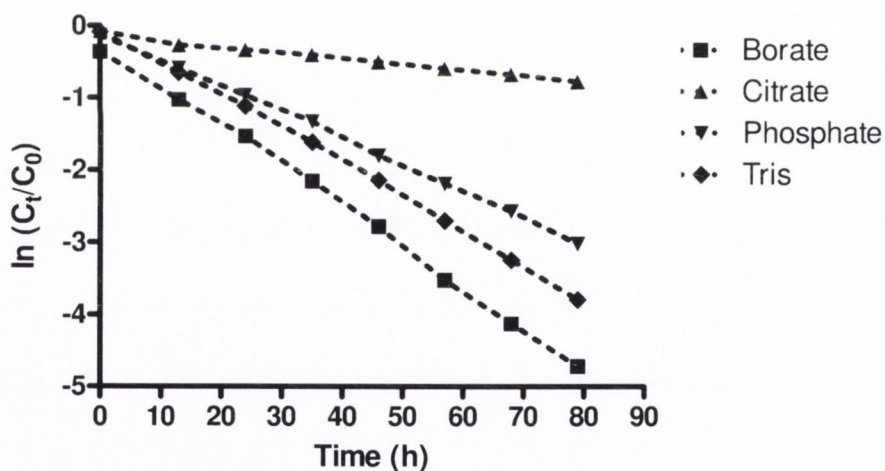


Figure 2.6 The effect of different buffer systems on the rate of degradation of bupropion at pH 7.4 @ 60°C, $I = 0.055$, adjusted with sodium chloride.

The degradation of bupropion was monitored in the temperature range 40–60°C at pH 10.7 and ionic strength, 0.055. This pH was chosen as degradation happened at a sufficiently fast rate to enable analysis over a 24 h period. The rate constant for each temperature was calculated from the slope of the first-order degradation profile (Table 4). When $\ln k$ was plotted against $1/T$ the equation of the line was Equation 2.5:

Equation 2.5

$$\ln k = -6497/R.1/T + \ln 16.69$$

the activation energy E_a for the degradation of bupropion was calculated to be $52.85 \text{ kJ.mol}^{-1}$, the frequency factor A , was found to be $1.78 \times 10^7 \text{ h}^{-1}$.

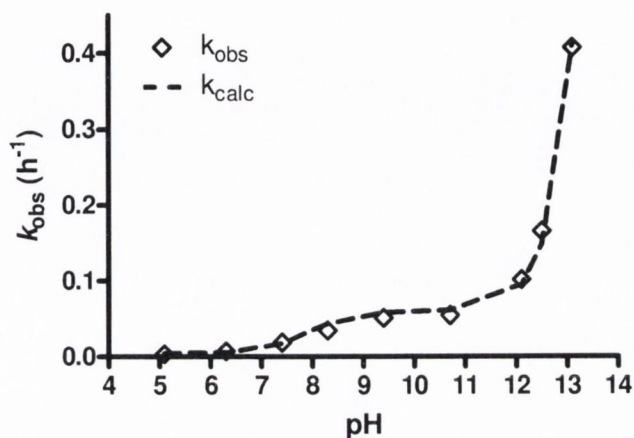
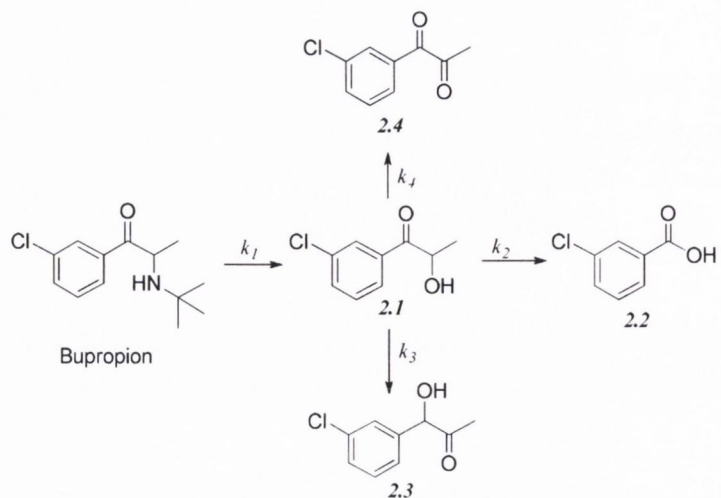


Figure 2.7 Shows the pH degradation profile of bupropion at 60°C , $I = 0.055$. Macro reaction constants have been calculated by non-linear regression analysis. The fitted line was constructed using Equation 2.3 and the data appearing in Table 2.2 and Table 2.3.

2.2.4 Identification of bupropion degradants and mechanistic proposal

Degradation products of bupropion were identified by matching the retention time and photodiode array UV spectra of eluted peaks from degraded samples with those of external standards run under similar conditions. Four main degradants were identified as **2.2**, **2.4**, **2.3** and **2.1** (Scheme 2.1). Bupropion related compounds **2.3**, **2.1** and **2.4** are poorly ionized by +ESI due to loss of the amino functionality. These degradants were all seen at $\text{pH} > 5$ but above $\text{pH} 10$ only *m*-chlorobenzoic acid **2.2** was seen at significant levels. Figure 2.8 shows the concentration versus time profiles for bupropion and its degradants at different pH values.



Scheme 2.1 Proposed pathway for base catalyzed degradation of bupropion in aqueous solution. 2.1 = 1-(3-chlorophenyl)-2-hydroxy-1-propanone, 2.2 = 3-chlorobenzoic acid, 2.3 = 1-(3-chlorophenyl)-1-hydroxy-2-propanone, 2.4 = 1-(3-chlorophenyl)-1,2-propanedione.

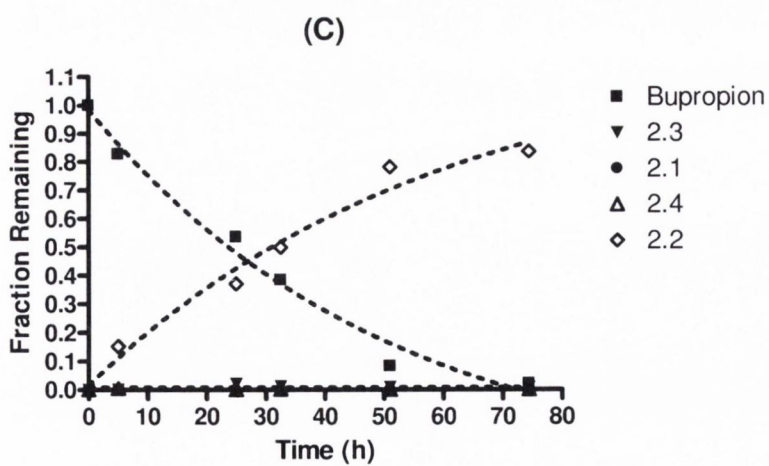
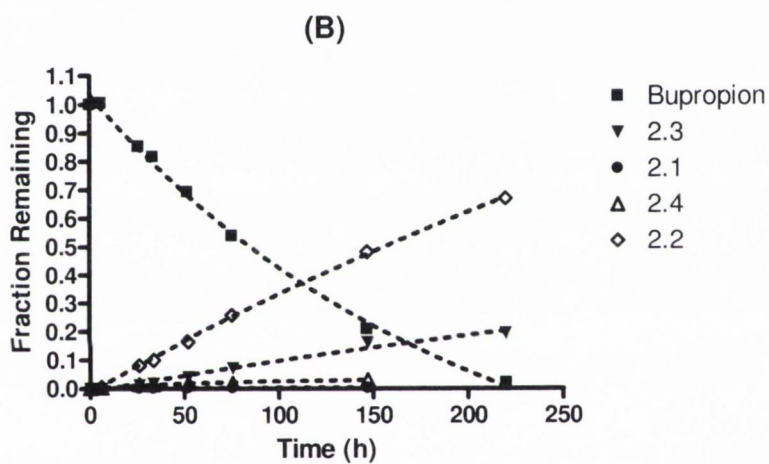
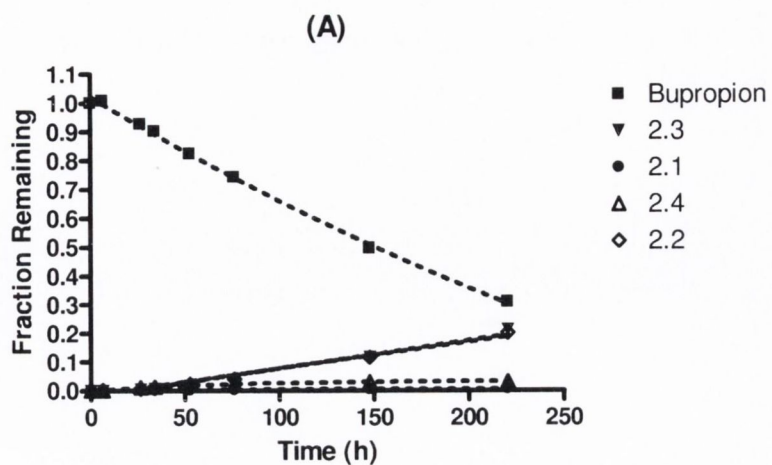


Figure 2.8 Shows the time course profile for degradation of bupropion at (A) pH 7.6, (B) pH 8.7 and (C) pH 10.9, 50°C, I = 0.12.

A proposed degradation pathway of bupropion is presented in Scheme 2.1. The mathematical model that best described the mechanism of degradation follows consecutive and parallel reactions. Degradation of bupropion was strongly pH dependent, and below pH 5 bupropion was protonated and stable. Above pH 5 and approaching its *pKa* bupropion becomes increasingly deprotonated and suffers from water catalysed and hydroxide catalysed degradation. This was evident from the pH rate profile of bupropion. Under these conditions the proposed reaction (Scheme 2.1) is kinetically possible.

Equation 2.6 The rate equation for decomposition of bupropion

$$\frac{d[bup]}{dt} = -k_1[bup]$$

Equation 2.7

$$[bupropion] = [bup]_0 e^{-k_1 t}$$

Bupropion's rate constant of decomposition was calculated by fitting a first-order plot using non-linear regression analysis, Equation 2.6. The first product of bupropion degradation at high pH is compound **2.1** formed from loss of the t-butylamine group during hydrolysis. The concentration of **2.1** during the course of the hydrolysis remained below 1 % of the total degradation products of bupropion. The rate of decomposition of **2.1** was faster than the rate of formation of **2.1** and therefore can be assumed at steady state throughout the time course of the reaction. The hydrolysis and oxidation products of **2.1** are the major apparent degradation products of bupropion. These are the two oxidation products, **2.2** and **2.4** and the tautomeric pair **2.3** and **2.1**. Equation 2.8-Equation 2.10 were used to calculate the rate constants of these parallel reactions. The experimental data fitted with these equations using non-linear regression analysis allowed calculation of the rate constants.

Equation 2.8 The rate equation for [2.2]

$$[2.2] = [2.2]_0 + \frac{[bup]_0 k_2 (1 - e^{-k_1 t})}{k_1}$$

Equation 2.9 The rate equation for [2.3]

$$[2.3] = [2.3]_0 + \frac{[bup]_0 k_3 (1 - e^{-k_1 t})}{k_1}$$

Equation 2.10 The rate equation for [2.4]

$$[2.4] = [2.4]_0 + \frac{[bup]_0 k_4 (1 - e^{-k_1 t})}{k_1}$$

The rate constants calculated at pH 8.7, 50°C, I = 0.12 were 0.0050, 0.0045, 0.00138 and 0.00023 h⁻¹ for k_1 , k_2 , k_3 and k_4 respectively.

The rate constants calculated at pH 7.6, 50°C, I = 0.12 were 0.0046, 0.0012, 0.0012 and 0.00028 h⁻¹ for k_1 , k_2 , k_3 and k_4 respectively.

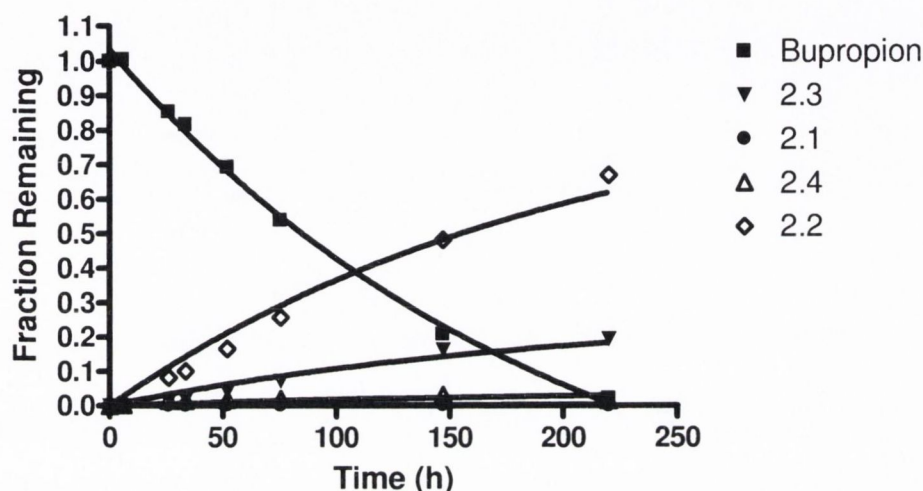


Figure 2.9 Shows actual data pH 8.7, 50°C, I = 0.12. The solid lines were constructed using Equation 2.8-Equation 2.10 with the calculated k_{obs} values.

2.2.5 Bupropion as a pro-oxidant

Bupropion shares its structural similarities with other endogenous α -aminoketones such as 5-aminolevulinic acid (ALA) and aminoacetone (AA). These α -aminoketones are well known to be pro-oxidizing and have been linked to toxicological effects [141]. Endogenous and xenobiotic polyphenols (e.g., homogentisic acid, divicine, hydroanthraquinones, 6-hydroxydopamine) and the enol form of carbonyl metabolites (e.g., ALA, AA) belong to organic functions expected to promptly donate one electron to dioxygen, especially in slightly alkaline medium containing phosphate ions [142]. Phosphate ions have been shown to catalyze carbonyl enolization, thus favoring substrate electron transfer to dioxygen [143]. Among other characteristics, α -aminoketones differ from primary amines for their property of undergoing rapid enolization in physiological pH and, in an aerated medium, subsequent oxidation by molecular oxygen via superoxide radical intermediate, forming α -dicarbonyls and H₂O₂ (Figure 2.10) [142].

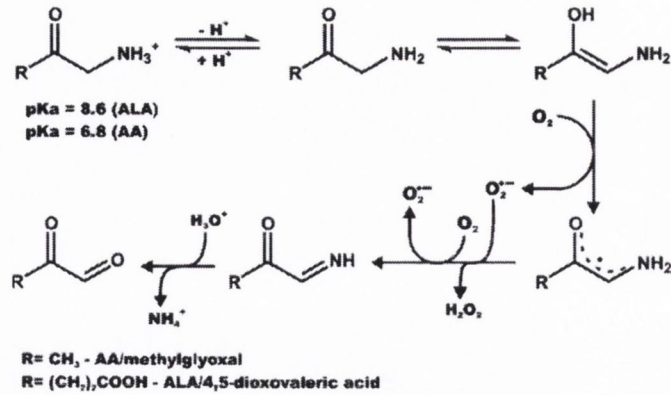


Figure 2.10 Non-enzymatic aerobic oxidation of α -aminoketones. Adapted from Bechara [141].

The end product of α -aminoketone oxidation, α -dicarbonyl compounds, it has been hypothesized that they could participate in deleterious biological processes, particularly in aging, based on their electronic configuration and high reactivity [144]. For example, formation of Schiff bonds between each of the carbonyl groups of the α -dicarbonylic compound and the amine group of proteins may cause protein aggregation and denaturation by cross-linking (Prot-N=CR-CR=N-Prot). Another important biological consequence of Schiff's reaction is the formation of fluorescent adducts called Advanced Glycation End products (AGEs), or Maillard products, such as pentosidines. Pentosidines are putative aging markers formed by cross-linking between lysine and arginine protein residues and oxidized pentose and other sugars. The AGEs are known for their ability to attach to specific cellular receptors, triggering various events such as the induction of cytokines and growth factors, oxidative stress and the regulation of cellular adhesion.

The reaction of aerobic oxidation on α -aminoketones has been shown to be catalysed by Fe(II) complexes which is particularly worrying considered the abundance of Fe(II)-heme *in vivo* (Figure 2.11) [141].

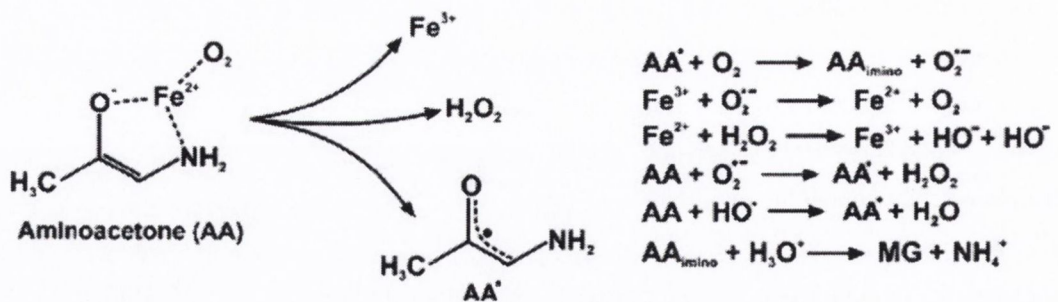


Figure 2.11 An example of Fe(II) catalysed aerobic oxidation of the α -aminoketone, aminoacetone which the end product of oxidation is the dicarbonyl MG (Methylglyoxal). Adapted from [141].

2.2.6 Hydroxyketones as inhibitors of urease

Two of bupropion's degradants are α -hydroxyketones. Similar to α -aminoketones these type compounds undergo enolization [145] and subsequent oxidation by dissolved molecular oxygen in slightly alkaline buffers to yield the α -dicarbonyl, amine ions and H_2O_2 [146]. This reaction was shown to be efficiently catalysed by iron complexes.

Urease (urea amidohydrolase; E.C.3.5.1.5) is a nickel containing enzyme that catalyzes the hydrolysis of urea to produce ammonia and carbamate [147]. The study of urease inhibition has medical, environmental and agronomic significance. For example, urease serves as a virulence factor in pathogens that are responsible for the development of kidney stones, pyelonephritis, peptic ulcers, and other medical complications [148]. Current efforts are focused on the discovery of novel urease inhibitors against *H. pylori* urease. Therefore, urease inhibitors have recently attracted much attention as potential new anti-ulcer drugs. Tanaka *et al.* have recently evaluated a variety of α -hydroxyketones and α -diketones for their effect on the jack bean urease [149]. They demonstrated that some α -hydroxyketone derivatives show urease inhibitory activity, possibly by binding to cysteinyl residues in the active site. This has implications for the pharmacological activity of these bupropion degradants. Although Tanaka *et al.* did not look specifically at these degradants, they are likely to have some pharmacological effect.

Aromatic α -hydroxyketones have also been shown to be easily oxidized by dioxygen in the presence of catalytic amounts of metals in solution to the α -dicarbonyl product [150].

2.2.7 Known pharmacological effects of the degradants of bupropion

The loss of the amino functionality during degradation is likely to render the degradants neuropharmacologically inactive.

The most polar and prominent degradant **2.2**, is likely the least problematic as this compound is reported to be easily metabolized and excreted in the urine as *m*-chlorhippuric acid [151]. However, high levels of **2.2** have been reported to inhibit thiopurine methyltransferase (TMPT)[152]. Ames *et al.* studied twenty-seven substituted benzoic acids and have been as inhibitors of partially purified human renal thiopurine methyltransferase. Amongst the benzoic acid analogues was 3-chlorobenzoic acid. They observed an IC_{50} value of 3.71 for the 3-chlorobenzoic acid degradant of bupropion. TMPT is best known for its role in the metabolism of the thiopurine drugs such as azathioprine, 6-mercaptopurine and 6-thioguanine.

Toxicological and pharmacological data on degradants **2.1**, **2.3** and the diketone **2.4** is absent. The latter is likely to be chemically active towards formulation components and *in vivo* towards proteins such as carboxylesterases (CEs) [153]. Although there is no toxicological data on the

chlorinated dicarbonyl degradant of bupropion **2.4**, Wadkins *et al.* have identified a class of compounds based on the dicarbonyl benzil (1,2-diphenylethane-1,2-dione) that are potent CE inhibitors, with K_i values in the low nanomolar range. The compound most structurally similar to **2.4** in their study was shown to have inhibition constants in the low micromolar range. Therefore **2.4** is likely to be pharmacologically active at inhibiting CE's.

CE's are involved in the detoxification of xenobiotics in both prokaryotes and eukaryotes. Bupropion is rapidly and extensively metabolised *in vivo* but the high lipophilicity of some of its degradants may have systemic effects due to accumulation in lipophilic tissues. Its metabolites contribute significantly to its pharmacological and toxicological profile. The rate data at pH 7.4 do not indicate that its chemical reactivity *in vivo* is likely to affect its pharmacological profile.

2.2.8 Addressing stability with a prodrug

There are two main processes leading to degradation of bupropion. The first is base-catalyzed hydrolysis of the α -hydroxyimine tautomer to the α -hydroxyketone (Figure 2.12). The second is oxidation to its main degradant 3-chlorobenzoic acid.

Bupropion when deprotonated will tautomerize into its enol form. Once in the enol/enamine configuration bupropion will tautomerize into the imine form which is easily hydrolysed to the α -hydroxyketone and t-butylamine. The reason for the enamine/imine tautomerism is the proton on the amino group. α -Aminoketones that are secondary amines will tautomerize to the imine under catalytic conditions. If the amino group is transformed into a tertiary amine this cannot occur. Therefore by derivatizing bupropion by alkylation at the amine will remove the liability of imine formation and hence improve the stability profile at higher pH. The tertiary α -aminoketone can still tautomerize to the enol form but not to the imine form (Figure 2.13).

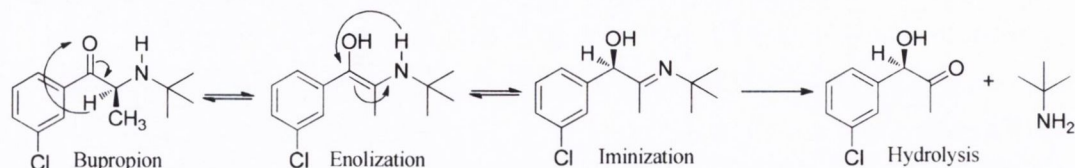


Figure 2.12 Base-catalyzed hydrolysis of bupropion

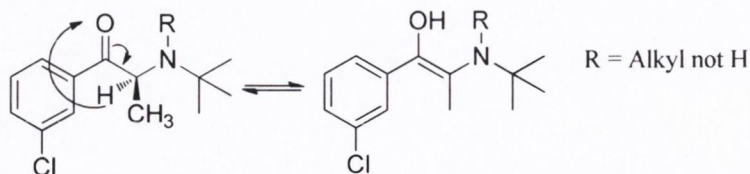


Figure 2.13 Removing the liability of imine formation by alkylation at the amine of bupropion

The second process leading to the degradation of bupropion in aqueous solution is by oxidation of bupropion directly and oxidation of its degradants **2.1** and **2.3** to the α -dicarbonyl **2.4** which is hydrolysed to the most abundant degradant 3-chlorobenzoic acid **2.2** (

Figure 2.14). Therefore oxidation is a major degradation pathway for bupropion in aqueous solution.

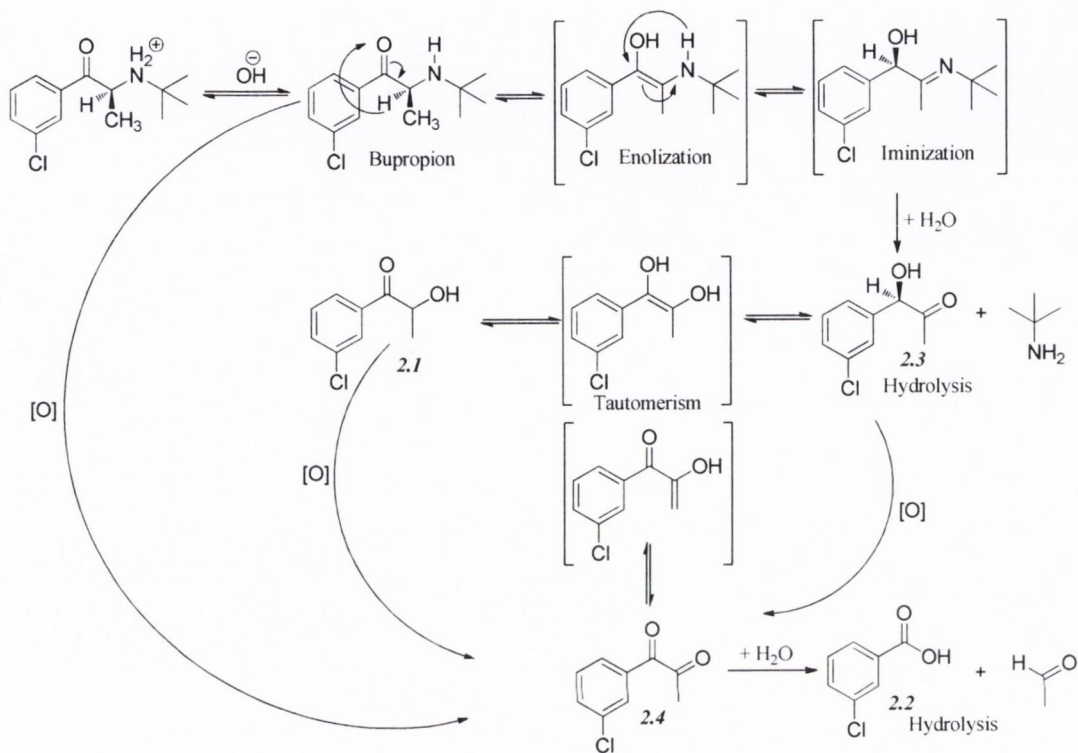


Figure 2.14 Degradation of bupropion, showing oxidation pathways. Compounds in brackets are theoretical and have not been isolated.

Bupropion is susceptible to oxidation via its enolization as described in 2.2.5. *N*-alkylation of bupropion (Figure 2.13) would give the tertiary aminoalcohol but this would still be prone to enolization and therefore would still be susceptible to oxidative degradation. One method to remove the potential for enolization would be to convert the carbonyl in bupropion to a non-enolizable group that can be transformed back to the ketone *in vivo*. A good example is the hydroxyimine group. The potential for intramolecular hydrogen bonding would also increase the stability of the molecule.

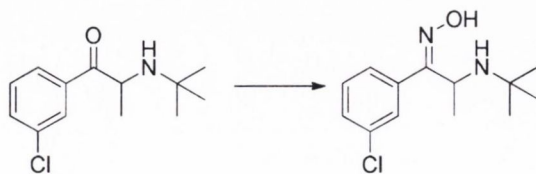


Figure 2.15 Removing the liability of enol formation by oxime conversion

2.3 Conclusion

Bupropion undergoes degradation in aqueous solution in a pH dependent manner. Its most prominent degradation pathway involves hydroxide ion catalysis of the free base form. Degradation involves loss of the t-butylamino group and the degradants are therefore likely to be neuropharmacologically inactive. The effect of ionic strength, buffer type and temperature on the kinetics were also characterised.

The poor stability profile of bupropion above pH 5 has implications for its formulation in drug delivery systems, its distribution *in vivo* and its analysis and storage in assay systems. The data shows that careful buffering below pH 5 during processing and formulation is needed in order to have the most stable product containing bupropion. There is also a need during sample preparation and storage to consider appropriate solvents and buffers which again keep the pH low. This stability issue could potentially be addressed by using a prodrug strategy.

2.4 Experimental

2.4.1 Chemicals

Methanol, acetonitrile and water were supplied by Fisher Scientific Ireland (LC-MS grade). Ammonium hydroxide solution (30% as NH_3), glacial acetic acid, formic acid, boric acid, citric acid monohydrate, sodium chloride and tripotassium phosphate were supplied by Sigma-Aldrich Ireland (reagent grade). Bupropion hydrobromide and related degradants were supplied as a gift from Biovail Technologies Ireland Ltd.

2.4.2 Instrumentation

A stability indicating HPLC-UV assay was used to monitor degradants of bupropion. The HPLC system consisted of a Waters Alliance 2695 separations module connected to a Waters 2996 Photodiode Array detector. The column was a Waters XBridge C18 250 mm \times 4.6 mm, 5 μm fitted with a Waters XBridge C18 guard column heated at 50°C. Mobile phase A was pH 10.0 ammonium acetate buffer (1.27 M)/water/acetonitrile, 10:80:10, mobile phase B was pH 10.0 ammonium acetate buffer (1.27 M)/water/acetonitrile, 10:20:70. Injection volume was 20 μL , flow rate 1.5 mL/min. Gradient; 0-42% B over 5 min, hold for 10 min, 42-100% B over 10 min, hold for 5 min and equilibrate to starting gradient. The retention time of bupropion standard was approximately 23 min. Detection wavelength 239 nm. This method was demonstrated to be linear over a working range of 0.01-0.50 mg/mL bupropion hydrobromide.

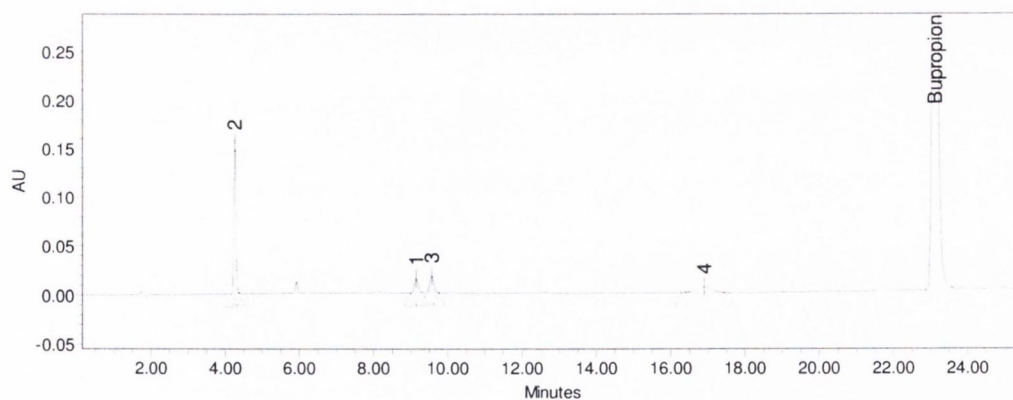


Figure 2.16 A typical LCUV chromatogram of bupropion hydrolysis at pH 8.7, 50°C, $I = 0.12$, $T = 144$ h. 2.1 = 1-(3-Chlorophenyl)-2-hydroxy-1-propanone, 2.2 = 3-Chlorobenzoic acid, 2.3 = 1-(3-Chlorophenyl)-1-hydroxy-2-propanone, 2.4 = 1-(3-Chlorophenyl)-1,2-propanedione.

Degradation kinetics and mass spectrometric measurements were carried out on a Thermo Accela Liquid chromatograph. The detector was a Thermo LTQ-XL-Orbitrap Discovery mass spectrometer. The column used for chromatographic separation was a Waters Xbridge C18, 2.1 x 50 mm 2.5 μm at 20°C. Mobile Phase A: 10:40:50, 0.5% Ammonium hydroxide solution in water, adjusted to pH 10.0 with formic acid: water: methanol. Mobile Phase B: 10:90, 0.5% Ammonium hydroxide solution in water, adjusted pH 10.0 with formic acid: methanol. Flow rate: 100 $\mu\text{L}/\text{min}$, Injection volume: 10 μL , run time: 15 min. Gradient, 0% B to 100% B over 8.00 min, hold until 12.00 min. 0% B at 12.01 min and equilibrate for 3 min. This method was validated as appropriate according to ICHQ2R and demonstrated to be linear over a working range of 1-250 ng/mL bupropion.

The LTQ-XL ion trap mass spectrometer was coupled to the Accela LC system via an electrospray ionization (ESI) probe. The capillary temperature was maintained at 400°C, sheath gas flow rate 50 arbitrary units, auxiliary gas flow rate 5 arbitrary units, sweep gas flow rate 0 arbitrary units, source voltage 3.20 kV, source current 100 μA , capillary voltage 43.00 V and tube lens 100 V. Bupropion was detected in positive ion mode using selected ion monitoring (SIM). Bupropion SIM 184, $(\text{M}+\text{H})^+ = 240$, retention time = 9.4 min. The optimum detector conditions were found by tuning the instrument to the highest sensitivity for bupropion most abundant fragment ion at 184 (m/z).

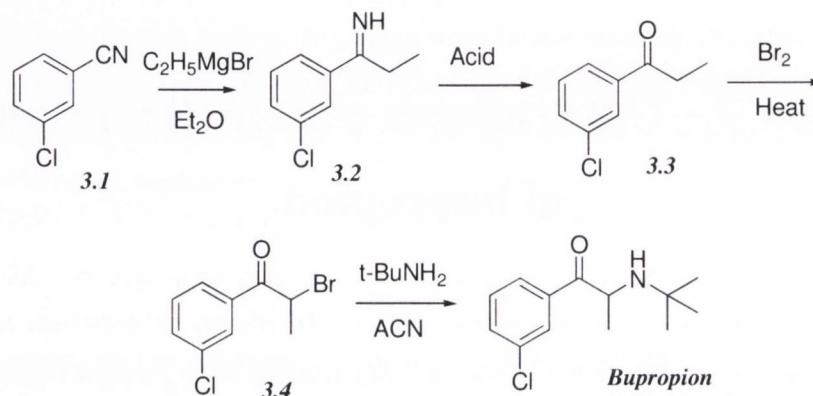
Chapter 3 - The synthesis of potential prodrugs of bupropion

This chapter begins with an overview of the synthesis of bupropion and the chemistry around this aminoketone. There are two functional groups that can be exploited as prodrug functional groups and each one is introduced with the potential prodrugs that can be derivatized from each one. Multistep prodrugs are introduced with a discussion on how this can be applied to bupropion. The methods used to synthesize each prodrug type are discussed with particular emphasis on the characterization and identification of each potential prodrug.

3 The synthesis of potential prodrugs of bupropion

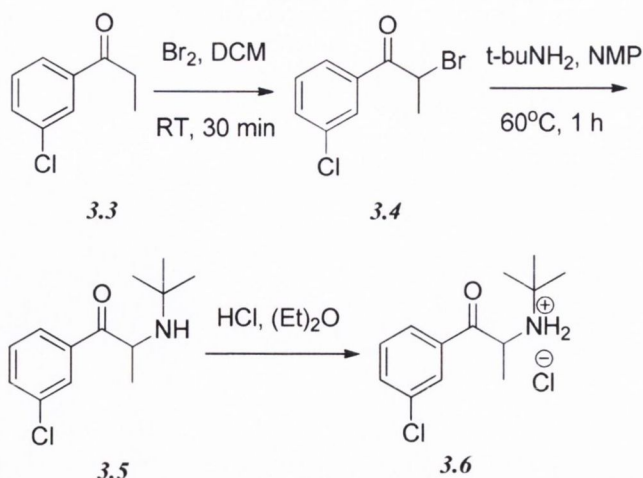
3.1 Brief overview of the commercial synthesis of bupropion

The first industrial synthesis of bupropion was described by Mehta in 1975 [3]. It was prepared in three steps from *meta*-chloro benzonitrile **3.1** (Scheme 1.1).



Scheme 3.1 Synthesis of bupropion via the method described by Mehta.

Our laboratory synthesis of bupropion mirrored the same route as that of Mehta, but is shorter as the propiophenone **3.3** is now commercially available. Treatment of 1-(3-chlorophenyl)propan-1-one **3.3** with bromine at room temperature in dry dichloromethane yielded the crude brominated ketone **3.4**. Removal of excess bromine and dichloromethane *in vacuo* afforded the bromo derivative which was then used directly in the next stage of the synthesis. Coupling of *t*-butylamine to **3.4** in *N*-methylpyrrolidone with gentle heating gave bupropion **3.5** in almost quantitative yield. After work up and purification, the free base was conveniently converted to the hydrochloride salt **3.6** by bubbling HCl gas through the freebase in a diethyl ether solution (Scheme 3.2).



Scheme 3.2 Synthesis of the hydrochloride salt of bupropion.

The ^1H NMR spectrum of bupropion is shown in Figure 3.1. There is one large singlet at 1.16 ppm which signifies the nine chemically equivalent protons associated with the *t*-butyl group. The three methyl protons resonate as a doublet at 1.34 ppm while the quartet at 4.60 ppm represents the methine proton. The broad peak at 5.0 ppm can be attributed to the NH signal.

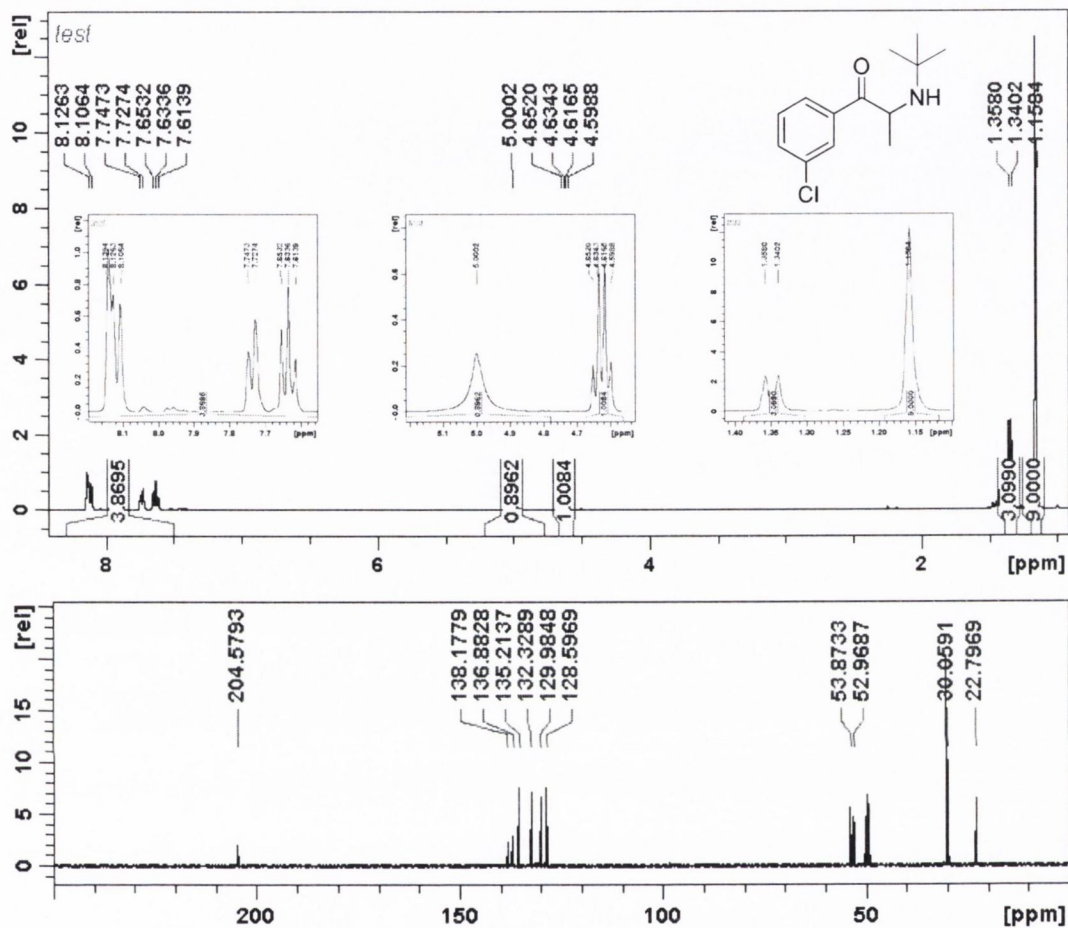


Figure 3.1 ^1H NMR and ^{13}C NMR spectra of bupropion hydrochloride 3.6 in deuterated methanol

The mass spectrum of bupropion (Figure 3.2) contains two main fragments, 184.0526 and 166.0420 amu. The first being formed from neutral loss of the *t*-butyl group and then subsequent dehydration to give the ion at 166.0420 amu. The most abundant ion is the molecular ion ($\text{M}+\text{H}^+$) at 240.1153 amu, illustrated in Figure 3.2. The loss of *t*-butyl (-56 amu), which is seen for most prodrugs of bupropion is a common neutral loss for these *t*-butylamines.

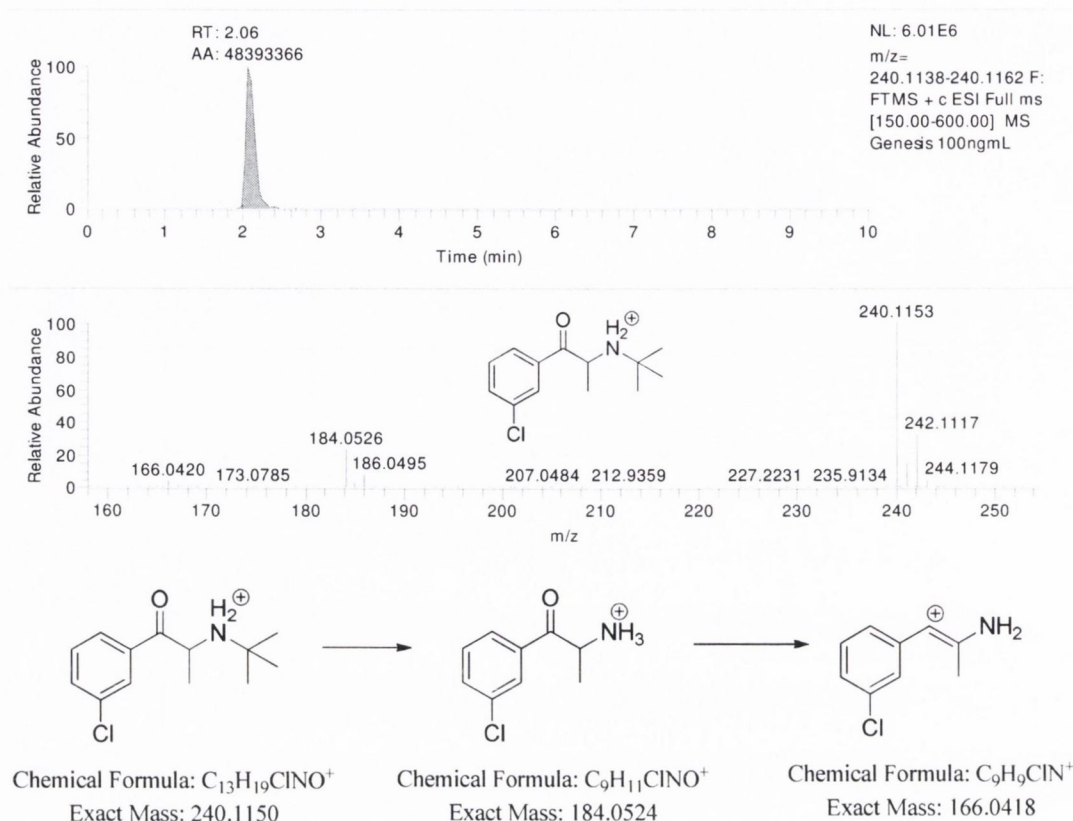


Figure 3.2 A high resolution LC-MS chromatogram/spectrum of bupropion 3.5 in +ESI mode and its proposed fragmentation pattern

3.2 Overview of the chemistry of bupropion

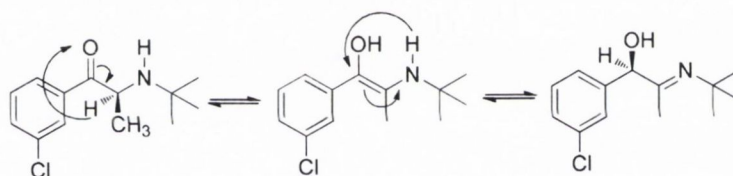
From our own published work and that outlined in Chapter 2, it was shown that bupropion is susceptible to base catalyzed hydrolysis and oxidation to four main degradation products [154] under aqueous conditions. Synthetic methods that utilised non-aqueous alkaline conditions also caused extensive degradation. At or above the pK_a of bupropion and especially at elevated temperatures, bupropion was not stable. Under acidic conditions, the opposite is true. When bupropion is ionised (protonated), that is at least two pK_a units below its pK_a , it is stable. The aqueous stability study demonstrated stability at elevated temperatures between pH 1-5. This was also true under non aqueous conditions especially during the synthesis of the protected ketal of bupropion, the mixture was refluxed for over 60 h at temperatures above 200 °C under strongly acidic catalytic conditions. Bupropion remained intact for the course of the reaction and no degradation products were detected by TLC.

Despite its many therapeutic applications there is very little work published on prodrug forms of bupropion or its active metabolite hydroxybupropion. The primary aim of the work described in this Chapter is to devise suitable prodrug forms of bupropion by exploiting in particular its keto

and amino functionalities. Although the keto group of bupropion can undergo the general reactions that typical aldehydes and ketones undergo, the neighbouring amino group and chlorine in the *meta*-position on the aromatic ring has an effect on the reactivity of the keto carbon due to their electronic properties. The diminished reactivity of chloro-substituted ketones has been studied before by Kalendra and Sickles [155].

The *t*-butyl substituent on the amino group of bupropion renders it less nucleophilic than would be expected of a typical secondary amine due to steric factors and as we shall see later does not readily undergo typical reactions of secondary amines. The second factor that may affect the nucleophilicity of the amine in bupropion is the electron withdrawing effects of the neighbouring carbonyl group.

In our hands, one method to improve the nucleophilicity of the amine of bupropion is to use alkaline conditions during substitution reactions. This has the effect of forming the enamine form of bupropion which is more nucleophilic than the keto form of bupropion. However, the drawback of this enhanced nucleophilicity in bupropion's case is its inherent instability under alkaline conditions. As depicted in Scheme 3.3, the enamine form of bupropion has the ability to tautomerize to the imine form and result in hydrolysis to the corresponding α -hydroxyketone derivative of bupropion.



Scheme 3.3 Keto-enol/enamine-imine tautomerism of bupropion

3.3 Prodrugs of bupropion

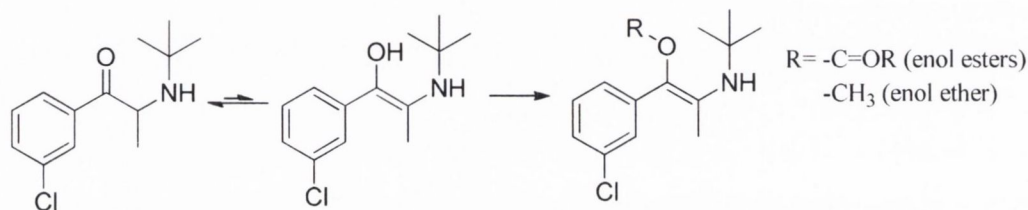
3.3.1 Prodrug formation at the amine site on bupropion

The main types of prodrugs associated with the amino group of known therapeutic agents are their carbamate and amide derivatives. Amides and carbamates prodrugs can be activated by the action of hydrolases. With bupropion, it is possible to acylate the amine or when in the enol form, its hydroxy group. Although not widely used as a prodrug strategy, it is also possible to effect an *N*-dealkylation step *in vivo*. With bupropion the amino group in principle can be readily alkylated with for example methyl and benzyl groups. Increasing bupropions' lipophilic character may ultimately result in higher amounts of the drug permeating across the blood brain barrier to the site of action. Typically enzyme types like the flavin containing mono-oxygenases (FMO's) and cytochrome P450 oxidases, which are known to be present in brain tissue, have the ability to dealkylate tertiary lipophilic amines to the more hydrophilic secondary or primary parent amine.

3.3.2 Prodrug formation at the keto site on bupropion

With the keto-group the most appropriate prodrug derivatives are its oxime and imine derivatives. These are prone to hydrolysis by non-enzymatic mechanisms but have also been known to be transformed by endogenous enzymes back to the parent ketone.

Perhaps a less obvious functional group that can be derivatized in bupropion lies from the potential that bupropion is enolizable (Scheme 3.4). Therefore the proton on the enol alcohol could be alkylated or esterified. Enol ethers and enol esters have been shown to be susceptible to enzymatic systems *in vivo*. *O*-dealkylation or *O*-de-esterification of a prodrug is potentially possible, giving back the enol that would tautomerize back to the ketone.



Scheme 3.4 Prodrugs associated with the enolization of bupropion.

3.3.3 Double prodrug forms of bupropion

Double or multistep prodrugs are ones that contain two or more functional groups that after metabolism or hydrolysis *in vivo* will release the active compound. One such example of this is Ximelagatran [156, 157], a double prodrug of melagatran. Melagatran is an anticoagulant which was expected to replace warfarin and aspirin in some therapeutic settings, such as deep vein thrombosis, prevention of secondary venous thromboembolism and complications of atrial fibrillation such as stroke. It is the prodrug that is dealkylated and dehydroxylated mainly in the liver and acts as a direct thrombin inhibitor.

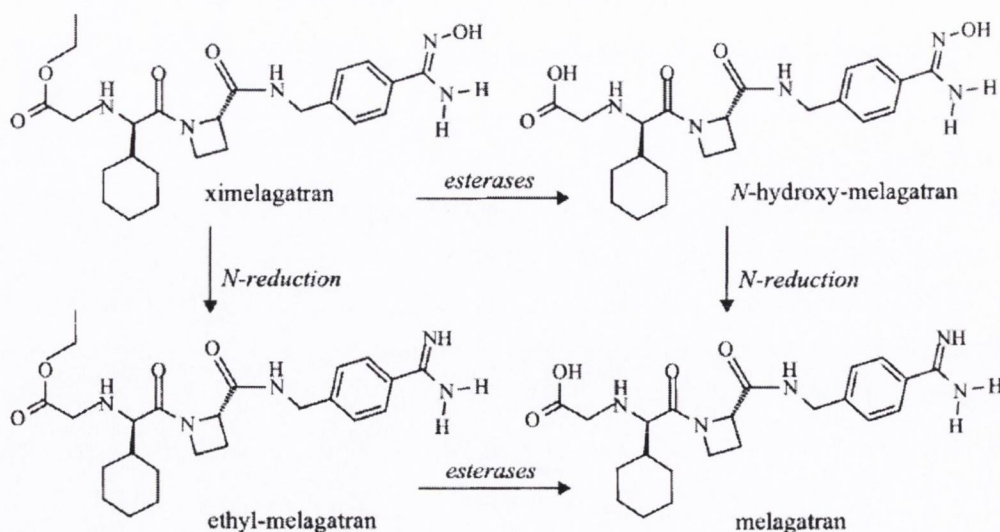
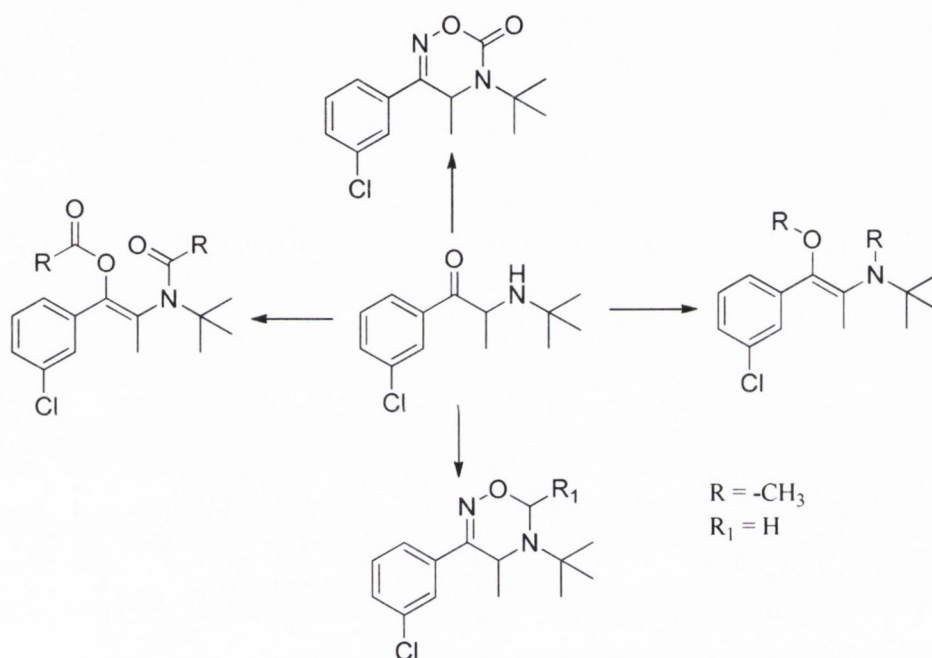


Figure 3.3 The multistep prodrug ximelagatran. Adapted from Clement [158]

The potential for more than one prodrug derivatization of the functional groups of bupropion could lead to a potential double prodrug of bupropion. Derivatization of both the keto- and amino-group in the same molecular structure, would lead to multistep prodrug compounds such as those presented in Scheme 3.5. A double prodrug may have higher lipophilicity and should traverse membranes such as the intestinal mucosa and blood brain barrier more efficiently than a less lipophilic drug.

Conversely, the increased lipophilicity would increase the drugs probability to metabolic conversion to a more hydrophilic metabolite which may render it inactive. It is also more difficult to predict the metabolic transformations and statistically more difficult to get back the parent compound from a double or multistep prodrug. Double prodrugs can be broken down in the body sequentially or in tandem either hydrolytically or enzymatically or both.



Scheme 3.5 Potential double prodrugs of bupropion

3.3.4 Carbamate type prodrugs of bupropion

Carbamates are widely used as prodrugs for alcohols and amines. The antihistamine agent loratadine, is one such example which undergoes a CYP450-mediated conversion *in vivo* to desloratadine [159]. Although hydrolysis, followed by spontaneous decarboxylation, is the likely mechanism leading to desloratadine, there is evidence that, in human liver microsomes its formation is catalyzed primarily by the CYP3A4 and CYP2D6 isozymes (Figure 3.4). Carbamates have also been shown to be hydrolysed by hydrolase enzymes [160].

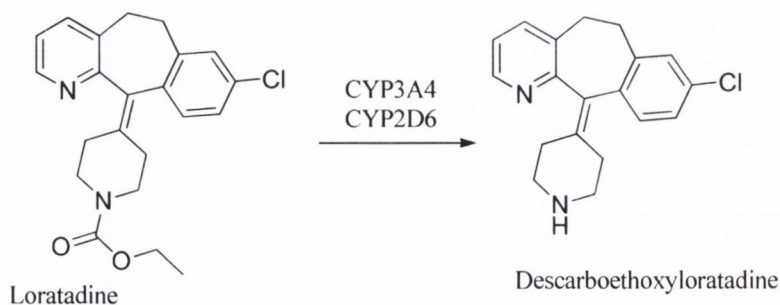
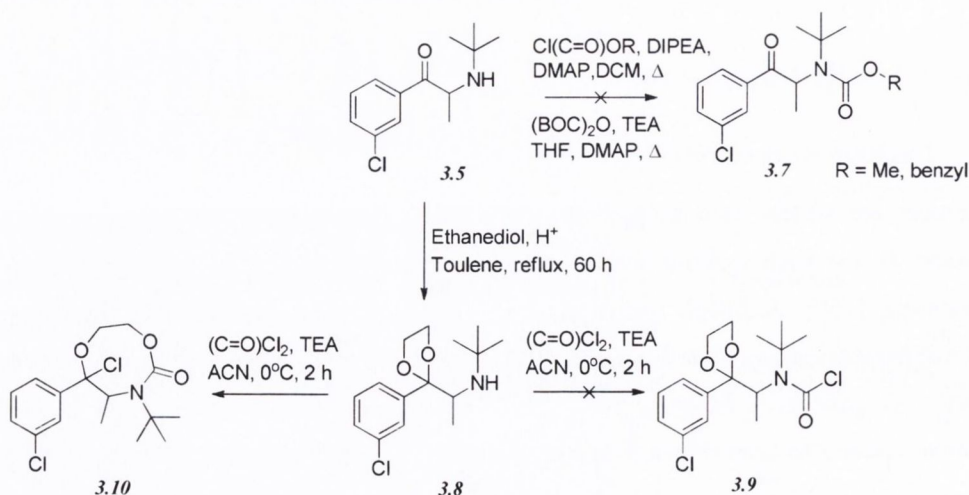


Figure 3.4 The carbamate prodrug loratadine. Adapted from Zhang [161]

3.3.4.1 Carbamates via derivatization of bupropion directly

Carbamates are generally easily prepared by treatment of the primary or secondary amine with the corresponding chloroformate in the presence of a tertiary base [162]. Attempts were made to furnish carbamate derivatives of bupropion **3.5** by treating it with methyl and benzyl chloroformates in the presence of diisopropylethylamine, *N,N*-dimethylaminopyridine as catalyst in dry DCM at room temperature as well as by conducting the reaction at elevated temperatures or by using microwave conditions but all were unsuccessful (Scheme 3.6). The reagent di-*tert*-butyl-dicarbonate was also used under similar conventional and microwave conditions but again there was no reaction. The inability of the amino group of bupropion to react with either chloroformates or di-*tert*-butyl-dicarbonate may be attributed to the reduced nucleophilicity of this particular amine. In an effort to increase the reactivity of the amine in bupropion, the neighbouring carbonyl was converted to the ketal **3.8**. This reaction was difficult to initiate and reproduce. The strictly anhydrous conditions of the reaction, the very high temperatures used and constant replacement of reagents over time was difficult to reproduce. This reaction was eventually optimized under Dean Stark conditions using sulphuric acid as catalyst, toluene as solvent and ethylene glycol as the ketal reagent.



Scheme 3.6 Attempted synthesis of a carbamate type potential prodrug of bupropion.

The successful synthesis of **3.8** was confirmed by ^1H NMR by the appearance of two multiplets at 3.72–4.10 ppm each representing the two methylene protons on the dioxolane ring (Figure 3.5) as well as the disappearance of the carbonyl signal and the presence of the two methylene signals at 64.3 and 64.5 ppm in the ^{13}C spectrum of the ketal **3.8**.

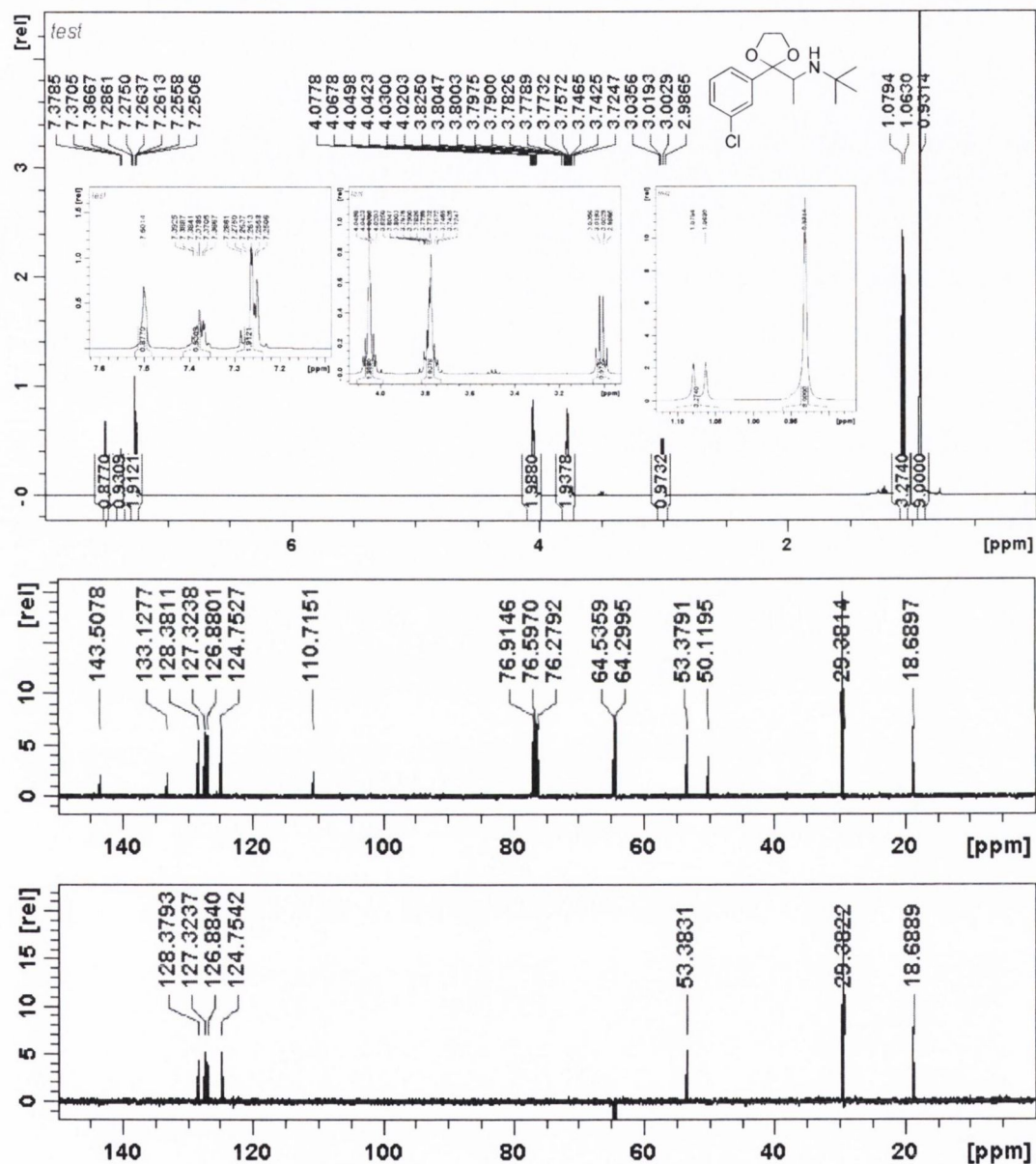
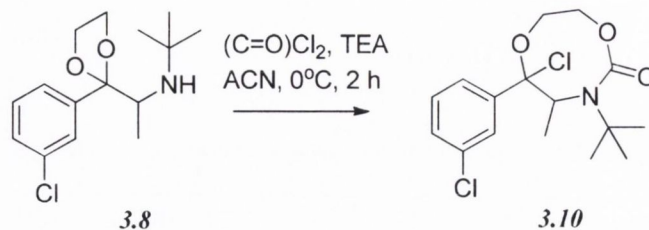


Figure 3.5 ^1H NMR, ^{13}C NMR and DEPT 135 spectrum of the ketal of bupropion **3.8**

Treatment of **3.8** under the conditions described above with bupropion failed to secure any of the desired carbamates. Our focus then turned to a two step procedure to secure the carbamate based prodrugs. The first step was to use phosgene to form the chloride derivative **3.9** and then it was hypothesised that treatment of this intermediate with a variety of alcohols should in principle secure the desired carbamates. However treatment of the ketal **3.8** with phosgene in

dichloromethane using triethylamine as base under a nitrogen atmosphere at 0°C afforded the cyclic carbamate **3.10** as a mixture of stereoisomers as evidenced by TLC, HPLC and NMR analysis of the purified diastereoisomeric products **3.10 a** and **b** (Scheme 3.7).



Scheme 3.7 Synthesis of **3.10**

When the ¹HNMR spectrum of **3.10a** was compared to the ketal **3.8** there were significant differences. Firstly the singlet from the t-butyl protons shifted from 0.93 to 1.47 ppm perhaps indicating coupling of an electron withdrawing carbonyl group to the amine while the methine signal also shifted from 3.00 to 3.40 ppm. Due to ring strain one of the 2H multiplets of the ketal has been split into two single proton multiplets on the dioxolane ring. The ¹³CNMR shows a significant shift in one of the methylene peaks when compared to the spectrum of **3.8**, the peak at 64.3 ppm has shifted to 43.1 ppm. The HRMS spectra of the two isomers showed two peaks, one from the protonated form and the other from the sodium adduct. The most abundant molecular ion peak was from the sodium adduct. The actual mass found was (M+H)⁺ = 346.0915 and (M+Na)⁺ = 368.0806, theoretical mass (M+H)⁺ = 346.0971 and (M+Na)⁺ = 368.0796 respectively.

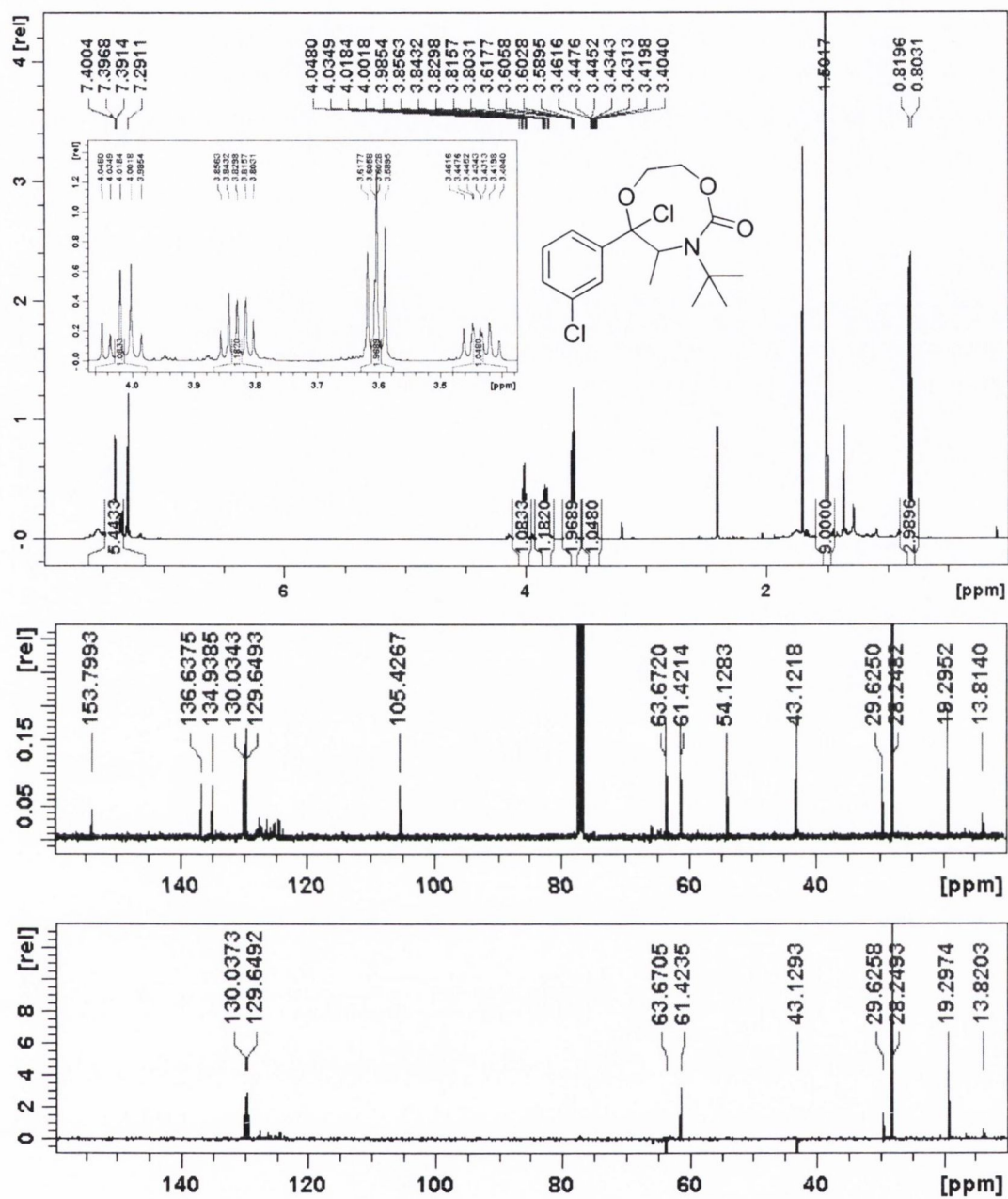
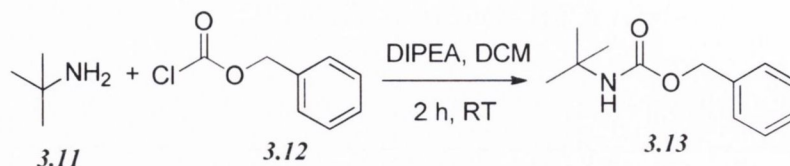


Figure 3.6 $^1\text{H NMR}$, $^{13}\text{C NMR}$ and DEPT135 spectra of a single diastereomer of the cyclic carbamate 3.10.

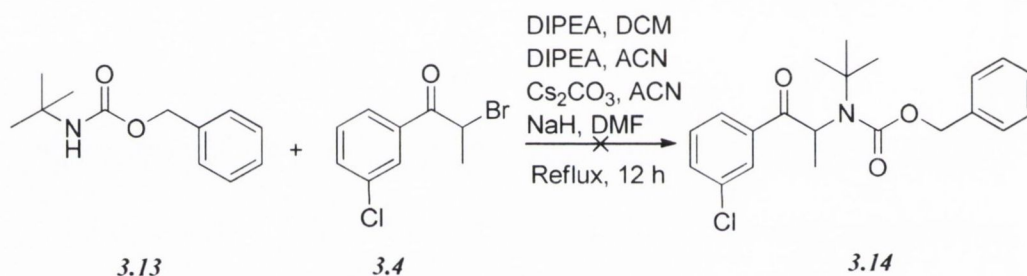
3.3.4.2 Carbamates via conjugation of benzyl tert butyl carbamate

Having failed to secure the desired carbamates by directly treating bupropion with a range of chloroformates, our attention turned to the idea of *N*-alkylating the bromo-ketone **3.4** with the carbamate **3.13**, which was readily furnished following treatment of benzyl chloroformate with *t*-butylamine (Scheme 3.8).



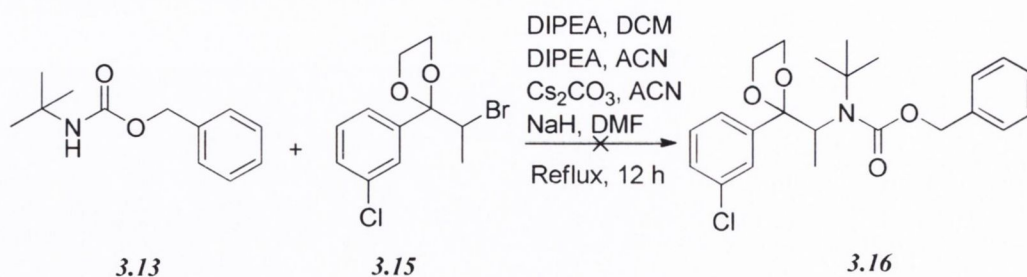
Scheme 3.8 Synthesis of benzyl tert butyl carbamate

Coupling of **3.13** to **3.4** was unsuccessful at room temperature and at elevated temperatures using DIPEA as base and DCM as solvent. Changing the solvent to acetonitrile or DMF and employing Cs₂CO₃ and NaH as bases also failed to furnish the desired product **3.14** (Scheme 3.9).



Scheme 3.9 Attempted synthesis of a benzyl carbamate prodrug of bupropion

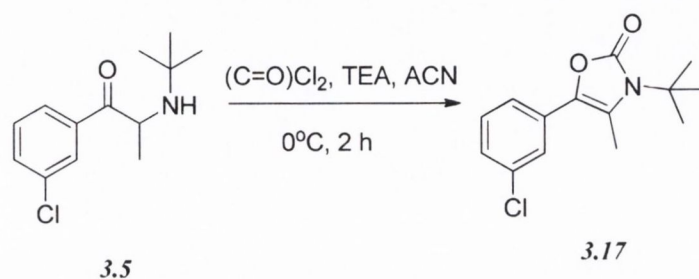
This alkylation step was also attempted with the ketal **3.15** using the same solvent/base systems but again there was no reaction (Scheme 3.10).



Scheme 3.10 Attempted synthesis of ketal protected benzyl carbamate prodrug of bupropion

3.3.4.3 A cyclic carbamate of bupropion (oxazole)

As oxazolidine prodrugs of ephedrine have been synthesised [104, 163], we hypothesised that using the method akin to that which resulted in the formation of the cyclic carbamate **3.10 a** and **b**, that it might be possible to furnish the oxazolone **3.17**. Treatment of bupropion **3.5** with phosgene in acetonitrile with triethylamine base at low temperature readily afforded the cyclic oxazolone **3.17** (Scheme 3.11). Indeed this compound has been synthesised previously by Hamad *et al.* [119] for a different application.



Scheme 3.11 Synthesis of an oxazolone type potential prodrug of bupropion.

The ^1H NMR spectrum of **3.17** (Figure 3.7) is uncomplicated as aside from the aromatic protons there are only two chemically different proton groups in the molecule. The t-butyl protons can be seen as one large singlet at 1.60 ppm while the methyl protons are also seen to resonate as a singlet at 2.30 ppm. The ^{13}C NMR spectrum is free from the carbonyl signal usually seen in bupropion above 200 ppm signifying removal of the aryl ketone group. This has been replaced by the carbonyl signal of the oxazolone moiety at 153 ppm. The HRMS confirmed the presence of the oxazolone with the M+1 ion at 266.0942 amu.

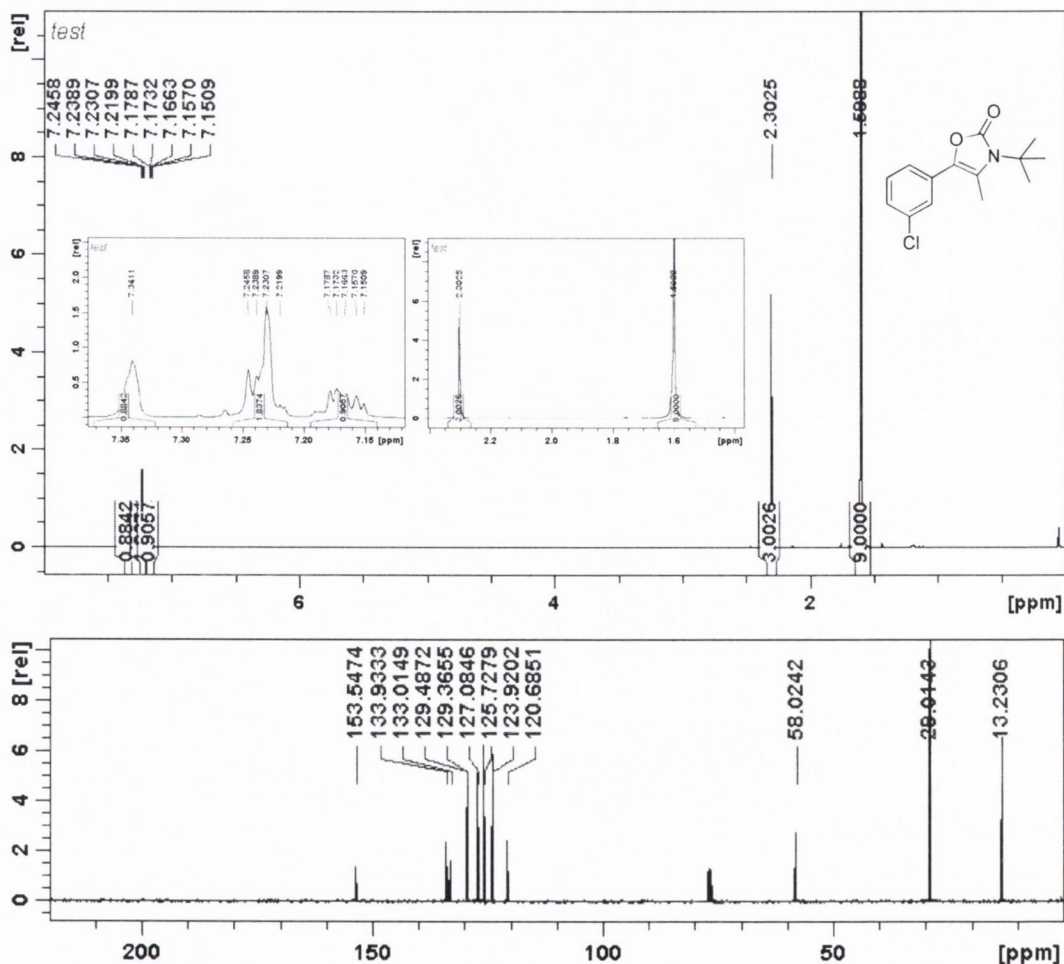


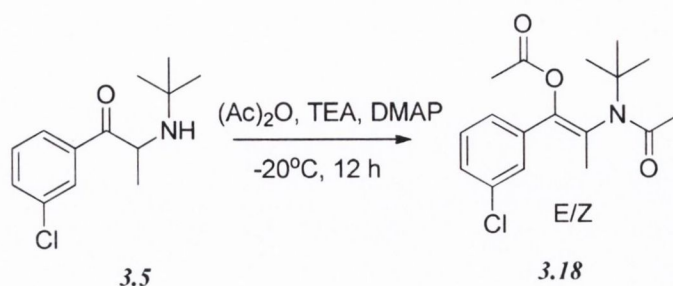
Figure 3.7 ^1H NMR and ^{13}C NMR of the cyclic carbamate oxazolone 3.17 type prodrug of bupropion in deuterated chloroform

3.3.5 Preparation of a double prodrug by acylation of bupropion

While in principle one might anticipate that treatment of bupropion with an acylation reagent might only furnish the corresponding amide derivative, it is also conceivable that under the conditions used the enolacyl ester derivative may also form. There are numerous examples of ester- and amide based prodrugs in the literature, but the idea of using both approaches in a single drug is a novel concept. Recent examples of amide-based prodrugs for neurological applications include docarpamine which has been shown to be converted back to dopamine when given orally [164].

In our situation the most appropriate route to double prodrugs of **3.5** is by its treatment with the corresponding anhydride in the presence of a tertiary base [162] (Scheme 3.12). The first approach used was by treatment of **3.5** with acetic anhydride, DMAP and TEA in acetonitrile at room temperature. This approach furnished the desired prodrug **3.18** in a poor yield and resulted in the formation of several degradation products of bupropion. This reaction was optimized by

simply using acetic anhydride as solvent and by conducting the reaction at -20°C . Generally both the syn and anti isomers formed as illustrated in the ^1H , ^{13}C NMR and LC-MS spectra of **3.18** (Figure 3.8 and Figure 3.9).



Scheme 3.12 The synthesis of a potential amide prodrug of bupropion.

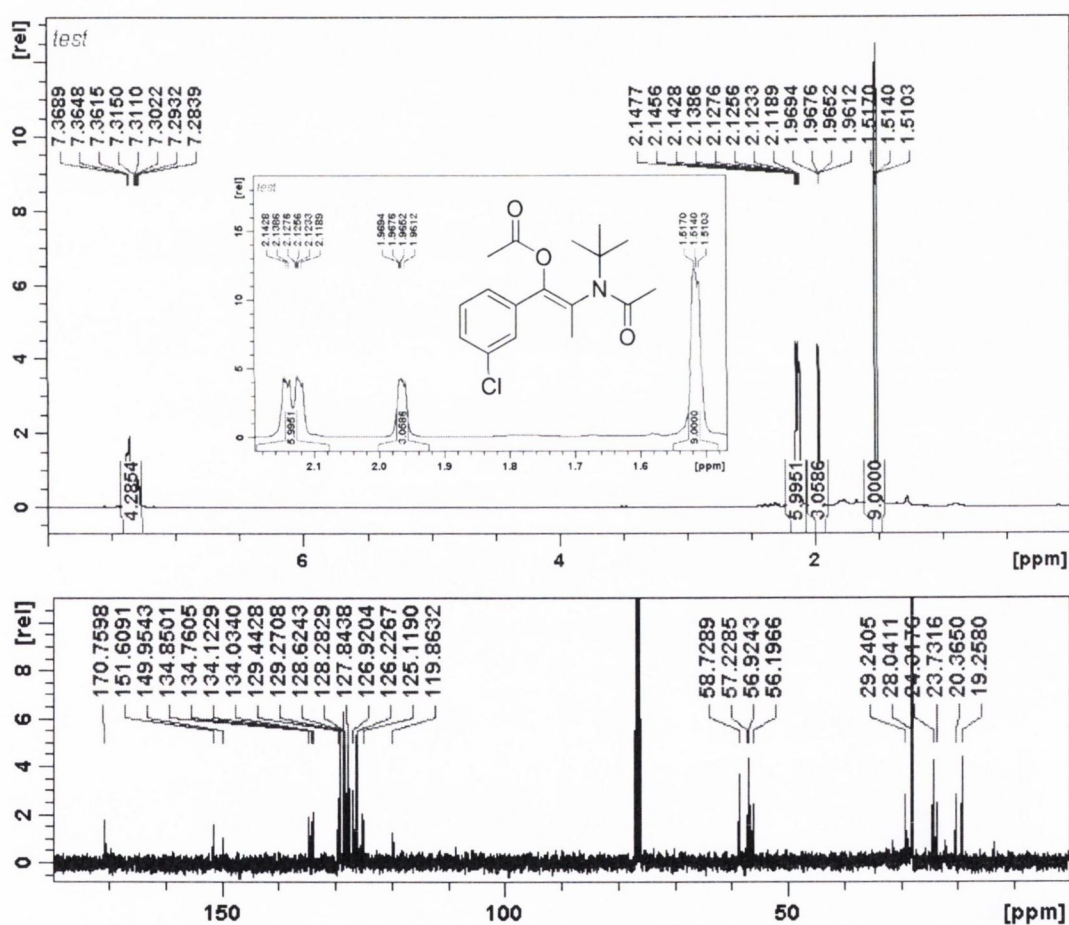


Figure 3.8 ^1H NMR of **3.18** shows the two isomers incompletely resolved. Peak singlet at 1.51 ppm indicates *t*-butyl protons, 1.98 ppm singlet $-\text{CH}_3$ protons, 2.12-2.15 ppm $2\times$ Acetyl group protons. ^{13}C NMR of **3.18** shows twice the number of carbons present that should be present, indicating two isomers present.

The positive electrospray fragmentation spectrum of **3.18** (Figure 3.9) has two main molecular ions, one from the sodium adduct ($M+Na^+$) = 346.1173 and one from the protonated species ($M+H^+$) = 324.1359. The main fragment from the molecular ion is from the neutral loss of one of the acetyl groups leaving a fragment ion at 282.1255. Neutral loss of the t-butyl group leaves the protonated secondary amide at 268.0731 and loss of both the acetyl and t-butyl group off the amine results in the protonated primary amine at 226.0626.

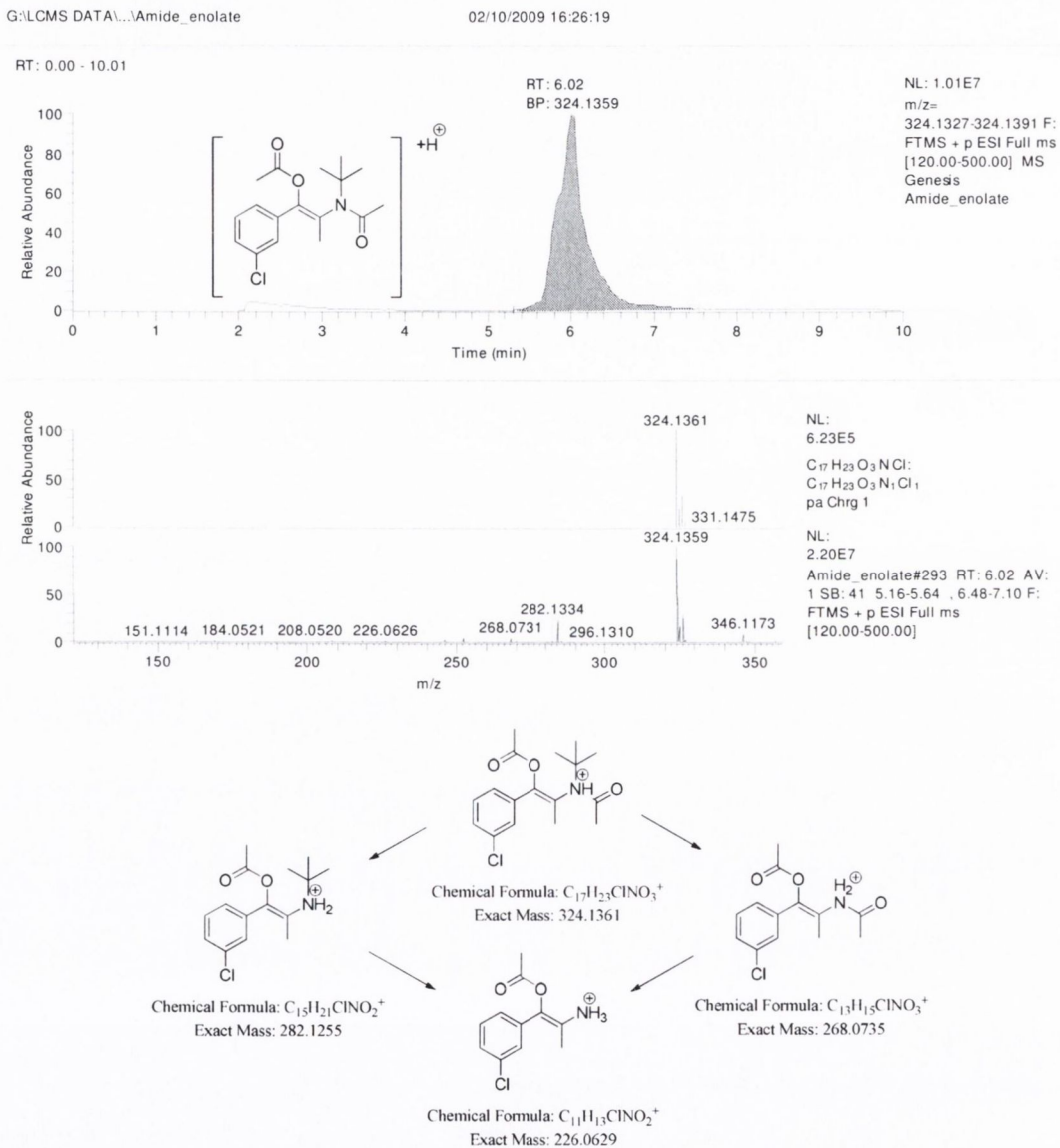


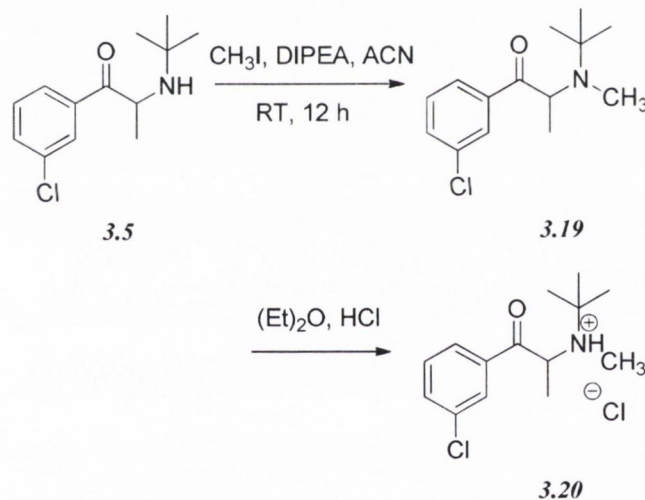
Figure 3.9 Shows an LC-MS chromatogram of **3.18**, and the proposed +ESI fragmentation pathway of **3.18**. The LC-plot shows asymmetry of the purified peak, which may indicate the presence of two isomers.

3.3.6 N-alkylation of bupropion

Some secondary and tertiary alkyl amines are reported to undergo dealkylation mediated by MAO-B to an amine and the corresponding aldehyde or ketone [165]. This has been investigated as a prodrug approach for the CNS active agent 2-phenylethylamine (PEA). In comparison with the free drug, *N,N*-dipropargyl-2-phenylethylamine and *N*-propargyl-2-phenylethylamine produced increased levels of PEA in the brain of rats following oral administration [166, 167].

Methylation of amino groups is commonly carried out by reacting the appropriate amine with an alkylating reagent such as methyl iodide or dimethyl sulphate under basic conditions or by treatment of the amine with formaldehyde in formic acid [168].

In our situation bupropion **3.5** was *N*-methylated with methyl iodide in the presence of diisopropylethylamine and acetonitrile at room temperature to form **3.19**. It was important to use a weak base as the use of stronger bases such as sodium hydride or lithium diisopropylamide may cause alkylation at either the oxygen or alpha carbon due to enolization. Treatment of **3.19** with HCl gas in diethyl ether afforded the hydrochloride salt **3.20** (Scheme 3.13).



Scheme 3.13 Synthesis of the *N*-alkylated potential prodrug of bupropion, *N*-methyl bupropion.

The ^1H NMR spectrum of **3.19** is similar to bupropion except for the addition of a singlet at 2.18 ppm which signifies alkylation of the amine with the methyl group. Like bupropion, it has one large singlet at 1.20 ppm relating to the nine *t*-butyl protons, a doublet at 1.27 ppm which is the methyl group adjacent to the alpha carbon and then one quartet which is the alpha proton adjacent to the methyl group. The ^{13}C NMR spectrum of *N*-methyl bupropion contains the extra methyl carbon signal at 28.7 ppm.

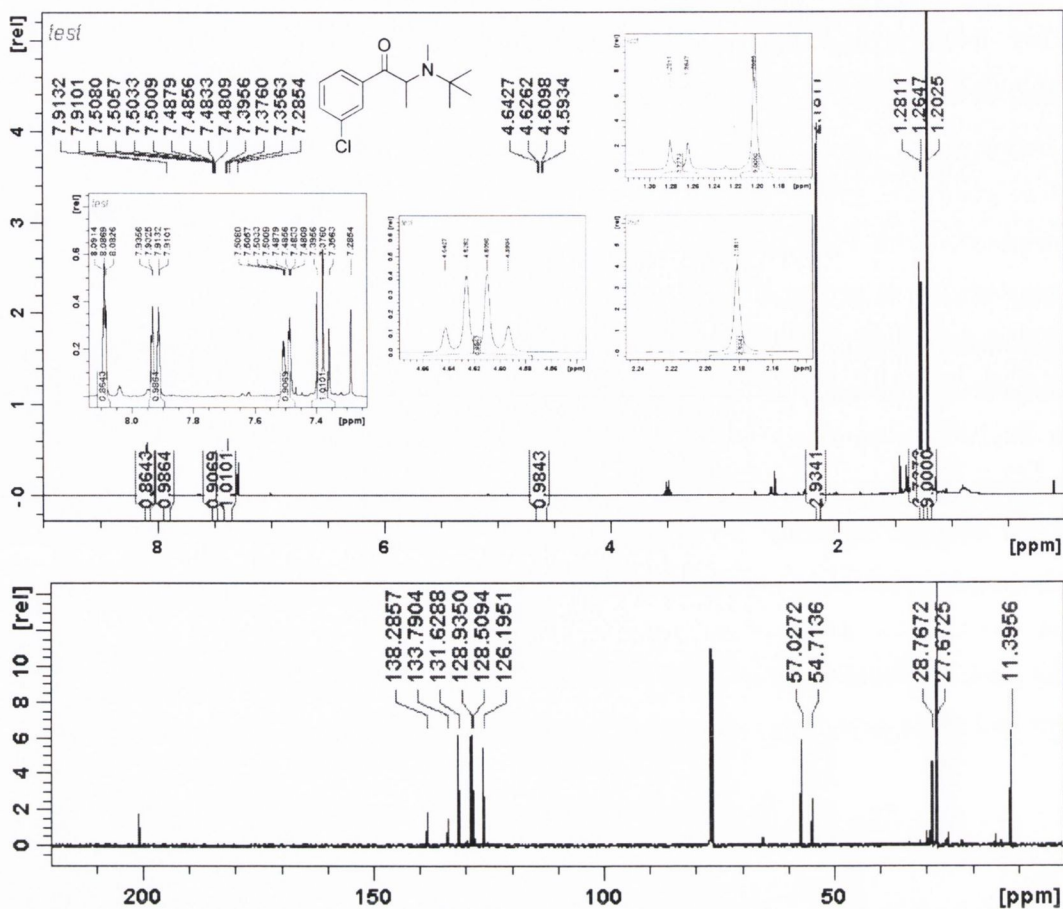


Figure 3.10 ¹H NMR and ¹³C NMR of N-methylated bupropion 3.19 in deuterated chloroform

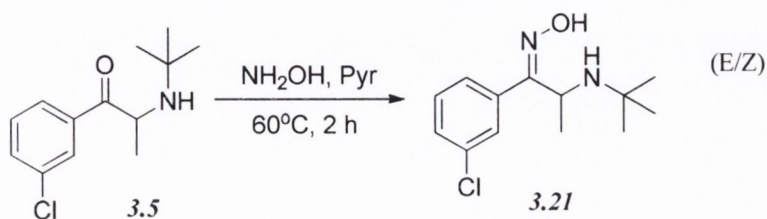
3.3.7 Oxime type prodrugs of bupropion

3.3.7.1 Hydroxyimine of bupropion

Oxime/hydroxyimine type prodrugs are a popular method for masking the reactivity of the carbonyl group of drug substances. As examples Buparvaquone hydroxyimine [112] and nabumetone hydroxyimine [113] are such examples both readily oxidized by CYP3A4 back to the parent ketone.

Bupropion 3.5 was initially converted to the hydroxyimine 3.21 by treatment with hydroxylamine hydrochloride in the presence of sodium acetate and ethanol under reflux conditions. This reaction was slow and yields were low due to degradation of bupropion under alkaline conditions. The yield was improved by removing the solvent and using pyridine as solvent/base under mild heating conditions (Scheme 3.14). The turnover of bupropion to the hydroxyimine was faster and less degradation of the parent compound was seen to occur using this method. As expected both the syn and anti isomers of 3.21 formed which were readily separated by flash column chromatography. This is most likely due to the fact that the syn

isomer can hydrogen bond to the neighbouring amino group. Perhaps surprising, there was no significant difference in the ^1H and ^{13}C NMR spectra of the two isomers. This may be due in part to the fact that the proton on the hydroxyimine group is exchangeable and therefore was not seen in the ^1H NMR. This proton signal would have shown the difference between the syn and anti isomers as the proton from the isomer that is intramolecularly hydrogen bonded would see a significant chemical shift over the isomer that was not hydrogen bonded.



Scheme 3.14 Synthesis of the potential hydroxyimine prodrug of bupropion.

The ^1H NMR spectrum of the hydroxyimine of bupropion **3.21** shows no significant difference to bupropion as the exchangeable protons are not present. The ^{13}C NMR spectrum of the hydroxyimine **3.21** shows that the carbonyl signal in the parent compound above 200 ppm is no longer present. The addition of a new signal in the aromatic region confirms the imine carbon is present. This carbon has significant aromatic character due to its unsaturation.

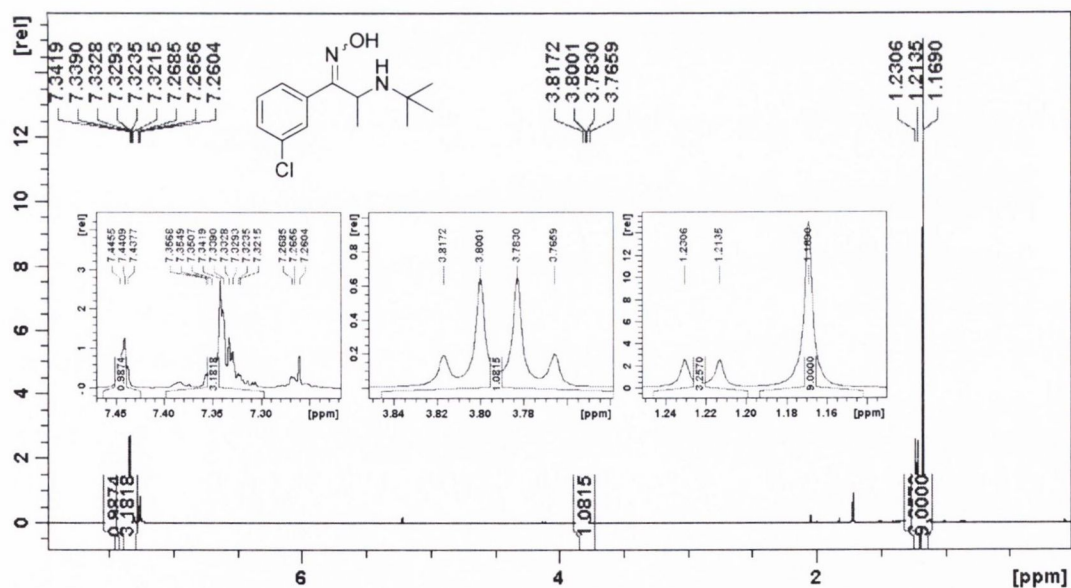


Figure 3.11 ^1H NMR of the hydroxyimine potential prodrug of bupropion **3.21**

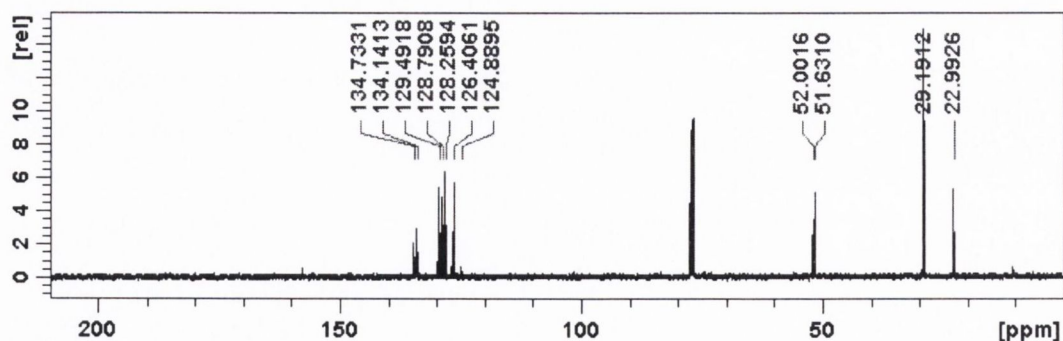
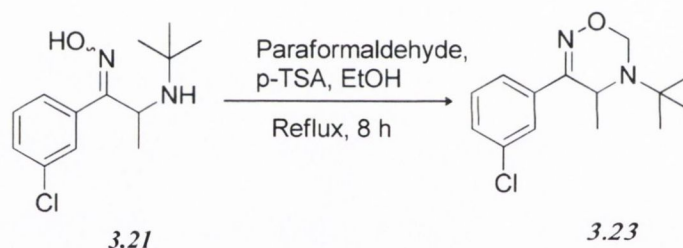


Figure 3.12 ^{13}C NMR of the hydroxyimine potential prodrug of bupropion **3.21**

3.3.7.2 Synthesis of potential double prodrug by formation of an oxadiazine derivative of the oxime **3.21**

Having succeeded with the synthesis of oxime **3.21**, it was felt that treatment of this oxime with formaldehyde and a catalytic amount of *p*-toluenesulfonic acid one could bridge the amine and hydroxyimine with a methylene group to form **3.23**, a potential double prodrug of bupropion. Treatment of the hydroxyimine **3.21** with paraformaldehyde in ethanol using *p*-toluenesulfonic acid under reflux yielded the oxadiazine **3.23** (Scheme 3.15).



Scheme 3.15 Synthesis of the double prodrug oxadiazine of bupropion

The ^1H NMR spectrum of the oxadiazine of bupropion **3.23** contains one singlet at 1.26 ppm for the 9 *t*-butyl protons, a doublet at 1.30 ppm for the 3 methyl protons, a quartet at 3.90 ppm which represent the methine proton and two doublets at 4.8 and 5.2 ppm for the methylene hydrogens. The ^{13}C NMR spectrum of the oxadiazine of bupropion **3.23** shows the additional methylene carbon signal at 75.2 ppm.

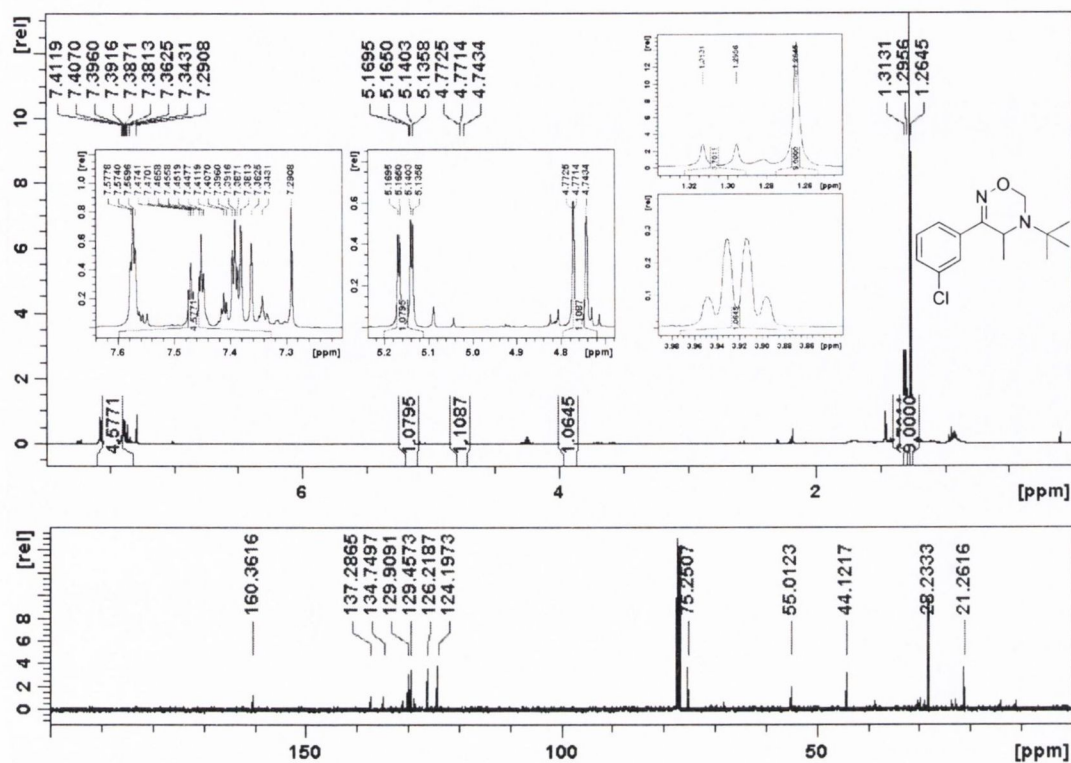
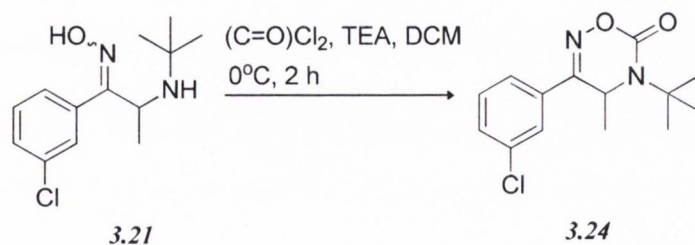


Figure 3.13 ^1H NMR and ^{13}C NMR spectra of the potential oxadiazine double prodrug of bupropion 3.23.

As oxodioxolones are readily hydrolysed back to the parent drug [169], we envisaged in an analogous fashion that perhaps the oxadiazinone derivative **3.24** of bupropion may also be converted back to bupropion *in vivo*. Treatment of the hydroxyimine **3.21** with phosgene in dry dichloromethane and triethylamine gave the ring closed oxadiazinone **3.24** (Scheme 3.16).



Scheme 3.16 Synthesis of the double prodrug oxadiazinone of bupropion

The ^1H NMR spectrum of the oxadiazinone of bupropion **3.24** is shown in Figure 3.14. The *t*-butyl singlet integrating as nine protons has been shifted downfield (1.6 ppm) due to its proximity to the carbonyl group. The methyl doublet is seen at 1.45 ppm and the single α -proton adjacent to the methyl group is split into a quartet, indicating the double bond on the oxadiazinone ring is between the carbon and nitrogen of the oxime group. The ^{13}C NMR spectrum of the oxadiazinone shows the oxadiazinone carbonyl peak at 160.3 ppm.

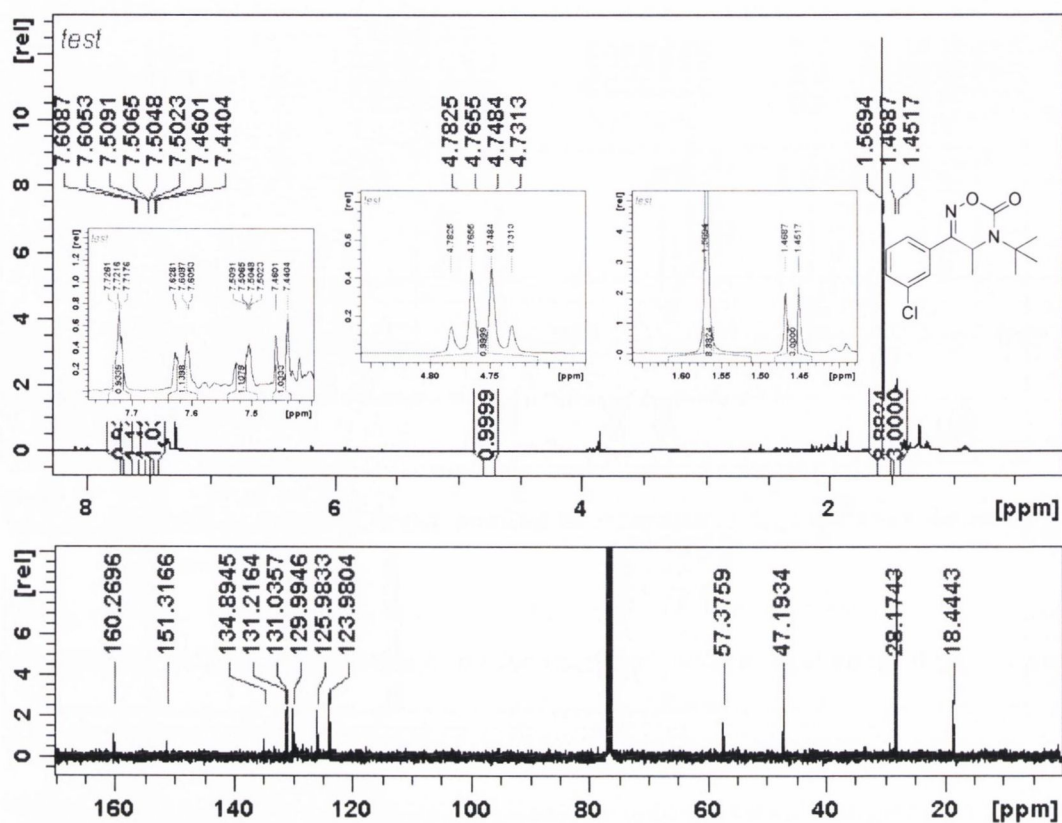
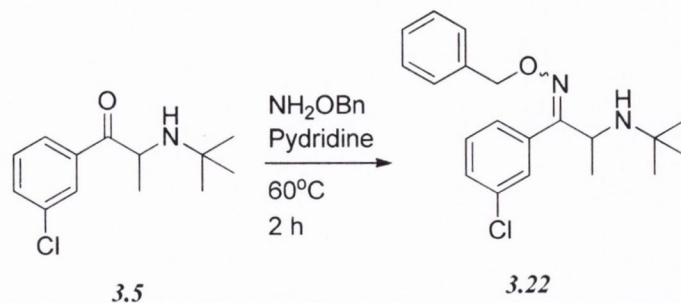


Figure 3.14 ^1H NMR and ^{13}C NMR of the potential oxadiazinone double prodrug of bupropion 3.24

3.3.7.3 Benzyl oxime of bupropion

Oximes, a substituted oxime, have also been shown to be viable prodrug alternatives to hydroxyimines. In the case of alprenolol, alprenoxime (the hydroxyimine prodrug) was shown to be readily transformed into the corresponding β -blocker [170]. An oximine analogue of alprenoxime was examined in an attempt to overcome the problem of low stability in aqueous solution. To this end, the methoxime analogue of alprenolol was prepared and evaluated. Stability in aqueous solution was greatly enhanced at neutral pH while topical administration to rabbits produced a decrease in intraocular pressure that had the same onset and intensity as that produced by alprenolol but lasted longer [171]. The evidence presented indicated that the methoxime to ketone reaction was enzymatic. Hydrolysis by an unknown hydrolase as postulated by the authors is a valid assumption but others state that the transformation involves oxidative *O*-demethylation to the oxime followed by spontaneous hydrolysis of the oxime to the ketone. Treatment of bupropion 3.5 with *O*-benzyl hydroxylamine in pyridine at elevated temperatures yielded the benzyl oximine 3.22. This reaction was slower than the corresponding hydroxyimine reaction and hence more degradation of the starting material was observed. The two syn and anti isomers were observed as products. These could be observed by thin layer chromatographic analysis and the impurities were separated from 3.22 by flash column chromatography.



Scheme 3.17 The synthesis of a benzyl oxime of bupropion

Important features of the ^1H NMR spectrum of **3.22** are the benzyl $-\text{CH}_2-$ protons at 5.24 ppm and the additional aromatic protons at 7.29-7.36 ppm.

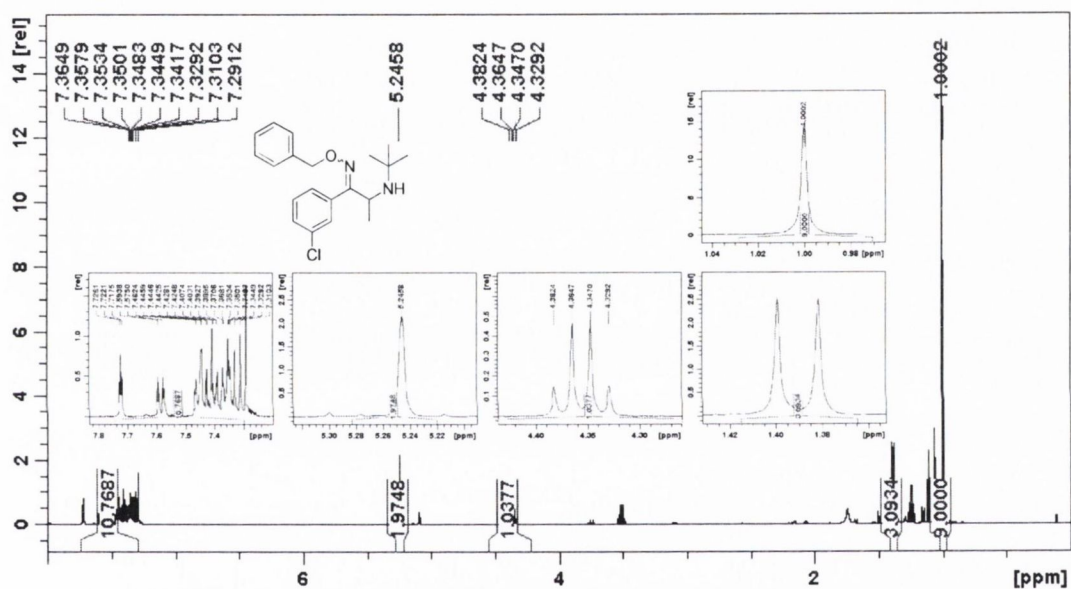
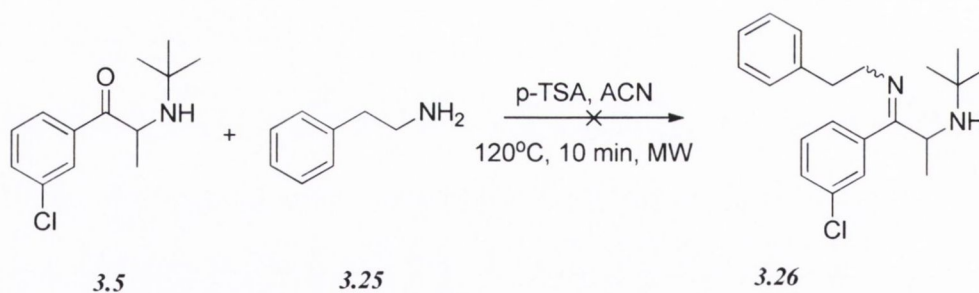


Figure 3.15 ^1H NMR of the benzyl oxime derivative of bupropion **3.22**

3.3.8 Imine prodrugs of bupropion

An alkyl (phenylethylamine) and aryl (anisidine) imine derivative of bupropion was attempted in an effort to find a suitable prodrug presentation of this compound. Imines are liable to chemical hydrolysis back to the parent ketone and although being quite unstable, they have been used as prodrug groups. Chemically activated azomethine prodrugs of the reference histamine H3 receptor agonist R- α -methylhistamine have been evaluated, as well as enzymatically activated prodrugs (amide, esters and carbamates) [172, 173]. R- α -methylhistamine is a potent and selective histamine H3 receptor agonist, but its use is limited by insufficient peroral absorption, poor brain penetration and rapid metabolism, especially by histamine *N*-methyltransferase.

The synthesis of an imine prodrug of bupropion was attempted by the acid catalysed condensation of bupropion with phenylethylamine. An equimolar mixture of bupropion **3.5** and phenylethylamine **3.25** were refluxed in acetonitrile using *p*-toluenesulfonic acid as the acid catalyst. This reaction was also attempted under microwave conditions, 120°C for 10 min (Scheme 3.18). In both cases bupropion and phenylethylamine were used up in the reaction and two major products formed, as seen by TLC. These were possibly the syn and anti isomers of an imine conjugate but it was not possible to isolate these products for characterization. One of the products decomposed on column during flash chromatography while the other product appeared to decompose during the drying step.



Scheme 3.18 Attempted synthesis of a potential imine prodrug of bupropion.

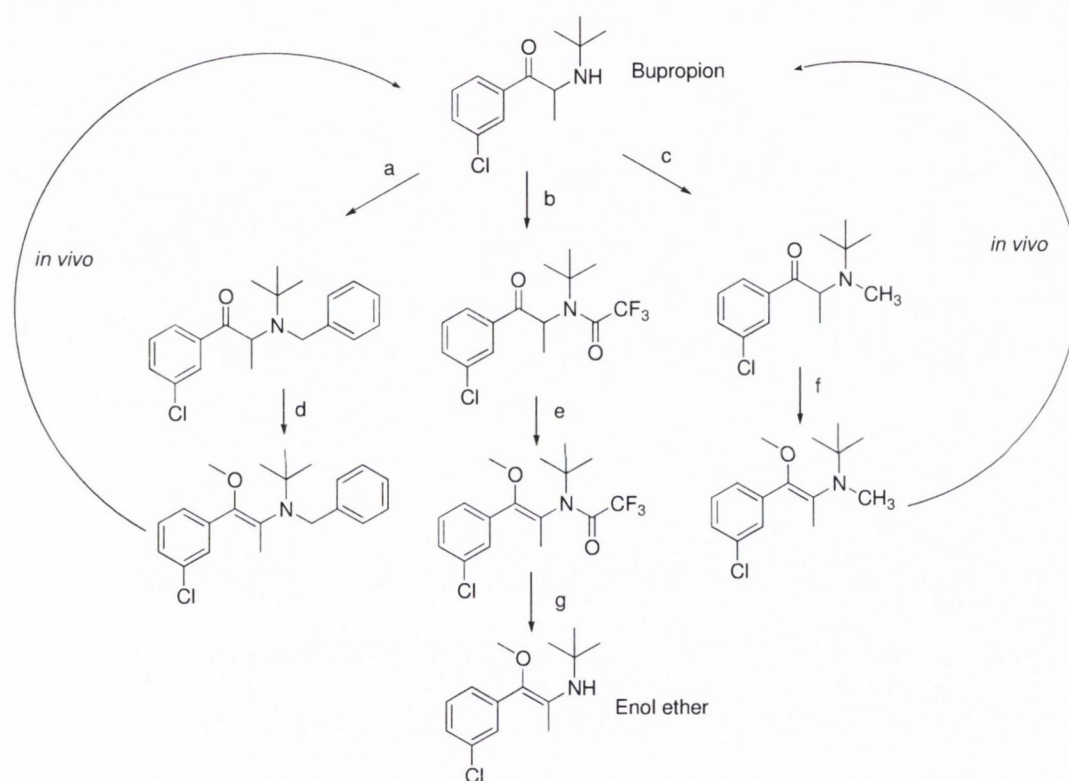
An alternative strategy was to prepare the aryl imine derivative as these are known to have better stability than alkyl imines due to extensive conjugation. Attempts were made to couple different aryl amines including *o*, *m* and *p*-anisidine with bupropion but all were unsuccessful.

3.3.9 O-alkylated prodrugs of bupropion

O-alkylation can be used as a masking group for the ketone. *O*-dealkylation is usually an enzymatic process and has been known to occur by both esterases [114] and P450 oxidative enzymes [117].

Since bupropion can be alkylated at three sites, the amino, the α -carbon and the oxygen during enolization, it was important to find a suitable protective group for the amine that could later be removed to provide the *o*-alkylated derivative of bupropion. Under ideal circumstances, a carbamate would have been a good protective group due to its ease of removal but as we have seen earlier in this chapter it was not possible to synthesize even a simple carbamate derivative of bupropion. Three protective group strategies were attempted in the synthesis of enol ethers of bupropion,

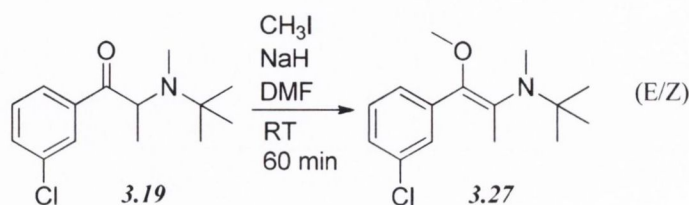
Scheme 3.19. Two were also double prodrug strategies, the benzyl and methyl. The TFA-protective group strategy was used to protect the amine during synthesis of the enol ether of bupropion.



Scheme 3.19 Protective group strategies for the amine of bupropion in order to synthesize double prodrugs of bupropion and an enol ether of bupropion. a) ACN, DIPEA, BnBr, reflux, 36 h, b) ACN, TEA, TFAA, RT, 15 min, c) ACN, DIPEA, CH₃I, RT, 12 h, d) NaH, CH₃I, DMF, RT, 30 min, e) NaH, CH₃I, DMF, RT, 30 min, f) DMF, NaH, CH₃I, RT, 2 h.

3.3.9.1 Dimethylated double prodrug of bupropion

Treatment of N-methyl bupropion **3.19** with sodium hydride in dimethylformamide resulted in formation of the sodium enolate of bupropion. The enolate was treated with a methylating reagent usually methyl iodide or dimethyl sulphate. Both approaches resulted in the successful synthesis of **3.27**.



Scheme 3.20 The synthesis of dimethylated bupropion

The most important feature of the ^1H NMR spectrum of **3.27** is the extra singlet at 3.39 ppm due to the methoxy-enol group. The methyl group at 2.48 ppm has collapsed from a doublet into a singlet due to the enol presentation of **3.27**. The ^{13}C NMR has most importantly lost the signal at 205 ppm signifying the removal of the carbonyl group.

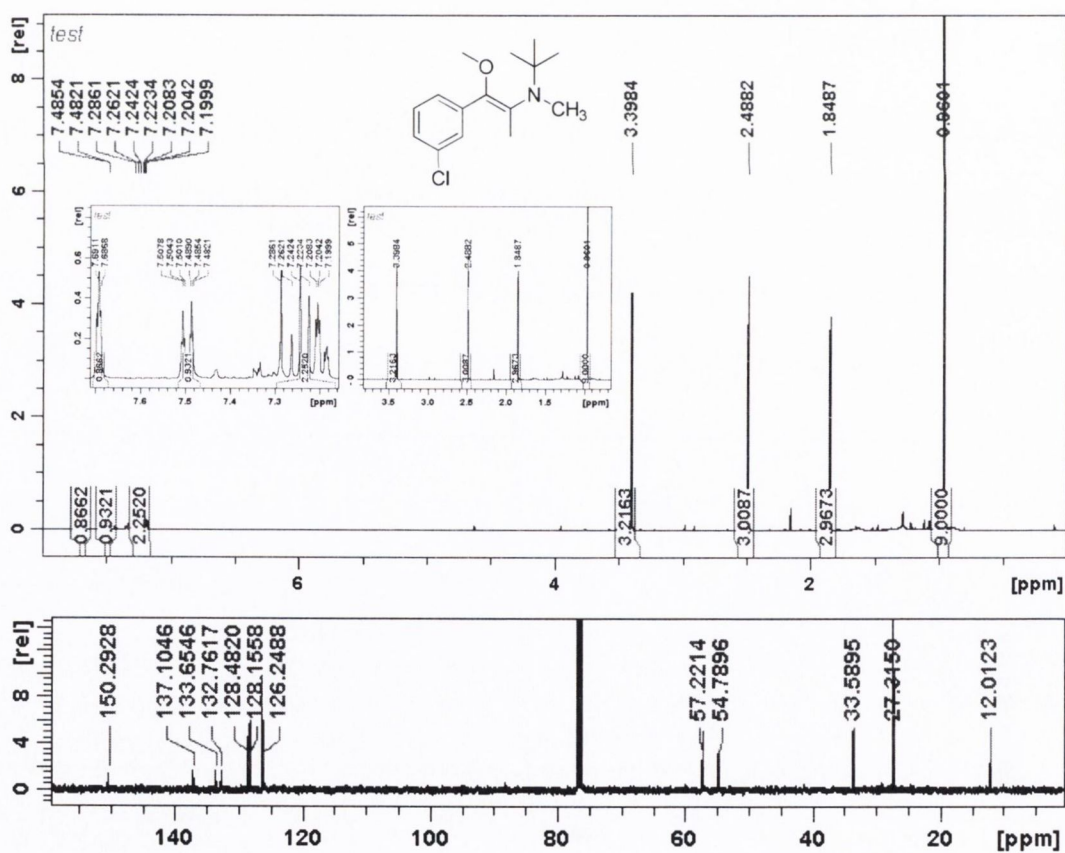


Figure 3.16 ^1H NMR and ^{13}C NMR spectra of N-methyl O-methyl bupropion **3.27** in deuterated chloroform

The introduction of the double bond in the form of the enol, brings the possibility of forming both the E and Z isomers. While there was little evidence by ^1H NMR and ^{13}C NMR spectral data, the LC-MS chromatogram of the dimethylated product **3.27** (Figure 3.17) clearly shows that the two isomers are present.

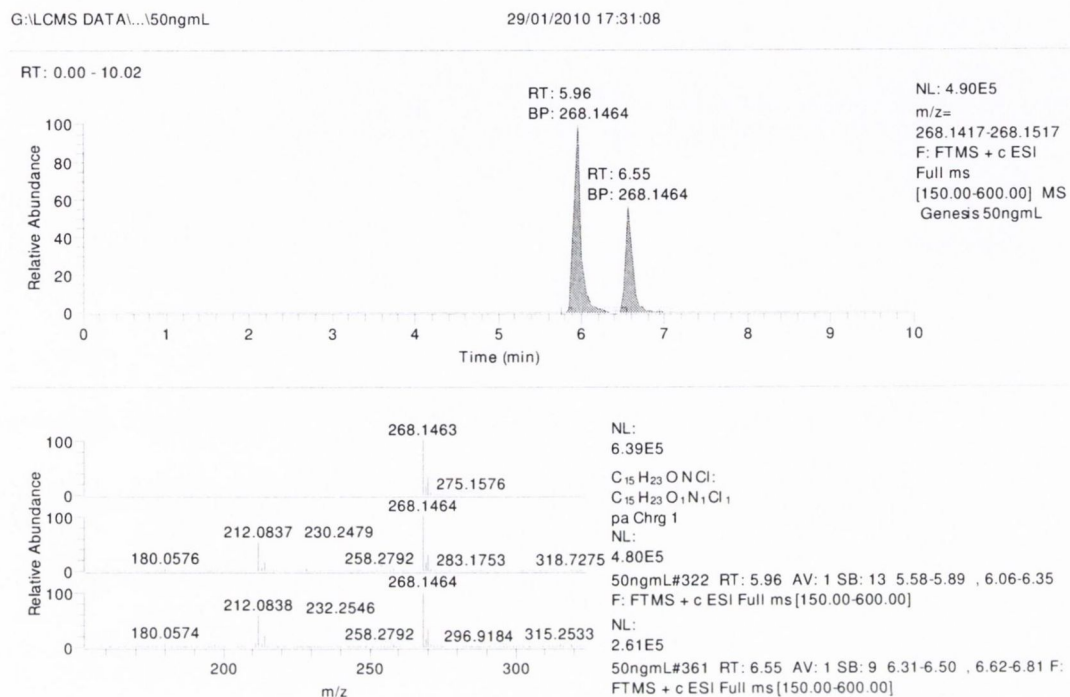
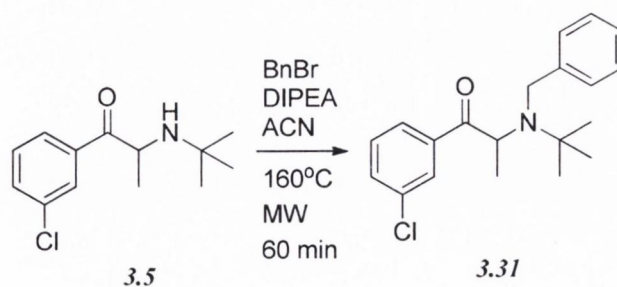


Figure 3.17 An LC-MS chromatogram of dimethyl bupropion **3.27**

3.3.9.2 *N*-benzyl *O*-methyl double prodrug of bupropion

Bupropion **3.5** was benzylated to **3.31** by treatment of the amine with benzyl bromide in diisopropylethylamine in acetonitrile, Scheme 3.21. The mixture was refluxed for 5 days but the reaction did not go to completion (~ 50 % yield). Increasing the amount of benzyl bromide did not improve the yield, so microwave conditions were evaluated. This improved the yield slightly and had the advantage of greatly improving the reaction time.



Scheme 3.21 The synthesis of *O*-methyl *N*-benzyl bupropion

The ^1H NMR spectrum of *N*-benzyl bupropion **3.31** is presented in Figure 3.18. The nine *t*-butyl protons are seen in the large singlet at 1.2 ppm, followed by the methyl doublet at 1.4 ppm. The two benzylic protons are seen as a double doublet at approximately 4.0 ppm and the quartet at 4.7 ppm signifies the α -proton to the keto group. The ^{13}C NMR spectrum of *N*-benzyl bupropion **3.31** contains ten chemically distinct carbon nuclei in the aromatic region. The ketone carbon can clearly be seen still present at 201 ppm.

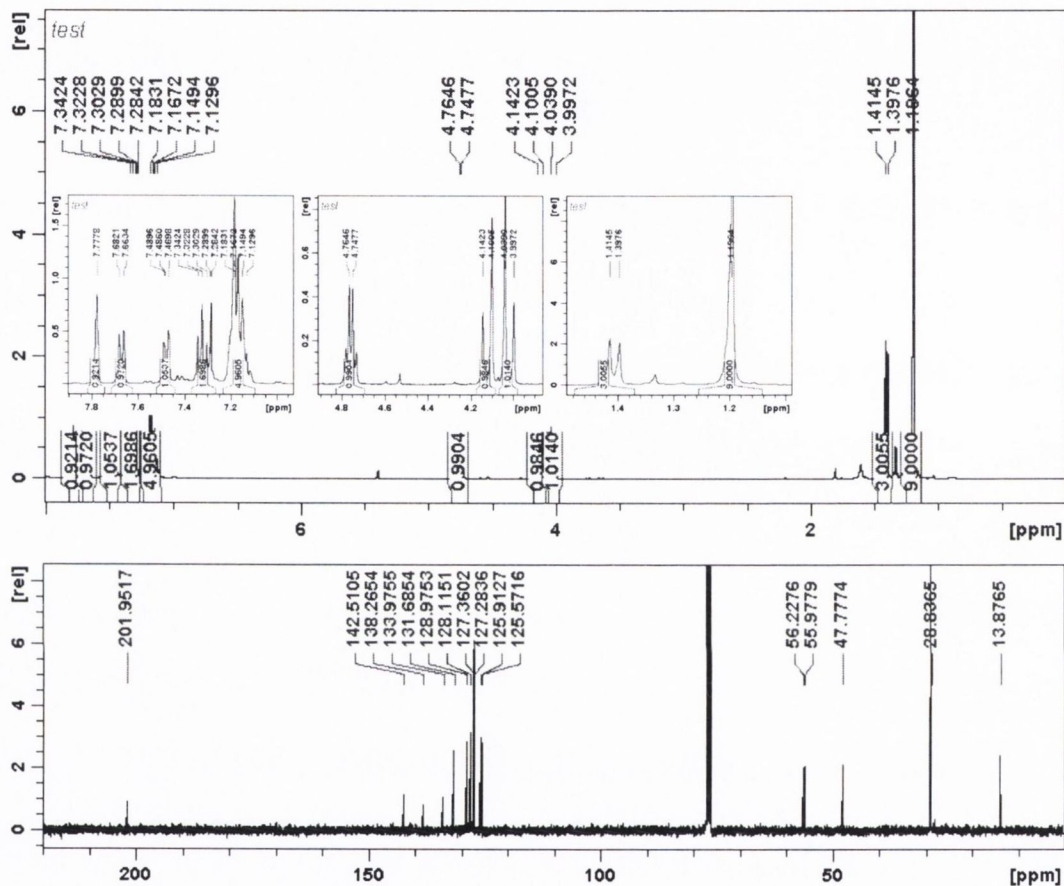
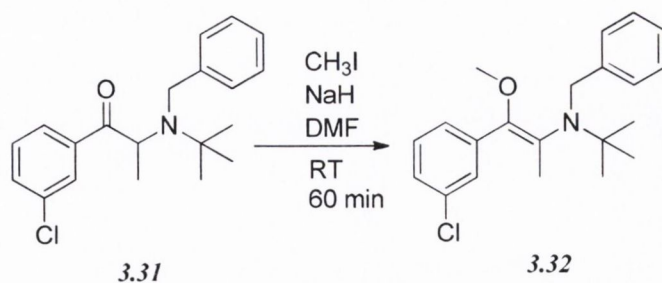


Figure 3.18 The ^1H NMR and ^{13}C NMR of *N*-benzyl bupropion **3.31**.

N-benzyl bupropion **3.31** was converted to the *O*-methyl analogue **3.32** by treatment with methyl iodide or dimethyl sulphate in the presence of sodium hydride. The ketone was converted to the enolate with sodium hydride in dimethylformamide followed by addition of the methylating reagent, Scheme 3.22.



Scheme 3.22 Synthesis of *N*-benzyl *O*-methyl bupropion

The ^1H NMR spectrum of the *O*-methylated *N*-benzylated product **3.32** shows the addition of a singlet at 3.2 ppm indicating the three methyl protons on the methyl enol ether group. The quartet at 4.7 ppm has been removed and the doublet of the methyl group has collapsed into a singlet indicating the unsaturation of the enol double bond. There is no evidence of the two *E/Z* isomers present in the proton ^1H NMR spectrum. The ^{13}C NMR spectrum does not contain the keto-group carbon, indicating successful methylation at the oxygen.

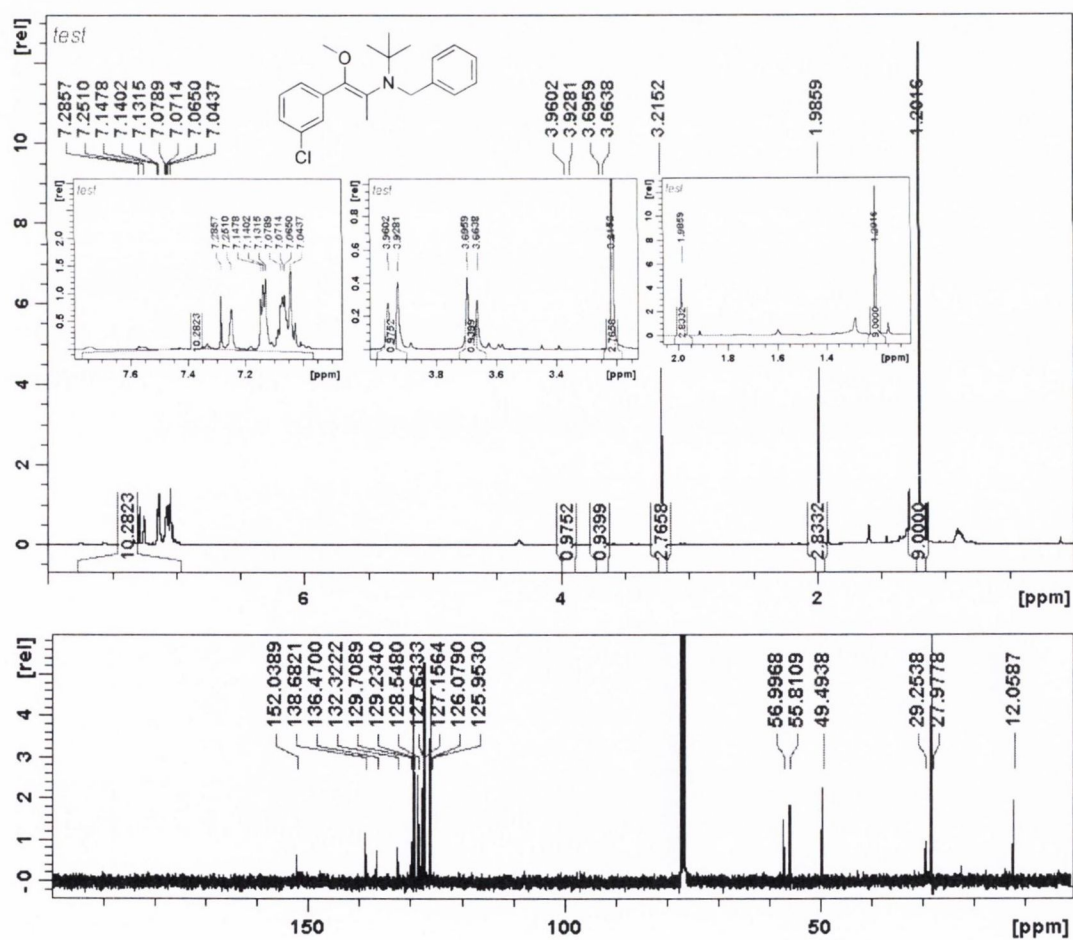
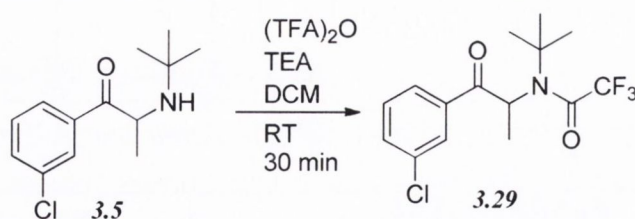


Figure 3.19 ^1H NMR and ^{13}C NMR spectra of *N*-benzyl protected methyl enol ether of bupropion **3.32** in deuterated chloroform

3.3.9.3 Attempted synthesis of an *O*-methylenol prodrug of bupropion

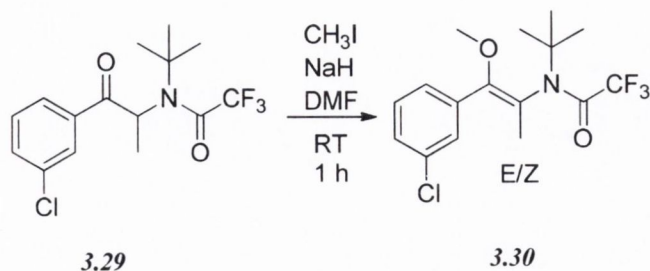
The initial step towards the synthesis of this prodrug required us to protect the amine group as a trifluoroacetamide derivative. Simple amides are generally prepared from the acid chloride or anhydride. There are also numerous other coupling agents and methodologies that have been developed for amide formation [174]. Amides are generally stable to acidic and basic hydrolysis, and they are classically hydrolysed by heating in strongly acidic or basic solutions. Among simple amides, hydrolytic stability increases from formyl > acetyl > benzoyl. Lability of haloacetyl derivatives to mild acid hydrolysis increases with substitution; acetyl < chloroacetyl < dichloroacetyl < trichloroacetyl < trifluoroacetyl [162]. Protection of amines as trifluoroacetamides is one of the more useful amine protecting groups because of the ease in which it can be removed under mildly basic conditions. The normal methods for TFA introduction is by treatment of the amine with an activated form of TFA such as trifluoroacetic anhydride (TFAA) or the ethyl ester derivative of trifluoroacetic acid under basic conditions in a polar aprotic solvent.

Protection of bupropion via a trifluoroacetamide was performed by treatment of bupropion **3.5** with TFAA with triethylamine as base in dichloromethane at room temperature (Scheme 3.23). The reaction was almost instantaneous but was left stirring for 30 minutes to ensure complete conversion to the TFA derivative. Unlike treatment of bupropion with acetic anhydride, TFA acetylation only occurred at one site on bupropion, the amino group. This was confirmed by one ^{19}F NMR signal in the spectrum at -67.87 ppm. The ^1H NMR spectrum of **3.29** showed the *t*-butyl group shifting slightly downfield to 1.40 ppm due to the strongly electronegative TFA group attached. The methyl group resonated as a doublet and the methine proton quartet remained which provided evidence that the structure was in its keto-form. This was confirmed by the ^{13}C NMR spectrum where the carbonyl signal was seen still present at 206 ppm.



Scheme 3.23 Synthesis of TFA-protected bupropion

Treatment of **3.29** with either methyl iodide or dimethyl sulphate using bases such as sodium hydride in DMF or potassium *tert*-butoxide in HMPA afforded **3.30** after work-up and purification by flash column chromatography. As expected, both *E* and *Z* isomers formed. It was not possible to separate these isomers by flash column chromatography as there was no selectivity between these isomers by normal phase chromatographic methods. Therefore both isomers can be seen as a mixture when analysed by NMR, Scheme 3.24.



Scheme 3.24 Synthesis of *N*-TFA *O*-methyl bupropion

The ^1H NMR spectrum of **3.30** clearly has two sets of peaks with an isomeric ratio of approximately 2:1. The addition of a new singlet representing the enol ether methyl group at approximately 3.2 ppm provides evidence of the *O*-methylated derivative. The quartet usually associated with the α -proton has disappeared, giving evidence of an enol ether double bond in the molecule. The doublet usually associated with the methyl group has collapsed into a singlet confirming removal of the methine proton. This signal has also shifted slightly downfield to 1.7 ppm. As expected the ^{13}C NMR spectrum of **3.30** has twice the number of carbon peaks indicating the presence of the E/Z isomers. The ^{19}F NMR spectrum also confirms the presence of the two isomers.

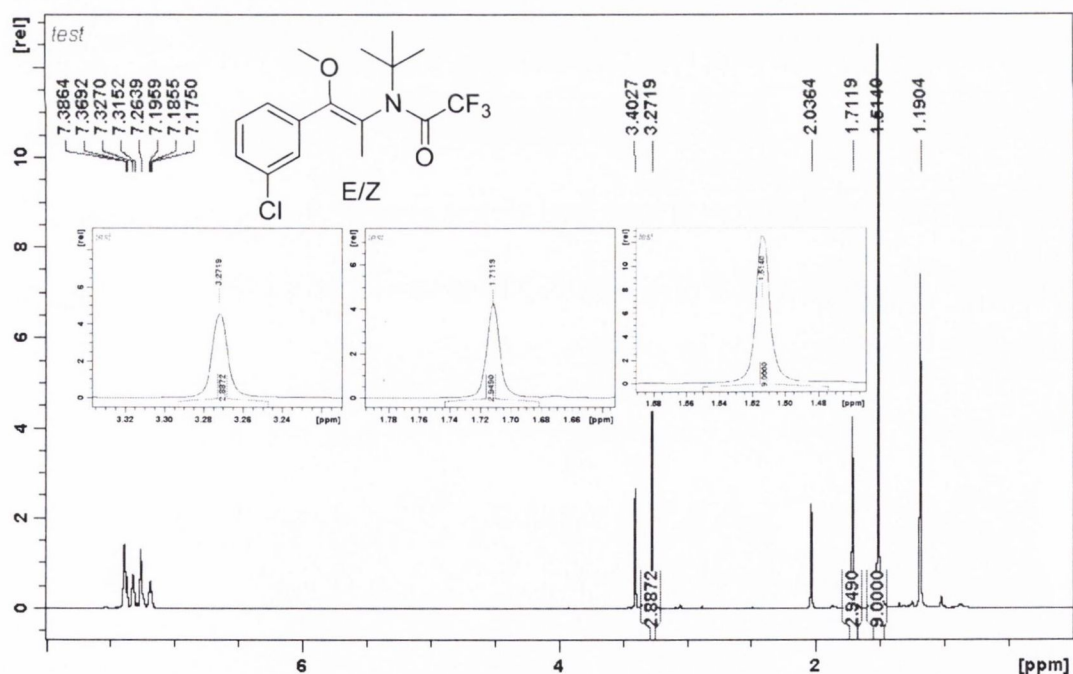


Figure 3.20 ^1H NMR spectrum of **3.30**

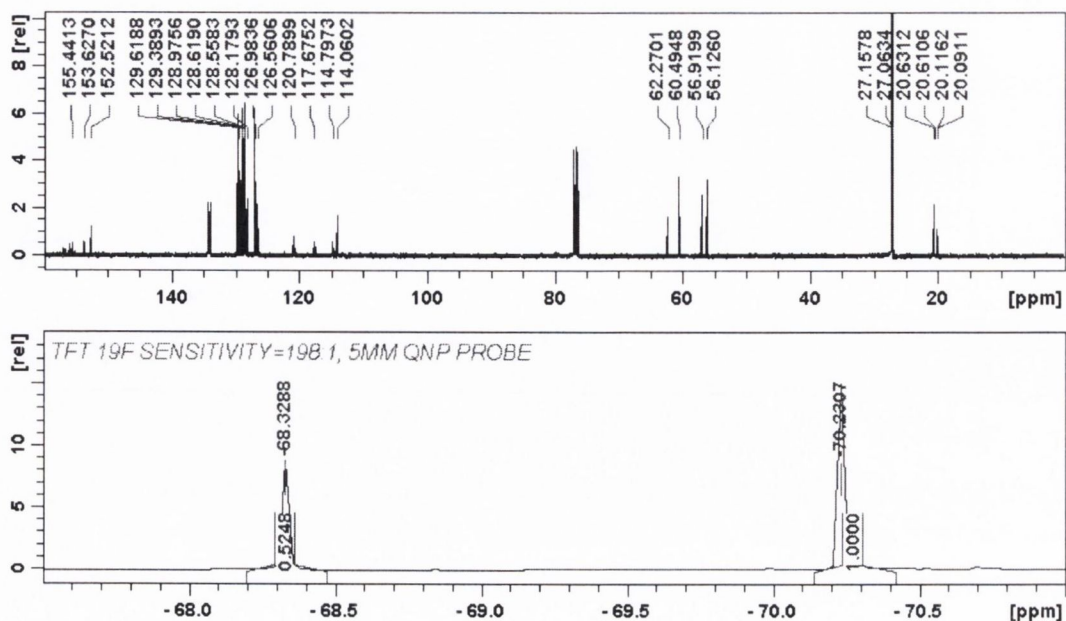
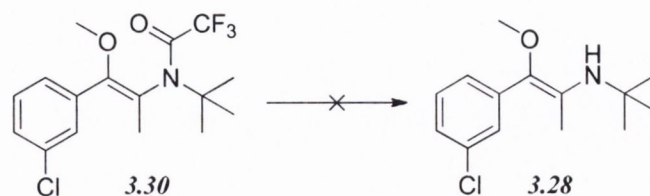


Figure 3.21 ^{13}C NMR and ^{19}F NMR spectra of 3.30

There are numerous methods for the deprotection of TFA amide groups. Most methods employ basic conditions for its removal. In the case of **3.30**, the methods used to remove the TFA group are summarized in Table 3.1. Regardless of the conditions employed the TFA group resisted removal.



Scheme 3.25 Attempted removal of the trifluoroacetyl protecting group

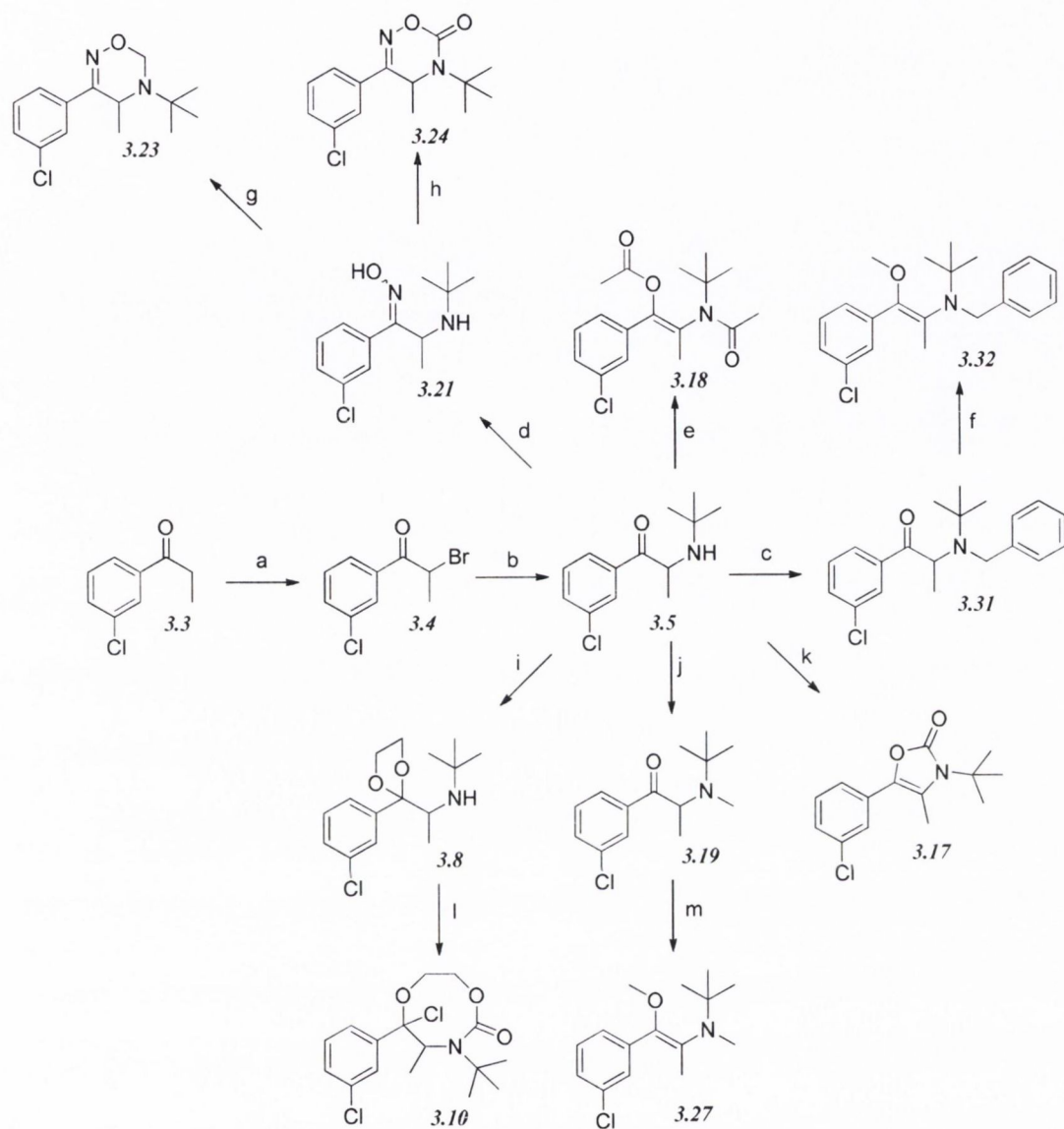
Reagent	Solvent	Temperature / Time	Reference
Potassium Carbonate	MeOH/H ₂ O	RT-reflux 24 h	[175]
Lithium hydroxide	THF/ MeOH/H ₂ O	RT-reflux 24 h	[176]
Potassium hydroxide/Et ₃ BnNH ₄ Cl	H ₂ O	RT-reflux 24h	[177]
NH ₃	Methanol	RT 24 h	[178]
KOH/Et ₃ BnNBr	H ₂ O/DCM	RT 24 h	[177]
0.2M Ba(OH) ₂	Methanol	RT-reflux 24 h	[179]
NaBH ₄	Ethanol	RT-reflux 24 h	[180]
HCl (conc)	MeOH	RT-reflux 24 h	[181]

Table 3.1 Deprotection strategies for N-TFA O-Me analogue of bupropion 3.30

3.4 Conclusion

This chapter describes the synthesis of potential prodrugs of bupropion. Scheme 3.26 summarises the successful syntheses leading to derivatives that may be transformed to bupropion *in vivo*. A number of prodrug types were successfully synthesized and fully characterised by spectroscopic methods. Some of the analogues are simple mono-prodrugs such as the amide, hydroxyimine, *N*-methylated and *N*-benzylated types. Others are more complex such as the oxazolone, oxadiazine, oxadiazinone and diacetyl enol amide, and may require a multistep prodrug pathway to return to them to the parent compound, bupropion.

The next phase of the project focuses on implementing appropriate *in vitro* screening tools to monitor the conversion of these potential prodrugs back to bupropion. It is hoped that these methods will mirror the behaviour of these compounds *in vivo*.



Scheme 3.26 Summary of successful synthesis of potential prodrugs of bupropion.

a) DCM, Br_2 , RT, 30 min, b) NMP, *t*-butylamine, 60°C , 1 h, c) ACN, DIPEA, BnBr, reflux, 36 h, d) Py, NH_2OH , reflux, 2 h, e) Ac_2O , TEA, DMAP, -20°C , 12 h, f) NaH, CH_3I , DMF, RT, 30 min, g) EtOH, *p*-TSA, paraformaldehyde, reflux, 8 h, h) DCM, TEA, phosgene, 0°C , 2 h, i) Toluene, H_2SO_4 , Ethanediol, reflux, 60 h, j) ACN, DIPEA, CH_3I , RT, 12 h, k) ACN, TEA, phosgene, 0°C , 2 h, l) DCM, TEA, phosgene, 0°C , 2 h, m) DMF, NaH, CH_3I , RT, 2 h.

3.5 *Experimental*

3.5.1 Reagents and chemicals

Bupropion hydrobromide reference standard was supplied from Biovail Technologies Ireland Ltd, Citywest Business Campus, Dublin 24, Ireland. Pooled human liver microsomes, pooled human intestinal microsomes, guinea pig S9 fraction, and NADP regenerating solutions were supplied by BDBiosciences, 1 Becton Drive, Franklin Lakes, NJ, USA, 07417. Citrated human plasma was obtained from healthy male and female volunteers from the School of Pharmacy and Pharmaceutical Sciences, Trinity College, Dublin. LC-MS grade solvents were purchased from Fisher Scientific Ireland. Pepsin, from porcine stomach mucosa, with an activity of 800 to 2500 units per mg of protein (Sigma-Aldrich catalogue number P7000). Pancreatin (Sigma-Aldrich catalogue number P8096). Phosphate buffered saline tablets, (Sigma-Aldrich catalogue number P4417). HPLC grade solvents and all other reagents were analytical grade and purchased from Sigma Aldrich Ireland. Bupropion hydrochloride reference standard and its metabolite standards were purchased from Toronto Research Chemicals, 2 Brisbane Road, North York, Ontario, Canada, M3J 2J8.

3.5.2 Instrumentation

Chromatographic analysis was carried out on a Thermo Accela liquid chromatograph. The detector was a Thermo LTQ-XL-Orbitrap Discovery mass spectrometer. Centrifugation was carried out on an IEC Micromax centrifugator. Vortex mixing was carried out on a Velp Scientifica Rx3 vortex mixer. Standards were stored in a Thermo Forma -80°C ULT freezer. Infra-red (IR) spectra were obtained using a Nicolet 205 FT Infra-red spectrometer. Band positions are given in cm^{-1} . Solid IR test samples were obtained as KBr discs; oils were analysed as neat films on NaCl plates. ^1H and ^{13}C NMR spectra were recorded at 27°C on a Bruker DPX 400 MHz FT NMR spectrometer (400.13MHz ^1H , 100.61MHz ^{13}C), in either CDCl_3 (tetramethylsilane as internal standard) or CD_3OD . For CDCl_3 , ^1H NMR spectra were assigned relative to the TMS peak at 0.00 δ and ^{13}C NMR spectra were assigned relative to the middle CDCl_3 triplet at 77.00ppm. For CD_3OD , ^1H and ^{13}C NMR spectra were assigned relative to the centre peaks of CD_3OD multiplets at 3.30 δ and 49.00 ppm respectively. Coupling constants are reported in Hertz. For ^1H NMR assignments, chemical shifts are reported: shift values (number of protons, description of absorption, coupling constant(s) where applicable, proton assignment). High resolution mass spectra were obtained on a Thermo LTQ XL-Orbitrap discovery at the School of Pharmacy and Pharmaceutical Sciences, Trinity College Dublin. Flash column chromatography was carried out on Merck Silica Gel 60 (particle size 0.040-0.063mm). Thin Layer Chromatography (TLC) was carried out on Merck Silica gel F254 plates.

3.5.3 Synthesis of 2-bromo-1-(3-chlorophenyl) propan-1-one (3.4)

To a stirred solution of **3.3** (10.0 g, 59.3 mmol) in dichloromethane (50 mL) in a round bottomed flask was added dropwise 1.0 M Br₂ in dichloromethane until the bromine colour remained. The residual dichloromethane and bromine was removed under vacuum to afford a brown oil. The brown oil was found to be pure by TLC analysis. (15g, 99 % yield). ¹H NMR δ (CDCl₃): 1.90-1.92 (d, 3H, J = 6.71 Hz, -CH₃), 5.22-5.27 (q, 1H, J = 6.59 and 6.97 Hz, -CH), 7.42-7.46 (t, 1H, J = 7.97 Hz, Ar-H), 7.56-7.58 (d, 1H, J = 8.04 Hz, Ar-H), 7.89-7.91 (d, 1H, J = 8.04 Hz, Ar-H), 7.99-8.00 (t, 1H, J = 1.75 Hz, Ar-H). ¹³C NMR ppm (CDCl₃): 19.5 (-CH₃), 40.8 (-CH-Br), 126.5, 128.5, 129.6, 133.1, 134.6, 135.1 (6 × Ar-C), 191.6 (-C=O). IR V_{max} (film): 1682 (-C=O). LRMS (M+H⁺); actual 246.95, found 247.1.

3.5.4 Synthesis of bupropion hydrochloride (3.6)

To a stirred solution of **3.4** (15.0g, 60.6 mmol) in N-Methyl-2-pyrrolidone (50 mL) in a round bottomed flask was added t-butylamine hydrochloride (6.64 g, 6.06 mmol). The mixture was heated to 60 °C for 60 min. The contents of the flask were then transferred to a separating funnel, 25 mL of water was added, and the mixture was extracted three times with 25-mL portions of ether. The combined ether extracts were washed with five 25-mL portions of water and dried over anhydrous magnesium sulphate. HCl gas was bubbled through the ether extracts providing the HCl salt. The excess ether was removed under vacuum and the solid remaining was washed with ether. After drying, a white solid remained. (16.6g, 99 % yield). ¹H NMR δ (CD₃OD): 1.16 (s, 9H, -C(CH₃)₃), 1.34-1.36 (d, 3H, J = 7.13 Hz, -CH₃), 4.60-4.65 (q, 1H, J = 6.86 and 7.15 Hz, -CH), 7.62-8.14 (m, 4H, 4 × Ar-H). ¹³C NMR ppm (CD₃OD): 22.8 (-CH₃), 30.1 (-C(CH₃)₃), 53.0 (-C(CH₃)₃), 53.9 (-CH), 128.6, 130.0, 132.3, 135.2, 136.9, 138.2 (6 × Ar-C), 204.6 (-C=O). IR V_{max} (KBr): 2771 (NH), 1692 (-C=O). HRMS (M+H⁺); actual 240.1150, found 240.1147.

3.5.5 Synthesis of a dioxolane of bupropion (3.8)

To a stirred solution of **3.5** (1.0 g, 3.1 mmol) in toluene (50 mL) in a double neck round bottomed flask was added ethanediol (2.0 mL, 32 mmol) and concentrated sulfuric acid (0.1 mL, 1.0 mmol). A dean stark apparatus was attached to the vertical neck of the flask and the mixture was refluxed for 60 h at 200 °C. The high temperature was required in order for the reaction to proceed as gentle reflux was not sufficient. Ethanediol and toluene were added to the reaction mixture as required by the removal across the dean stark with water. An aqueous solution of saturated sodium bicarbonate (10 mL) was added. The mixture was extracted with 3 x 10 mL portions of ethyl acetate. The ethyl acetate washings were combined and dried over anhydrous magnesium sulphate. The ethyl acetate was removed under vacuum. Methanol (10 mL) was added. With gentle stirring, sodium borohydride (0.1 g, 2.6 mmol) was added slowly,

to convert any remaining ketone to the alcohol. This aided in the purification of the mixture. An aqueous solution of saturated sodium bicarbonate (10 mL) was added. The mixture was extracted with 3 x 10 mL portions of ethyl acetate. The ethyl acetate washings were combined and dried over anhydrous magnesium sulphate. Silicon dioxide (1 g) was added and the ethyl acetate removed under vacuum. This mixture was separated and purified into homogenous fractions by flash column chromatography using hexane : ethyl acetate (9:1) as mobile phase. The solvent was removed under vacuum. After drying, a clear oil remained, 0.6 g (68 %) yield. $^1\text{H NMR } \delta$ (CDCl_3): 0.93 (s, 9H, $-\text{C}(\text{CH}_3)_3$), 1.06-1.08 (d, 3H, $J = 6.56$ Hz, $-\text{CH}_3$), 2.99-3.04 (q, 1H, $J = 6.55$ and 6.56 Hz, $-\text{CH}$), 3.72-3.83 (m, 2H, $-\text{CH}_2-$), 3.40-4.10 (m, 2H, $-\text{CH}_2-$), 7.25-7.50 (m, 4H, $4 \times \text{Ar-H}$). $^{13}\text{C NMR ppm}$: 18.7 ($-\text{CH}_3$), 29.4 $-\text{C}(\text{CH}_3)_3$, 50.1 $-\text{C}(\text{CH}_3)_3$, 53.4 $-\text{CH}$, 64.3 $-\text{CH}_2-$, 64.5 $-\text{CH}_2-$, 110.7 $-\text{CO}_2-$, 124.8, 126.9, 127.3, 128.4, 133.1, 143.5 ($6 \times \text{Ar-C}$). IR V_{max} (film): 3462 (NH), 1175 ($-\text{CO}_2-$). LRMS ($\text{M}+\text{H}^+$); actual 284.14, found 284.1.

3.5.6 Synthesis of a 8-membered ring cyclic carbamate of bupropion (3.10)

To a stirred solution of **3.8** (0.3 g, 1.0 mmol) in dry dichloromethane (5 mL) in a round bottomed flask under a nitrogen atmosphere was added triethylamine (0.3 g, 3.0 mmol). The mixture was chilled to 0 °C and phosgene (20 % in toluene, 1.0 g, 2 mmol) was added dropwise. The mixture was allowed to equilibrate to room temperature over 2 h. A gentle stream of nitrogen gas was passed through the mixture to remove any residual phosgene. An aqueous solution of saturated sodium bicarbonate (10 mL) was added slowly. The mixture was extracted with 3 x 10 mL portions of diethyl ether. The diethyl ether washings were combined and dried over anhydrous magnesium sulphate. Silicon dioxide (1 g) was added and the diethyl ether removed under vacuum. This mixture was separated and purified into homogenous fractions by flash column chromatography using initially 100 % hexane, but with an increasing gradient of ethyl acetate as mobile phase. The solvent was removed under vacuum. After drying, two compounds remained, a colourless oil 0.12 g (35 %) yield, and a yellow oil 0.07 g (20 %) yield. Diastereomer 1; $^1\text{H NMR } \delta$ (CDCl_3): 0.78-0.80 (d, 3H, $J = 6.61$ Hz, $-\text{CH}_3$), 1.48 (s, 9H, $-\text{C}(\text{CH}_3)_3$), 3.38-3.45 (m, 1H, $-\text{CH}_2-$), 3.56-3.59 (m, 2H, $-\text{CH}_2-$), 3.75-3.82 (m, 1H, $-\text{CH}_2-$), 3.96-4.01 (q, 1H, $J = 6.61$ and 6.61 Hz, $-\text{CH}$), 7.37-7.52 (m, 4H, $4 \times \text{Ar-H}$). $^{13}\text{C NMR ppm}$: 19.3 $-\text{CH}_3$, 28.2 $-\text{C}(\text{CH}_3)_3$, 43.1 $-\text{CH}_2-$, 54.1 $-\text{C}(\text{CH}_3)_3$, 61.4 $-\text{CH}$, 63.6 $-\text{CH}_2-$, 105.4 $-\text{COCl}$, 123.9, 125.9, 129.6, 130.0, 134.9, 136.6 ($6 \times \text{Ar-C}$), 153.8 ($-\text{C}=\text{O}$). IR V_{max} (KBr): 3330, 1729, 1263. LRMS ($\text{M}+\text{H}^+$); actual 346.09, found 346.2.

Diastereomer 2; $^1\text{H NMR } \delta$ (CDCl_3): 0.80-0.82 (d, 3H, $J = 6.61$ Hz, $-\text{CH}_3$), 1.50 (s, 9H, $-\text{C}(\text{CH}_3)_3$), 3.40-3.46 (m, 1H, $-\text{CH}_2-$), 3.59-3.62 (m, 2H, $-\text{CH}_2-$), 3.90-3.86 (m, 1H, $-\text{CH}_2-$), 3.99-4.05 (m, 1H, $-\text{CH}$), 7.30-7.61 (m, 4H, $4 \times \text{Ar-H}$). $^{13}\text{C NMR ppm}$: 19.3 $-\text{CH}_3$, 28.2 $-\text{C}(\text{CH}_3)_3$, 43.1 $-\text{CH}_2-$, 54.1 $-\text{C}(\text{CH}_3)_3$, 61.4 $-\text{CH}$, 63.6 $-\text{CH}_2-$, 105.4 $-\text{COCl}$, 123.9, 125.9, 129.6, 130.0,

134.6, 136.6 (6 × Ar-C), 153.8 (-C=O). IR V_{\max} (film): 3333, 1735, 1251. LRMS (M+H⁺); actual 346.09, found 346.1.

3.5.7 Synthesis of the dioxolane brominated starting material (3.15)

To a stirred solution of **3.4** (1.0 g, 4.0 mmol) in toluene (20 mL) in a round bottomed flask was added ethylene glycol (5 mL, 80 mmol) and a catalytic amount of p-toluenesulfonic acid. A dean stark apparatus with condenser was attached and the mixture was refluxed 3 hours. The toluene was removed under vacuum and a saturated solution of sodium bicarbonate was added (25 mL). The mixture was extracted with 3 x 10 mL portions of diethyl ether and the extracts were pooled and ether removed under vacuum. Methanol (25 mL) and sodium borohydride (0.15 g, 4 mmol) were added. The methanol was reduced under vacuum and water (20 mL) was added. This mixture was extracted with 3 x 10 mL portions of diethyl ether and the extracts were pooled and ether removed under vacuum. This mixture was separated and purified into homogenous fractions by flash column chromatography on silica gel with a 100 % hexane mobile phase. After drying, the major product was a pale yellow oil, 0.69 g (75 %) yield. ¹H NMR δ (CDCl₃): 1.58-1.60 (d, 3H, J = 7.00 Hz, -CH₃), 3.85-3.89 (m, 2H, -CH₂-), 4.13-4.17 (m, 2H, -CH₂-), 4.30-4.36 (q, 1H, J = 6.90 and 6.90 Hz, -CH-), 7.29-7.52 (m, 4H, 4 × Ar-H). ¹³C NMR ppm: 20.8 -CH₃, 53.5 -CH-, 65.7 -CH₂-, 66.0 -CH₂-, 108.8 -CO₂-, 125.0, 127.0, 128.7, 129.4, 134.0, 141.4 (6 × Ar-C).

3.5.8 Synthesis of the oxazolone of bupropion (3.17)

To a stirred solution of **3.5** (1.0 g, 3.1 mmol) in dry dichloromethane (30 mL) in a round bottomed flask under a nitrogen atmosphere was added triethylamine (1.7 g, 12.5 mmol). The mixture was chilled to 0 °C and phosgene (20 % in toluene, 10 g, 20 mmol) was added dropwise. The mixture was allowed to equilibrate to room temperature over 2 h. A gentle stream of nitrogen gas was passed through the mixture to remove any residual phosgene. An aqueous solution of saturated sodium bicarbonate (10 mL) was added slowly. The mixture was extracted with 3 x 10 mL portions of diethyl ether. The diethyl ether washings were combined and dried over anhydrous magnesium sulphate. Silicon dioxide (1 g) was added and the diethyl ether removed under vacuum. This mixture was separated and purified into homogenous fractions by flash column chromatography using initially 100 % hexane, but with an increasing gradient of ethyl acetate as mobile phase. The solvent was removed under vacuum. After drying, a white solid remained, 0.6 g (73 %) yield. ¹H NMR δ (CDCl₃): 1.60 (s, 9H, -C(CH₃)₃), 2.30 (s, 3H, -CH₃), 7.14-7.34 (m, 4H, 4 × Ar-H). ¹³C NMR ppm: 13.2 -CH₃, 29.0 -C(CH₃)₃, 58.0 -C(CH₃)₃, 120.7 (-C=C-), 123.9 (Ar-CH), 125.7 (Ar-CH), 127.1 (Ar-CH), 129.4 (Ar-CH), 129.5 (-C=C-), 133.0 (Ar-C), 133.9 (Ar-C), 153.5 (-C=O). Melting point range 178-180°C. V_{\max} (KBr): 1645 (-C=O), 1152 (-CO-). LRMS (M+H⁺); actual 266.09, found 266.1.

3.5.9 Synthesis of the (E/Z)-N,O-diacetylated bupropion (3.18)

To a stirred solution of **3.5** (0.5g, 1.6 mmol) in acetic anhydride (5 mL) at -20 °C in a round bottomed flask was added triethylamine (0.5g, 5 mmol) and a catalytic amount of dimethylaminopyridine. The solution was stirred overnight and allowed to equilibrate to room temperature. While stirring, a solution of saturated aqueous sodium bicarbonate was added dropwise slowly until the effervescence of carbon dioxide ceased and a precipitate remained. The aqueous solution was transferred quantitatively to a separating funnel. The mixture was extracted with 3 x 20 mL portions of hexane. The hexane extracts were combined and dried over anhydrous magnesium sulphate. Silicon dioxide (5 g) was added and the solvent removed under vacuum. This mixture was separated and purified into homogenous fractions by flash column chromatography using 9:1 hexane : ethyl acetate as mobile phase. The solvent was removed under vacuum. The E and Z isomers could not be resolved. The major product was a clear oil, yield 0.19 g (37.1 %). ¹H NMR δ (CDCl₃): 1.51-1.52 (m, 9H, -C(CH₃)₃), 1.96-1.97(m, 3H, -CH₃), 2.12-2.15 (m, 6H, 2 x C=OCH₃), 7.29-7.38 (m, 4H, 4 x ArH). ¹³C NMR ppm: 20.4 (-CC=OCH₃), 20.6 (-CC=OCH₃), 23.7 -CH₃, 28.0 -C(CH₃)₃, 58.0 -C(CH₃)₃, 126.3, 127.9, 128.7, 129.3 (4 x Ar-CH), 128.2, 133.9, 135.4, 143.9 (4 x Ar-C), 167.8 -C=O, 169.5 -C=O. V_{max} (film): 1742, 1685. HRMS (M+H⁺); actual 324.1361, found 324.1357.

3.5.10 Synthesis of N-methyl bupropion (3.19)

To a stirred solution of **3.5** (1.0 g, 3.1 mmol) in acetonitrile (25 mL) in a round bottomed flask was added diisopropylethylamine (0.8 g, 6.3 mmol) and methyl iodide (1.0 g, 7.1 mmol). The mixture was allowed to stir overnight at room temperature. An aqueous solution of saturated sodium bicarbonate (10 mL) was added. The mixture was extracted with 3 x 10 mL portions of ethyl acetate. The ethyl acetate washings were combined and dried over anhydrous magnesium sulphate. Silicon dioxide (2 g) was added and the ethyl acetate removed under vacuum. This mixture was separated and purified into homogenous fractions by flash column chromatography using hexane : ethyl acetate (9:1) as mobile phase. The solvent was removed under vacuum. After drying, a pale yellow oil remained, 0.5 g (63 %) yield. ¹H NMR δ (CDCl₃): 1.21 (s, 9H, -C(CH₃)₃), 1.27-1.28 (d, 3H, J = 6.55 Hz, -CHCH₃), 2.18 (s, 3H, -NCH₃), 4.59-4.64 (q, 1H, J = 6.46 and 6.58 Hz, -CHCH₃), 7.36-8.09 (m, 4H, 4 x ArH). ¹³C NMR ppm: 11.4 -CHCH₃, 27.7 -C(CH₃)₃, 28.7 -NCH₃, 54.7 -C(CH₃)₃, 57.0 -CHCH₃, 126.2, 128.5, 128.9, 131.6, 133.8, 138.3 (6 x ArC), 200.7 -C=O. V_{max} (film): 1701. HRMS (M+H⁺); actual 254.1306, found 254.1299.

3.5.11 Synthesis of bupropion hydroxyimine (3.21)

To a stirred solution of **3.5** (1.0 g, 3.12 mmol) in pyridine (10 mL) in a round bottomed flask was added hydroxylamine hydrochloride (0.28 g, 4.0 mmol). The solution was refluxed for 2 h. Toluene (25 mL) was added and the solvent removed under vacuum at elevated temperature.

This was repeated twice more to remove the remaining solvent. Ethyl acetate (10 mL was added) and then silicon dioxide (5 g). The remaining solvent was removed under vacuum. This mixture was separated and purified into homogenous fractions by flash column chromatography using 9:1 dichloromethane : methanol as mobile phase. The solvent was removed under vacuum. The major product were a white solid, two isomers yield 0.2 g (37.5 %). ^1H NMR δ (CDCl_3): 1.21 (s, 9H, $-\text{C}(\text{CH}_3)_3$), 1.26-1.28 (d, 3H, $J = 6.87$ Hz, $-\text{CHCH}_3$), 3.82-3.87 (q, 1H, $J = 6.77$ and 6.81 Hz, $-\text{CHCH}_3$), 7.29-7.47 (m, 4H, 4 x ArH). ^{13}C NMR ppm (CDCl_3): 22.9 - CHCH_3 , 29.1 $-\text{C}(\text{CH}_3)_3$, 51.7 $-\text{CHCH}_3$, 52.2 $-\text{C}(\text{CH}_3)_3$, 126.4, 128.3, 128.9, 129.5, 134.2, 134.5 (6 x ArC), 157.6 $-\text{C}=\text{N}$ -. Melting point range; 202-206°C. V_{max} (KBr): 3434, 3301, 1651. HRMS ($\text{M}+\text{H}^+$); actual 255.1259, found 255.1249.

3.5.12 Synthesis of the benzyl oximine of bupropion (3.22)

Bupropion **3.5** (1.26 g, 3.9 mmol), benzyloxyamine hydrochloride (0.69 g, 4.3 mmol), sodium acetate (0.53 g, 6.5 mmol) were refluxed in an ethanol:water mixture (4:1, 40 mL) in a round bottomed flask for 6 hours. The ethanol was removed under vacuum and the mixture was extracted with 3 x 10 mL portions of diethyl ether. The extracts were combined and reduced under vacuum. The resulting mixture was separated and purified into homogeneous fractions on silica gel with a mobile phase of hexane:ethyl acetate (80:20). After drying, a clear oil remained, two isomers, 0.5 g (33%) yield. ^1H NMR δ (CDCl_3): 1.00 (s, 9H, $-\text{C}(\text{CH}_3)_3$), 1.38-1.40 (d, 3H, $J = 7.10$ Hz, $-\text{CH}_3$), 4.33-4.38 (q, 1H, $J = 7.07$ and 7.13 Hz, $-\text{CHCH}_3$), 5.25 (s, 2H, $-\text{CH}_2-$), 7.29-7.72 (m, 9H, 9 x ArCH). ^{13}C NMR ppm (CDCl_3): 11.4 $-\text{C}(\text{CH}_3)_3$, 15.3 $-\text{CHCH}_3$, 68.2 $-\text{C}(\text{CH}_3)_3$, 74.6 $-\text{CHCH}_3$, 76.1 $-\text{CH}_2-$, 124.9 ArCH, 126.9 ArCH, 128.0 ArCH, 128.1 (2 x ArCH), 128.3 ArCH, 128.5 (2 x ArCH), 129.9 ArCH, 134.6 $-\text{C}=\text{N}$ -, 137.6, 142.1, 157.6 (3 x ArC). LRMS ($\text{M}+\text{H}^+$); actual 345.17, found 345.3.

3.5.13 Synthesis of an oxadiazine of bupropion (3.23)

To a stirred solution of **3.21** (0.3 g, 1.2 mmol) in ethanol (10 mL) in a round bottomed flask was added paraformaldehyde (1.1 g) and a catalytic amount of p-toluenesulfonic acid. This mixture was refluxed for 8 h. An aqueous saturated sodium bicarbonate solution (10 mL) was added and the mixture was quantitatively transferred to a separating funnel. The mixture was extracted with 3 x 10 mL portions of ethyl acetate. The ethyl acetate washings were combined and dried over anhydrous magnesium sulphate. Silicon dioxide (1 g) was added and the ethyl acetate removed under vacuum. This mixture was separated and purified into homogenous fractions by flash column chromatography using 9:1; hexane : ethyl acetate as mobile phase. The solvent was removed under vacuum. After drying, a white solid remained, 0.1g (31 %) yield. ^1H NMR δ (CDCl_3): 1.26 (s, 9H, $-\text{C}(\text{CH}_3)_3$), 1.30-1.31 (d, 3H, $J = 7.00$ Hz, $-\text{CH}_3$), 3.90-3.95 (q, 1H, $J = 6.86$ and 6.69 Hz, $-\text{CHCH}_3$), 4.74-4.77 (d, 1H, $J = 11.23$ Hz, $-\text{CH}_2$), 5.14-5.17 (dd, 1H, $J = 1.81$

and 9.88 Hz, $-\text{CH}_2$), 7.34-7.57 (m, 4H, 4 x ArCH). ^{13}C NMR ppm: 21.3 $-\text{CHCH}_3$, 28.2 $-\text{C}(\text{CH}_3)_3$, 44.1 $-\text{CHCH}_3$, 55.0 $-\text{C}(\text{CH}_3)_3$, 75.3 $-\text{CH}_2$, 124.2, 126.2, 129.5, 129.9, 134.7, 137.3 (6 x ArC), 160.4 $-\text{C}=\text{N}-$. Melting point range; 169-175°C. V_{max} (KBr): 1673. HRMS ($\text{M}+\text{H}^+$); actual 267.1259, found 267.1250.

3.5.14 Synthesis of an oxadiazinone of bupropion (3.24)

To a stirred solution of **3.21** (0.5 g, 2.0 mmol) in dry dichloromethane (30 mL) in a round bottomed flask under a nitrogen atmosphere was added triethylamine (0.7 g, 7.1 mmol). The mixture was chilled to 0 °C and phosgene (20 %, 2.0 g, 4 mmol) was added dropwise. The mixture was allowed to equilibrate to room temperature over 2 h. A gentle stream of nitrogen gas was passed through the mixture to remove any residual phosgene. An aqueous solution of saturated sodium bicarbonate (10 mL) was added slowly. The mixture was extracted with 3 x 10 mL portions of diethyl ether. The diethyl ether washings were combined and dried over anhydrous magnesium sulphate. Silicon dioxide (1 g) was added and the diethyl ether removed under vacuum. This mixture was separated and purified into homogenous fractions by flash column chromatography using initially 100 % hexane, but with an increasing gradient of ethyl acetate as mobile phase. The solvent was removed under vacuum. After drying, a yellow oil remained, 0.1 g (18 %) yield. ^1H NMR δ (CDCl_3): 1.45-1.47 (d, 3H, $J = 6.89$ Hz, $-\text{CH}_3$), 1.57 (s, 9H, $-\text{C}(\text{CH}_3)_3$), 4.73-4.78 (q, 1H, $J = 6.86$ and 6.82 Hz, $-\text{CHCH}_3$), 7.44-7.72 (m, 4H, 4 x ArCH). ^{13}C NMR ppm: 18.4 $-\text{CH}_3$, 28.2 $-\text{C}(\text{CH}_3)_3$, 47.2 $-\text{CHCH}_3$, 57.4 $-\text{C}(\text{CH}_3)_3$, 124.0, 126.0, 130.0, 131.0, 131.2, 134.9 (6 x ArC), 151.3 $-\text{C}=\text{N}-$, 160.3 $-\text{C}=\text{O}$. V_{max} (film): 1692, 1641. HRMS ($\text{M}+\text{H}^+$); actual 281.1051, found 281.1040.

3.5.15 Synthesis of *N,O*-dimethylated bupropion (3.27)

To a stirred solution of **3.19** (0.05 g, 0.18 mmol) in dry dimethylformamide in a round bottomed flask was added sodium hydride (60 % in mineral oil, 0.01 g, 0.4 mmol). The solution was left stirring at room temperature for 30 min under a nitrogen atmosphere. Methyl iodide (0.03 g, 0.2 mmol) was added dropwise. After 2 h the reaction was quenched by addition of a saturated aqueous solution of sodium bicarbonate (10 mL). The mixture was extracted with 3 x 5 mL portions of diethyl ether. The diethyl ether washings were combined and dried over anhydrous magnesium sulphate. Silicon dioxide (1 g) was added and the diethyl ether removed under vacuum. This mixture was separated and purified into homogenous fractions by flash column chromatography using hexane : ethyl acetate (9:1) as mobile phase. The solvent was removed under vacuum. After drying, a yellow oil remained, 0.02 g (42 %) yield. ^1H NMR δ (CDCl_3): 0.96 (s, 9H, $-\text{C}(\text{CH}_3)_3$), 1.85 (s, 3H, $-\text{CH}_3$), 2.49 (s, 3H, $-\text{NCH}_3$), 3.40 (s, 3H, $-\text{OCH}_3$), 7.20-7.70 (m, 4H, 4 x ArCH). ^{13}C NMR ppm: 12.0 $-\text{CH}_3$, 27.3 $-\text{C}(\text{CH}_3)_3$, 33.6 $-\text{NCH}_3$, 54.8 $-\text{C}(\text{CH}_3)_3$, 57.2

-OCH₃, 126.2 (2 x ArCH), 128.2 ArCH, 128.5 ArCH, 132.7, 133.7 (2 x ArC), 137.1, 150.3 (2 x -C=C-). V_{max} (film): 1621, 1211. HRMS (M+H⁺); actual 268.1463, found 268.1461.

3.5.16 Synthesis of *N*-benzyl bupropion (3.31)

To a stirred solution of **3.5** (0.5 g, 1.6 mmol) in acetonitrile (5 mL) in a round bottomed flask was added di-isopropylethylamine (0.60 g, 4.5 mmol) and benzyl bromide (0.29 g, 1.7 mmol). The mixture was refluxed for 36 h. The contents of the flask were washed into a separating funnel with 2 x 5 mL aliquots of water, then ethyl acetate (10 mL). The mixture was washed with 3 x 10 mL portions of ethyl acetate and the aqueous layer was discarded. The remaining organic layer was dried over anhydrous magnesium sulphate (5 g) and reduced under vacuum. Silicon dioxide (5 g) was added and the remaining solvent was removed under vacuum. This mixture was separated and purified into homogenous fractions by flash column chromatography using 95:5 hexane : ethyl acetate as mobile phase. The solvent was removed under vacuum. The major product was a bright yellow oil, yield 0.2 g (37.5 %). ¹H NMR δ (CDCl₃): 1.20 (s, 9H, -C(CH₃)₃), 1.39-1.41 (d, 3H, J = 6.76 Hz, -CHCH₃), 3.99-4.04 (d, 1H, J = 16.70 Hz, -CH₂-), 4.10-4.14 (d, 1H, 16.68 Hz, -CH₂-), 4.73-4.78 (q, 1H, J = 6.65 and 6.96 Hz, -CHCH₃), 7.11-7.77 (m, 9H, 9 x ArCH). ¹³C NMR ppm (CDCl₃): 13.9 -CH₃, 28.8 -C(CH₃)₃, 47.7 -CHCH₃, 55.9 -C(CH₃)₃, 56.2 -CH₂-, 125.5 ArC, 125.9 ArC, 127.2 (2 x ArCH), 127.4 (2 x ArCH), 128.1 ArC, 128.9 ArC, 131.7 ArC, 133.9 ArC, 138.2 ArC, 142.5 ArC, 201.9 -C=O. V_{max} (film): 1732. HRMS (M+H⁺); actual 330.1619, found 330.1611.

3.5.17 Synthesis of (*E/Z*)-*O*-methyl *N*-benzyl bupropion (3.32)

To a stirred solution of **3.31** (0.1 g, 0.3 mmol) in dry dimethylformamide (3 mL) at room temperature in a round bottomed flask was added sodium hydride (0.01 g, 0.3 mmol). The solution was allowed to stir at room temperature for 30 min. Methyl iodide (0.05 g, 0.3 mmol) was added slowly and left stirring at room temperature for 2 h. A saturated aqueous solution of sodium bicarbonate was added (10 mL) and the mixture was quantitatively transferred to a separating funnel. The mixture was extracted with 3 x 10 mL portions of hexane. The hexane extracts were combined and dried over anhydrous magnesium sulphate. Silicon dioxide (1 g) was added and the solvent removed under vacuum. This mixture was separated and purified into homogenous fractions by flash column chromatography using 50:1 hexane : ethyl acetate as mobile phase. The solvent was removed under vacuum. After drying, a yellow oil remained, yield 0.02g (15 %). ¹H NMR δ (CDCl₃): 1.20 (s, 9H, -C(CH₃)₃), 1.99 (s, 3H, -CH₃), 3.21 (s, 3H, -OCH₃), 3.66-3.96 (dd, 2H, J = 13.2 and 93.3 Hz, -CH₂-), 7.00-7.75 (m, 9H, 9 x ArCH). ¹³C NMR ppm: 12.0, 28.0, 29.3, 49.5, 55.8 -, 57.0, 126.0, 126.1, 127.1, 127.6, 128.5, 129.3, 129.7, 132.3, 136.5, 138.7. V_{max} (film): 1610, 1016. HRMS (M+H⁺); actual 344.1776, found 344.1785.

Chapter 4 - The screening and evaluation of potential prodrugs of bupropion

This chapter describes the development of an *in vitro* screening tool to assess the potential prodrugs synthesized in Chapter 3. A successful tool was developed for *in vitro* screening of potential prodrugs of bupropion which utilised 5 different media that a drug substance would encounter via the oral route of delivery. Two direct prodrugs of bupropion were discovered using the prodrug screening tool, *N*-methyl bupropion **3.19** and *N*-benzyl bupropion **3.31**. The *N*-methyl, *N*-benzyl and oxadiazine were all *N*-dealkylated by human liver and human intestinal microsomes indicating that the tertiary amine is susceptible to oxidation by the CYP or FMO enzymes. Two potential multistep prodrugs of bupropion were discovered, *N,O*-dimethyl bupropion **3.27** and *N*-benzyl *O*-methyl bupropion **3.32**, which in themselves are prodrugs of *N*-methyl and *N*-benzyl bupropion respectively. *N*-methyl bupropion **3.19** was evaluated for its enzyme kinetics, pharmacology and stability. *N*-methyl bupropion was also shown to be reduced to the amino alcohol, this new metabolite could also have potential pharmacotherapies. *N*-methyl bupropion was shown to have a similar stability profile to bupropion below pH 5. The pharmacological profile of *N*-methyl bupropion was screened in a DAT, NET, SERT, nAChR and nMAChR assay. It was shown to be less active than bupropion. *N*-methyl bupropion was deemed a good candidate as a potential prodrug of bupropion for an *in vivo* proof of concept study.

4 The screening and evaluation of potential prodrugs of bupropion

4.1 Introduction

There are numerous barriers that hinder drug discovery and delivery. In a biological system, multiple mechanisms exist to protect the system from exposure to foreign substances while preserving nutrient uptake. The physiological arrangement and the chemical and biochemical barriers associated with the physiological structures form the first line of defence. How a drug molecule interacts with these barriers is determined by the properties of the molecule. These properties are the physicochemical and/or biochemical characteristics of the molecule. Pharmacokinetics and pharmacodynamics provide a general approach by allowing modelling of the interaction of a drug molecule with the entire biological system to predict drug concentrations in the systemic circulation and therefore providing a prediction of pharmacological responses. Developability in drug delivery is an overall assessment of the above factors.

After synthesis of potential prodrug candidates, an *in vitro* assay was needed to predict the viability of these prodrugs and to determine which of these prodrugs would be a good candidate for a proof of concept *in vivo* study. The majority of drug molecules are delivered as oral medications and this would be the most likely route of administration for a prodrug of bupropion. For the oral route of delivery, numerous factors have to be met to have a successful drug candidate. Solubility is important because a drug molecule has to be dissolved to be absorbed. Some lipophilicity is essential because the drug molecule has to cross cell membranes by diffusion. In order to reach the systemic circulation, the molecule has to survive various chemical and biochemical attacks in the gastrointestinal system and liver. The order in which these factors occur can also be the order of logical thinking when one plans to tackle an oral drug delivery problem but some of these problems can be addressed by other methods such as formulation development after a drug molecule has been developed.

It is believed that the permeability and metabolic stability of a drug molecule are the two major factors in drug delivery or in the prediction of drug absorption when the molecule is in solution [182]. During ADME studies, both absorption and metabolism can be assessed by *in vitro* methods with good correlation to *in vivo* data but distribution and elimination are usually best studied with *in vivo* methods.

The oral route of administration is subject to a wide variety of metabolic enzymatic systems with a high variability in pH. The stomach can be as low as pH 1 while along the GI tract this can increase to a high of pH 9 during the fed state in the intestinal duct. Numerous pre-systemic enzymatic systems are present before the potential prodrug reaches its desired target, the brain. The most ideal prodrug would be one that is metabolically and hydrolytically stable both

presystemically and in the blood circulation but is transformed at the site of its target to the parent drug. There are numerous presystemic and first-pass metabolic systems ranging from phase I esterases, cytochrome P450 enzymes, flavin containing monooxygenases to phase II glucuronosyl transferases.

Phase I metabolism is sometimes called a 'functionalization reaction', since it results in the introduction of new hydrophilic functional groups to a molecule. The introduction or unveiling of functional groups such as -OH, -NH₂, -SH, -COOH, all incorporate a higher polarity and hence hydrophilicity to the compound which facilitate the excretion of the compound from the body. The main reaction types associated with phase I metabolism are oxidation, reduction and hydrolysis. The oxygenases and oxidases consist of cytochrome P450 (P450 or CYP), flavin containing monooxygenases (FMO), peroxidase, monoamine oxidase (MAO), alcohol dehydrogenase, aldehyde dehydrogenase and xanthine oxidase. The reductase enzymes are aldehyde and ketone reductases and quinone reductase. The main hydrolytic enzymes are esterases, amidases, aldehyde oxidase and alkylhydrazine oxidase. Some enzymes can scavenge reduced oxygen. These include the superoxide dismutases, catalase, glutathione peroxidase, epoxide hydrolase, γ -glutamyl transferase, dipeptidase and cysteine conjugate β -lyase.

Phase II metabolism includes what are known as conjugation reactions. In general, the conjugation reaction with endogenous substrates occurs on the metabolite(s) of the parent compound after phase I metabolism; however, in some cases, the parent compound itself can be subject to phase II metabolism. The unveiled functional groups are conjugated or derivatized with endogenous substrates. The reaction types are glucuronidation, sulfation, glutathione-conjugation, *N*-acetylation, methylation and conjugation with amino acids (e.g. glycine, taurine or glutamic acid). The main enzymes responsible for phase II metabolism are uridine diphosphate-glucuronosyltransferase (UDPGT), sulfotransferase (ST), *N*-acetyltransferase, glutathione S-transferase (GST), methyl transferase and amino acid conjugating enzymes.

4.1.1 Biochemical barriers to oral drug delivery

4.1.1.1 Phase I enzymes

4.1.1.1.1 Esterase/Amidase enzymes

Esterase activity can be found in many mammalian tissues and in blood [183-185] and can be the result of catalysis by a number of distinct enzyme families, including carboxylesterases, paraoxonase and cholinesterases. The esterase enzymes generally have wide substrate specificities and are capable of performing a wide range of hydrolytic biotransformations, although certain members such as cholinesterase have highly specialized functions. Esters, amides, hydrazides, carbamates and thioesters are all hydrolysed by esterases.

The most important family of esterase enzymes is the carboxylesterase family (EC 3.1.1.1), and members of this family are responsible for the hydrolysis of a variety of drugs [186]. These enzymes are localized in the endoplasmic reticulum and are strongly inhibited by sulfonyl or phosphonyl fluorides. The enzymes employ a Ser-His-Glu triad as their catalytic domain. The major forms of the enzymes are designated hCE-1, hCE-2 and hCE-3 [187]. The carboxylesterase enzymes are responsible for the hydrolysis of the majority of prodrug esters.

Although the highest esterase activity is normally found in the liver, the intestine is also high in this activity. The carboxylase most abundant in human intestinal tissue is designated hCE-2 [186]. This enzyme is also found in human liver but hCE-1 is the most abundant liver carboxylesterase enzyme [186]. Esterases are generally ubiquitous though and can be found in kidneys (proximal tubules), testis, lung, plasma and red blood cells too.

4.1.1.1.2 Cytochrome P450 enzymes

The cytochrome P450 (CYP) enzymes are a large family of related enzymes expressed predominantly in the liver, but found in many tissues, that play a role in the metabolic clearance of well over 50 % of drugs. The enzymes have broad and somewhat overlapping substrate specificity. They play a major role in the biosynthesis and catabolism of various endogenous compounds such as steroid hormones, bile-acids, fat-soluble vitamins and fatty acids. CYP enzymes are also considered the most important metabolizing enzymes for xenobiotics (>85 % of the drugs in the market are metabolized by CYPs)[188]. Although over 50 human CYP enzymes have been characterized, only 5 seem to be responsible for the majority of drug metabolism; CYP1A2, CYP2C9, CYP2C19, CYP2D6 and CYP3A4. Of these, by far the most important enzyme is CYP3A4. The enzyme is found in the greatest quantity (>30 % of total liver CYP enzyme) [189] and has the broadest range of known substrates [188].

The mechanism of action of the enzymes is a complex multistep process that leads to the biotransformation of substrate, most often to the oxidized product (Figure 4.1). This mechanism has been described in great detail [190]. The process of oxidation involves high energy intermediates and often involves the generation of reactive electrophilic intermediates at the enzyme active site that are sometimes released and can react with cellular components. This process is thought to contribute to the acute toxicity displayed by some compounds [191].

The main reaction type of the CYP enzymes is oxidation (Figure 4.1) in the presence of oxygen or reduction under low oxygen tension. Nicotinamide-adenine-dinucleotide-phosphate (NADPH) and oxygen are the cofactors needed for this enzyme to carry out its duty.

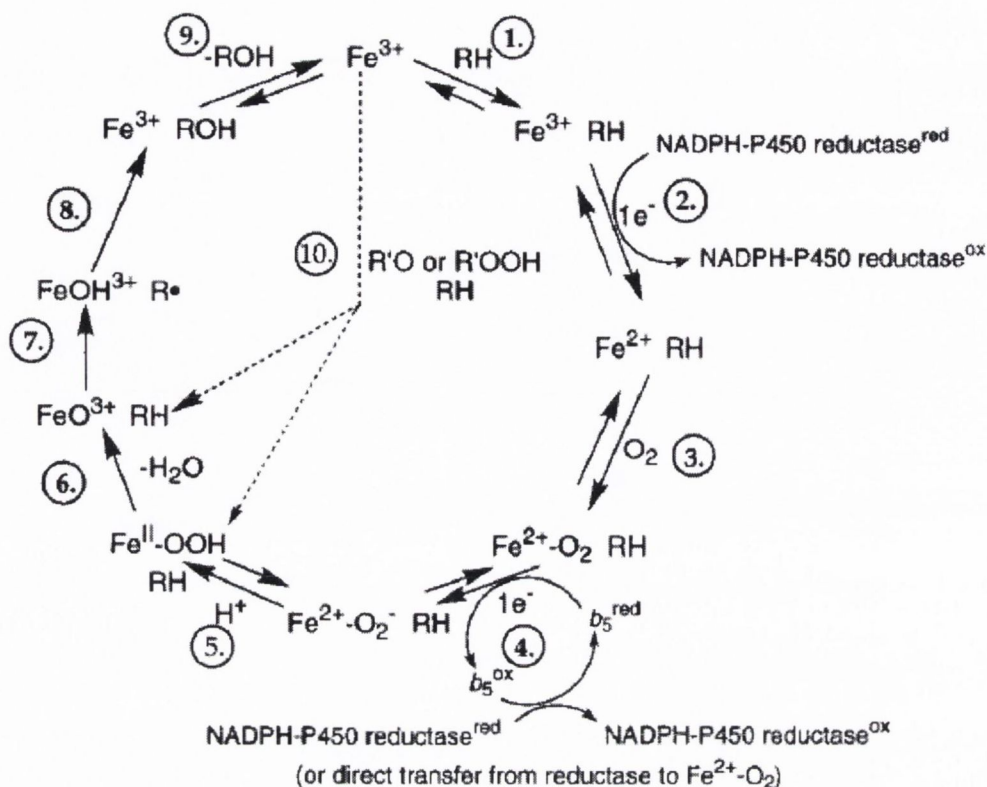


Figure 4.1 The generalized P450 catalytic cycle adapted from Guengerich [190]

There are numerous other types of oxidation performed by CYP enzymes; aromatic hydroxylation, aliphatic hydroxylation, N, O, S-dealkylation, N-oxidation, S-oxidation, epoxidation and dehalogenation. The reduction reactions are azo- or nitroreduction and dehalogenation. CYPs have also been shown to hydrolyse esters and can also dehydrogenate compounds. CYPs are distributed ubiquitously especially in the liver, intestine, kidney, lung, skin and brain. They are localized in the endoplasmic reticulum.

4.1.1.1.3 Flavin-containing monooxygenase

In addition to the CYPs, hepatic microsomes contain a second class of monooxygenase, the flavin-containing monooxygenase (FMO). Although the FMO's are considered to be important for metabolizing heteroatom (N, S, Se or P)-containing compounds rather than direct oxidation at a carbon atom, the quantitative role of FMO's in hepatic drug metabolism in humans is limited. The main reaction type is oxidation of compounds containing a heteroatom and again, NADPH and oxygen are the necessary cofactors.

4.1.1.1.4 Alcohol dehydrogenase

Alcohol dehydrogenase (ADH) is a major enzyme responsible for oxidation of ethanol to acetaldehyde.

4.1.1.1.5 Aldehyde dehydrogenase

Aldehyde dehydrogenase (ALDH) is the major enzyme responsible for oxidation of xenobiotic aldehydes to acids. In particular, acetaldehyde formed from ethanol by alcohol dehydrogenase is oxidized to acetic acid which is further oxidized to carbon dioxide and water. Both aromatic and aliphatic aldehydes though can also be oxidized to the corresponding acid.

4.1.1.1.6 Monoamine Oxidase

Monoamine oxidase (MAO) has been seen to be related to the metabolism of exogenous tyramine. MAO catalyzes the oxidative deamination of biogenic amines.

4.1.1.2 Phase II enzymes

4.1.1.2.1 Glucuronosyl Transferases (UGTs)

The uridine diphosphate glucuronosyltransferases are a family of enzymes found in the endoplasmic reticulum that catalyze the transfer of glucuronic acid to nucleophilic sites on drugs and xenobiotics. The enzymes have broad substrate specificity and can conjugate phenols, acids, alcohols, amines, nitrogen containing heterocycles and other moieties. UGT enzymes often catalyze the conjugation of metabolites of the CYP enzymes, which leads to their designation as phase II enzymes: however, it is also known that the enzymes can conjugate substrates directly.

4.1.1.2.2 Sulfotransferase (ST)

Sulfation mediated by sulfotransferase is a predominant conjugation reaction of a compound at a low concentration, whereas glucuronidation becomes an important conjugation pathway at a higher substrate concentration. Sulfation is considered in general a high-affinity low capacity reaction. Generally oxygen and nitrogen nucleophiles are sulfated.

4.1.1.2.3 N-acetyltransferase (NAT)

N-acetyltransferase is an enzyme that catalyzes the transfer of acetyl groups from acetyl-CoA mainly onto arylamines, particularly serotonin. They have a wide specificity for aromatic amines. Other common *N*-acetylation reactions by NAT are on sulfonamides or hydrazine derivatives.

4.1.1.2.4 Glutathione S-transferase (GST)

GST represents an integral part of the phase II detoxification system. GST protects cells from oxidative and chemical induced toxicity and stress by catalysing the glutathione conjugation

reaction with an electrophilic moiety of lipophilic and often toxic xenobiotics. In the liver, GST accounts for up to 5 % of the total cytosolic proteins.

4.1.1.2.5 Amino acid conjugation

Exogenous carboxylic acid, especially esters, can be activated to coenzyme A derivatives (acyl CoA thioether) in vivo by acyl-CoA synthetase and further conjugated with endogenous amines such as amino acids by acyl-CoA:amino acid *N*-transferase. Amino acid conjugates of xenobiotics are eliminated primarily in urine by tubular active secretions. These enzymes are found mainly in the liver and kidney in the mitochondria and endoplasmic reticulum for acyl-CoA synthetase, and cytosol and mitochondria for acyl-CoA:amino acid *N*-transferase.

4.1.2 Physiological barriers to oral drug delivery

The luminal side of the gastrointestinal tract is covered with an aqueous mucus layer that is secreted by the goblet cells. Before reaching the epithelial layer of the intestinal mucosa, a drug must penetrate this mucus layer, which has a thickness of about 100 μm . The mucus layer acts as a filter for molecules with a molecular mass of 600-800 amu. The mucus is composed of glycoproteins, which trap water within the layer with a turnover rate of 12-24 hours. Drug transport through this mucus and unstirred water layer is the rate limiting step before the drug reaches the surface of the epithelial cells of the intestine [192].

Immediately below the mucus layer are the columnar epithelial cells, joined together by tight intercellular junctions. The layer of cells is composed of enterocytes, goblet cells, endocrine cells and paneth cells. A drug can cross the intestinal mucosa via several different mechanisms, depending on its physicochemical properties. Hydrophobic drugs that can partition through the cell membranes are more likely to cross the intestinal mucosa through the transcellular pathway. Hydrophilic drugs cannot penetrate the cellular membranes; therefore, they must use the paracellular pathway. Unfortunately, this pathway is restricted by the presence of tight junctions. Only molecules that have a hydrodynamic radius of less than 11 Å can pass through this pathway. Therefore, the transport of peptides via this pathway is limited. Another way in which a drug can penetrate the intestinal mucosa involves receptor-mediated uptake of the drug. Some dipeptide transporters have been found to transport drugs from the lumen to the blood side of the intestinal mucosa. Finally, the intestinal mucosa has efflux pumps that can create an efflux of drugs, which have been partitioned through the membranes. P-glycoprotein is a known efflux pump located within the brush borders of the villus tips of the intestine. The substrate specificity for P-gp covers a broad range of molecular structures, a common feature of the substrates is hydrophobicity.

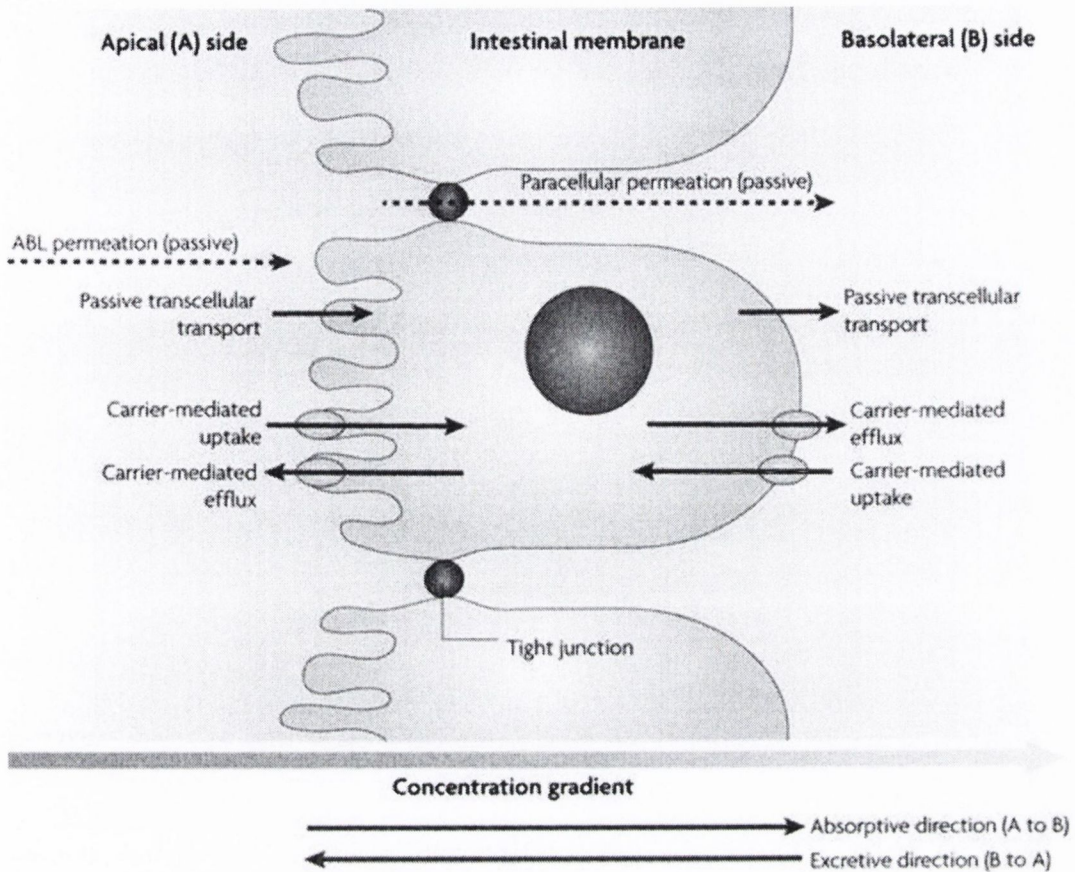


Figure 4.2 A schematic representation is shown of how compounds can permeate the intestinal membrane. Transcellular permeation is the route passing through the epithelial cells (that consists of passive transcellular and carrier-mediated permeation). Paracellular permeation is the route passing between the cells. The aqueous boundary layer (ABL) is adjacent to a membrane and could be a permeation barrier. Uptake refers to transport into a cell and efflux refers to transport out of a cell. Adapted from Sugano et al.[193]

4.1.3 Chemical barriers to oral drug delivery

The chemical structure of a drug determines its solubility and permeability profile. In turn, the concentration at the intestinal lumen and the permeation of the drug across the intestinal mucosa are responsible for the rate and extent of absorption.

Hydrogen bonding potential has been shown to be an important factor in the permeation of drugs. Studies *in vivo* and in models of the blood brain barrier and intestinal mucosa indicate that desolvation or hydrogen bonding potential regulates the permeation of drugs [194]. For small organic molecules, the octanol-water partition coefficient is the best predictor of cell membrane permeation. Other properties that greatly affect passage of drugs via the paracellular route are size, charge and hydrophilicity [195].

4.1.4 Development of a screening tool to evaluate drug metabolic stability

Figure 4.3 summarizes the workplan utilized when developing prodrugs of bupropion. It contains six main steps and can be applied to the development of any drug candidate.

The workplan starts out with a concept which in this case was bupropion. At this stage prodrug candidates are identified and the literature is searched for transformations that have been done in the past and methods used to carry out these transformations. This gave a background into the novelty of the prodrug concept for bupropion and allowed preparation for the synthetic approach.

Synthesis of the desired analogues of bupropion was carried out, always followed by work-up of the crude reaction mixture and purification of the final product usually by flash column chromatography.

The final product was characterized by spectroscopic techniques and high-performance liquid chromatography to accurately identify the structure of the final product. ^1H NMR and ^{13}C NMR were used to identify the exact structure of the analogues, while HPLC-MS was used to elucidate any isomers present and purity. FT-IR was used to evaluate functional group transformations and in some cases a melting point of salts were determined to further characterize the products.

After characterization, the potential prodrugs were evaluated using an *in vitro* screening process that would mimic the oral route of administration. A number of different media containing a range of pH and enzyme types were selected to screen if the prodrug was activated *in vitro*. Prodrugs that were activated in the *in vitro* screen were then characterized for their kinetics. If enzymes carried out the transformation, a substrate saturation study was conducted and the Michaelis-Menten enzyme kinetics were evaluated. If the prodrug was hydrolysed chemically, the kinetics and order of the reaction was determined.

Finally, the most likely prodrug candidate was selected for an *in vivo* study to assess if prodrug concept could be demonstrated in an animal model. The pharmacokinetics and metabolism were evaluated with the parent (bupropion) as a control. The pharmacological activity of the potential prodrug was also studied.

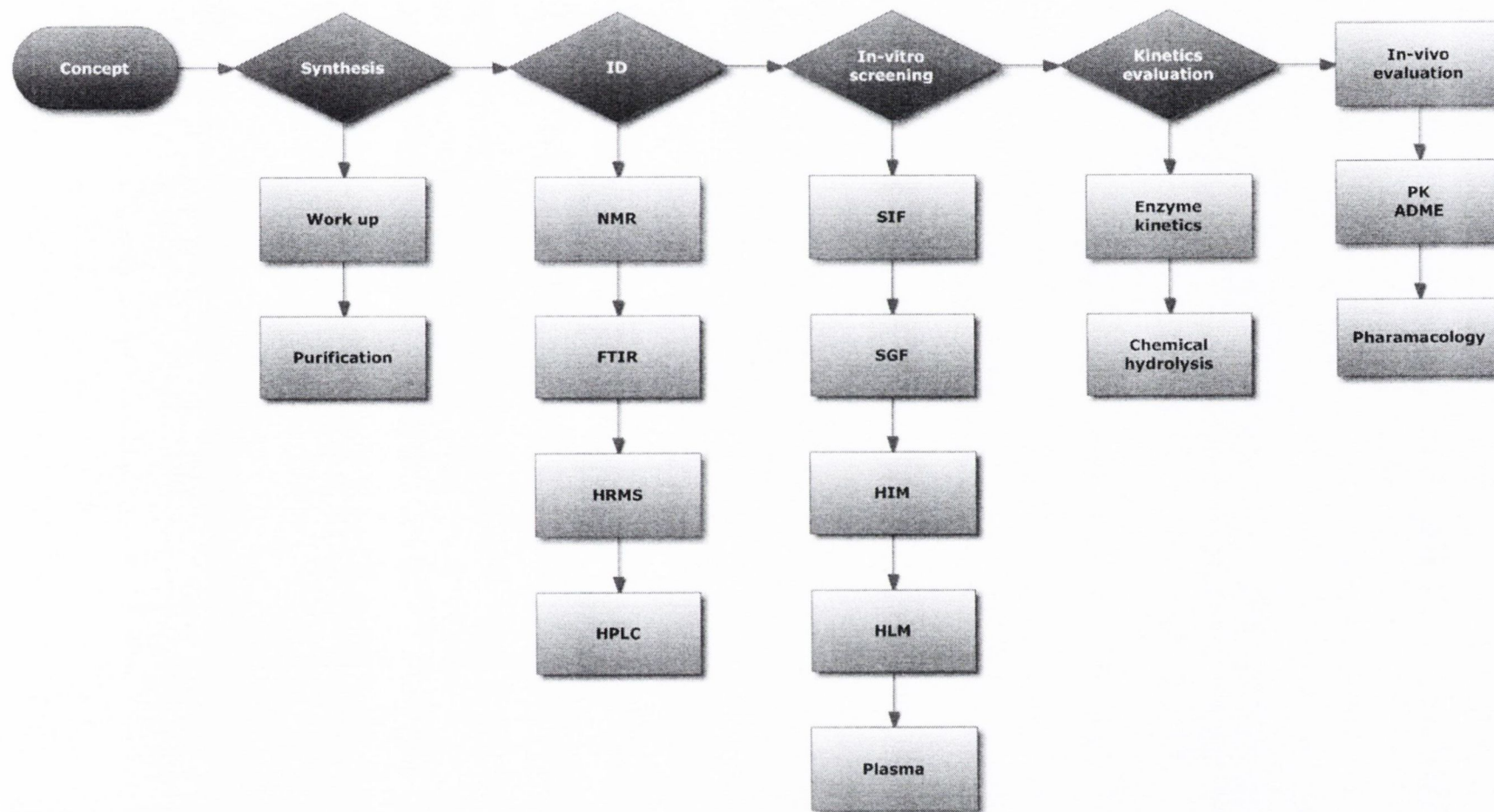


Figure 4.3 The prodrug assessment scheme used to develop potential prodrugs of bupropion.

4.1.4.1 Metabolic screening tools already available

Determination of metabolic properties is one of the most important steps during drug discovery and development. *In vitro* methods are used for estimation and prediction of *in vivo* metabolism. It is possible to determine the metabolic stability as well as the risk for drug-drug interactions (DDIs) related to inhibition and induction of drug metabolic enzymes with *in vitro* methods. Metabolic stability is defined as the susceptibility of a chemical compound to biotransformation and in prodrug design it is an integral part of the development process. In drug development, the goal is to design a pharmaceutical with good metabolic stability while in prodrug development, the goal is to design a pharmaceutical which is transformed *in vivo* to an active product and so in prodrug design we use the enzymatic systems to metabolize our prodrug. There are four main *in vitro* models used to study drug metabolism.

4.1.4.1.1 Recombinant expressed enzymes

Recombinant expressed enzymes are routinely used for predicting drug clearance [196] and the risk for DDI's related to enzyme inhibition [197, 198]. The recombinant expressed enzyme system is the simplest *in vitro* model that contains the individual enzymes usually produced in the endoplasmic reticulum of eukaryotic host cells. The major advantage of this model is its simplicity, and providing an opportunity to study the activity of the specific enzymes separately. The major disadvantage is the difference in the activity of metabolic enzymes per unit of microsomal proteins compared to that in human liver microsomes.

4.1.4.1.2 Microsomes

Microsomes can easily be prepared from different tissues, most commonly from the liver of animals and human donors by ultracentrifugation and have become very popular [199]. The enzymatic activities are stable during prolonged storage of the microsomes. By supplementing the microsomes with relevant cofactors and other reaction components, it is possible to investigate and distinguish between CYPs, flavin-containing monooxygenase (FMO) and glucuronosyltransferase (UGT) activities. Therefore, this model is widely used by pharmaceutical companies for prediction of clearance of NCEs *in vivo*. The major disadvantage of the model is the limited incubation time (the enzyme activities decrease after 2 h of incubation).

4.1.4.1.3 Fresh and cryopreserved hepatocytes

Fresh and cryopreserved hepatocytes are valuable *in vitro* models for estimation and prediction of clearance and DDI of NCEs [200]. This model contains all, phase I and II metabolic enzymes as well as all necessary co-factors. Therefore, depending on the conditions

used, incubation times can be long (up to 96–120 h for primary cultures). The limited availability of fresh human hepatocytes is the major disadvantage of this model.

4.1.4.1.4 Tissue slices

Tissue slices are the most complex *in vitro* model, the most closely mimicking the *in vivo* situation. Tissue slices are a useful model to study formation of metabolites, but this model is not well established for prediction of metabolic clearance and DDIs [201]. Use of liver slices provides advantages over previous *in vitro* techniques because this preparation allows for maintenance of the functional acinar architecture of the liver and has displayed drug metabolism over a span of hours to days.

4.1.4.2 Mass analyzers for liquid chromatography

Due to the high specificity, speed and selectivity offered by HPLC–MS/MS, this approach has long been adopted in the pharmaceutical industry to assess certain properties of drug molecules, such as metabolic stability.

4.1.4.2.1 Quadrupole mass analyzers

Single-Stage quadrupole mass spectrometers (SSQMS) as well as triple-stage quadrupole mass spectrometers (TSQMS) are commonly used by the pharmaceutical industry for both qualitative and quantitative studies [202]. Whilst quadrupole mass analysers have the ability to operate in both negative and positive ion modes, specific advantages of SSQMS instruments include low cost and their relatively small size, whilst TSQMS instruments have greater discrimination against chemical background resulting in real gains in selectivity and sensitivity. However detection sensitivity decreases dramatically when wide mass range is analysed in a scanning mode; which can be a limitation in its application for screening of ‘unknown’ drug metabolites.

4.1.4.2.2 Ion trap mass analyzers

Like quadrupole instruments, ion traps are relatively inexpensive and compatible with a wide range of systems. Ions generated are focused towards the centre of the trap allowing measurement of all ions retained in the trapping step. Consequently, sensitivity losses during the full-scan mode are avoidable. Whilst TSQMS retains sensitivity advantage for quantification when operated in SRM mode, ion-trap instruments provide more sensitivity for structure elucidation than TSQMS. This is due to the fact that ion traps can obtain richer mass spectra, with more efficient trapping and scanning of ions; this MS mode can be more structurally informative when compared to triple quadrupole or Quadrupole time-of-flight (Q-TOF)-mass spectrometers. The ion-trap analysers can be used for quantification in full-scan

mode, with little difference between sensitivity in SIM or MRM modes. When operated in a full-scan mode, the sensitivity gains, ability to measure a wide mass range and acquisition of full-scan data can make these instruments ideal for screening-type applications in which qualitative information is paramount (such as metabolite identification studies) [203]. These instruments have traditionally shown increased variability at the limits of detection due to the slow ion accumulation time. This coupled with the relatively slow data acquisition rate, limits their use in high-speed quantitative LC-MS applications, such as fast UPLC analyses. In recent years, hybrid instruments have become available, where both tandem and trap MS functionality can be used (for both quantitative and qualitative applications).

4.1.4.2.3 LTQ-Orbitrap mass analyzers

LTQ-Orbitrap is a hybrid, high-resolution mass spectrometer composed of a 2-D linear ion trap (LTQ) front-end that is coupled to an electrostatic ion trap on the back-end (Orbitrap). Ions are formed traditionally using a wide variety of ionization techniques: APCI, ESI, and APPI. The orbitrap provides very high mass resolution for ions delivered by LTQ used as a pre-selection of measured ions. Given this, the LTQ-Orbitrap is an effective alternative to the TOF instruments used for metabolite profiling [204]. Also, this instrument is capable of high sensitivity screening over a wide mass range and tandem mass spectrometry with accurate mass data for both parent and fragment ions. The LTQ-Orbitrap, like other ion-trap systems suffers from a slow data acquisition rate compared to TOF instruments and hence, is not suitable for very fast chromatography applications.

4.1.4.2.4 Time of flight (TOF) mass analyzers

TOF MS involves measuring the time taken for an analyte ion to travel from the ion source to the detector. TOF instruments are generally used with electrospray ion sources in which ions are pulsed orthogonally into the flight tube. This together with the use of electrostatic mirrors can enable operation at very high mass resolution. This increased mass resolution can help with the accurate determination of undefined metabolites, hence TOF instruments are primarily used for metabolic identification studies [205]. Quadrupole time of flight (Q-TOF) mass spectrometers are relatively simple, and capable of recording all the ions produced in the source on a microsecond time scale offering increased sensitivity. The time taken for an ion to reach the detector is proportional to its m/z ratio and this is used to differentiate the ions mass down the path of the instrument flight tube. Q-TOF instruments have the ability to operate with relatively high mass resolution and to make accurate mass measurements, providing a degree of selectivity since it is able to discriminate between interference and among mass peaks having similar nominal masses but different exact masses. This instrument can operate at relatively high scanning rates which makes them ideal for use with high resolution liquid

chromatography (LC) methodology such as ultra performance liquid chromatography (UPLC).

4.1.4.3 Ionization methods

The application of atmospheric pressure ionization (API) methods in particular electrospray and pneumatically assisted electrospray, have provided a breakthrough for the combination of liquid separation techniques with mass spectrometry. The two most significant API techniques used to date have been atmospheric pressure chemical ionization (APCI) and electrospray ionization (ESI) [206]. Ionization of non-polar compounds at atmospheric pressure was made possible following the introduction of atmospheric pressure photoionization (APPI) [207].

4.1.4.3.1 Automation approaches for metabolic screening

Automation for use in drug metabolism in vitro ADME studies can be utilised to varying degrees depending on the data required to advance discovery projects. Fully automated systems are available that are adapted to high capacity and simple assay protocols [208], these tend to be implemented at early stages in the drug discovery continuum where sparse sampling (e.g. single time point) screens are often operated. These systems are optimised for the relatively high compound numbers encountered. A fully automated approach can be adopted, using a centralised robotic arm integrated with other robotic liquid handlers, which carry out the assays [209]. These systems are designed for fully automated sample preparation, data analysis and management of results generated from in vitro ADME assays. Although these systems take longer to develop and require more capital investment, they can be very successful in situations where maximum efficiency, short data feedback times, high-throughput and unattended (overnight) operation is required. Introduction of semi-automated approaches for in vitro ADME assays have the advantage of offering sufficient flexibility to operate different assay configurations, enabling manual intervention at crucial stages of the assay. It also provides a robotic platform that is easily reconfigured when assays evolve.

4.1.4.3.2 Sample preparation techniques for metabolic screening

Sample preparation is a key step in quantitative bio-analysis and can potentially be a bottleneck in the process in developing robust and efficient screening methodologies. This is attributed to the complex nature of macromolecular compounds, such as proteins and non-volatile endogenous substances, that have to be removed from the in vitro sample and separated from the analytes to eliminate matrix interferences prior to the LC-MS/MS analyses. Due to the high specificity of LC-MS/MS detection, sample preparation is typically achieved by protein precipitation with an organic solvent such as acetonitrile and subsequent

on-line HPLC separation [210]. The advantage of using a protein precipitation technique is that this sample preparation stage is usually incorporated into the in vitro assay protocol, by utilising it as the actual termination step.

4.1.4.4 Media selection

Prodrugs of bupropion that are to be delivered orally face five main metabolic stability obstacles before they cross the blood-brain barrier and reach their target. The first obstacle is the stomach. All orally delivered drugs have to be stable at low pH in order to survive the harsh acidic conditions of the stomach. The stomach also contains digestive enzymes, mainly pepsin. Pepsin is an enzyme whose precursor form (pepsinogen) is released by the chief cells in the stomach and that degrades food proteins into peptides. Pepsin is one of three principal protein-degrading, or proteolytic enzymes in the digestive system, the other being trypsin and chymotrypsin. Pepsin is most efficient at cleaving peptide bonds between hydrophobic and preferably aromatic amino acids such as phenylalanine, tryptophan and tyrosine. In order to simulate the pH and digestive enzymes of the stomach, USP simulated gastric fluid (SGF) was used as the first media for screening of prodrugs.

The second obstacle once the drug has passed through the stomach is the intestine. The intestine's pH rises to approximately neutral pH. Along with intestinal microflora there are digestive enzymes present, a mixture called pancreatin. Amylase, lipase, protease, trypsin and chymotrypsin are all present in pancreatin. The trypsin found in pancreatin works to hydrolyze proteins in oligopeptides; amylase hydrolyzes starches into oligosaccharides and the disaccharide maltose; lipase hydrolyzes triglycerides into fatty acids and glycerol; and Chymotrypsin preferentially cleaves peptide amide bonds where the carboxyl side of the amide bond (the P1 position) is a tyrosine, tryptophan or phenylalanine. This media was simulated using USP simulated intestinal fluid (SIF).

After traversing the intestinal duct, the next obstacle the drug or prodrug will face is crossing the intestinal membrane into the portal vein. It is here the drug will face its first round of phase I and phase II metabolic enzymes. The intestinal cells contain cytochrome P450 enzymes, flavin monooxygenases, esterases and UDP glucuroyl transferases. This media was simulated by using human intestinal microsomes. Microsomes are prepared by differential centrifugation from a crude tissue homogenate. The intestinal tissue is homogenized in buffer and subjected to a 9000g centrifugation. The supernatant from this centrifugation (often referred to 'S9') is recovered and then centrifuged at 100,000g. The pellet from this high speed centrifugation is referred to as 'microsomes' and the supernatant is referred to the 'cytosol'. The microsomes from this first 100,000g centrifugation are resuspended in buffer and centrifuged again 100,000g. The pellet from this final centrifugation is resuspended in 250 mM sucrose and the protein concentration is adjusted. Microsomes are principally

derived from the endoplasmic reticulum, however membranes from other cellular organelles are typically present. Microsomes therefore provide an enriched source of membrane bound drug metabolizing enzymes. Pooled human intestinal microsomes (HIM) were used in order to simulate the potential metabolism that occurs when the prodrug passes through the intestinal membrane into the portal vein.

After passing through the intestinal membrane into the portal circulation the prodrug quickly enters the liver. The liver is the major metabolizing organ of the body. The blood plasma perfuses the liver from the portal vein. The liver cells contain another rich source of cytochrome P450 enzymes, flavin monooxygenases, esterases and UDP glucucroyl transferases. This metabolic media was simulated in the present work by using pooled human liver microsomes (HLM).

The final obstacle of metabolism for the prodrug before it reaches the brain, is its stability in blood plasma. The plasma contains dissolved proteins, glucose, clotting factors, mineral ions, hormones and carbon dioxide. Plasma was pooled from three human donors. This pooled human plasma (PHP) was used to evaluate the prodrugs stability in human blood.

The five media (SGF, SIF, HIM, HLM and PHP) best represent the transit a drug or prodrug would take if delivered by the oral route of administration. Obviously for drug delivery, the compound is expected to be as stable as possible so it reaches its target at maximum concentrations. For prodrug delivery, it is expected that one or more of the media can metabolize or hydrolyse the prodrug back to parent drug, so metabolic lability is more important. Stability in gastric fluid can be addressed by formulation development, *i.e.* with enteric coated tablets but once the tablet formulation is dissolved in the intestine, the compounds stability is under attack from the hydrolytic and metabolic enzymatic systems until it reaches its target.

4.1.4.5 Sample preparation

It was possible to fully automate the sample preparation process of our screening by using the capabilities of the Accela autosampler, for online dilutions, spiking, mixing, incubating etc. The only step that could not be automated was after addition of acetonitrile to quench the reaction and precipitate the proteins, the sample needed to be centrifuged and this centrifugation could not be done online in our laboratory. It was possible though to direct inject the metabolite-media mixtures onto the column by using a guard column and switching valve, diverting the first few minutes of the chromatogram away from column and detector.

4.1.4.6 Chromatographic method

In order to evaluate the metabolic mixtures, a chromatographic method had to be developed that would separate and purify each mixture into its separate components. Although the mass spectrometer could separate out the masses of the individual compounds, the chromatographic method was still important as diastereomers, namely the bupropion amino alcohols, had the exact same mass and therefore needed to be separated chromatographically in order to be adequately identified and quantified. The chromatographic method was also needed to separate out any inorganic salts or water soluble proteins from the mixture so these could be diverted to waste.

Reverse phase LC methods are the most widely used for separating organic compounds. A high pH reverse phase gradient method was chosen to purify the prodrug and metabolite mixtures entering the detector. The benefit of using a high pH gradient method is due to ionisation suppression of basic analytes. The pK_a of bupropion, its ionisable prodrugs and metabolites are all between 7-9 as they are all amines. Performing a separation above the pK_a of the amines ensures that the analytes are unionised, and hence are retained on the column. Better retention means better separation between analytes and therefore improved resolution. Working at high pH also reduces the tendency for amines to tail, which is a significant problem in reverse phase methods. The reduced tailing also improves peak shape and hence increase resolution. The improved peak shape also improves sensitivity allowing for lower limits of detection for the analytes. A high pH reversed phase column was selected, Xbridge C18, which is a silica-polymeric hybrid column capable of withstanding pH 2-12 at elevated temperatures.

Two high pH buffer systems were identified to control the pH of the mobile phase, ammonium bicarbonate and ammonium formate. Both buffers are volatile and are suitable for high pH applications but ammonium formate was chosen as the pH was more easily adjusted as the acid and base component could be added separately. The stock buffer system was prepared by diluting a 0.5 % ammonium hydroxide solution in water and adjusting to pH 10.5 with formic acid. This solution was then diluted to 10 % in mobile phase A and B (water and acetonitrile). The initial gradient chosen was from 10 % B to 90 % over 10 mins but was later adjusted to suit the chromatography and improve run times. Bupropion and its metabolites were separated in the first three minutes, and the potential prodrugs were separated thereafter as they were all more lipophilic than bupropion. The first 0.5 minutes of the chromatogram were diverted to waste, to ensure no inorganic salts and water soluble proteins entered the detector.

4.1.4.7 Mass spectrometric method

To achieve maximum sensitivity of both known and unknown metabolites with the Orbitrap mass spectrometric detector, the system was set up with two scan types. The first scan was selective ion monitoring, looking specifically for the accurate mass molecular ions of bupropion and its metabolites. The second scan type was full scan total ion chromatogram. This was used to get a mass spectrum of each unknown coming into the detector. Appended to this scan, the instrument was set up in data dependent acquisition mode. When the instrument detected a mass ion with a chlorine isotope pattern, this triggered a MS/MS and that ion was sent into the ion trap for MS³ analysis. This greatly improved the selectivity of the instrument for MSⁿ analysis as instantly only compounds relating to bupropion could be selected out due to their inclusion of the chlorine isotope. For very low levels of chlorine containing compounds, it was more difficult to detect the M+2 isotope and other conditions were set up to trigger data dependent analysis. The data dependent acquisition was also set up to trigger MS³ on the maximum abundance ion on each full scan. To save workspace on the Orbitraps memory, dynamic exclusion was used. This performed MS/MS on the most abundant ion only three times and then excluded this ion onto a list for 30 seconds in order to stop the instrument repeating itself again and again. For qualitative analysis, this was the best setup for the analyzer as accurate mass full scans on each product would be acquired along with MS³ analysis which gave fragmentation data on each of the most abundant ions.

4.2 Screening results

Table 4.1 summarizes the results obtained when each prodrug was incubated in each metabolic media at 37°C for one hour. Physiological temperature was used to best represent the human internal temperature and to optimize the activity of the enzymes present in each media. A one hour incubation was used as the maximum time a drug or prodrug would be immersed in the media. One hour metabolism or hydrolysis was sufficient time to generate detectable levels of metabolites. A blank media was used in each analysis to subtract a background from each LC-MS sample chromatogram. A t_0 sample was also used to identify impurities related to each prodrug.

After one hour incubation of each prodrug in each media, the mixture was quenched with acetonitrile and the sample was centrifuged to remove precipitated proteins. The supernatant solution was injected directly by the autosampler and the LC-MS chromatogram was obtained with data dependent acquisition analysis. This data was then screened using Networks software in order to establish what metabolites were present and more importantly, if bupropion or its metabolites were present. Bupropion and its metabolite standards were run with every prodrug analysis. A linear curve generated of each bupropion and its metabolites was the determining factor if the system was suitable for analysis. The linear range for bupropion and metabolites was 1-250 ng/mL, $R^2 \geq 0.9950$.

For microsome solutions (HIM and HLM), a control media was used to determine if the microsomes were active or not. This control solution was a bupropion standard. Bupropion was hydrolylated to hydroxybupropion when the microsomes were active. This transformation is commonly used to assess activity of oxidative enzyme CYP2B6 in human liver and intestinal microsomes. The microsomes certificate of analysis also described the enzyme activities of each media.

Results reported as <LOD (less than limit of detection), indicated that bupropion, its metabolites or any of the other prodrugs were not detected in the media after a one hour incubation at 37°C ($n = 2$). The limit of detection was 0.1 ng/mL for bupropion and metabolites. It was important to report if any of the other prodrugs were detected if for instance a possible multistep-prodrug was found. It was also important to report the metabolites of bupropion if for instance the prodrug was converted to bupropion but then subsequently metabolized to one of its metabolites immediately. Detection of bupropion or its metabolites would be a positive screening result, indicating that the prodrug may be worth an *in vivo* assessment. A positive screen would also initiate the next level of analysis on the prodrug assessment scheme, Figure 4.3, either determination of enzyme kinetics or determination of hydrolysis kinetics. This generic screen can also be used to assess drug stability for the oral route of administration.

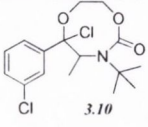
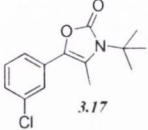
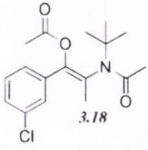
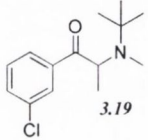
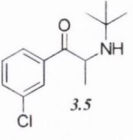
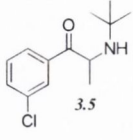
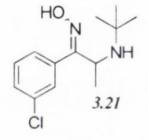
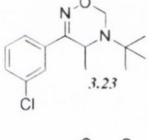
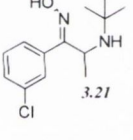
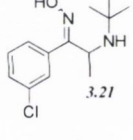
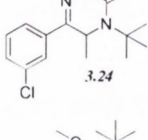
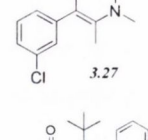
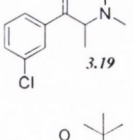
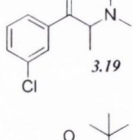
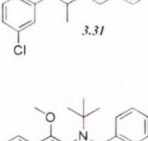
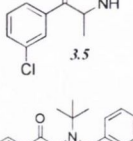
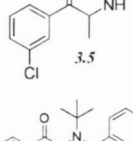
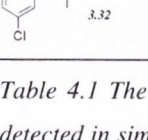
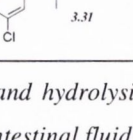
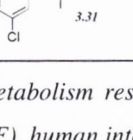
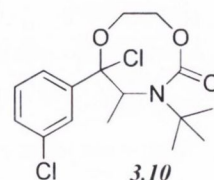
Compound	SGF	SIF	HIM	HLM	PHP
 3.10	<LOD	<LOD	<LOD	<LOD	<LOD
 3.17	<LOD	<LOD	<LOD	<LOD	<LOD
 3.18	<LOD	<LOD	<LOD	<LOD	<LOD
 3.19	<LOD	<LOD	 3.5	 3.5	<LOD
 3.21	<LOD	<LOD	<LOD	<LOD	<LOD
 3.23	<LOD	<LOD	 3.21	 3.21	<LOD
 3.24	<LOD	<LOD	<LOD	<LOD	<LOD
 3.27	<LOD	<LOD	 3.19	 3.19	<LOD
 3.31	<LOD	<LOD	 3.5	 3.5	<LOD
 3.32	<LOD	<LOD	 3.31	 3.31	<LOD

Table 4.1 The testing matrix of potential prodrugs and hydrolysis/metabolism results of compounds detected in simulated gastric fluid (SGF), simulated intestinal fluid (SIF), human intestinal microsomes (HIM), human liver microsomes (HLM) and pooled human plasma (PHP). <LOD = less than limit of detection, n = 2 (0.1 ng/mL for bupropion and metabolites).

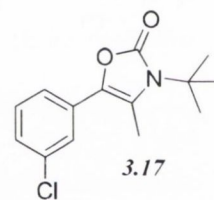
4.2.1 Cyclic carbamate derivative of bupropion (3.10)

The 8-membered ring cyclic carbamate **3.10** was the first compound selected for screening in the five media. Neither bupropion or its metabolites were detected in any media. This would suggest that **3.10** is stable to hydrolysis or enzymatic metabolism under the conditions used in the method. The carbamate group in this molecule would be labile to catalysed hydrolysis under strong acid or base conditions but under physiological conditions this is more difficult. The carbamate group should also be labile to esterase activity and cleavage would be expected in most other carbamate cases, releasing the free amine. **3.10** is most likely too sterically crowded around the nitrogen to fit in the active site for hydrolysis to occur. Even if hydrolysis at the amine occurred it is unlikely that further hydrolysis would occur around the oxygen and bupropion would not be recovered. **3.10** is therefore an unlikely prodrug candidate of bupropion.



4.2.2 Oxazolone of bupropion (3.17)

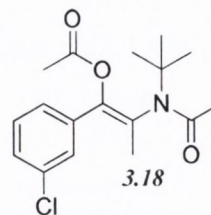
Compound **3.17** was an oxazolone of bupropion. The oxazolone contains a ring whereby a carbamate functionality is joined in a ringed system by two adjacent carbons. These two carbons are unsaturated. The oxazolone ring should be prone to acid or base catalysed hydrolysis as the carbon in the carbamate functional group will be electrophilic. The possibility of ring opening and further dealkylation could return bupropion. Although the concentration of the oxazolone was decreasing over time, the screening of the oxazolone in each media did not generate bupropion or any of its metabolites and it is therefore unlikely that **3.17** could be a human bupropion prodrug.



There is no previous literature on oxazolone type prodrugs but oxazolidine type prodrugs have been used successfully for aminoalcohols. Oxazolidines are structurally very similar to oxazolone with the exception of the unsaturation on the two carbons linking the nitrogen to the oxygen on the ring. Oxazolidine prodrugs of ephedrine have been shown to be hydrolysed successfully in rats, yielding ephedrine [163, 211, 212]. This prodrug strategy could be used on the amino alcohol metabolites of bupropion or possibly on bupropion when it is enolized. A group of structurally related prodrugs are the oxodioxolyl-methyl esters (daloxates) which are susceptible to base catalysed hydrolysis yielding the corresponding carboxylic acid [169].

4.2.3 *N,O*-diacetylated bupropion (3.18)

N,O-diacetylated bupropion **3.18** contained two potential prodrug groups that would be liable to hydrolysis. Therefore this compound was a potential double prodrug of bupropion. Deacetylation at the oxygen would give back the keto-amide, while deacetylation at the amide would give back the amino-enol ester. Amide and ester prodrugs are widely used and have been



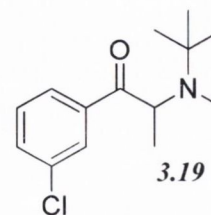
investigated extensively in the past [213]. Prodrugs of enol esters are not so widely used but this has been used successfully to deliver ketone drugs [115, 116, 214, 215]. Burkhart *et al.* have described the synthesis of α -keto ester enol acetates and have shown these are converted back to the ketone drugs by esterases.

After deacetylation at the amine, the amino-enol ester would ionize well in the mass spectrometer as it contains the free amino group but the keto-amide would be more difficult to ionize and detect. The tertiary amide would likely be more difficult to hydrolyse.

Incubation of **3.18** in each media did not show any hydrolysis back to bupropion or its metabolites. It is possible though, that a mono-deacetylation occurred on the oxygen and the keto-amide was returned but the poor ionisation of the amide gave poor sensitivity on the detector and this was not detected. Since a deacetylation on the amine would have been much easier detected and was not seen, the tertiary-*t*-butylated amide is probably too sterically hindered for hydrolysis of the amide by hydrolases.

4.2.4 *N*-methyl bupropion (3.19)

N-methyl bupropion **3.19** was a good candidate as a potential prodrug of bupropion. *N*-dealkylation is a common bio-transformation for xenobiotics *in vivo*, and oxidative enzymes have been shown to dealkylate quite sterically hindered groups. **3.19** was incubated in all five media and as anticipated, bupropion was detected in both the human liver and human



intestinal microsome media. An enzyme or enzymes common to both media were able to *N*-demethylate **3.19** back to parent bupropion **3.5**. Further deconvolution of the data by Metworks software was able to show a reduced metabolite of *N*-methyl bupropion, *N*-methyl amino alcohol of bupropion **4.1** (RT = 4.49 min). An example of an LC-MS chromatogram of the metabolized *N*-methyl bupropion in human liver microsomes is given in Figure 4.4.

Bupropion (RT = 2.14 min) in the sample is seen at the same retention time of the bupropion standard that was run on the same day and accurate mass spectrum of bupropion in the sample also agrees with the standard fragmentation spectrum confirming the identity and presence of bupropion.

G:\LCMS DATA\...NMeBup_HLM_07

08/03/2010 21:51:15

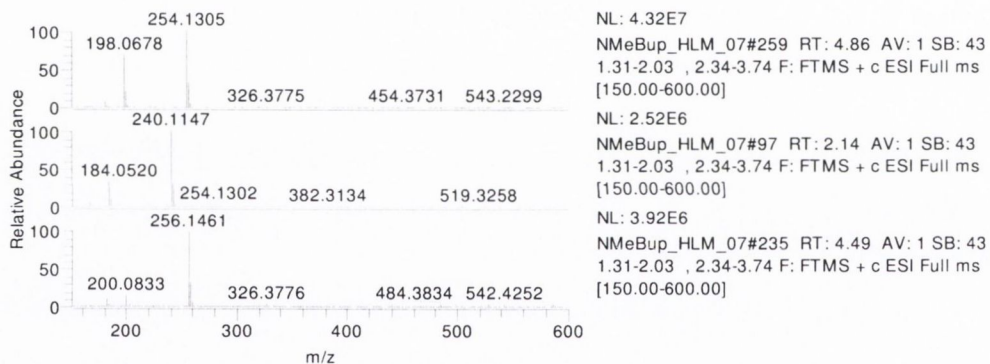
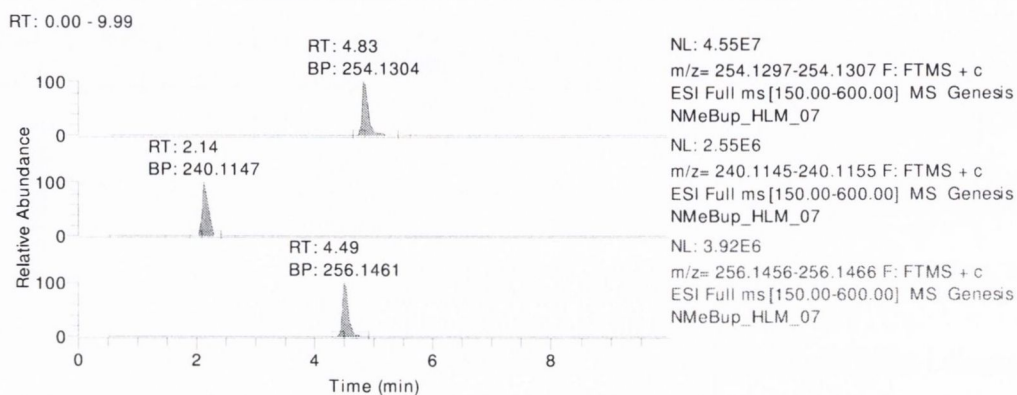
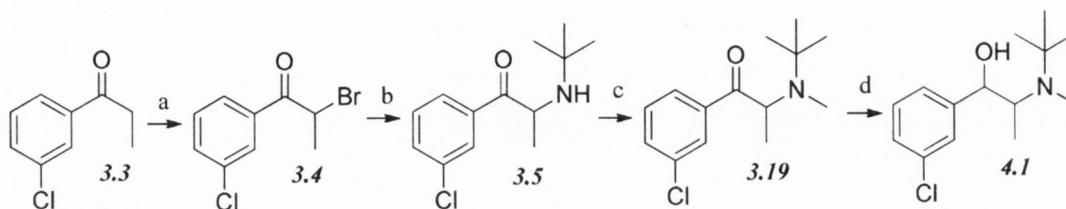


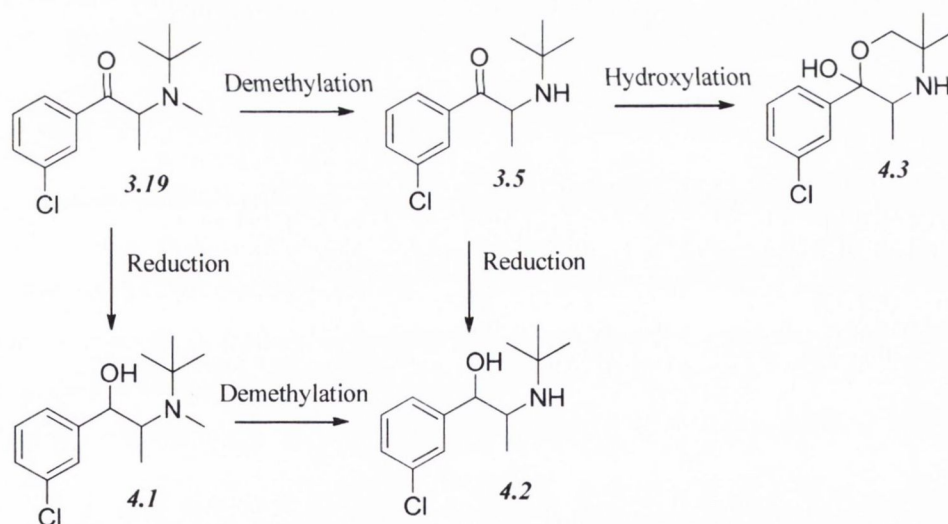
Figure 4.4 A typical LC-MS chromatogram of *N*-methyl bupropion incubated with human liver microsomes. The retention times of *N*-methyl bupropion (254.1305), bupropion (240.1147) and *N*-methyl amino alcohol (256.1461) are 4.83, 2.14 and 4.49 minutes respectively

The presence of an amino alcohol of *N*-methyl bupropion **4.1** showed that *N*-methyl bupropion **3.19** and bupropion **3.5** are metabolized similarly, by reduction. This amino alcohol **4.1** was later confirmed as the threo-diastereomer by synthesis of a standard (Scheme 4.1) and comparison with the sample chromatogram and fragmentation spectrum. This stereoselective metabolism of *N*-methyl bupropion to *N*-methyl threo-amino alcohol is also seen in the metabolism of bupropion to the threo-amino alcohol. The threo isomer usually predominates over the erythro-isomer in human and guinea-pig metabolism.



Scheme 4.1 Synthesis of *N*-methyl amino alcohol of bupropion. a) Br_2 , DCM, RT, 30 min, b) *t*-butylamine, NMP, 60°C , 30 min, c) MeI, DIPEA, ACN, RT, 12 h d) NaBH_4 , EtOH, RT, 30 min.

Scheme 4.2 summarizes the *in vitro* metabolism of *N*-methyl bupropion **3.19** in the presence of human intestinal and liver microsomes, showing the two main metabolites, bupropion **3.5** and *N*-methyl threo-amino alcohol **4.1**. This positive *in vitro* result was a good indication that *N*-methyl bupropion was a potential bio-precursor prodrug of bupropion. The generation of a new metabolite related to the amino-alcohol of bupropion was also a new drug candidate with potential pharmacological activity related to the metabolites of bupropion. This new metabolite is also a potential prodrug of the threo-amino alcohol metabolite of bupropion **4.2**. *N*-demethylation of **4.1** would give the threo-amino alcohol metabolite of bupropion **4.2** which itself is also pharmacologically active.

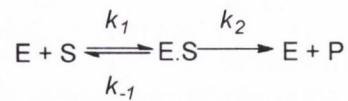


Scheme 4.2 Metabolism of *N*-methyl bupropion in human intestinal and liver microsomes

4.2.4.1 Enzyme kinetics

After establishing that *N*-methyl bupropion is transformed to bupropion *in vitro* by human liver microsomes, some basic enzyme kinetics were determined to understand if true non-linear pharmacokinetics was occurring *in vitro*. Generally, the initial rate of an enzyme reaction such as the demethylation of *N*-methyl bupropion to bupropion is directly

proportional to the concentration of the substrate at low concentrations. However, as the substrate concentration increases, the reaction reaches a certain maximum rate. In the simplest case, the overall processes of an initial enzymatic reaction can be described by the following scheme:



In brief, the substrate (S) binds to free enzyme molecule (E) and forms an enzyme-substrate complex (ES), which then can either dissociate back to E and S, or further break down to E and product (P); k_1 and k_{-1} are the association and dissociation rate constants, respectively; and k_2 is the rate constant for the production of P. During the early stages of the reaction, the reverse process, *i.e.*, $E + P \rightarrow ES$, is assumed to be negligible, because the concentration of P is essentially zero. The equation describing the initial rate of the reaction as a function of the substrate concentration can be derived from this scheme, and is known as the Michaelis-Menten equation, Equation 4.1, first proposed by Henri in 1903 and originally formulated from the equation describing a simple *in vitro* enzymatic reaction. This equation is most useful for describing apparent non-linear plasma concentration-time profiles of drugs in both *in vivo* and *in vitro* situations.

Equation 4.1 The Michaelis-Menten equation

$$v = \frac{V_{max} \cdot C}{K_m + C}$$

C is the original concentration of the substrate ([S]) at the beginning of the reaction; v is the initial rate of the reaction [substrate depletion (-dC/dt), or product formation (dP/dt)]; K_m is the Michaelis-Menten constant ($[E] \cdot C / [EC]$); and V_{max} is the maximum rate of the reaction ($k_2 \cdot [E]_t$), with $[E]_t$ being the total concentration of the enzyme. In practice, consumption of no more than 5 % of the original amount of substrate is considered acceptable for estimating the initial reaction rate with the original substrate concentration at the beginning of a reaction to satisfy the Michaelis-Menten equation. K_m is inversely related to the affinity between the substrate and the enzyme, *i.e.*, the smaller the K_m value, the stronger the affinity between the substrate and the enzyme and vice versa. K_m is also equal to the substrate concentration at which the rate of the process is half of V_{max} . V_{max} would be attained at infinite substrate concentration where all the enzymes are saturated with the substrate and present as ES, and is directly proportional to the total enzyme concentration. The important assumptions required for the Michaelis-Menten equation include;

- a) Only a single substrate and a single enzyme-substrate complex with a 1:1 stoichiometry between substrate and enzyme are involved, and the enzyme-substrate complex breaks down directly to form free enzyme and the product,
- b) The reaction rate is measured during the very early stages of the process so that the reverse reaction from the enzyme and the product to the enzyme-substrate complex ($E + P \rightarrow ES$) is negligible,
- c) The substrate concentration is significantly higher than the enzyme concentration so that the formation of an enzyme-substrate complex does not alter the substrate concentration to any significant extent.

Another important parameter that can be estimated from the Michaelis-Menten parameters is clearance. Clearance is a measure of the ability of the body or an organ to eliminate a drug from the blood circulation. Systemic clearance is a measure of the ability of the entire body to eliminate the drug, whereas organ clearance such as hepatic or renal clearance is a measure of the ability of a particular organ to eliminate the drug. Using liver microsomes we can estimate the liver clearance. The liver is the most important organ in the elimination of a drug from the blood. It is highly perfused and under normal conditions receives approximately 75 % of its blood supply from the portal vein and 25 % from the hepatic artery. The highly branched capillary system and fenestrated endothelium enable direct contact between the blood components and all cell types within the organ. Hepatocytes, the principal cell type in the organ, contain the various metabolizing enzymes and are well equipped with active transporters for efficient uptake of drug and excretion into the bile. In general, hepatic drug clearance implies clearance via both metabolism and biliary excretion. Intrinsic hepatic clearance, $Cl_{i,h}$ reflects the inherent ability of the liver to eliminate the drug not bound in blood components (to be exact, drug molecules not bound to tissue components within the hepatocytes) and is governed solely by the activities of metabolizing enzymes and/or biliary excretion (both active and passive transport of a drug into the bile). In theory, it is the same as the hepatic clearance of a drug when there are no limitations in drug delivery to the liver (sufficient and fast blood flow), protein binding (no protein binding), and other factors such as cofactor availability when needed. Intrinsic hepatic clearance can be calculated using

Equation 4.2 Intrinsic hepatic clearance

$$Cl_{i,h} = \frac{V_{\max}}{K_m}$$

There are three physiological factors that affect hepatic clearance, blood flow rate, fraction of drug not bound to blood components and the intrinsic hepatic clearance. The most important value of hepatic clearance models is probably their ability to elucidate how the different physiological factors are related to each other. In some models, the effects of the degree of blood dispersion inside the liver on clearance can also be taken into account.

The Michaelis-Menten parameters for *N*-methyl bupropion **3.19** were determined by fixing the concentration of human liver microsomes and its necessary co-factors in a PBS buffer. Varying amounts of substrate were added and the velocity of formation of bupropion was determined by LC-MS analysis over a timeframe so the sensitivity of bupropion was above the quantitation limit of the method, this was usually 20 min. The velocity of formation of product (bupropion) versus substrate (*N*-methyl bupropion) concentration was plotted and Equation 4.1 was solved using least squares non-linear regression. *N*-methyl bupropion was transformed to bupropion using human liver microsomes with a V_{max} value of 900.4 ± 74 pmol/min/mg HLM and a K_m value of 96.8 ± 24.4 μ M. The intrinsic hepatic clearance ($Cl_{i,h}$) was found to be 9.28 L/min. This *in vitro* experiment was conducted with six replicates at each concentration level (Figure 4.5). As a comparison, bupropion has been shown to be hydroxylated by human liver microsomes with substantial variation, with V_{max} rates between 85-662 pmol/min/mg HLM, K_m values of 109-162 μ M and $Cl_{i,h} = 0.5$ -6.1 L/min. The hydroxylation has also been shown to be stereoselective with the rate of (S,S)-hydroxybupropion 1.5 fold greater than that of (R,R)-hydroxybupropion using human liver microsomes [129]. This was shown using CYP2B6 when racemic bupropion was incubated at therapeutic concentrations. The rate of (S,S)-hydroxybupropion formation was approximately threefold greater than that of (R,R).

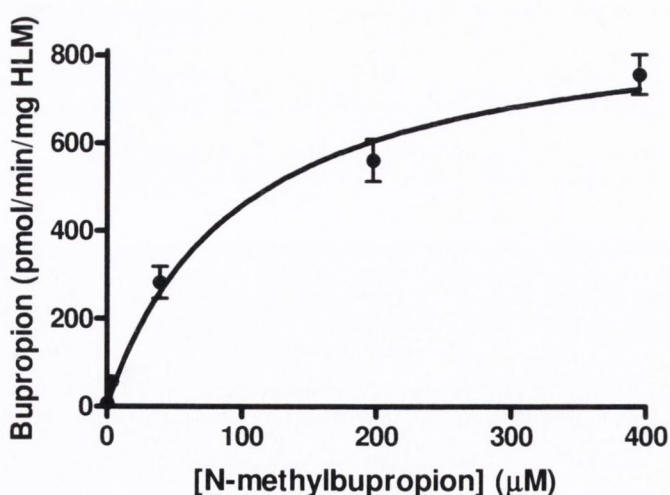


Figure 4.5 Substrate saturation study in pooled human liver microsomes of *N*-methyl potential prodrug of bupropion. $V_{max} = 900.4 \pm 73.8$ pmol/min/mg HLM, $K_m = 96.8 \pm 24.4$ μ M, $R^2 = 0.9289$, $n = 6$.

4.2.4.2 Pharmacology

In order to determine if *N*-methyl bupropion was truly a prodrug of bupropion it was important to show that the pharmacological activity of the prodrug was less active than bupropion. From a structure activity relationship point of view, *N*-methyl bupropion was likely to have some pharmacological activity since the amino group in the molecule was still basic, *i.e.* the free lone pair electrons on the nitrogen were still available for bonding at the site of activity. If this pair of electrons was tied up for bonding in a group such as a carbamate or amide group, this molecule would most likely have lost all activity. The pharmacology of *N*-methyl bupropion at a number of different neurotransmitter sites in the brain was determined using *in vitro* methods and bupropion as a control.

Since bupropion's activity in depression was known to be related to its dual reuptake inhibition of dopamine and norepinephrine, these two transporter systems were evaluated. Serotonin inhibition was also evaluated in case *N*-methyl bupropion showed some triple reuptake inhibition including the serotonin transport system. Bupropion is also known to act upon nicotinic acetylcholine receptors, which lead to its activity as a smoking cessation agent. Therefore activity at nicotinic acetylcholine receptors was also evaluated. Finally, activity was evaluated at the muscarinic acetylcholine receptor. A summary of the pharmacological screen is presented in Table 4.2. IC₅₀ values were calculated using non-linear least squares regression, inhibition constants (K_i) were calculated using the equation of Cheng and Prusoff and the Hill coefficient (n_H) defines the slope of the competitive binding curve. Hill coefficients significantly different from 1.0 may suggest that the binding displacement does not follow the law of mass action with a single binding site.

<i>N</i> -methyl bupropion				Bupropion		
IC ₅₀ (μM)	K_i (μM)	n_H	Target	IC ₅₀ (μM)	K_i (μM)	n_H
39.3	12.3	0.957	Muscarinic non-selective, central	86.5	27	1.42
71.6	49.2	0.836	Nicotinic Acetylcholine	>100	-	-
3.71	2.95	0.924	Transporter, dopamine (DAT)	<1	-	-
57.9	54.4	0.764	Transporter, norepinephrine (NET)	19.9	19.8	0.835
>100	-	-	Transporter, serotonin (SERT)	>100	-	-

Table 4.2 Pharmacological screen of *N*-methyl bupropion and bupropion determined by MDS Pharma Services

4.2.4.2.1 Dopamine transporter system (DAT)

The dopamine active transporter is a membrane spanning protein that pumps dopamine out of the synapse back into the cytosol, from which other transporters sequester dopamine into vesicles for later storage and release. Dopamine reuptake via DAT provides the primary mechanism through which dopamine is cleared from synapses except in the prefrontal cortex, where dopamine uptake via the norepinephrine transporter plays that role [216]. DAT is thought to be implicated in a number of dopamine related disorders, including ADHD, bipolar disorder, clinical depression and alcoholism. DAT's mechanism of action is based upon its ability to act as a symporter that moves dopamine across the cell membrane by coupling the movement to the energetically favourable sodium ions moving from high to low concentration into the cell. DAT function requires the sequential binding and co-transport of two Na⁺ ions and one Cl⁻ ion with the dopamine substrate.

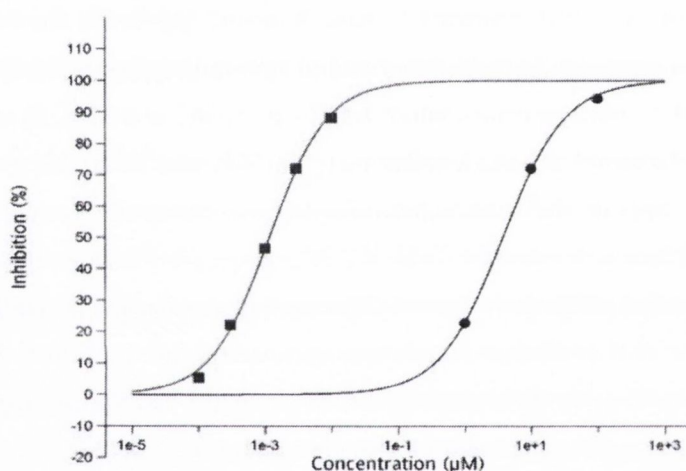


Figure 4.6 Dose response curve for *N*-methyl bupropion (circles) versus vancouverine reference (squares) in the DAT assay

The pharmacological screening of *N*-methyl bupropion versus bupropion in the dopamine transporter assay showed that *N*-methyl bupropion was much less active than bupropion in the reuptake of dopamine (Table 4.2). Although some activity was reported for *N*-methyl bupropion, $IC_{50} = 3.71 \mu M$ (Figure 4.6), this was at least one order of magnitude less active than bupropion, which in the pharmacological screen was shown to be in the nM range. From a prodrug perspective, if *N*-methyl bupropion and bupropion were dosed in an equimolar formulation and delivered by the oral route of administration, the *in vitro* screening results have shown that *N*-methyl bupropion would be extensively metabolised to bupropion pre-systemically in the intestine and liver. The pharmacological screen has also shown that any remaining unmetabolized prodrug would be only one-tenth as potent as bupropion at the DAT. This reduced activity at DAT reinforced its use as a potential prodrug of bupropion.

4.2.4.2.2 Serotonin transport system (SERT)

This protein is an integral membrane protein that transports the neurotransmitter serotonin from synaptic spaces into presynaptic neurons [216]. Transport of serotonin by the SERT protein terminates the action of serotonin and recycles it in a sodium-dependent manner. This protein is a target of psychomotor stimulants, such as amphetamine, cocaine and MDMA, and is a member of the sodium:neurotransmitter symporter family. A repeat length polymorphism in the promoter of this gene has been shown to affect the rate of serotonin uptake and may play a role in sudden infant death syndrome, aggressive behavior in Alzheimer disease patients, post traumatic stress disorder and depression-susceptibility in people experiencing emotional trauma.

Neither *N*-methyl bupropion nor bupropion showed activity in the serotonin transporter in the pharmacological screen ($IC_{50} > 100 \mu M$). This was a positive prodrug result from a pharmacological point of view as bupropion has no activity at the SERT.

4.2.4.2.3 Norepinephrine transporter (NET)

The sodium dependent norepinephrine transporter also known as the norepinephrine transporter or NET (or noradrenaline transporter (NAT)) is a monamine transporter that transports the neurotransmitters norepinephrine and dopamine from the synapse back to cytosol, from which other transporters VMAT sequester DA and NE into vesicles for storage and release [216].

Certain antidepressant medications act to raise noradrenaline, such as the SNRI's and the tricyclic antidepressants (TCAs). In other words, these medications prevent the noradrenaline transporter from doing its job. Noradrenaline therefore remains in the synapse longer, allowing it to reach more normal levels. Since the noradrenaline transporter is responsible for most of the dopamine clearance in the prefrontal cortex, SNRIs would also raise dopamine levels in synapses there. However, dopamine in most brain regions is cleared primarily by the dopamine transporter, which works roughly 10 times faster.

Although *N*-methyl bupropion and bupropion were shown to have similar activities at the NET, *N*-methyl bupropion was less active. Bupropion ($IC_{50} = 19.9 \mu M$) was approximately three times more active than *N*-methyl bupropion ($IC_{50} = 57.9 \mu M$) at the norepinephrine transporter, Table 4.2. These values represent weak reuptake inhibition of norepinephrine as the standard reference control, desipramine is active in the pM range ($IC_{50} = 0.89 nM$), Figure 4.7.

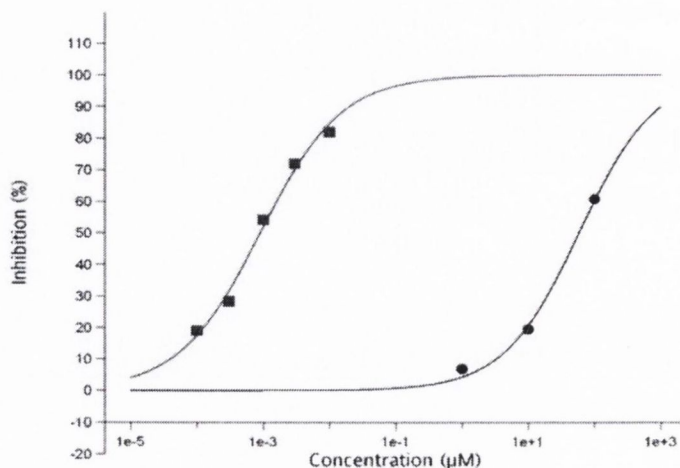


Figure 4.7 Dose response curve for *N*-methyl bupropion (circles) versus desipramine reference (squares) in the NET assay

4.2.4.2.4 Muscarinic acetylcholine receptor (mAChR)

Muscarinic receptors, or mAChRs, are G-coupled acetylcholine receptors found in the plasma membrane of certain neurons and other cells. They play several roles, including acting as the main end-receptor stimulated by acetylcholine released from postganglionic fibers in the parasympathetic nervous system. Muscarinic receptors were named as such because they are more sensitive to muscarine than to nicotine.

N-methyl bupropion and bupropion showed little activity at the muscarinic receptor. The IC_{50} values obtained from the screen were 39.3 and 86.5 μ M for *N*-methyl bupropion and bupropion respectively (Table 4.2). Although *N*-methyl bupropion was lower, these values are insignificant compared to reference atropine (1.54 nM), Figure 4.8.

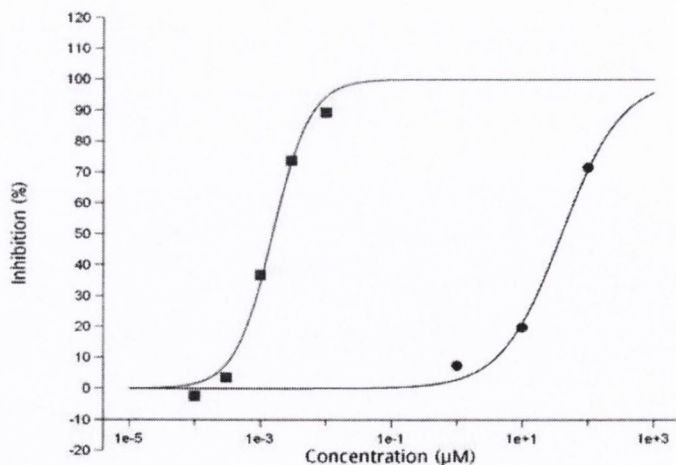


Figure 4.8 Dose response curves for *N*-methyl bupropion (circles) versus atropine reference (squares) in the muscarinic assay

4.2.4.2.5 Nicotinic acetylcholine (nAChR)

Nicotinic acetylcholine receptors, or nAChRs, are cholinergic receptors that form ligand gated ion channels in the plasma membrane of certain neurons and on the postsynaptic side of the neuromuscular junction. Being ionotropic receptors, nAChRs are directly linked to an ion channel and do not make use of a second messenger as metabotropic receptors do. Like the other type of acetylcholine receptors, muscarinic acetylcholine receptors (mAChRs)-the nAChR is triggered by the binding of the neurotransmitter acetylcholine (ACh). However, whereas muscarinic receptors are also activated by muscarine, nicotinic receptors are also opened by nicotine. Nicotinic acetylcholine receptors are present in many tissues in the body and are the best-studied of the ionotropic receptors. The neuronal receptors are found in the central nervous system and the peripheral nervous system. The neuromuscular receptors are found in the neuromuscular junctions of somatic muscles; stimulation of these receptors causes muscular contraction.

The pharmacological screen of *N*-methyl bupropion and bupropion at the nicotinic acetylcholine receptor did not show activity at any appreciable binding. Although *N*-methyl bupropion did have a lower IC_{50} value of 71.6 μ M, bupropion's IC_{50} was $> 100 \mu$ M (Table 4.2), these values are still insignificant to the reference compound epibatidine ($IC_{50} = 0.123$ nM), Figure 4.9. This assay was most likely not specific enough as bupropion is a known nicotinic antagonist for the $(\alpha 3)_2(\beta 4)_3$ receptor. In an effort to assess if *N*-methyl bupropion had any activity at a more specific receptor, three more specific nicotinic acetylcholine receptors were evaluated, namely $\alpha 1$, $\alpha 4\beta 2$ and $\alpha 7$. Bupropion and *N*-methyl bupropion did not show activity at these receptors in the range 1-100 μ M.

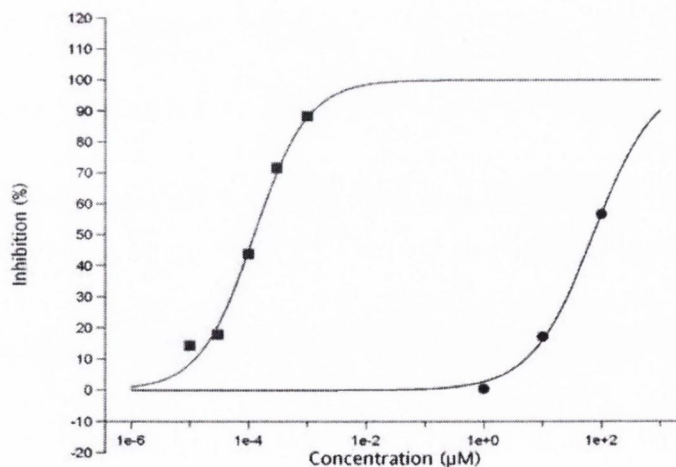


Figure 4.9 Dose response curves for *N*-methyl bupropion (circles) versus epibatidine reference (squares) in the nicotinic acetylcholine assay

4.2.4.2.6 A potential pharmacotherapy for cocaine addiction

A recent study released in December 2009 by Carroll *et al.* has suggested the potential use of *N*-methyl bupropion as a pharmacotherapy for cocaine addiction [123]. A series of bupropion analogues were synthesized and their *in vitro* and *in vivo* pharmacological properties were evaluated with the goal of developing an analogue of bupropion that had better properties for treating addiction. Although *N*-methyl bupropion was not the ideal candidate in this case, it did show some interesting properties. Bupropion has been shown to be a good candidate for treating cocaine addiction, given its dopaminergic properties and its success in dependency studies for cocaine, methamphetamine and nicotine. Their study's goal was to develop a bupropion analogue with increased dopaminergic properties as determined by its DA uptake with reduced NE uptake properties to reduce the potential for cardiotoxicity. Since the increased dopaminergic properties could also increase abuse potential, the desired analogue would need to have slow onset and long duration of action properties that are believed to reduce abuse potential. Although dopamine uptake inhibition was lower for *N*-methyl bupropion over bupropion, *N*-methyl bupropion performed well in other tests. *N*-methyl bupropion showed locomotor stimulant efficacy similar to cocaine and had periods of maximum stimulatory effect at times of 1 h or greater following injection. It also had a duration of locomotor activity greater than 3 h. The study showed some interesting pharmacotherapies for *N*-methyl bupropion but failed to recognize the extensive metabolism of this drug analogue that was shown in this chapter. An interesting study would be to assess potential synergistic pharmacological effects of dosing both *N*-methyl bupropion and bupropion.

4.2.4.2.7 A potential pharmacotherapy for smoking cessation

Another recent study by the Carroll group have also suggested a possible aid to smoking cessation for *N*-methyl bupropion [124].

The use of bupropion for treating nicotine addiction emerged from serendipitous observations that patients taking bupropion as an antidepressant were more successful in smoking cessation attempts. It was known that bupropion inhibited DA and NE uptake activity, but the discovery that it also preferentially antagonized $\alpha 3\beta 4^*$ -nAChR suggested that more than one of these targets might be involved in its smoking cessation efficacy. It is possible that bupropion SR is achieving its effects by increasing dopamine levels through DA uptake inhibition and shielding against nicotine induction of nAChR-mediated dopamine elevation. Although it is not clear what part if any is played by the ability of bupropion to inhibit NE uptake in its smoking cessation activity, it is likely to contribute to nicotine withdrawal amelioration. The goals of the study were to find bupropion analogues that possessed increased inhibitory

activity for DA and NE uptake inhibition and/or nAChR antagonism while retaining the druglike properties of bupropion.

N-methyl bupropion was the only compound of all synthesized that had higher selectivity (4-fold) for NE uptake inhibition relative to DA inhibition. Bupropion was shown to have a 4-fold selectivity for the $\alpha 3\beta 4^*$ -nAChR over other subtypes but *N*-methyl bupropion had > 10-fold selectivity. In the hot-plate assay, *N*-methyl bupropion had approximately a 2-fold more potency than bupropion suggesting that several mechanisms might impact supraspinal mechanisms of nicotine-mediated antinociception. *N*-methyl bupropion had an improved selectivity for $\alpha 3\beta 4^*$ -nAChR over DA uptake inhibition.

Once again though the authors had failed to recognize that *N*-methyl bupropion would be extensively metabolized presystemically before reaching its desired target so its use as a drug is limited.

4.2.4.3 Aqueous Stability

The aqueous stability of *N*-methyl bupropion was determined in the exact same manner as the determination of the aqueous stability of bupropion described in Chapter 2 [154]. This study was carried to establish if *N*-methyl bupropion had an improved stability profile over bupropion which could be used to its advantage in the formulation of *N*-methyl bupropion prodrug delivery systems. In particular, it was already seen that bupropion had a poor stability profile above pH 5 and any improved profile above this pH would have commercial benefits in formulating *N*-methyl bupropion.

The pH stability profile of bupropion and *N*-methyl bupropion at 40°C is presented in Figure 4.10. Both bupropion and *N*-methyl bupropion follow pseudo-first order decay kinetics in aqueous media. Below pH 5, *N*-methyl bupropion and bupropion had similar degradation rates, where they are both stable. Above pH 5, *N*-methyl bupropion degraded faster than bupropion. From pH 6 to 12, the rate of degradation of *N*-methyl bupropion increased almost linearly but above pH 12 the rate of degradation decreased quite dramatically. The opposite is true for bupropion where above pH 12, the rate of degradation increases significantly.

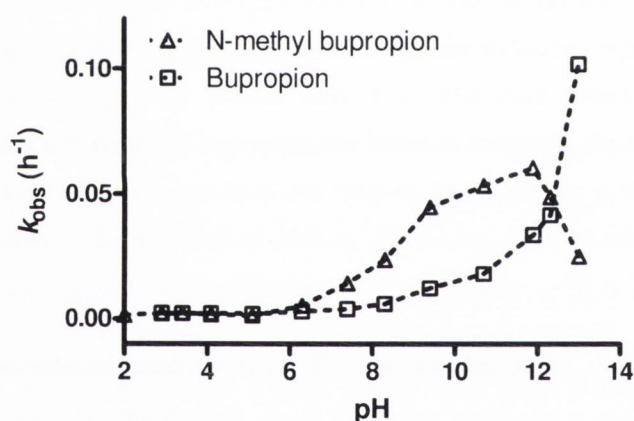


Figure 4.10 The pH stability profile of *N*-methyl bupropion compared to bupropion at 40°C

The reason for this improved stability of *N*-methyl bupropion at high pH is most likely due to the inability of the tertiary amine to form the imine. When bupropion is exposed to high pH it tautomerizes from ketone to enol/enamine to imine, whereas when *N*-methyl bupropion is exposed to high pH it may only tautomerize from ketone to enol, the imine cannot form as there is no free proton on the amino group of the tertiary amine. The imine is much more unstable and prone to hydrolysis which is the reason why bupropion's rate of degradation increases rapidly at high pH. It is unlikely though that *N*-methyl bupropion would be exposed to such a pH under physiological or formulation conditions so its improved stability at this pH confers no practical advantage.

4.2.4.4 Caco-2 cell permeability

N-Methylation of bupropion increases its lipophilicity by removing the hydrogen bond donor of the secondary amine, thus transforming it into a tertiary amine. This increase in lipophilicity should in turn increase its ability to traverse cell membranes such as the intestinal cell wall or the blood brain barrier. In order to assess if *N*-methylation improved cell permeability, a CACO-2 cell permeability experiment was conducted.

CACO-2 cells, derived from human colon adenocarcinoma, differentiate into a highly functionalized epithelial barrier with biochemical similarity to small intestinal columnar epithelium. These differentiated monolayers can be used to assess the membrane transport properties of novel compounds. The apparent permeability P_{app} values obtained from CACO-2 transport experiments have been shown to correlate with human intestinal absorption [217].

The experiment is conducted by growing a cell monolayer of CACO-2 cells on a porous membrane. The substrate is then placed in a donor well which can be on the apical (AP) side of the cell monolayer to measure passive diffusion or the basolateral (BL) side of the cell monolayer which is used to measure active transport diffusion (Figure 4.11). The amount of substrate transported into the receiver well is quantified and the apparent permeability can be calculated.

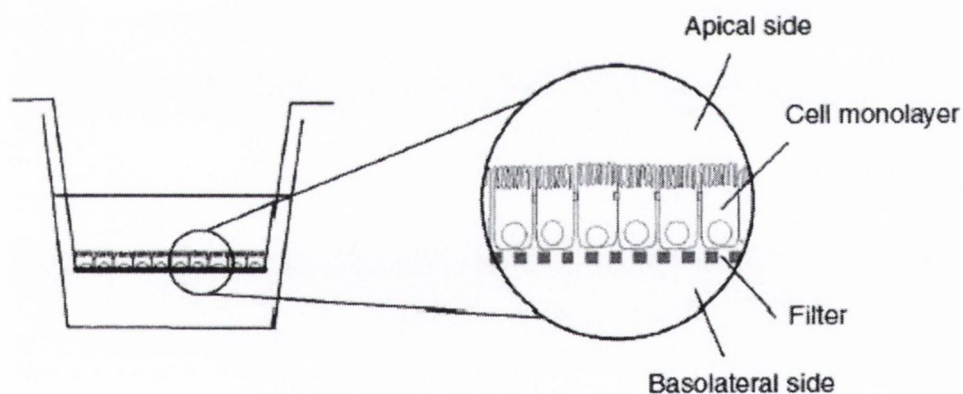


Figure 4.11 A schematic of the CACO-2 cell permeability experiment adapted from [218]

The transport assay donor solution contained 100 μM *N*-methyl bupropion in transport medium containing 100 μM Lucifer yellow and 1 % DMSO (pH 7.4 PBS buffer). The LC-UV method used to quantify *N*-methyl bupropion had an LOQ of 1 μM and the method was linear to at least 1 mM. System suitability was established on the day of use by repeat injections ($n = 6$) of 100 μM standard. The RT and peak area % RSD ≤ 2.0 %. Three methods were used to evaluate the integrity of the cell monolayer on the membrane, firstly by optical microscope visually, secondly by measuring the TEER (transepithelial electrical resistance) and thirdly by measuring the amount of Lucifer yellow that had passed through the membrane into the

receiver well. The TEER values indicate the degree of monolayer confluence and tight junction development. Lucifer yellow was used as an internal control for each monolayer to verify tight junction integrity during the entire assay period. Variations in tight junctions can significantly affect permeability rates for compounds using the paracellular transport route. P_{app} values of Lucifer yellow were quantified at the end of experiment. The normal range for Lucifer yellow permeability in CACO-2 monolayers ≤ 10 nm/sec.

Apparent permeability (P_{app}) values were calculated using Equation 4.3

Equation 4.3

$$P_{app} = \left(\frac{dQ}{dt}\right) \times \frac{1}{C_0} \times \frac{1}{A}$$

where dQ/dt is the permeability rate, C_0 is the initial concentration in the donor compartment, and A is the surface area of the filter. Permeability rate was calculated by plotting the percent of initial AP drug mass (peak area) found in the BL compartment versus time and determining the slope of the line. The P_{app} value for *N*-methyl bupropion was calculated from 15 minute data to ensure that < 10 %of initial compound was found in the receiver compartment.

After ensuring all the quality controls were met for the experiment, the P_{app} values were calculated and are presented in Table 4.3.

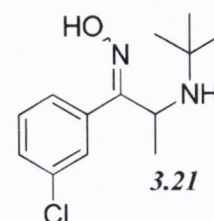
	P_{app} (cm/sec)	(nm/sec)	Efflux ratio	Bupropion P_{app} (nm/sec)
Apical to basolateral	$5.16 \pm 1.12 \times 10^{-6}$	4710 ± 1020	2.42	1500 ± 220 [219]
Basolateral to apical	$12.5 \pm 2.9 \times 10^{-6}$	6820 ± 1600		

Table 4.3 CACO-2 cell permeability values for *N*-methyl bupropion. Bupropion literature data is also shown

The AP to BL P_{app} of 5.16×10^{-6} cm/sec for *N*-methyl bupropion is a typical value for a compound that is completely absorbed from the human intestine [218]. This rate is also three times higher than the value obtained for bupropion, which reflect its increased permeability due to increased lipophilicity. The basolateral to apical P_{app} was faster than the apical to basolateral P_{app} indicating active transport is also occurring through the cells. *N*-methyl bupropion is most likely protein bound and transported through the CACO-2 cell monolayer. Efflux ratios greater than 1 are an indication of an active transport process. The efflux ratio is defined as the quotient of the secretory permeability and the absorptive permeability ($P_{app, ba} / P_{app, ab}$). The increased lipophilicity and permeability of *N*-methyl bupropion improve its prodrug like qualities and its ability to penetrate the blood brain barrier and reach its potential target.

4.2.5 Hydroxyimine of bupropion (3.21)

The hydroxyimine of bupropion **3.21** was screened in each of the five metabolic media, SGF, SIF, HIM, HLM and PHP. Neither bupropion nor any of its metabolites were detected during the course of the screening in any media. This was unexpected as oximes are generally susceptible to hydrolysis and are also prone to metabolism by CYP enzymes [113]. It was unusual too that an analogue of bupropion was showing such high stability.



A short stability study was conducted on the hydroxyimine of bupropion **3.21** versus bupropion in two media at 37°C to see if the hydroxyimine had greater overall stability. Simulated gastric fluid was chosen to establish if any hydrolysis would occur to the hydroxyimine at low pH but none was detected, bupropion and the hydroxyimine of bupropion had similar stability profiles in this media. At physiological pH though, the hydroxyimine of bupropion had much greater stability than bupropion. This was likely due to intramolecular hydrogen bonding between the hydrogen on the hydroxyl group of the hydroxyimine and the amino nitrogen. This added stability of the hydroxyimine may have been the contributing reason why no metabolism to bupropion was occurring. The stability study results are presented in Figure 4.12.

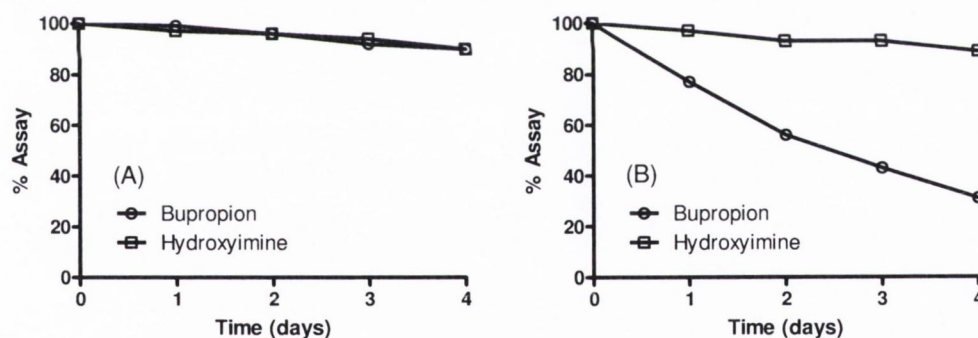


Figure 4.12 Stability of the hydroxyimine of bupropion versus bupropion in (A) simulated gastric fluid pH 1.2 at 37°C and (B) phosphate buffered saline solution pH 7.4 at 37°C

Although the hydroxyimine has no potential as a prodrug of bupropion, its excellent hydrolytic stability profile and inertness to metabolic enzymes make it a very good potential drug candidate. Chromatographically, it has the same retention time as bupropion so most likely has similar lipophilicity as the pK_a would also be similar to bupropion. Therefore the hydroxyimine would likely cross the blood brain barrier quite easily. It would be an interesting compound to evaluate for its pharmacological profile. The structures of bupropion

and the hydroxyimine are very similar but one isomer of the hydroxyimine is likely locked in one configuration due to intramolecular hydrogen bonding.

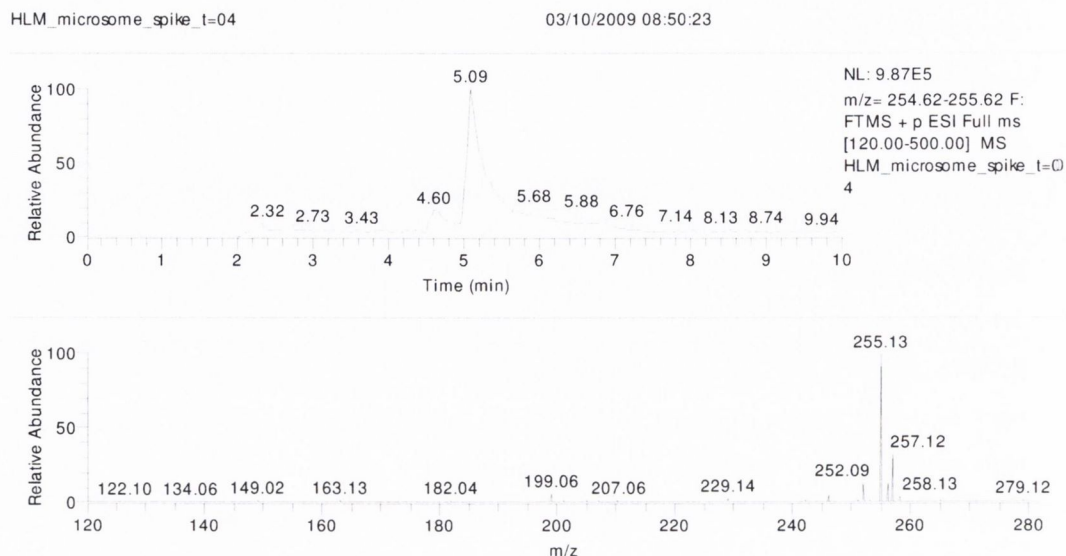
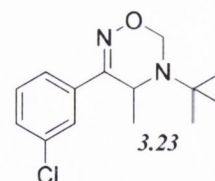


Figure 4.13 A +ESI LC-MS spectrum of the hydroxyimine of bupropion 3.21

4.2.6 Oxadiazine of bupropion (3.23)

The oxadiazine of bupropion **3.23** was an interesting compound for two reasons. Firstly, did it have the potential to be a double prodrug of bupropion? Possible *N*-dealkylation and metabolism of the remaining alkyl-oximine would give back bupropion. It was already shown that the *N*-methylated analogue of bupropion was susceptible to *N*-dealkylation, and this could easily be the case for the oxadiazine. Secondly, if the hydroxyimine **3.21** was a possible prodrug of bupropion or even a new drug candidate, the oxadiazine **3.23** could be a prodrug for the hydroxyimine **3.21**.



Screening of the oxadiazine of bupropion **3.23** in each of the five metabolic media did not produce bupropion or any of its metabolites but the main transformation that was occurring was conversion to the hydroxyimine. Two successive de-alkylations were giving back the hydroxyimine. The hydroxyimine again was most likely too stable then for further metabolism. Both the human intestinal and human liver microsome suspensions were able to metabolize the oxadiazine **3.23** back to the hydroxyimine of bupropion **3.21**. An example of the accurate mass LC-MS chromatogram is presented in Figure 4.15.

RT: 0.00 - 15.03

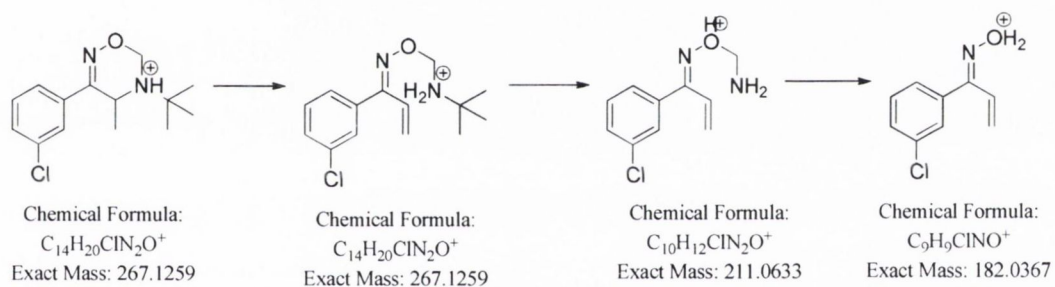
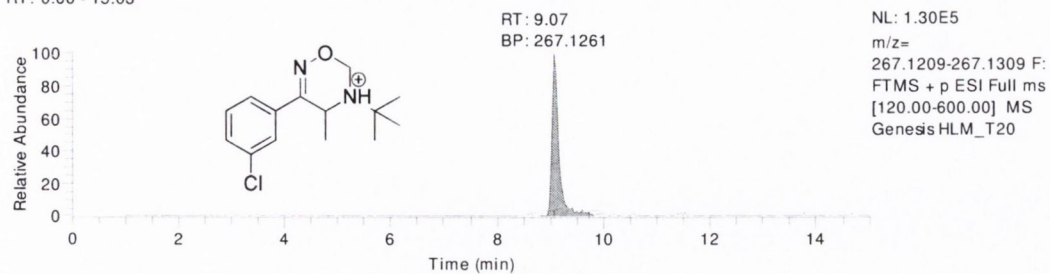


Figure 4.14 An LC-MS chromatogram of the oxadiazine prodrug of bupropion 3.23 and the proposed fragmentation pattern

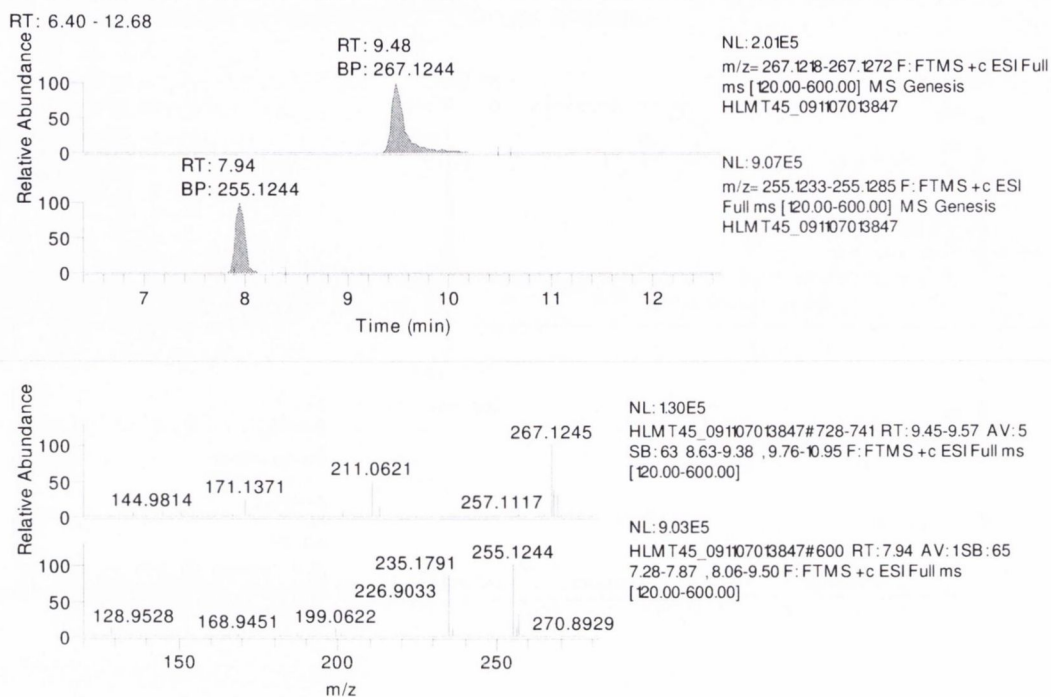
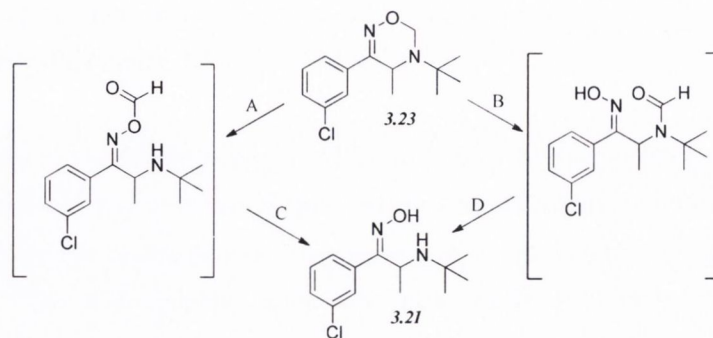


Figure 4.15 A typical LC-MS chromatogram of the oxadiazine of bupropion incubated in human liver microsomes for one hour at 37°C. The retention times of the oxadiazine and hydroxyimine are 9.48(267.1245) and 7.94 (255.1244) min respectively.

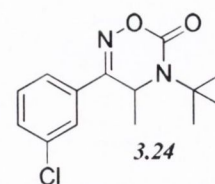
The likely mechanism of transformation of the oxadiazine **3.23** to the hydroxyimine **3.21** is via a double dealkylation of the oxadiazine ring. *N*-dealkylation, step A Scheme 4.3, is the most likely first dealkylation with subsequent loss of formaldehyde, step C to yield the hydroxyimine. This is more likely as step B would yield an amide intermediate which is likely to be too stable for further hydrolysis back to the hydroxyimine (as seen in section 4.2.3.).



Scheme 4.3 The possible mechanisms of oxidative dealkylation of the oxadiazine by human intestinal and human liver microsomes. A) Oxidative *N*-dealkylation B) Oxidative *O*-dealkylation C) and D) loss of formaldehyde

4.2.7 Oxadiazinone of bupropion (3.24)

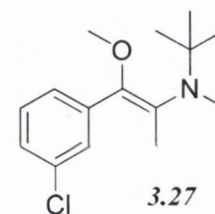
The oxadiazinone of bupropion **3.24** was synthesized as another potential prodrug of the hydroxyimine of bupropion, and possibly a multistep prodrug of bupropion itself. The oxadiazinone is a six membered ring containing both a carbamate and oxime functionality linked together. The carbamate carbonyl should be liable to hydrolysis. The structure is relatively novel as a structure search yielded no drug like structures with any similarity to the oxadiazine of bupropion.



Screening of the oxadiazinone of bupropion in each of the five metabolic media, showed the compound to be stable over the course of the experiment. Neither bupropion nor any of its metabolites were detected in the media. There was no detection of any other prodrug either so there was no transformation back to the hydroxyimine. The oxadiazinone was too stable to act as a prodrug for bupropion.

4.2.8 *N,O*-dimethyl bupropion (3.27)

Dimethyl bupropion **3.27** was synthesized by *O*-methylation of the enolate of *N*-methyl bupropion **3.19**. This compound was synthesized as a potential multistep prodrug of bupropion **3.5**. It was already shown that *N*-methyl bupropion **3.19** was quite easily demethylated to bupropion **3.5**, and an *N,O*-dimethylated analogue **3.27** could just as easily be *O*-demethylated to



N-methyl bupropion **3.19**. Enol-ether prodrugs have been used successfully in the past and can be converted to the corresponding ketone by acid catalysed hydrolysis, without the use of metabolizing enzymes [220]. Enol ether prodrugs of Erythromycin have been shown to have half lives in the order of minutes for conversion to their corresponding ketones at pH's 1 and 2.

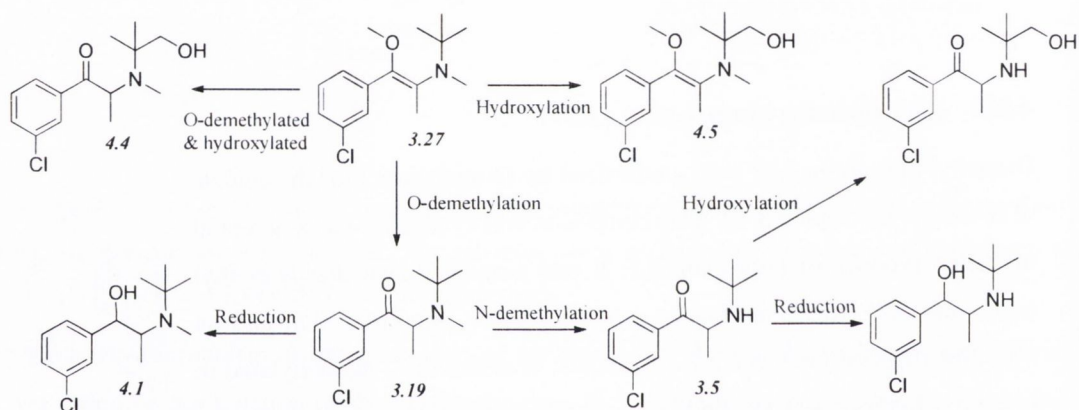
The dimethylated prodrug was transformed to *N*-methyl bupropion in human intestinal and human liver microsomes. It was also shown to be unstable in the other media, SGF, SIF and PHP but neither bupropion, its metabolites or any other prodrug were detected so it was likely degrading to unknown compounds that the mass spectrometer could not pick up in positive ion mode. *O*-demethylation of the dimethylated prodrug and subsequent *N*-demethylation meant that the dimethylated prodrug was a potential double prodrug of bupropion.

A number of new metabolites of dimethyl bupropion **3.27** were detected. The major metabolite of dimethyl bupropion was *N*-methyl bupropion formed by *O*-demethylation. Two other minor metabolites were also detected, specifically the hydroxylated metabolite and a

metabolite of two mass units greater than the substrate, most likely formed by *O*-demethylation and subsequent formation of the *N*-oxide. The hydroxylated metabolite was also shown to be hydroxylated on one of the *t*-butyl arms. This was evident from the fragmentation pattern of the metabolite.

This result indicated that dimethyl bupropion was a good multistep prodrug of bupropion and a prodrug of *N*-methyl bupropion. The extra dimethyl groups increased the lipophilicity of the compound and hence it should have improved absorption and better permeation across the blood-brain barrier. The lone pair of electrons are still available on the nitrogen so the dimethyl analogue can be transformed into a quaternary ammonium salt to improve solubility and improve its stability upon formulation.

A number of new drug candidates emerged too relating to dimethyl bupropion, in fact the *O*-demethylated, hydroxylated metabolite was a prodrug of *N*-methyl bupropion. Both these new metabolites were likely to be pharmacologically active.



Scheme 4.4 Metabolism of dimethyl bupropion 3.27 in human liver and human intestinal microsomes

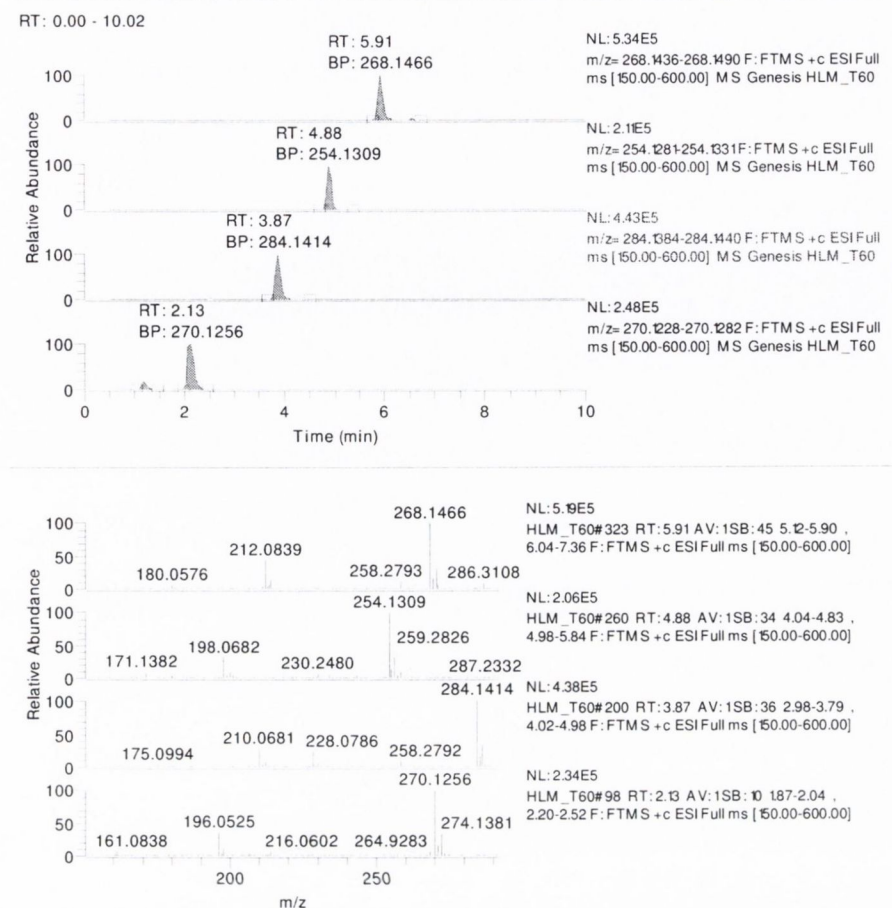
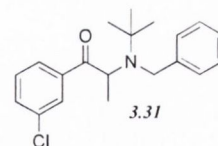


Figure 4.16 A typical HPLC-MS chromatogram of the metabolism of dimethyl bupropion in human liver microsomes. Dimethyl bupropion (268.1466 amu), *N*-methyl bupropion (254.1309 amu), hydroxylated dimethyl bupropion (284.1414 amu) and mono-demethylated & hydroxylated dimethyl bupropion (270.1256 amu), retention times are 5.91, 4.88, 3.87 and 2.13 minutes respectively

4.2.9 *N*-benzyl bupropion

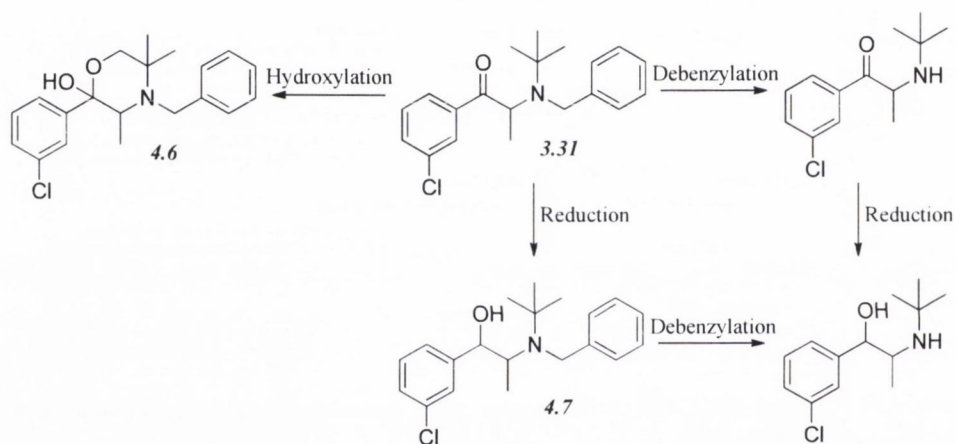
Bupropion was *N*-benzylated in order to protect the amine group during further reactions on the enolate as shown in chapter 3. Catalytic reduction and oxidative methods failed to remove the benzyl group without further degradation of the product so adequate deprotection methods were not



found for *N*-debenzylation. Attempts were made to debenzylate using the metabolic enzyme mixtures. *N*-benzyl bupropion was screened using SGF, SIF, HIM, HLM and PHP. Bupropion and new metabolites related to the *N*-benzyl compound were detected in both human intestinal and human liver microsomes. Therefore although the microsomes were used to debenzylate *N*-benzyl bupropion, we had serendipitously found a potential prodrug of bupropion. An example of the metabolic screen is shown in Figure 4.17.

The major metabolite from the microsomal screen was bupropion so debenzylation is the main mechanism of metabolism but a reduced and hydroxylated metabolite were also seen. Reduction of the ketone to the alcohol was most likely the reduced metabolite as seen with bupropion and *N*-methyl bupropion. The retention time and accurate mass spectrum of the reduced metabolite were as expected.

Hydroxylation took place on one of the *t*-butyl arms and rearrangement occurred. This rearrangement leads to more stable phenylmorphinol ring and is evidenced by the accurate mass spectrum of the metabolite. The major fragment from the molecular ion (346 amu) is at 328 amu signifying loss of water. If rearrangement didn't occur, *i.e.* hydroxylation occurred elsewhere on the molecule, one of the major fragments would be loss of the *t*-butyl group (-56 amu). When rearrangement to the phenylmorphinol metabolite occurs, the *t*-butyl fragment cannot be lost. The metabolism is summarized in Scheme 4.5.



Scheme 4.5 Metabolism of *N*-benzyl bupropion in human liver and intestinal microsomes

The unexpected debenzylation of the *N*-protected amine lead to the conclusion that an *N*-benzyl prodrug of bupropion would also be a good prodrug candidate. After showing *N*-demethylation (4.2.4), *N*-debenzylation and ring opening on the oxadiazine (4.2.6), it was likely that this nitrogen was very susceptible to oxidative *N*-dealkylation by microsomal enzymes.

Two new drug candidates related to *N*-benzyl bupropion were also discovered which could later be synthesized and evaluated for their pharmacological activity. Like bupropion, the reduced metabolite, the amino alcohol and the hydroxylated phenylmorphinol were most likely going to have some activity which would increase the therapeutic profile of *N*-benzyl bupropion.

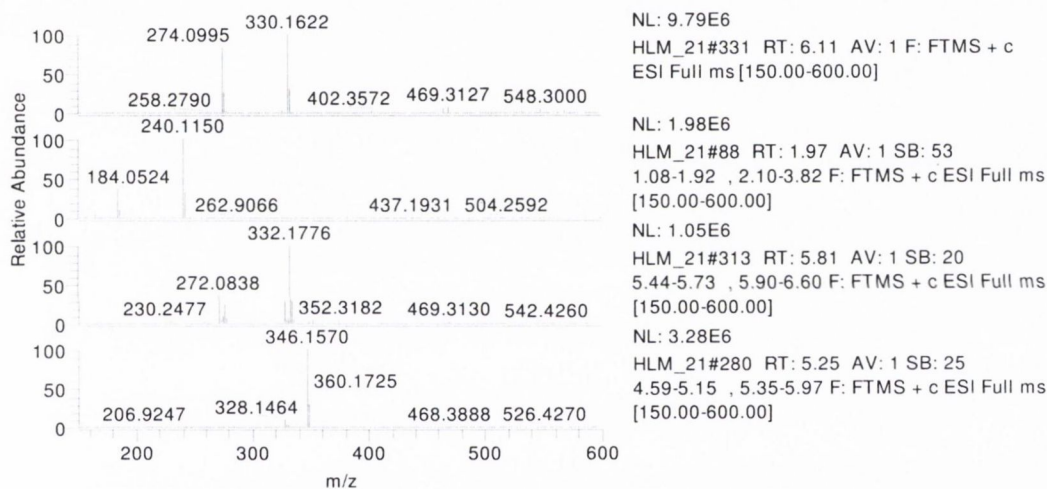
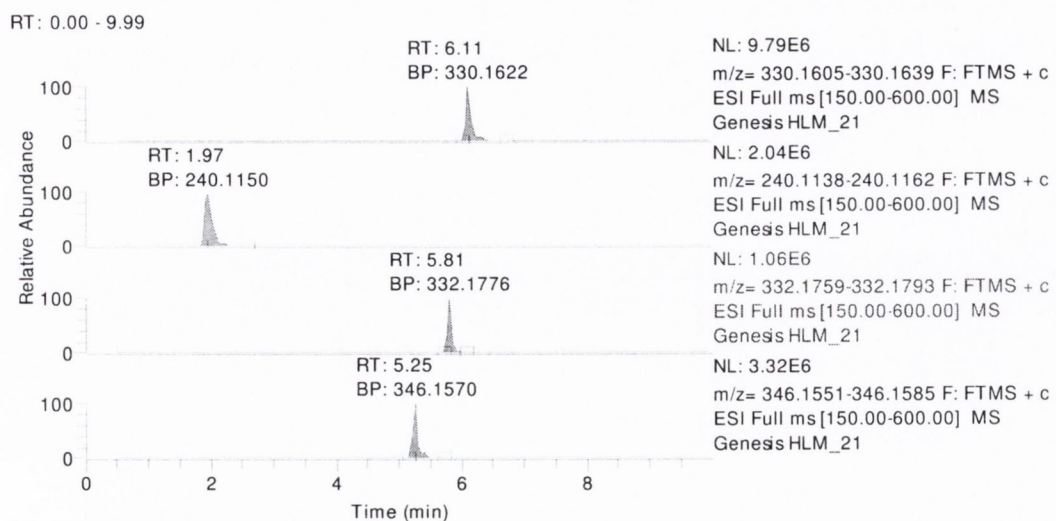


Figure 4.17 A typical HRLC-MS chromatogram of *N*-benzyl bupropion incubated with human liver microsomes. The retention times of *N*-benzyl bupropion (330.1622 amu), bupropion (240.1150 amu), *N*-benzyl amino alcohol (332.1776 amu) and *N*-benzyl bupropion hydroxylated (346.1570 amu) are 6.11, 1.97, 5.81 and 5.25 minutes respectively

4.2.9.1 Enzyme kinetics

The enzyme kinetics were evaluated according to the Michaelis-Menten equation. The enzyme concentration, co-factors and buffer concentration were fixed while the substrate concentration was varied. The velocity of bupropion formation was quantified by LC-MS and the data was fitted to the Michaelis-Menten equation using least squares non-linear regression analysis, Figure 4.18. The V_{max} was calculated at 1323 ± 42.2 pmol/min/mg HLM, the K_m was 15.2 ± 2.8 μ M and the intrinsic hepatic clearance ($Cl_{i, h}$) was found to be 87 L/mg.

Compared to the enzyme kinetic data obtained for the transformation of *N*-methyl bupropion to bupropion, the conversion of *N*-benzyl bupropion to bupropion had a higher velocity and a greater enzyme-substrate affinity as seen with the lower Michaelis-Menten constant, K_m . Hence there is almost a 10-fold higher intrinsic hepatic clearance for *N*-benzyl compared to *N*-methyl bupropion.

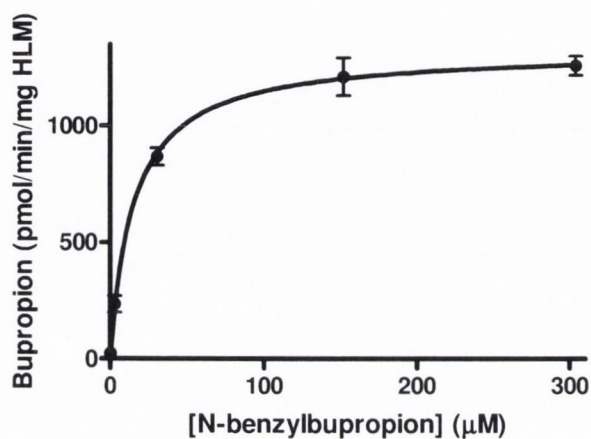


Figure 4.18 Substrate saturation study in pooled human liver microsomes of *N*- benzyl potential prodrug of bupropion. $V_{max} = 1323 \pm 42.2$ pmol/min/mg HLM, $K_m = 15.2 \pm 2.8$ µM, $R^2 = 0.9601$, $n = 6$.

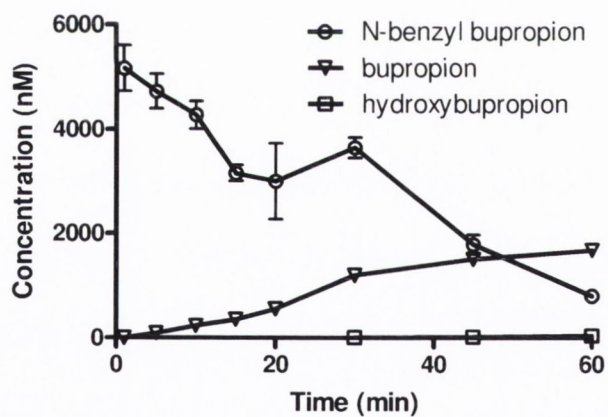
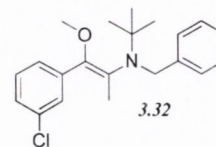


Figure 4.19 Metabolism of *N*-benzyl bupropion during a 60 minute incubation in HLM

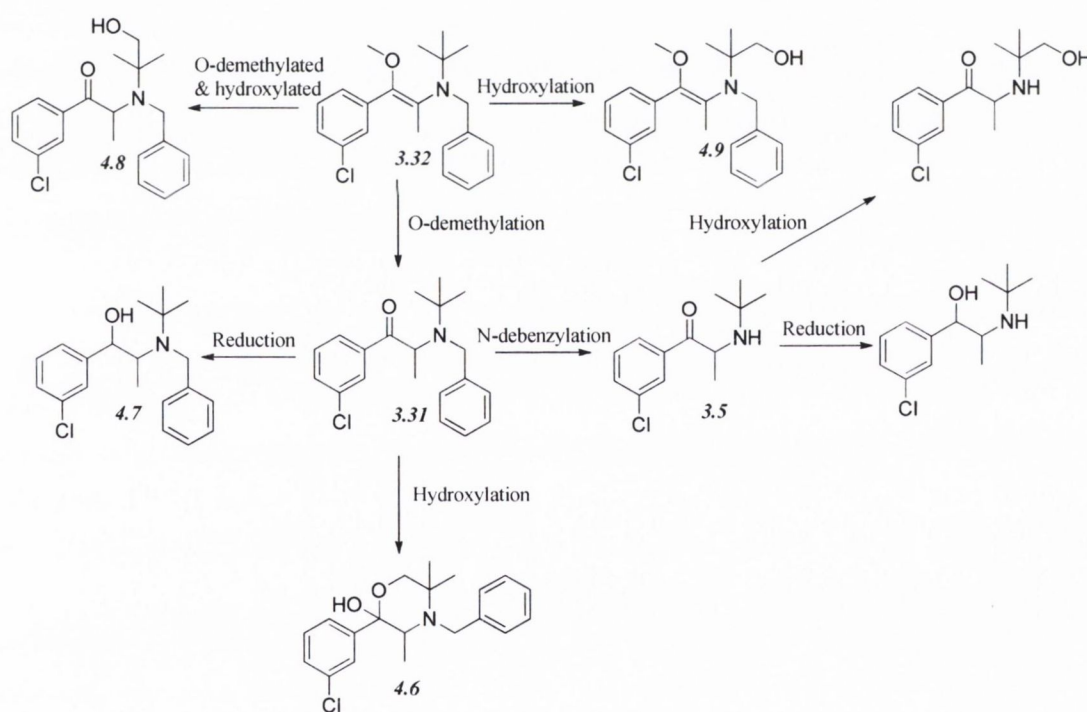
4.2.10 *N*-benzyl *O*-methyl bupropion (3.32)

During the course of trying to synthesize *O*-methyl bupropion, the *N*-benzyl protected *O*-methylated product 3.32 was made as an intermediate. After unsuccessful attempts to remove the benzyl protecting group, it was decided to use the intermediate as is. This compound could potentially be a double prodrug of bupropion if *O*-demethylation and *N*-debenzylation occurred. It was already shown that *N*-debenzylation was a realistic possibility with compound 3.31 and *O*-demethylation also occurred with compound 3.27.



3.32 was screened in the five metabolic media and was shown to be *O*-demethylated to *N*-benzyl bupropion in human liver and human intestinal microsomes. New metabolites were also detected but the general mechanism of metabolism followed the same pathway as *N,O*-dimethyl bupropion (

Scheme 4.4). The same benzylated metabolites were detected (Scheme 4.6), a hydroxylated 4.9, demethylated and oxidized 4.8 and debenzylated 3.31.



Scheme 4.6 Metabolism of *N*-benzyl, *O*-methyl bupropion in human liver microsomes

N-benzyl *O*-methyl bupropion 3.32 has the potential to be a multistep prodrug of bupropion by *O*-demethylation and *N*-debenzylation in liver and intestinal microsomes. Numerous metabolites relating to the above were detected, all with possible pharmacological activity and therefore potentially new drug candidates.

4.3 Conclusion

A successful tool was developed for *in vitro* screening of potential prodrugs of bupropion which utilised 5 different media that a drug substance would encounter via the oral route of delivery. This screening tool can be used generically to evaluate drug and prodrug stability for oral delivery.

Two direct prodrugs of bupropion were discovered using the prodrug screening tool, *N*-methyl bupropion **3.19** and *N*-benzyl bupropion **3.31**. *N*-benzyl bupropion was found serendipitously while trying to find a suitable protective group for the amine of bupropion. An oxadiazine **3.23** bioprecursor of the hydroxyimine **3.21** of bupropion was found. The hydroxyimine **3.21**, being a potential new drug entity with potential pharmacology similar to bupropion was found to have an excellent stability profile. The *N*-methyl, *N*-benzyl and oxadiazine were all *N*-dealkylated by human liver and human intestinal microsomes indicating that the tertiary amine is susceptible to oxidation by the CYP or FMO enzymes. It is therefore quite likely that other *N*-alkyl groups such as ethyl, propyl or codrugs linked via an alkyl bridge could be appended to bupropion and would be successfully metabolized off.

Two potential multistep prodrugs of bupropion were discovered, *N,O*-dimethyl bupropion **3.27** and *N*-benzyl *O*-methyl bupropion **3.32**, which in themselves are prodrugs of *N*-methyl and *N*-benzyl bupropion respectively. These pro-prodrugs of bupropion are metabolized as follows to reach bupropion; *O*-dealkylation followed by *N*-dealkylation. Therefore enol-ethers are susceptible to the oxidative enzymes of the CYP and FMO family. A number of new metabolites of these prodrugs were identified with potential pharmacological activity.

N-benzyl bupropion **3.31** was evaluated for its enzyme kinetics using human liver microsomes. It was transformed to bupropion at a higher rate than *N*-methyl bupropion and it had a higher enzyme-substrate affinity. A number of new metabolites relating to *N*-benzyl bupropion were found, namely the reduced form *N*-benzyl amino alcohol and a hydroxylated *N*-benzyl bupropion. These metabolites could all have potential pharmacological activities. *N*-benzyl bupropion may also be a good prodrug candidate of bupropion.

N-methyl bupropion **3.19** was evaluated for its enzyme kinetics, pharmacology and stability. *N*-methyl bupropion was also shown to be reduced to the amino alcohol, this new metabolite could also have potential pharmacotherapies. *N*-methyl bupropion was shown to have a similar stability profile to bupropion below pH 5, but between pH 5-11 was less stable. The pharmacological profile of *N*-methyl bupropion was screened in a DAT, NET, SERT, nAChR and nMAChR assay. It was shown to be less active than bupropion. *N*-methyl bupropion was deemed a good candidate as a potential prodrug of bupropion for an *in vivo* proof of concept study.

4.4 Experimental

4.4.1 Materials

Bupropion hydrobromide reference standard was supplied from Biovail Technologies Ireland Ltd, Citywest Business Campus, Dublin 24, Ireland. Pooled human liver microsomes, pooled human intestinal microsomes, guinea pig S9 fraction, and NADP regenerating solutions were supplied by BDBiosciences, 1 Becton Drive, Franklin Lakes, NJ, USA, 07417. Citrated human plasma was obtained from healthy male and female volunteers from the School of Pharmacy and Pharmaceutical Sciences, Trinity College, Dublin. LC-MS grade solvents were purchased from Fisher Scientific Ireland. Pepsin, from porcine stomach mucosa, with an activity of 800 to 2500 units per mg of protein (Sigma-Aldrich catalogue number P7000). Pancreatin (Sigma-Aldrich catalogue number P8096). Phosphate buffered saline tablets, (Sigma-Aldrich catalogue number P4417). HPLC grade solvents and all other reagents were analytical grade and purchased from Sigma Aldrich Ireland. Bupropion hydrochloride reference standard and its metabolite standards were purchased from Toronto Research Chemicals, 2 Brisbane Road, North York, Ontario, Canada, M3J 2J8.

4.4.2 Chromatographic method for screening potential prodrugs

The column used for chromatographic separation was a Waters Xbridge C18, 2.1 x 50 mm 2.5 μm at 30°C. Mobile phase A: 10:40:50, 1.0 % ammonium hydroxide solution in water, adjusted to pH 10.5 with formic acid: water: acetonitrile. Mobile phase B: 10:90, 1.0 % ammonium hydroxide solution in water, adjusted to pH 10.5 with formic acid: acetonitrile. Flow rate : 250 $\mu\text{L}/\text{min}$, injection volume: 10 μL , run time: 10 min. Gradient, 100 % A hold for 1 min, 0 % B to 100 % B over 4 min, hold 100 % B for 4.5 min, 0 % B at 9.51 minutes and equilibrate for 0.5 min.

4.4.3 Mass Spectrometer conditions for detection of potential prodrugs

The LTQ-XL-Orbitrap mass spectrometer was coupled to the Accela LC system via an electrospray ionization (ESI) probe. The capillary temperature was maintained at 350°C, sheath gas flow rate 50 arbitrary units, auxiliary gas flow rate 5 arbitrary units, sweep gas flow rate 0 arbitrary units, source voltage 3.20 kV, source current 100 μA , capillary voltage 43.00 V and tube lens 100 V. Compounds were detected in positive ion mode using selected ion monitoring (SIM). Hydroxybupropion was detected $(\text{M}+\text{H})^+ = 256.1099$, RT = 1.0 min, Rac-erythrohydrobupropion $(\text{M}+\text{H})^+ = 242.1306$, RT = 2.3 min, Rac-threohydrobupropion $(\text{M}+\text{H})^+ = 242.1306$, RT 2.8 min, bupropion $(\text{M}+\text{H})^+ = 240.1150$, RT = 2.0 min. The optimum detector conditions were found by tuning the instrument to be most sensitive for bupropion's most abundant ion at 240 (m/z).

4.4.4 Networks software

Networks 1.1.0 software from Thermo Electron Corporation was used to screen accurate mass LC-MS chromatograms for phase I and phase II metabolic transitions. This was done in three steps. The sample (metabolized TIC/MSⁿ) chromatogram and a blank chromatogram are selected from the sample run. The blank is subtracted from the sample to clean up the background spectra. The analyte(s) being metabolized are selected or inputted into the software, namely the exact mass molecular weight. Metabolite modifications are selected from the software or can be entered into the software manually. These modifications are the exact mass transitions that would be expected from the analyte of interest if the metabolic modification has taken place. The chromatogram is then screened by the software for each modification and the results are presented. The software increases productivity by automatically searching for each analyte metabolites with exact mass specifications.

4.4.5 Human liver microsome stock solution preparation

HLM (0.5 mL) stock was added to PBS solution (9.5 mL). Final concentration; 1 mg/mL. This solution was sub-aliquotted to reduce freeze-thaw cycles, and stored at -80°C. 20 x 500 µL aliquots were sufficient. The PBS solution was prepared by addition of one USP PBS tablet (Sigma-Aldrich catalogue number P4417) dissolved in 200 mL deionised water.

4.4.6 Human intestinal microsome stock solution preparation

HIM (0.2 mL) stock was added to PBS solution (9.8 mL). Final concentration; 0.2 mg/mL. This solution was sub-aliquotted to reduce freeze-thaw cycles, and stored at -80°C. 20 x 500 µL aliquots were sufficient.

4.4.7 NADPH regenerating solution A stock solution preparation

NADPH solution A (5.0 mL) was added to PBS solution (5.0 mL). Final concentration; 13 mM NADP⁺. This solution was sub-aliquotted to reduce freeze-thaw cycles, and stored at -80°C. 20 x 500 µL aliquots were sufficient.

4.4.8 NADPH regenerating solution B stock solution preparation

NADPH solution B (1.0 mL) was added to PBS (9.0 mL). Final concentration; 4 U/mL G-6-PDH. This solution was sub-aliquotted to reduce freeze-thaw cycles, and stored at -80°C. 20 x 500 µL aliquots were sufficient.

4.4.9 Pooled human plasma solution preparation

Citrated human plasma was pooled together from three separate donors. This solution was sub-aliquoted to reduce freeze-thaw cycles, and stored at -80°C. 20 x 500µL aliquots were sufficient.

4.4.10 USP simulated gastric fluid preparation

Sodium chloride (0.02 g) and purified pepsin (0.032 g) that is derived from porcine stomach mucosa with an activity of 800 to 2500 units per mg of protein were dissolved in 0.07 mL of hydrochloric acid and sufficient water to make 10 mL. This test solution had a pH of about 1.2. This solution was sub-aliquoted to reduce freeze-thaw cycles, and stored at -80°C. 20 x 500µL aliquots are sufficient.

4.4.11 USP simulated intestinal fluid preparation

Monobasic potassium phosphate (0.068 g) was dissolved in 2.5 mL of water and mixed. Sodium hydroxide (0.77 mL of 0.2 N) and water (5.0 mL) were added. Pancreatin (0.1 g) was added and the pH adjusted with either 0.2 N sodium hydroxide or 0.2 N hydrochloric acid to a pH of 6.8 ± 0.1 . The solution was diluted to 10 mL with water. This solution was sub-aliquoted to reduce freeze-thaw cycles, and stored at -80°C. 20 x 500µL aliquots are sufficient.

4.4.12 Determination of microsomal metabolic stability

Microsomes, NADPH regenerating solutions A and B were thawed rapidly to 37°C, then kept on wet ice until ready for use. The prodrug was prepared to 5 mM in ACN. To a 1.7 mL microcentrifuge tube in a 37°C water bath was added, 349 µL phosphate buffered saline solution, 50 µL NADPH regenerating solution A, 50 µL NADPH regenerating solution B, 1 µL prodrug solution. After incubation for 5 minutes, 50 µL microsome solution was added and the metabolism was initiated. The tube was inverted twice or vortex mixed. The final concentrations in this solution was 10 µM prodrug, 0.1 mg/mL HLM or 0.02 mg/mL HIM, 1.3 mM NADP⁺, 0.4 U/mL glucose-6-phosphate dehydrogenase and 0.2 % organic solvent. This solution was incubated for 60 minutes at 37°C. The reaction was quenched by addition of 500 µL of acetonitrile. The mixture was centrifuged at 10,000 x g for 10 minutes. The supernatant was analysed by LC-MS analysis.

4.4.13 Synthesis of *N*-methyl amino alcohol of bupropion (4.1)

To *N*-methyl bupropion **3.19** (0.05 g, 0.2 mmol) was added sodium borohydride (0.04 g, 1.0 mmol) in 5 mL methanol:ethanol, 1:4 at room temperature. The mixture was stirred for 30

minutes. The colour changed from slight yellow to clear cloudy. The reaction was complete when no *N*-methyl bupropion was detected by thin layer chromatographic analysis. 10 mL water was added and the mixture was extracted with 3 x 10 mL portions of hexane. The hexane extracts were combined and dried over anhydrous magnesium sulphate. The hexane was removed under vacuum on a rotary evaporator. After drying a white solid remained.

Two diastereomers. (Yield 0.05 g, 100 %, 66 % erythro, 33 % threo by NMR and LCMS).

N-methyl erythro amino alcohol, $^1\text{H NMR } \delta$ (CDCl_3): 0.96-0.98 (d, 3H, $J = 7.0$ Hz, $-\text{CHCH}_3$), 1.10 (s, 9H, $-\text{CH}(\text{CH}_3)_3$), 1.99 (s, 3H, $-\text{NCH}_3$), 3.36-3.43 (q, 1H, $J = 6.65$ and 6.11 Hz, $-\text{CHCH}_3$), 4.48-4.49 (d, 1H, $J = 5.36$ Hz, $-\text{CHOH}$), 7.19-7.39 (m, 4H, Ar-H).

$^{13}\text{C NMR ppm}$: 12.72 $-\text{CHCH}_3$, 26.7 $-\text{CH}(\text{CH}_3)_3$, 30.5 $-\text{NCH}_3$, 54.5 $-\text{CHCH}_3$, 54.5 $-\text{C}(\text{CH}_3)_3$, 73.9 $-\text{CHOH}$, 124.6, 126.4, 126.5, 128.3 (4 x Ar CH), 133.2, 144.7 (2 x Ar C). HRMS (M+H) actual 256.1463 found 256.1460.

N-methyl threo amino alcohol, $^1\text{H NMR } \delta$ (CDCl_3): 0.88-0.90 (d, 3H, $J = 6.41$ Hz, $-\text{CHCH}_3$), 1.19 (s, 9H, $-\text{CH}(\text{CH}_3)_3$), 2.25 (s, 3H, NCH_3), 2.95-3.01 (m, 1H, $-\text{CHCH}_3$), 4.02-4.04 (d, 1H, $J = 5.36$ Hz, $-\text{CHOH}$), 7.19-7.39 (m, 4H, Ar-H).

$^{13}\text{C NMR ppm}$: 11.72 $-\text{CHCH}_3$, 27.3 $-\text{CH}(\text{CH}_3)_3$, 27.3 $-\text{NCH}_3$, 57.7 $-\text{CHCH}_3$, 55.0 $-\text{C}(\text{CH}_3)_3$, 73.5 $-\text{CHOH}$, 125.3, 126.9, 127.2, 128.9 (4 x Ar CH), 133.7, 144.9 (2 x Ar C). HRMS (M+H) actual 256.1463 found 256.1455.

4.4.14 Determination of Michaelis-Menten kinetic parameters

Microsomes, NADPH regenerating solutions A and B were thawed rapidly to 37°C, then kept on wet ice until ready for use. A number of different concentration substrate solutions were prepared where the maximum concentration of DMSO was 1 %, and the concentration of microsomes, NADP regenerating solution B and phosphate buffer was fixed. After incubation for 5 minutes, NADP regenerating solution A was added and the metabolism was initiated. Final volume was 100 μL . The tube was inverted twice and vortex mixed. The final concentrations in this solution was 1-500 μM prodrug, 0.1 mg/mL HLM or 0.02 mg/mL HIM, 1.3 mM NADP^+ , 0.4 U/mL glucose-6-phosphate dehydrogenase and 1.0 % DMSO. This solution was incubated for 20 minutes at 37°C. The reaction was quenched by addition of 100 μL of acetonitrile. The mixture was centrifuged at 10,000 x g for 10 minutes. The supernatant was analysed by LC-MS analysis.

4.4.15 Pharmacological screening of *N*-methyl bupropion

The pharmacological screens were carried out by MDS Pharma Services Taiwan. The methods used are detailed in the following references, NET [221], DAT [222, 223], Muscarinic acetylcholine receptor [224], nicotinic acetylcholine receptor [225, 226] and SERT [227, 228]. The specific nicotinic acetylcholine assays are detailed in the following

references, nicotinic acetylcholine $\alpha 1$ [229], nicotinic acetylcholine $\alpha 4\beta 2$ [230, 231] and nicotinic acetylcholine $\alpha 7$ [232]. The original reports, methods and results can be found in the Appendices.

4.4.16 CACO-2 cell transport experiment

4.4.16.1 Materials

Cell culture media and buffer components were purchased from Gibco BRL (Gaithersburg, MD). Caco-2 cells were obtained from the ATCC (American Type Culture Collection, Rockville, MD). Transwell-COL tissue culture inserts collagen-coated PTFE (poly(ethylene terephthalate)) were purchased from Costar Corporation (Cambridge, MA). An EndOhm volt-ohm meter and electrode were purchased from World Precision Instruments (Sarasota, FL). All other chemicals were from Sigma Ireland Chemical Company.

4.4.16.2 Cell Culture

Caco-2 cells were maintained in Dulbecco's Modified Eagle Medium (DMEM) containing 10% FBS, 1% nonessential amino acids, and 2 mM fresh L-glutamine. Cells were cultured at 37 °C in an atmosphere of 5% CO₂ and 95% relative humidity. Cells were passaged at 80-90% confluence (every 3-4 days) using Trypsin-EDTA solution (Gibco #25300-047). Culture inserts were preincubated with culture medium (1 h, 37 °C) and then seeded with cells. Caco-2 monolayers were fed with fresh medium 24 h after seeding and then 3 times per week. Caco-2 monolayers were cultured for 14-21 days before use.

4.4.16.3 Transport Assays

Monolayer Screening - Cell monolayers were fed with the appropriate culture medium on the day of assay. Two hours after feeding, monolayers were washed with transport medium (Hanks' Balanced Salt Solution (HBSS, Gibco #14025-092) + 10 mM Hepes, pH 7.4). Monolayers were equilibrated in transport medium for 30 min at 37 °C, in 95% humidity. The electrical resistance of each monolayer was measured at 37 °C at three locations using an STX-2 "chopstick" electrode and volt-ohm meter. The resistance of bare filter inserts was subtracted from monolayer resistance values. Monolayer resistance values were multiplied by the membrane area and averaged to calculate transepithelial electrical resistance (TEER (Ωcm^2)) values for each monolayer. Transport assay donor solution consisted of 100 μM test compound in transport medium containing 100 μM lucifer yellow and 1% DMSO (pH 7.4). Lucifer yellow, a fluorescent marker for the paracellular pathway, was used as an internal control in every test to verify tight junction integrity during the assay. All compounds were tested in six replicate monolayers. Monolayers were incubated with donor and acceptor solutions for 60 min at 37 °C, 95% humidity, with 30 rpm reciprocal shaking. BL compartments were sampled at 15, 30, and 60 min. AP compartments were sampled at 60 min.

Chapter 5 - *In vivo* evaluation of N-methyl bupropion

This chapter describes an *in vivo* pharmacokinetic study of N-methyl bupropion in the guinea-pig. The guinea-pig was chosen as it is reported to best represent human metabolism of bupropion. N-methyl bupropion was also shown to be N-demethylated using guinea-pig S9 liver fractions and the enzyme kinetics are presented. An LC-MS method was developed to determine N-methyl bupropion (prodrug), bupropion and metabolites in guinea-pig plasma and brain. This method was validated according to the FDA guidelines on bioanalytical method validation. Two pharmacokinetic studies were carried out in a guinea-pig animal model. The first study involved intraperitoneal injection (IP) with a parallel dosing of bupropion as reference. The second study was dosed via oral gavage (PO) again with bupropion as reference. The pharmacokinetic results showed marked differences in the PK profile when dosing IP versus PO but the prodrug showed an almost identical PK plasma profile to bupropion when dosed orally. A number of new metabolites of N-methyl bupropion were identified, all potentially pharmacologically active. The chapter concludes that N-alkylated prodrugs of bupropion are susceptible to N-dealkylation *in vivo* and some recommendations are proposed for future work on this project.

5 In-vivo evaluation of N-methyl bupropion

5.1 Introduction

In chapter 4 potential prodrugs of bupropion were evaluated using an *in vitro* screening tool. Two direct prodrugs of bupropion emerged as candidates for an *in vivo* study. The *N*-methyl and *N*-benzyl analogues of bupropion both showed *N*-dealkylation back to bupropion by human liver and intestinal microsomes. The potential prodrug *N*-methyl bupropion was chosen as the preferred candidate for a proof of concept *in vivo* animal study. This decision was based on a number of factors. *N*-benzyl bupropion was discovered at quite a late stage in the project's time line and full evaluation of its stability or pharmacological profile had not been achieved. *N*-methyl bupropion had been fully evaluated. Its stability profile was similar to bupropion. Its pharmacological activity was determined, and its CACO-2 cell intestinal permeability was evaluated.

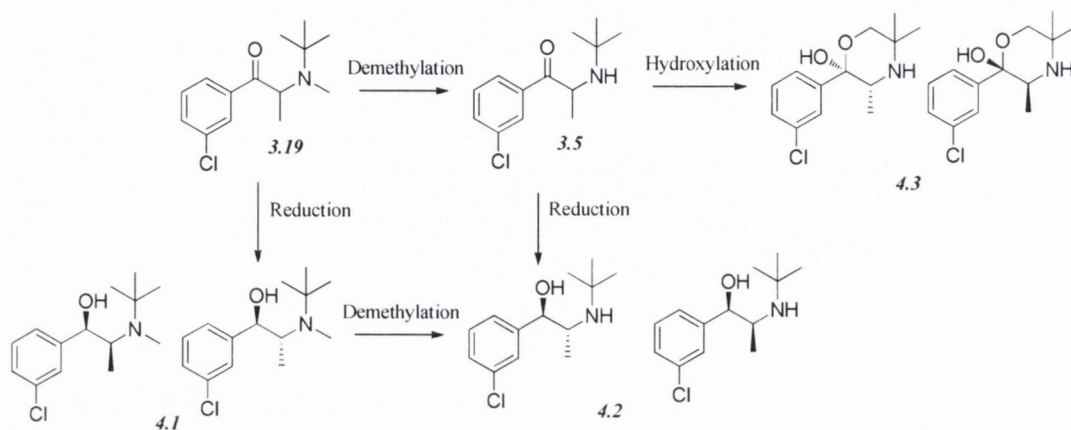
The next stage of the project was to develop an LC-MS method for determination of *N*-methyl bupropion, bupropion and their metabolites in plasma and brain for a proof of concept PK animal study. The method had to be capable of resolving all the known and novel metabolites of bupropion and the prodrug *N*-methyl bupropion. Sufficient resolution between the diastereomeric pairs of metabolites of bupropion and *N*-methyl bupropion was required as these diastereomers had the same exact mass and could not be resolved by the mass spectrometer.

An animal had to be selected for the study and a number of factors had to be taken into account during the selection process. The cost of the study was a significant factor in study design as the actual animal handling and animal dosing would be performed externally while the analysis would be carried out in-house. Generally, the smaller the mammal in the study, the more cost efficient the study but other factors besides cost were important considerations when selecting an appropriate animal. An animal with similar metabolism to humans had to be selected based on the metabolism of bupropion so the results could be correlated best with a clinical study.

The method needed to be fully validated after development, but before the study commenced in order to achieve confidence in the analytical results. Once validated to the guidance of FDA bioanalytical method validation, the plasma and brain of the animals could be analysed post dosing to assess the pharmacokinetic profile of *N*-methyl bupropion versus bupropion. The PK results would be able to discriminate if *N*-methyl bupropion could be used as a successful prodrug of bupropion in a clinical trial. The route of administration was also an important factor as this would significantly affect the pharmacokinetic profile of the drugs.

5.1.1 LC-MS methods already known

Bupropion is extensively metabolised in the liver producing three basic active metabolites, hydroxybupropion, threohydrobupropion and erythrohydrobupropion. Plasma levels of the metabolites are several times higher than bupropion following oral dosing in man. The metabolic and pharmacokinetic profile of bupropion is scientifically interesting and clinically significant because the metabolites contribute to the pharmacological [233] and side effect profile of bupropion [17]. There has accordingly been a number of reports on bioanalytical methods for bupropion. However there have been few reports of methods suitable for the quantitation of bupropion and its basic active metabolites and none including potential prodrugs of bupropion.



Scheme 5.1 *N*-methyl bupropion, its metabolites, bupropion and its active metabolites as determined by *in vitro* evaluation in chapter 4

There are a number of analytical methods in literature suitable for the determination of bupropion. Generally, these use conventional low pH RP-LC conditions coupled to MS. Some methods have been developed solely for determination of bupropion, some include its hydroxylated metabolite and some include all three metabolites.

Petsalo, Turpeinen and Tolonen [234] have developed a qualitative LC-MS method which identified numerous phase I and phase II metabolites using a 0.1 % acetic acid and ammonium acetate mobile phase with a run time of 20 min by LC-MS. Human urinary metabolism of the antidepressant bupropion was studied using liquid chromatography/time-of-flight mass spectrometry (LC/TOFMS) and liquid chromatography/tandem mass spectrometry (LC/MS/MS). A total of 20 metabolites were detected and identified. The phase I metabolism included formation of morpholinohydroxybupropion, threo- and erythrohydrobupropion, aromatic hydroxylation, butyl group hydroxylation with ketone

hydrogenation and dihydroxylation. These metabolites were detected either as the free form or as glucuronide and/or sulphate conjugates. In addition also *m*-chlorohippuric acid was detected. Of the phase I metabolites, a dihydroxylation to the aromatic ring and to the methyl group in the middle of the substrate molecule was reported here for the first time, as well as eight of the glucuronide conjugates (to hydroxy, dihydroxy, hydroxyl and hydrogenation metabolites) and three of the sulphate conjugates (to aromatic hydroxy and hydroxy and hydrogenation metabolites). This was an excellent qualitative LC-MS method for determining unknown metabolites in the urine but was unsuitable for quantitation of metabolites in plasma or brain. Our in-house method needed to have both a quantitative and qualitative advantage in order to be able to quantify known metabolites but also to identify unknown metabolites.

Loboz *et al.* [235] developed a specific and reproducible HPLC assay to simultaneously quantify bupropion and its major metabolites hydroxybupropion, threohydrobupropion and erythrohydrobupropion in human plasma. The analysis was performed on an Aqua C18 HPLC column, with a mobile phase consisting of 45:55 of methanol:0.05 M phosphate buffer (pH 5.5) and simultaneous UV detection at 214 nm (bupropion metabolites) and 254 nm (bupropion, internal standard timolol maleate). The assay showed a linear response for bupropion (2.5–250 ng/mL), threohydrobupropion (5–250 ng/mL), erythrohydrobupropion (10–250 ng/mL) and hydroxybupropion (10–1000 ng/mL). Extraction recovery was reproducible and greater than 55 % for each analyte. The inter- and intra-day assay variability (measured as percent coefficient of variation; % CV) was less than 15 % for all analytes. Limit of quantification was 2.5 ng/mL for bupropion, 5 ng/mL for threohydrobupropion and 10 ng/mL for hydroxybupropion and erythrohydrobupropion. This assay was more sensitive than the currently published methods using HPLC with UV detection for the simultaneous quantitation of bupropion and metabolites and can be used for assessing CYP2B6 activity *in vivo* following a single dose of bupropion. This was an excellent method for those with access to UV detection only, as the levels of quantitation were significantly lower than even existing LC-MS methods.

Arellano *et al.* developed a rapid, sensitive and selective LC-MS method for the simultaneous assay of bupropion and its metabolite hydroxybupropion during its intestinal absorption, studied with the rat everted gut sac model [128]. The method was validated in the concentration range of 1–15 μ M (0.024–3.58 μ g/mL) for bupropion and 0.005–1 μ M (0.00127–0.25 μ g/mL) for hydroxybupropion with 10 μ L injected. Its major metabolite hydroxybupropion was found in the serosal media of the gut sac showing that the isoenzyme of the 2B group was active in the intestinal mucosa and metabolized bupropion during its passage across the mucosa. The metabolite was also quantified in the mucosal media

indicating its ability to cross the apical membrane of the epithelial cells. This method was unsuitable for our analysis as the limits of detection were too high and there was no analytical data relating to the aminoalcohol metabolites.

Stewart *et al.* used a method developed by Glaxo Wellcome Inc. to determine the single dose pharmacokinetics of bupropion in adolescents [236]. Bupropion, the internal standard, and its metabolites were eluted with a 5 mL aliquot of ethyl acetate into glass culture tubes containing 0.1 ml of 0.1 N HCl. The samples were evaporated to dryness using nitrogen, reconstituted with 200 μ L of 50:50 water:acetonitrile, and analyzed by APCI LC/MS/MS using the heated nebulizer in the positive-ion mode. Chromatography was performed using an Inertsil C4 column (150 x 4.6 mm) with a mobile phase B (100 % acetonitrile) under isocratic flow. The range of the standard curves for bupropion, hydroxybupropion, and threohydrobupropion was 1.25 ng/mL to 200 ng/mL based on a 0.15 mL sample. There is no mention of which mobile phase A was used and interestingly, under the chromatographic conditions used for the assay, threohydrobupropion and erythrohydrobupropion coeluted. The authors do mention that previous clinical studies have shown that the ratio of threohydrobupropion and erythrohydrobupropion is constant. Therefore, the results for threohydrobupropion and erythrohydrobupropion are reported as a sum using threohydrobupropion as the standard.

Borges *et al.* [237] developed a high-throughput LC/MS/MS method using a Chromolith RP-18 (50 mm x 4.6 mm) monolithic column and partially validated for the determination of bupropion and its metabolites, hydroxybupropion and threo-hydrobupropion (TB), in human, mouse, and rat plasma. A modern integrated liquid chromatograph and an LC/MS/MS system with a TurboIonSpray (TIS) interface were used for the positive electrospray selected reaction monitoring (SRM) LC/MS analyses. Spiked control plasma calibration standards and quality control (QC) samples were extracted by semi-automated 96-well liquid-liquid extraction (LLE) using ethyl acetate. A mobile phase consisting of 8 mM ammonium acetate-acetonitrile (55:45, v/v) delivered isocratically at 5 ml/min, and split post-column to 2 ml/min directed to the TIS, provided the optimum conditions for the chromatographic separation of bupropion and its metabolites within 23 s. The isotope-labeled d6-bupropion and d6-hydroxybupropion were used as internal standards. The method was linear over a concentration range of 0.25–200 ng/ml (bupropion and threo-hydrobupropion), and 1.25–1000 ng/ml (hydroxybupropion). The intra- and inter-day assay accuracy and precision were within 15 % for all analytes in each of the biological matrices. The monolithic column performance as a function of column backpressure, peak asymmetry, and retention time reproducibility was adequately maintained

over 864 extracted plasma injections. This method had an extremely fast throughput but suffers from high solvent flows and poor resolution as there is no separation of the threo- and erythro- amino alcohol metabolites.

Kharasch and Coles have stereoselectively analysed the *in vitro* and *in vivo* transformation of bupropion to hydroxybupropion. The run time was 20 min [129, 238]. The assay used solid phase extraction, LC-MS-MS and was developed and validated for the analysis of (R)- and (S)- bupropion and its major metabolite (R,R)- and (S,S)-hydroxybupropion in human plasma and urine. Plasma or glucuronidase-hydrolyzed urine was acidified, then extracted using a Waters Oasis MCX solid phase 96-well plate. HPLC separation used an α -acid glycoprotein column, a gradient mobile phase of methanol and aqueous ammonium formate, and analytes were detected by electrospray ionization and multiple reaction monitoring with an API 4000 Qtrap. The assay was linear in plasma from 0.5 to 200 ng/ml and 2.5 to 1000 ng/ml in each bupropion and hydroxybupropion enantiomer, respectively. The assay was linear in urine from 5 to 2000 ng/ml and 25 to 10,000 ng/ml in each bupropion and hydroxybupropion enantiomer, respectively. Intra- and inter-day accuracy was > 98 % and intra- and inter-day coefficients of variations were less than 10 % for all analytes and concentrations. The assay was applied to a subject dosed with racemic bupropion. The predominant enantiomers in both urine and plasma were (R)-bupropion and (R,R)-hydroxybupropion. This was the first LC-MS/MS assay to analyze the enantiomers of both bupropion and hydroxybupropion in plasma and urine. This method was suitable for stereoselective analysis of bupropion and hydroxybupropion but again lacked the inclusion of the aminoalcohol metabolites.

5.1.2 Choice of chromatographic conditions

The analysis of bupropion and its metabolites by RP LC poses similar challenges to those widely associated with amines. The interaction of amines with residual silanol groups on poorly endcapped columns at low pH causes significant tailing leading to poor resolution. Working at low pH under RP conditions also leads to poor retention, which affects resolution and quantitation. Utilizing a high pH mobile phase, at least two units above the pK_a of the amine under RP conditions can eliminate both of these problems.

Polymeric and zirconium dioxide/titanium dioxide RP columns permit high pH analysis, however they have not entered routine use because of several disadvantages compared with silica-based phases. Polymeric columns are prone to shrinking or swelling in response to organic gradients. Furthermore it has proven difficult to control particle size and pore size distribution and therefore reproducibility can be compromised. They also offer a relatively

limited range of surface chemistries. Zirconium and titanium-based stationary phases generally require higher temperatures which can affect solute stability [239].

The emergence of silica-polymeric hybrid columns such as Phenomenex Gemini and Waters Xterra/Xbridge has greatly improved the analysis of amines at high pH. High pH hybrid columns combine the aqueous stability of polymeric stationary phases with the rigidity and robustness of the derivatized silica particles.

Coupling a high pH RP method to a high resolution high sensitivity mass spectrometer such as the Orbitrap greatly improves the sensitivity and specificity of amine analyte analysis. The Orbitrap mass spectrometer gives FT-accurate mass analysis with exceptional signal to noise ratio resulting in sub-nanogram per mL detection limits with a dynamic working range of over three orders of magnitude in the nanogram per mL range.

This chapter presents a rapid, sensitive high pH RP LC method coupled to an Orbitrap MS for the determination of *N*-methyl bupropion, bupropion and its basic metabolites in guinea-pig brain and plasma. The LC method gives excellent peak shape, retention and selectivity, while the Orbitrap MS adds sensitivity and specificity.

5.1.3 Method development

The chromatographic method was developed initially by running four different scouting gradients over two different time intervals. The standard sample mixture consisted of bupropion and its three metabolites, hydroxybupropion, threohydrobupropion and erythrohydrobupropion; *N*-methyl bupropion and its two metabolites *N*-methyl threohydrobupropion and *N*-methylethrohydrobupropion. Two different aqueous buffers were examined for the mobile phase, a pH 2.5 ammonium formate and pH 10.0 ammonium formate buffer. Two different organic solvents were evaluated as organic modifiers, ACN and MeOH. Linear gradients from 10 % B to 90 % B over 10 min and 30 min were examined. Resolution, selectivity and peak shape were determined in assessing the optimum mobile phase. Working at low pH, there was inadequate retention on the RP column, due to all analytes being in their ionised form. The poor retention caused inadequate resolution between bupropion and its metabolites. High pH mobile phase gave excellent retention on the column as all analytes were unionised. ACN gave a better overall peak shape but there was a loss of resolution between bupropion and threohydrobupropion. The use of MeOH in the mobile phase gave better overall resolution at pH 10.0. Adjustment of the pH to 10.5 gave better resolution using ACN as organic modifier. The retention time of bupropion was affected considerably by changes in the pH of mobile phase but pH 10.5 gave the best resolution between all metabolites, bupropion and prodrug. The gradient was then optimized to shorten run time and improve efficiency. A sample chromatogram is presented in Figure 5.1.

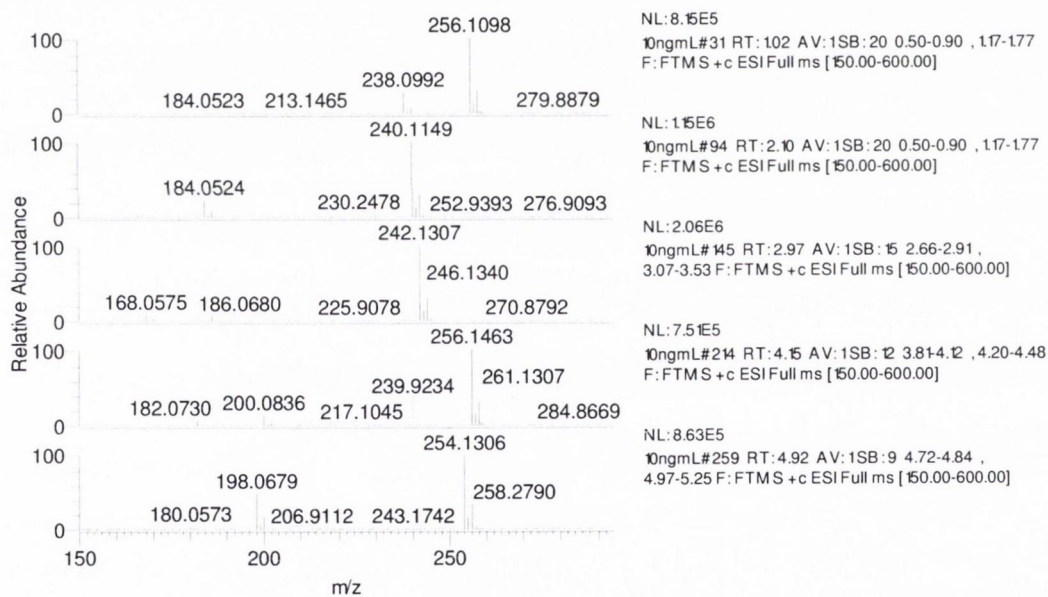
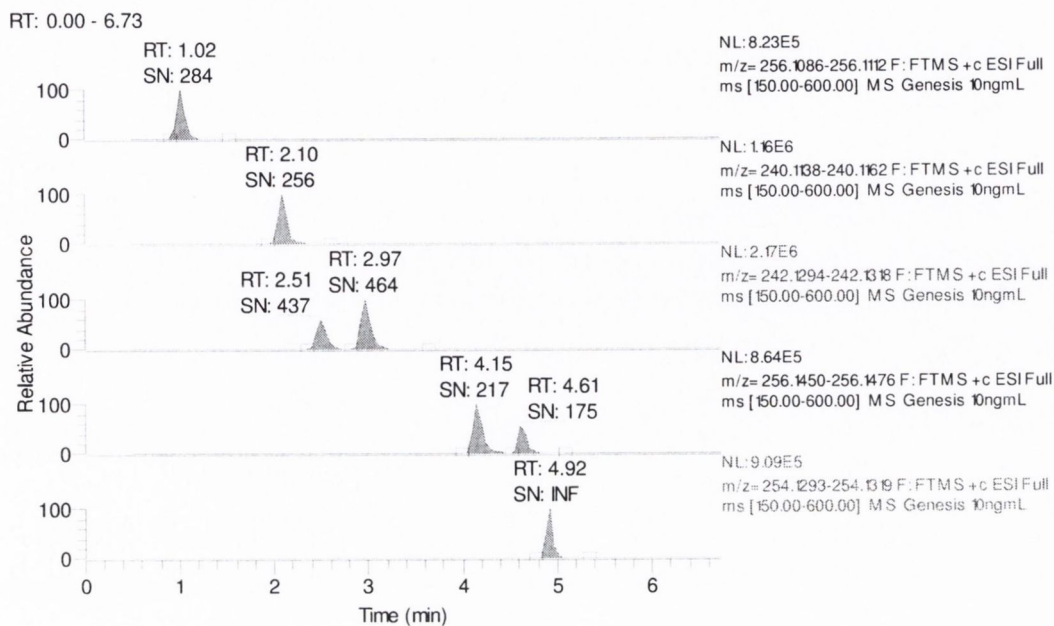


Figure 5.1 LC-FTMS chromatogram of hydroxybupropion 1.02 min, bupropion 2.1 min, erythrohydrobupropion 2.51 min and threohydrobupropion 2.97 min, N-methylethreohydrobupropion 4.15 min, N-methylthreohydrobupropion 4.61 min and the prodrug N-methyl bupropion 4.92 min each at 10 ng/mL. Under the peak retention times is the signal to noise ratio SN.

During the optimization of the chromatographic conditions, the mass spectrometer was monitoring peaks coming off in positive ion electrospray mode. The instrument was tuned on bupropion's (M+H⁺) peak, 240.1150 amu. Sheath gas was optimized to improve nebulization of the sample solution in the electrospray. The auxiliary gas was optimized to improve the vapour plume coming from the electrospray. This helped focus the spray to the ion source and improved desolvation. No sweep gas was used as this did not affect the sensitivity of the electrospray at any value. The capillary temperature was optimized by running the same experiments three times at different capillary temperatures, 200, 300 and 400°C. The temperature was chosen which gave the best sensitivity. The capillary voltage, tube lens and other focusing lenses were autotuned using the MS tune software.

5.1.4 Optimization of protein precipitation

A number of different protein precipitation techniques were evaluated to ensure full extraction of analytes. Our initial in-house method utilized addition of a 2 % zinc sulfate solution in 50 % ACN to the plasma samples, which was effective for precipitating plasma proteins. However it also caused precipitation of the principal analyte possibly through a chelation effect with the Zn. Experimentally, the samples that were quenched with zinc sulphate had much lower bupropion recovery. Plasma protein precipitation was then evaluated with ACN, MeOH and THF. ACN afforded the best recovery and reproducibility. It was also chosen as it was our organic modifier in our chromatographic method, so injection of this up to 50 % composition would not adversely affect chromatography.

5.2 Guinea pig enzyme kinetics

To establish the best species for dosing the prodrug and bupropion, an assessment of past pharmacokinetic literature of bupropion was carried out. As far back as 1986 Suckow *et al.* performed a study involving three species, the rat, mouse, and guinea pig, as animal models to evaluate bupropion metabolism. The pharmacokinetic profiles of bupropion and its major basic metabolites, BW 306U (hydroxybupropion) and BW A494U (threohydrobupropion), were determined following the ip administration of 40 mg/kg bupropion to these animals. Pharmacokinetic profiles of the parent drug and metabolites from plasma and brain samples were obtained using a liquid chromatographic method. Investigation of the reduced bupropion metabolite BW A494U was carried out by the ip administration of this metabolite to these animals and assaying the plasma and brain samples 90 min after dosing. Analysis of the pharmacokinetic data revealed that the rat quickly metabolized bupropion, but no basic metabolites accumulated. The mouse metabolized bupropion predominantly to BW 306U, whereas the guinea pig converted bupropion to reduced bupropion (BW A494U) as well as

BW 306U. Brain/plasma ratios of bupropion among these animals did not vary significantly. However, both metabolites showed dramatic differences in their brain/plasma ratios among these species. When reduced bupropion (BW A494U) was injected, almost 3% of the plasma concentration of BW A494U was determined to be bupropion in the rat. Lesser amounts were converted in the mouse and guinea pig. Therefore, they demonstrated that distinct differences exist in the metabolism of bupropion in various species of animals. The conclusion drawn at the end of the study was that the guinea pig, when compared to the rat or mouse, appeared to constitute a model that most closely resembles that of human bupropion metabolism [240].

Further work on potential co-drugs of bupropion [241] and prodrugs of hydroxybupropion [242] have also been carried out in the guinea pig which suggests this model is the most appropriate for studying bupropion metabolism.

To verify that the guinea pig could also *N*-dealkylate *N*-methyl bupropion, a substrate saturation study was performed using guinea pig S9 liver fraction. The concentration of guinea pig S9 liver fraction, buffer and co-factors was fixed and the concentration of *N*-methyl bupropion was varied. The velocity of formation of bupropion from *N*-methyl bupropion was determined by LC-MS analysis. A substrate saturation curve is presented in Figure 5.2 and the Michaelis-Menten parameters were determined by solving the Michaelis-Menten equation by non-linear regression analysis to the experimental data. The V_{max} was determined at 419.2 ± 13.65 pmol/min/mg S9 and the K_m constant was 114.0 ± 14.77 μ M. This result verified that the guinea pig would be a suitable model to determine the pharmacokinetics of *N*-methyl bupropion and bupropion. The guinea pig could be used as a good model to replicate human metabolism in a prodrug proof of concept study.

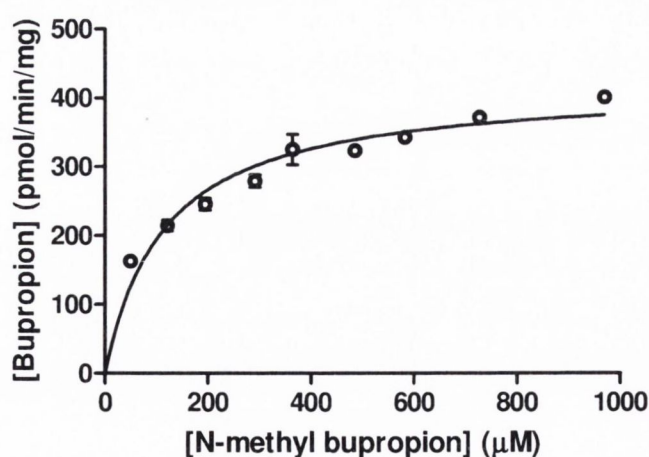


Figure 5.2 A substrate saturation curve for *N*-methyl bupropion in guinea pig S9 liver fraction, $V_{max} = 419.2 \pm 13.65$ pmol/min/mg S9, $K_m = 114.0 \pm 14.77$ μ M ($n = 3$)

5.2.1 Method validation

5.2.1.1 Specificity

The method was shown to be specific for all analytes by injection of all standards, plasma and diluent solutions separately. No interfering peaks were observed with mass values similar to the analytes of interest. The ability of the Orbitrap to extract ions ± 2.0 ppm routinely during the course of the analysis significantly improves the signal to noise ratio affording excellent specificity and sensitivity. The diastereomeric pair rac-erythrohydrobupropion and rac-threo hydrobupropion which have identical mass (242.1306 amu) required baseline resolution for accurate quantitation. Resolution between these two compounds over the linear range was > 1.5 which was considered acceptable. The same resolution was observed for the diastereomeric pair of *N*-methyl amino alcohol metabolites. For use of this method for determination of bupropion and metabolites in guinea-pig plasma and brain, selectivity is not an issue for rac-erythrohydrobupropion as this is not generated in guinea-pigs in significant amount[240].

5.2.1.2 Linearity

Standard	Linear Range (ng/mL)	r^2
Hydroxybupropion	1-250	0.9984
Rac-erythrohydrobupropion	1-250	0.9951
Rac-threo hydrobupropion	1-250	0.9970
Rac- <i>N</i> -methyl-erythrohydrobupropion	1-165	0.9989
Rac- <i>N</i> -methyl-threo hydrobupropion	1-85	0.9995
<i>N</i> -methyl bupropion	1-500	0.9996
Bupropion	1-250	0.9991

Table 5.1 Shows correlation levels for bupropion and its principal human metabolites in the range 1-250 ng/ml.

Linearity was determined by injection of a range of standards from 0.1 ng/mL to 1000 ng/mL. The linear part of the calibration curve was evaluated by least squares-linear regression analysis where the linear range was calculated by the range of points with a correlation coefficient of greater than 0.995. The method was found to be linear for all analytes for at least three orders of magnitude, with a minimum correlation coefficient of $r^2 \geq 0.995$. Table 5.1 presents the correlation coefficient values for bupropion, *N*-methyl bupropion and their metabolites. The linear range for rac-*N*-methyl aminoalcohols was lower as this standard was 2:1 mixture of the two diastereomers. *N*-methyl bupropion had the largest range of quantitation, 1-500 ng/mL. An example least squares-regression linear curve for bupropion is presented in Figure 5.3.

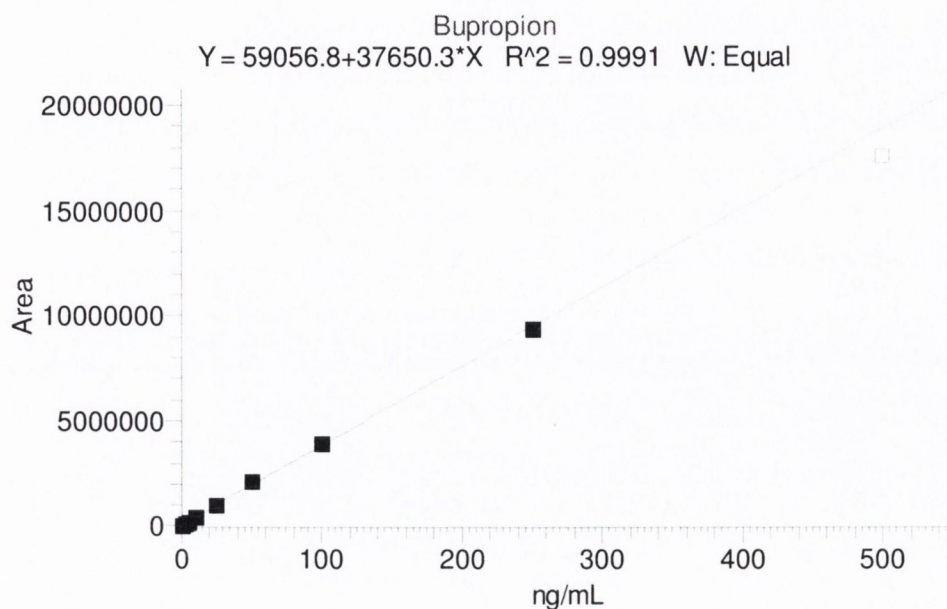


Figure 5.3 The least squares linear – regression curve for bupropion. The last point on the curve was omitted (500 ng/mL) as this concentration point deviated from the line (R^2 value < 0.995).

5.2.1.3 Carryover

Carryover was assessed by injection of a blank sample after the highest concentration linearity sample. Initially during the method development there was significant carryover (> 2 %) of bupropion but after careful adjustment of needle flushing and washing between injections, this was eliminated. The needle wash solution was optimized as 0.5 % formic acid in MeOH. The acidified needle wash improved system suitability, reproducibility and eliminated carryover almost completely (< 0.1 %).

5.2.1.4 Limit of detection

The LOD of the method was determined by injection of standards from highest to lowest level. The limit of detection was determined as the lowest peak detected with a minimum signal to noise ratio of three. The LOD of *N*-methyl bupropion, bupropion and metabolites was shown to be in the pg/mL range (Table 5.2).

Standard	LOD (ng/mL)	S/N
Hydroxybupropion	0.25	4
Erythrohydrobupropion	0.25	3
Threo hydrobupropion	0.25	3
<i>N</i> -Methyl bupropion	0.25	4
Bupropion	0.50	5

Table 5.2 Signal to noise ratios (S/N) at the nominal LOD levels.

5.2.1.5 Accuracy and precision

The accuracy/recovery and precision of the method was evaluated using human plasma. Six replicate plasma samples were analysed at three different levels across the linear range. Each was spiked with *N*-methyl bupropion, bupropion and metabolites in the expected pharmacokinetic concentration range. All accuracy results were within 85-115 %, % RSD \leq 15 % (Table 5.3), as required by FDA guidance on validation of bioanalytical methods. The accuracy and precision of the method was not determined for the aminoalcohol metabolites of *N*-methyl bupropion. The Orbitrap mass spectrometer working in accurate mass mode was routinely able to filter out all ions for analysis to \leq 2.0 ppm, which greatly improved the signal to noise ratio and removed any interfering ions from matrix effects.

Theoretical Conc. Level (ng/mL)	Actual Conc. Level (ng/mL)	\pm (SD)	%RSD	Accuracy (%)
Hydroxybupropion				
10.00	10.23	0.35	3.43	102.33
50.00	53.04	1.67	3.16	106.07
100.00	100.64	4.70	4.67	100.64
Mean			3.75	103.01
Threohydrobupropion				
10.00	11.02	0.40	3.60	110.25
50.00	59.22	2.08	3.62	118.44
100.00	109.39	3.96	3.62	109.39
Mean			3.61	112.69
Bupropion				
10.00	9.03	0.58	6.41	90.33
50.00	51.34	1.92	3.74	102.67
100.00	97.77	3.73	3.82	97.77
Mean			4.65	96.92
<i>N</i>-Methyl bupropion				
10.00	9.33	0.56	5.95	93.31
50.00	57.61	2.75	4.77	115.21
100.00	113.79	4.38	3.85	113.79
Mean			4.86	107.44

Table 5.3 Accuracy/precision results for hydroxybupropion, threohydrobupropion, bupropion and *N*-methyl bupropion.

5.2.1.6 LLOQ-Accuracy and precision

Plasma lower limit of quantitation-accuracy and precision was established at the 1 ng/mL level for *N*-methyl bupropion, bupropion and metabolites. At 1 ng/mL each analyte had a signal to noise ratio of greater than 10. The results are tabulated in Table 5.4.

Standard	Theoretical Conc. Level (ng/mL)	Actual Conc. Level (ng/mL)	± (SD)	%RSD	Accuracy (%)
Hydroxybupropion	1.0	1.09	0.05	4.90	108.97
Threohydrobupropion	1.0	0.96	0.23	24.37	95.88
<i>N</i> -Methyl bupropion	1.0	1.18	0.24	20.28	118.34
Bupropion	1.0	1.18	0.12	10.19	118.14

Table 5.4 Plasma LOQ accuracy and precision results.

Brain LLOQ was determined at 12.5 ng/mL and accuracy/recovery at 125 ng/mL, the CV of six replicates at each level was higher than that of plasma samples. This was attributed to dissolved protein precipitating out of solution during the sample preparation. This displaces the solution volume and can have an effect of concentrating the solutions. Results are tabulated in Table 5.5.

Compound	Level (ng/mL)	Mean (ng/mL)	SD	%RSD	Accuracy (%)
Hydroxybupropion	12.5	14.87	1.00	6.75	118.93
	125	132.71	4.35	3.28	106.17
Threohydrobupropion	12.5	14.98	0.80	5.37	119.87
	125	137.30	5.01	3.65	109.84
Bupropion	12.5	16.50	1.58	9.56	131.98
	125	145.59	6.90	4.74	116.47
<i>N</i> -Methylated bupropion	12.5	15.10	0.64	4.27	120.84
	125	166.10	5.04	3.03	132.88

Table 5.5 Brain LOQ/accuracy and precision results.

5.2.1.7 Sample and standard stability

Short term sample and standard stability was evaluated over 24 h. Samples and standards were shown to be > 90% assay after 24 h at 5 °C. Medium and long term stability was not established. Sample and standard stability in plasma is already documented in literature for bupropion and metabolites [134, 243]. Bupropion plasma samples are stable at low pH and metabolite samples are stable from pH 2.5-10.0. It was for this reason that our samples and

standards were prepared in 0.001 M HCl. This is also the standard sample preparation procedure in the current USP monograph for preparation of assay samples for bupropion hydrochloride extended release tablets [244]. Standard stability was demonstrated throughout the run and at the end of the run by calculating the %RSD of a repeat injection standard. This verified standard stability over the course of the analysis.

5.3 *In vivo study results & discussion*

5.3.1 Guinea pig pharmacokinetics via IP injection

The pharmacokinetics of bupropion has been studied in several species [240, 245, 246]. The species that best represents human metabolism is the guinea-pig. The rat and mouse model do not produce significant amounts of the reduced metabolite threohydrobupropion which is a significant metabolic product of human metabolism. Erythrohydrobupropion is not a prominent metabolite in animal models. The main basic metabolites found in human metabolism are shown in Scheme 5.1. The IP route of administration was chosen for guinea pig administration in the present work because it is considered to be a route that involves the first-pass effect and therefore gains access to the hepatic-portal system, making it similar to oral administration. Thus, the effect of the liver metabolizing enzymes could be assessed in the pharmacokinetics. A 40 mg/Kg bupropion dose was chosen for the guinea-pig so the data could be directly compared to literature [240] to establish the validity of our method, an equimolar amount of prodrug was dosed alongside bupropion.

The pharmacokinetic data was interpreted using a one-compartment model. The one compartment model views the entire body as a single kinetically homogenous compartment where the drug is eliminated by first-order kinetics. In first order pharmacokinetic processes the rate of change of concentration of the drug in biological fluids is directly proportional to its concentration. The rate constant for the kinetics is usually called the elimination constant. The amount of drug present in the body at any given time t [$A(t)$] in a one-compartment model is described in Equation 5.1;

Equation 5.1 Drug concentration

$$A(t) = C_p(t).V$$

where $C_p(t)$ and V are the drug concentration in the plasma and the apparent volume of distribution respectively. Following PO or IP administration of drugs some important parameters can be obtained from the plasma exposure to describe the pharmacokinetics. C_{max} was determined from the highest concentration observed after administration; t_{max} is the time at which C_{max} is observed. The terminal half life $t_{1/2}$, is the time at which the concentration is approximately half its initial concentration and can be affected by both its absorption and

elimination rates. When calculating these factors sampling time points are critical in order to estimate these parameters accurately. At least five sample time points are recommended, which include at least one time point before t_{max} and three time points during the terminal phase for half-life estimation. AUC, C_{max} and t_{max} were estimated directly from PK data but terminal half life was calculated by plotting the natural logarithm of concentration versus time, the slope of which gave the elimination rate constant β . The terminal half life $t_{1/2}$ was determined from Equation 5.2;

Equation 5.2 Terminal half-life

$$t_{\frac{1}{2}} = \frac{0.693}{\beta}$$

The terminal half-life of a drug is probably the most important parameter in assessing the duration of drug exposure. If there is a direct correlation between plasma exposure levels of a drug and its pharmacological response, absolute exposure levels during the terminal phase and $t_{1/2}$ can be important in assessing the duration of its efficacy.

Regardless of the route of administration, $t_{1/2}$ of a drug after multiple dosing becomes close to that during the true terminal phase after single dosing; *i.e.*, $t_{1/2}$ after multiple dosing is dictated by the true terminal $t_{1/2}$ after single dosing. It is not uncommon to see the apparent $t_{1/2}$ of a drug after multiple doses being longer than that after a single dose. This can be simply because the true terminal $t_{1/2}$ after a single dose cannot be readily measured owing to assay limitations or inadequate sampling time points.

The time to reach steady state after multiple dosing is directly related to $t_{1/2}$ after a single dose. It usually takes about five half-lives to reach steady state drug concentrations after multiple dosing for a drug exhibiting one-compartment kinetic characteristics.

The pharmacokinetic data after dosing bupropion and *N*-methyl bupropion via intraperitoneal injection are given in Table 5.6, Table 5.7 and Table 5.8. These results are demonstrated graphically in Figure 5.4, Figure 5.5, Figure 5.6 and Figure 5.7.

After dosing bupropion 40 mg/Kg, the metabolite with the highest AUC was threohydrobupropion (THB) (2.86 $\mu\text{g/mL.h}$), followed by hydroxybupropion (BUPOH) (2.33 $\mu\text{g/mL.h}$). Bupropion (BUP) is seen at lower levels than both metabolites with an AUC of 1.34 $\mu\text{g/mL.h}$. This is the expected profile seen in the guinea pig, illustrating the extensive first pass hepatic metabolism of bupropion. The t_{max} for threohydrobupropion and bupropion are 20 min, and hydroxybupropion was 40 min. The C_{max} for threohydrobupropion, hydroxybupropion and bupropion were 1228 ± 307 , 945 ± 178 and 869 ± 190 ng/mL respectively. Bupropion and metabolite levels in the brain do not show a similar profile. The

level of bupropion in the brain was higher than that of the metabolites even though plasma levels of the metabolites were higher. This is expected as bupropion is more lipophilic than its metabolites and can therefore pass the blood brain barrier more easily. A direct comparison of the PK levels in the brain cannot be made with literature data as the sampling time points are different (20 min versus 90 min [240]). The brain/plasma ratios of bupropion and metabolites were calculated at 20 min (Table 5.7). Bupropion has the highest B/P of 11.25, followed by threohydrobupropion 6.54 and hydroxybupropion 6.30. This is reflective of its lipophilicity and is consistent with literature data [240].

After dosing 42 mg/Kg *N*-methyl bupropion, the AUC values for BupOH, Bup, THB follow a similar profile to dosing of bupropion but the levels are lower. THB had the highest AUC at 2.31 $\mu\text{g}\cdot\text{h}/\text{mL}$ followed by BupOH 1.80 $\mu\text{g}\cdot\text{h}/\text{mL}$ then Bup 0.64 $\mu\text{g}\cdot\text{h}/\text{mL}$. The levels of bupropion after administration of bupropion were approximately twice that after administering *N*-methyl bupropion.

This result indicated that the prodrug was successfully transformed to bupropion *in vivo* but the plasma levels of bupropion were there at equimolar concentrations. Significant amounts of *N*-methyl bupropion (*N*-MeBup) was present in the plasma AUC = 0.23 $\mu\text{g}\cdot\text{h}/\text{mL}$ and the *N*-methyl amino alcohol (*N*-MeTHB) was also present AUC = 0.13 $\mu\text{g}\cdot\text{h}/\text{mL}$. The C_{max} data reflected the plasma AUC's but there was a change in the t_{max} for both THB and BupOH. The longer t_{max} for THB and BupOH indicated the time spent in conversion from prodrug to bupropion then to metabolites. The increased t_{max} could be an advantage as the metabolites of bupropion, THB and particularly BupOH have been directly related to seizure incidence [17]. The levels of THB, BupOH and Bup in the brain was similar when prodrug was dosed (Figure 5.7) versus bupropion (Figure 5.6) but there was a significant difference in the brain/plasma ratios, Table 5.7 and Table 5.8. When the prodrug was dosed there was an increase in bupropion in the brain compared to when bupropion was dosed, even though plasma levels were almost half as much. This could be due to *N*-methyl bupropion crossing the blood brain barrier and being demethylated and metabolized *in situ* by brain oxidative enzymes. After prodrug dosing all metabolites including bupropion had a higher brain/plasma ratio.

These results were positive, in that the prodrug concept of *N*-methyl bupropion had been demonstrated in the guinea pig. *N*-methyl bupropion was successfully converted to bupropion and metabolites *in vivo*. The best result would have shown lower levels of THB and BupOH and increased levels of bupropion but once bupropion is systemic it is naturally metabolized to these metabolites. Significant levels of *N*-methyl bupropion and its aminoalcohol metabolite were detected in the plasma and brain. Depending on pharmacological activity and therapeutic use these may have a synergistic effect with bupropion .

Drug dosed	Parameter	BupOH	Bup	THB	N-Me Bup	N-Me THB
Bup 40 mg/Kg	AUC	2.33	1.34	2.86	-	-
N-Me 42 mg/Kg	($\mu\text{g}\cdot\text{h}/\text{mL}$)	1.80	0.64	2.31	0.23	0.13
Bup 40 mg/Kg	C_{max}	$0.95 \pm$	$0.87 \pm$	$1.22 \pm$	-	-
N-Me 42 mg/Kg		0.17	0.19	0.31	$0.18 \pm$	$0.08 \pm$
	($\mu\text{g}/\text{mL}$)	$0.72 \pm$	$0.38 \pm$	$0.97 \pm$	0.08	0.02
Bup 40 mg/Kg	t_{max} (h)	0.66	0.33	0.33	-	-
N-Me 42 mg/Kg		1.00	0.33	1.0	0.33	0.33
Bup 40 mg/Kg	$t_{1/2}$ (h)	6.8	1.2	3.3	-	-
N-Me 42 mg/Kg		5.2	1.5	4.0	0.7	1.1

Table 5.6 The pharmacokinetic parameters for N-methyl bupropion, bupropion and metabolites following equimolar dosing via intraperitoneal injection in guinea pig IP PK study (n = 5)

	Brain levels		Plasma levels		Brain/plasma ratio
	$\mu\text{g}/\text{g}$	SD	$\mu\text{g}/\text{mL}$	SD	
BupOH	5.67	1.06	0.90	0.13	6.30
Bup	9.79	0.37	0.87	0.19	11.25
THB	8.04	2.92	1.23	0.31	6.54

Table 5.7 The brain/plasma ratio of bupropion and metabolites in the guinea-pig 20 min post IP injection of 40 mg/Kg bupropion (n = 5)

	Brain levels		Plasma levels		Brain/plasma ratio
	$\mu\text{g}/\text{g}$	SD	$\mu\text{g}/\text{mL}$	SD	
BupOH	5.02	1.60	0.66	0.25	7.61
Bup	6.49	1.56	0.38	0.09	17.07
THB	10.89	1.03	0.90	0.49	12.1
N-MeTHB	1.01	0.72	0.08	0.02	12.63
N-MeBup	3.64	1.73	0.18	0.08	20.22

Table 5.8 The brain/plasma ratio of N-methyl bupropion and metabolites in the guinea-pig 20 min post IP injection of 42 mg/Kg N-methyl bupropion (n = 5)

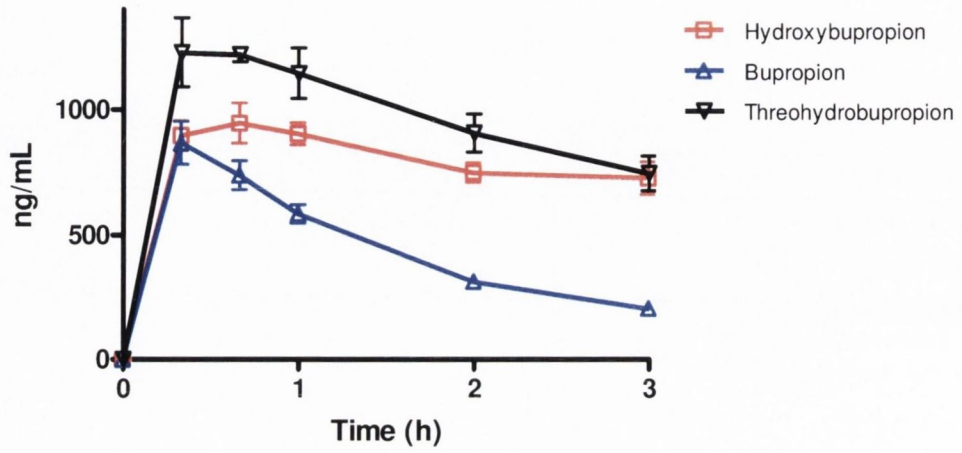


Figure 5.4 The mean plasma levels of bupropion and metabolites after dosing 40 mg/Kg bupropion to guinea pigs by intraperitoneal injection (n = 5)

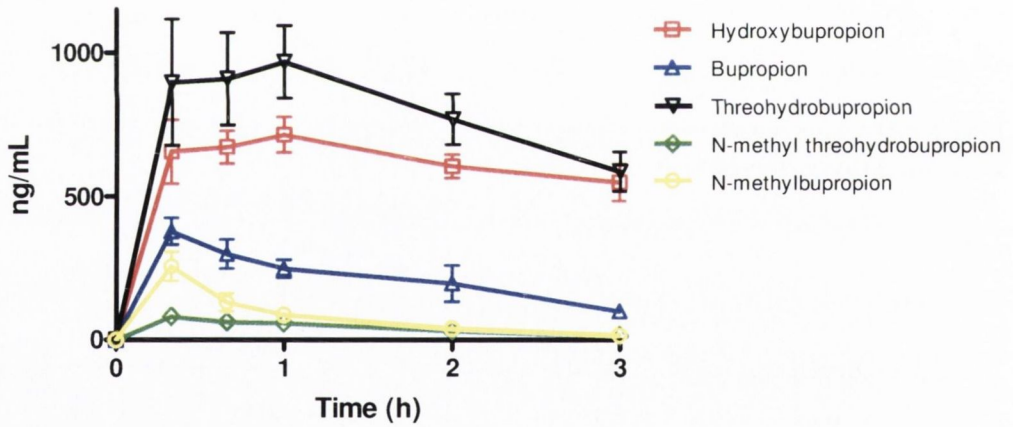


Figure 5.5 The mean plasma concentrations of N-methyl bupropion and metabolites after dosing 42 mg/Kg N-methyl bupropion to guinea pigs by intraperitoneal injection (n = 5)

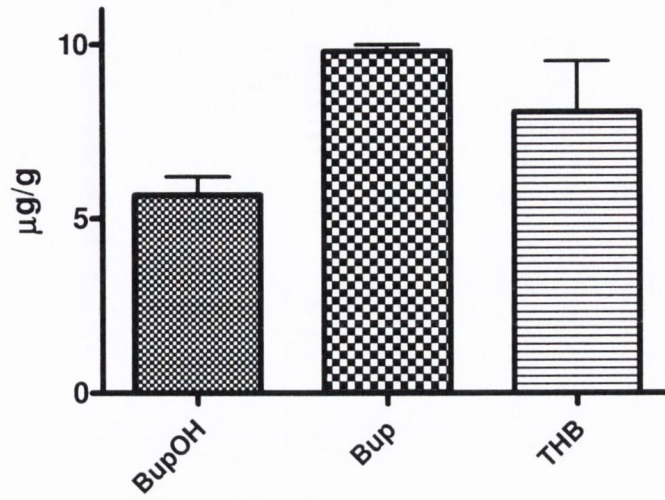


Figure 5.6 The mean brain concentrations of bupropion and metabolites 20 min after dosing 40 mg/Kg bupropion to guinea pig by intraperitoneal injection (n = 5)

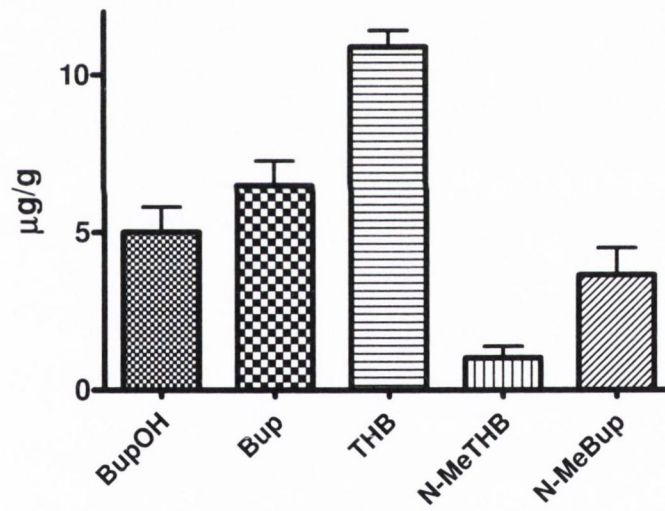


Figure 5.7 The mean brain concentrations of N-methyl bupropion and metabolites 20 min after dosing 42 mg/Kg N-methyl bupropion to guinea pigs by intraperitoneal injection (n = 5)

5.3.2 Guinea pig pharmacokinetics via oral administration (PO)

A second PK guinea pig study was performed using a different route of administration, by oral delivery. The reason for this was to determine if delivery by oral route would lead to much lower plasma and brain levels of the intact prodrug *N*-methyl bupropion. If little or no prodrug was detected in plasma or brain after administration, its pharmacological activity if any could be discounted and it would fit a true prodrug definition. It would also be an interesting comparison to evaluate if the IP route of administration truly represented the oral route (PO). When delivered via intraperitoneal injection, the drug solution is placed in the abdominal cavity which encases the organs of the abdomen. The abdominal cavity is surrounded by a rich blood flow direct to the portal vein and onto the liver. Although first pass hepatic metabolism occurs during IP injection, the first pass effect of the intestine is avoided. Oral delivery involves the full first pass metabolic effect, which includes stability in the stomach, stability in the GI tract and absorption through the intestinal membrane. The increased metabolism of the intestine was expected to cause lower plasma levels of *N*-methyl bupropion.

The oral PK study was performed by MSD Pharma Services with similar animal handling and sampling so the study could be compared directly with IP study results. The dosages of bupropion and *N*-methyl bupropion were kept the same; 40 mg/Kg and 42 mg/Kg respectively. The sampling time points were increased to six hours post dosing and brain was removed at 20 min to evaluate brain/plasma ratios. The brain levels were determined on a separate group. The pharmacokinetic results are shown in Table 5.9, Table 5.10 and Table 5.11. The results are demonstrated in Figure 5.8, Figure 5.9, Figure 5.10 and Figure 5.11.

At first glance, the PK results obtained by dosing orally were much more similar to each other. The plasma AUC's for THB, BupOH and Bup were almost identical when the prodrug is dosed equimolarly to bupropion. The t_{max} for bupropions metabolites, THB and BupOH was extended out to 1 hour which can lower the probability of adverse effects relating to these metabolites. The C_{max} values for THB, Bup and BupOH was almost identical. Probably the most important result was very low levels of the prodrug in plasma compared to IP dosing. The amount of prodrug found in the brain was also below the limit of quantitation. The *N*-methyl amino alcohol metabolite (*N*-MeTHB) of the prodrug was detected in the plasma and brain, so further evaluation of the pharmacological activity of this metabolite should be evaluated. These PK results indicate that the prodrug versus bupropion were bio-equivalent. Interestingly, the oral PK results do not agree with the IP results, which indicates that intraperitoneal injection is not a good route of administration if one wants to study first pass PK metabolism.

Drug dosed	Parameter	BupOH	Bup	THB	<i>N</i> -Me	<i>N</i> -Me
					Bup	THB
Bup 40 mg/Kg	AUC	2.25	0.11	2.31	-	-
<i>N</i> -Me 42 mg/Kg	($\mu\text{g}\cdot\text{h}/\text{mL}$)	2.10	0.08	2.11	0.08	0.01
Bup 40 mg/Kg	C_{max}	0.73 \pm	0.09 \pm	0.83 \pm	-	-
<i>N</i> -Me 42 mg/Kg		($\mu\text{g}/\text{mL}$)	0.15	0.03	0.11	0.02 \pm
Bup 40 mg/Kg	t_{max} (h)	0.33	0.33	0.66	-	-
<i>N</i> -Me 42 mg/Kg		1.00	0.33	1.0	0.33	0.33
Bup 40 mg/Kg	$t_{1/2}$ (h)	1.7	0.9	1.3	-	-
<i>N</i> -Me 42 mg/Kg		1.6	0.8	1.1	<LOQ	1.7

Table 5.9 Estimated pharmacokinetic parameters for *N*-methyl bupropion, bupropion and metabolites following equimolar dosing via oral gavage. Dosed equimolar to bupropion 40 mg/Kg ($n = 5$)

	Brain levels		Plasma levels		Brain/plasma ratio
	$\mu\text{g}/\text{g}$	SD	$\mu\text{g}/\text{mL}$	SD	
BupOH	0.37	0.14	0.73	0.15	0.50
Bup	0.43	0.21	0.09	0.03	4.78
THB	0.97	0.51	0.83	0.11	1.17

Table 5.10 The brain/plasma ratio of bupropion and metabolites in the guinea-pig 20 min post dose of 40 mg/Kg bupropion via oral gavage ($n = 5$)

	Brain levels		Plasma levels		Brain/plasma ratio
	$\mu\text{g}/\text{g}$	SD	$\mu\text{g}/\text{mL}$	SD	
BupOH	0.22	0.04	0.55	0.22	0.40
Bup	0.46	0.40	0.05	0.02	9.20
THB	0.62	0.19	0.54	0.30	1.15
<i>N</i> -MeTHB	0.57	0.49	0.04	0.05	14.25
<i>N</i> -MeBup	<LOQ	<LOQ	0.02	0.01	<LOQ

Table 5.11 The brain/plasma ratio of *N*-methyl bupropion and metabolites in the guinea-pig 20 min post dose of 42 mg/Kg *N*-methyl bupropion via oral gavage ($n = 5$)

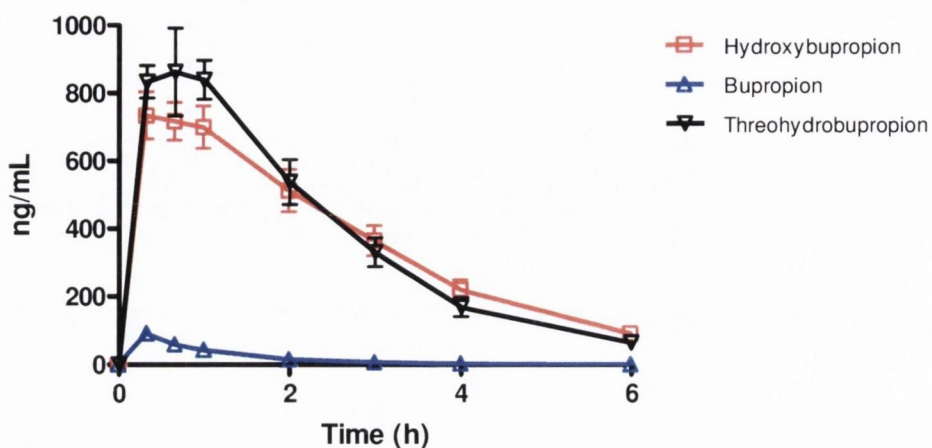


Figure 5.8 The mean plasma concentrations of bupropion and metabolites after dosing 40 mg/Kg bupropion to guinea pigs by oral gavage (n = 5)

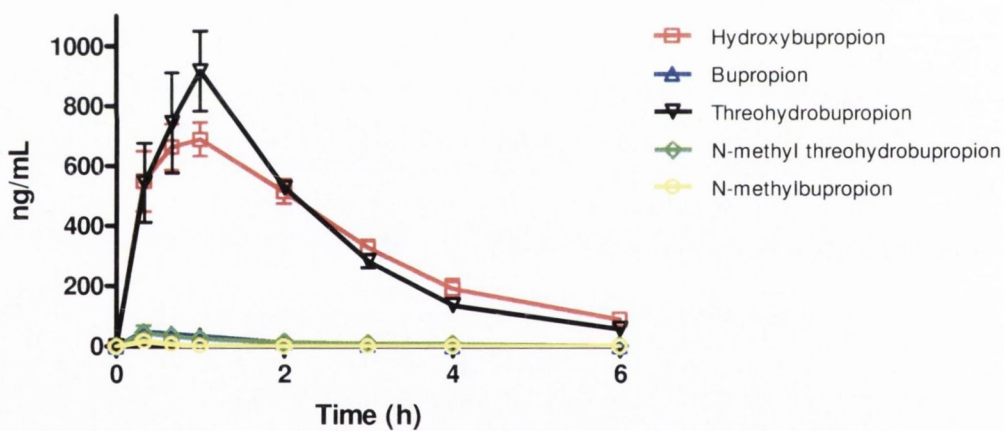


Figure 5.9 The mean plasma concentrations of N-methyl bupropion and metabolites after dosing 42 mg/Kg N-methyl bupropion to guinea pigs by oral gavage (n = 5)

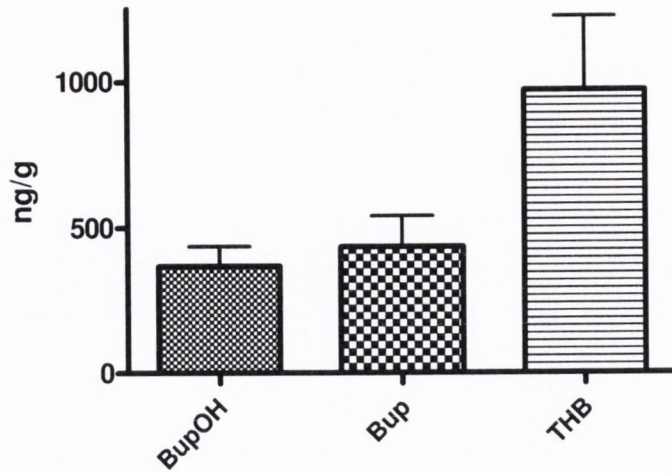


Figure 5.10 Mean brain concentrations of bupropion and metabolites 20 min after dosing 40 mg/Kg bupropion in guinea pig by oral gavage (n = 5). Concentrations are expressed in terms of ng of compound per g of brain tissue.

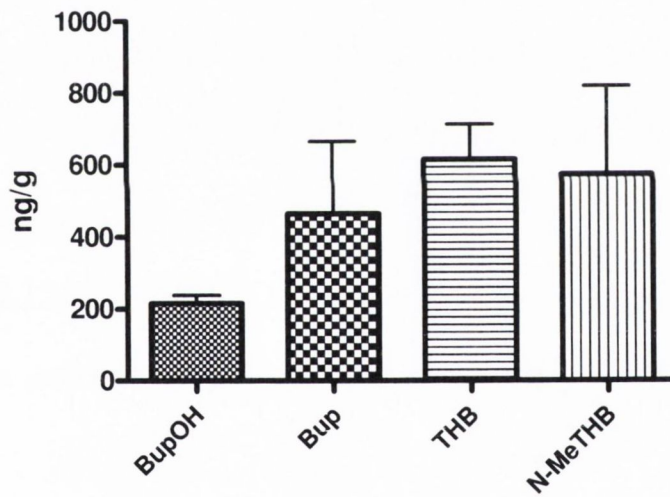


Figure 5.11 Mean brain concentrations of N-methyl bupropion and metabolites 20 min after dosing 42 mg/Kg N-methyl bupropion in guinea pig by oral gavage (n = 5). Concentrations are expressed in terms of ng of compound per g of brain tissue.

5.4 Identification of new *in vivo* metabolites of *N*-methyl bupropion

During both pharmacokinetic studies a number of new metabolites relating to *N*-methyl bupropion were identified. These were filtered out from the accurate mass full scans. The mass defect filter on the data dependent acquisitions was set to < 5.0 ppm therefore it is highly probable that the molecular formula for these metabolites is correct. The instrument was also set in chlorine isotope mode where it selected out mass ions with a chlorine isotope for data dependent MS/MS. Four main metabolites were identified with stereoisomers (Figure 5.12).

The most polar new metabolite was the dihydroxylated metabolite of *N*-methyl bupropion (mass 286.1204 amu) at a retention time of approximately 0.6 min. There is most likely a number of stereoisomers present due to two chiral centres but only one peak appeared in the chromatogram. It is likely that the diastereomers are not resolved in the chromatogram due to inadequate retention on the column. It must also be noted that the positions of hydroxylation are ambiguous as there was a lack of MSⁿ data to say with any certainty the positions of the hydroxyl groups but at least one is likely on the *t*-butyl group causing cyclisation.

Two diastereomers of the dimethylated-dihydroxylated metabolite were present (mass 272.1048) with retention times of 0.8 and 1.1 min respectively. The positions of these hydroxyl groups are also ambiguous due to lack of MS data.

The mono-hydroxylated metabolite of *N*-methyl bupropion was present at 2.0 min (mass 270.1255). The position of this hydroxyl group is also ambiguous due to lack of MS data. This mono-hydroxylated metabolite also has two chiral centres and therefore should exist as two diastereomeric peaks in the chromatogram but only one was present.

The last pair of metabolites were confirmed as the *O*-methylated metabolite of *N*-methyl bupropion (mass 268.1463), retention time 5.92 and 6.53 min. There were two isomers present, *syn* and *anti* due to the double bond in the enol group and each of the *syn* and *anti* isomers is chiral. Their identity could be confirmed as we had previously made these as potential prodrugs of bupropion.

Although these four sets of metabolites were present as only minor metabolites, they may have potential pharmacological activity, with activity higher than the prodrug *N*-methyl bupropion. This abundance of metabolites of *N*-methyl bupropion shows the prodrug is extensively metabolised in the guinea-pig animal model. It would be a tedious exercise to synthesize and characterize all these metabolites and isomers for pharmacological activity assessment. The best way to understand if they work synergistically would be to perform an animal efficacy study. Only then, after comparison to an equimolar dose of bupropion could it be decided if the prodrug concept has alternative benefits to a regular bupropion dose.

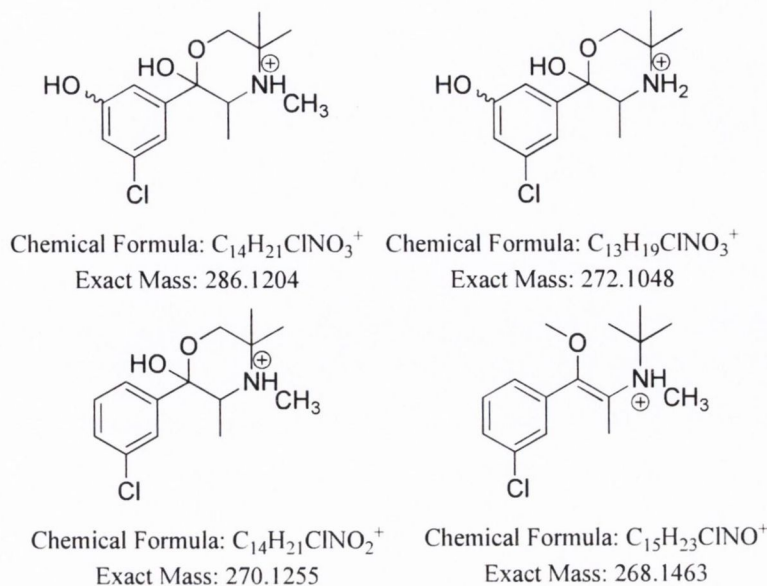


Figure 5.12 Proposed four new metabolites that were recovered after dosing *N*-methyl bupropion in both PK guinea-pig studies. Note metabolites are protonated to correlate off MS data

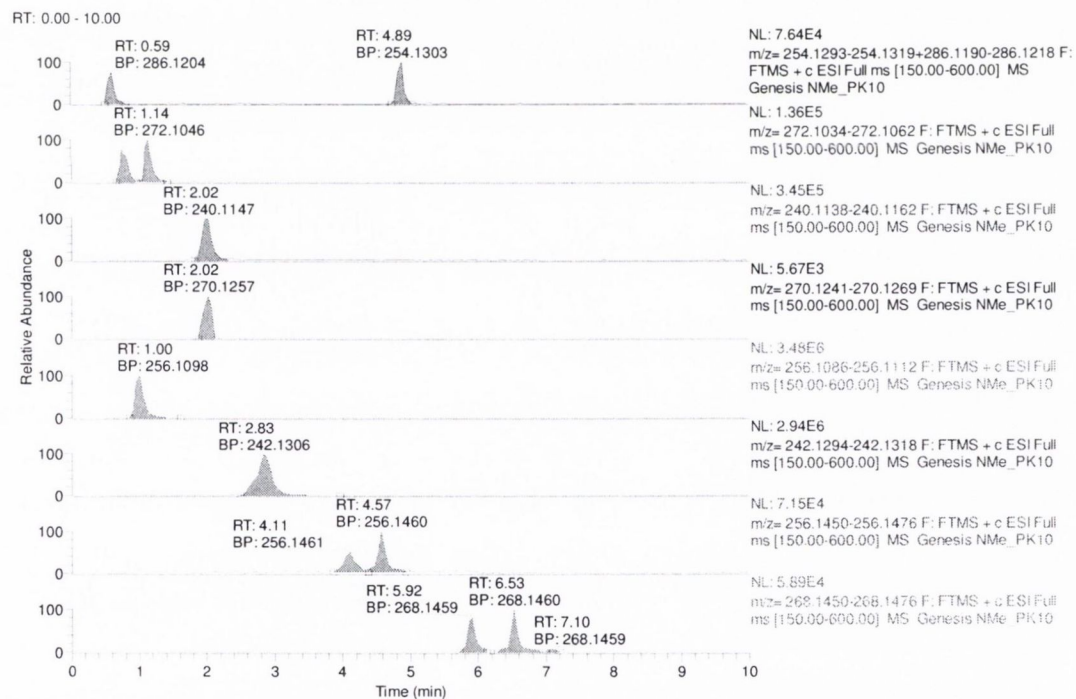


Figure 5.13 LC-MS chromatogram of guinea-pig plasma at $t = 40$ min post prodrug dose. Bupropion (2.02), threohydrobupropion (2.83), hydroxybupropion (1.00), *N*-methyl bupropion (4.89), *N*-methyl hydrobupropion isomers (4.11 and 4.57), dihydroxylated metabolite (0.59), demethylated-dihydroxylated metabolite (0.75 and 1.14), mono-hydroxylated metabolite (2.02), methylated metabolites (5.92 and 6.53)

5.5 Conclusion

The objectives of this chapter were to describe the evaluations of a bupropion prodrug in an animal model. After initial *in vitro* enzyme kinetic evaluation, the guinea pig was selected as an adequate model to demonstrate metabolism of the prodrug to bupropion and their relating metabolites. In order to evaluate if the prodrug was converted to bupropion *in vivo*, a method for the determination of *N*-methyl bupropion, bupropion and their metabolites in guinea-pig plasma and brain was developed. The method utilized a high-pH reversed phase separation on the Accela UPLC system, coupled to an LTQ-XL Discovery-Orbitrap mass spectrometer. The high pH separation afforded much better selectivity and separation efficiency compared to low pH reversed phase LC methods. Coupling this separation to the dual LTQ-iontrap (nominal mass) - Orbitrap (accurate mass) offered extremely high sensitivity for both quantitative analysis of the known analytes but also in identification of unknown metabolites. This method was subsequently validated using the guidelines proposed by the FDA on validation of bioanalytical methods.

After validation was performed, guinea pigs were dosed with equimolar amounts of bupropion or *N*-methyl bupropion via intraperitoneal injection. The intraperitoneal PK study showed that *N*-methyl bupropion was being transformed to bupropion *in vivo* and that the predicted metabolites, *N*-methylthreohydrobupropion, threohydrobupropion and hydroxybupropion were present in the plasma and brain of the guinea-pig.

A second PK guinea-pig study was performed by oral delivery to assess if the added pre-systemic metabolic enzymes and route of delivery would affect the prodrug and plasma-brain concentrations. After administering bupropion or *N*-methyl bupropion in equimolar doses by oral gavage, the plasma AUC and C_{max} of bupropion, threohydrobupropion and hydroxybupropion were shown to be almost identical. *N*-methyl bupropion was shown to be a good bio-precursor prodrug of bupropion. In addition to this, the t_{max} for hydroxybupropion and threohydrobupropion was shown to be extended to one hour from 20 min with bupropion. This extended t_{max} for these metabolites was welcomed as these two metabolites and their stereo-isomers are known to contribute to the side effect profile of bupropion, particularly in seizure liability. The delayed or sustained onset of these metabolites might mitigate the impact of these metabolites.

The two PK studies effectively showed that *N*-alkylated analogues of bupropion can be used as bio-precursor prodrugs of bupropion. They also demonstrated that the IP route of administration is not a bioequivalent to dosing orally. Very different plasma profiles were obtained following dosing IP and PO. The nitrogen in bupropion is susceptible to oxidative *N*-dealkylation *in vivo* which opens the doors to many prodrug and co-drug concepts that can be used for the emerging treatments associated with this versatile compound.

5.6 Proposed future work

The successful outcome of this project by no means closes the door on this work. This thesis simply opens the door and lays a platform for new concepts relating to bupropion. The compound is versatile, in that it can be used for a number of indications including CNS disorders like depression, SAD, ADHD, smoking cessation, obesity, sexual dysfunction or even as a replacement for drugs of abuse but can also be used as an anti-viral and to treat inflammatory disorders like Crohn's disease. The sensitivity of the amino group to oxidative *N*-dealkylation means that prodrug and co-drugs of bupropion can be linked via alkyl linkages through the amine of bupropion leading to new chemical entities for the above treatments. The susceptibility of the amino group to *N*-dealkylation can also be used to its advantage for different routes of delivery. For example, the solubility and stability of the compound can be increased or decreased by changing different types of *N*-alkyl groups. If lipophilicity is increased, an *N*-alkylated prodrug or co-drug could be administered via a transdermal or intranasal delivery, which would by-pass the pre-systemic metabolic enzymes, delivering more prodrug to the brain where it can be metabolized to bupropion *in situ*.

There are obvious advantages and disadvantages to some of the above concepts but this is an area of research that needs to be developed and much further work lies ahead. Some proposed future work is listed below with expansions on some of the concepts above and some new developing areas.

5.6.1 Identification of CYP450 enzymes responsible for metabolism

Since the concept has been demonstrated, it would be important to identify which intestinal and liver enzymes are responsible for the de-alkylation of the prodrug. This has a number of implications. First of all, drug-drug interactions can be evaluated if the enzyme responsible can be identified. Enzyme induction and inhibition are two extremely important parameters that need to be identified. Knowledge of these enzyme parameters can be used to ones advantage. For example, bupropion is metabolized to hydroxybupropion by CYP2B6 and to the aminoalcohols by an unstudied reductase enzyme. If the prodrug was too de-alkylated by CYP2B6 and had a much higher affinity for the enzyme (lower Michaelis constant, K_m), there would be competition for the active site on the enzyme between prodrug and converted bupropion and if the prodrug had a higher affinity for the enzyme then less bupropion would be hydroxylated to hydroxybupropion, in turn lowering plasma levels of hydroxybupropion and increasing levels of bupropion. This can be taken a step further; the best case scenario would be if the prodrug was an inhibitor of CYP2B6, therefore blocking conversion of bupropion to hydroxybupropion completely. This would lead to much decreased levels of

unwanted metabolite hydroxybupropion and increased systemic and brain levels of bupropion, hence lowering therapeutic dose.

Another possibility is to study the induction and inhibition of *N*-methyl and *N*-benzyl bupropion metabolites. These prodrug metabolites could possibly be substrates for CYP2B6 or even the reductase enzyme responsible for conversion of bupropion to the aminoalcohol metabolite. If they were to be substrates for CYP2B6 or the reductase enzyme with higher lower K_m values, or even inhibitors of these enzymes, the same reduced levels of unwanted metabolites would occur and higher levels of bupropion.

5.6.2 *In vivo* efficacy and toxicology

Following on from the work presented in this chapter, if the plan was to focus on *N*-methyl bupropion the next stage of the project would involve an *in vivo* efficacy study. The idea would be to dose bupropion and *N*-methyl bupropion in an animal model preferably a guinea pig or some other animal that had similar pharmacokinetics, and monitor the therapeutic effect.

For example, if the therapeutic indication was depression, the prodrug would be dosed versus bupropion and a behavioural despair test (AKA forced swimming test or Porsolt test) would be assessed. The behavioural despair test is a test used to measure the effect of anti-depressant drugs on the behaviour of animals. Animals are subjected to two trials during which they are forced to swim in an acrylic glass cylinder filled with water, and from which they cannot escape. The trial lasts 15 min, then after 24 hours a second trial is performed that lasts 5 min. The time that the test animal spends without moving in the second trial is measured. This immobility time is decreased by anti-depressants [247].

A statistical evaluation of the results would determine if the prodrug has the same or improved efficacy as an antidepressant. This can also be shown using the tail suspension test. The tail suspension test is an experiment used to assess mood levels in rodents. Changes in mobility time indicate changes in mood and it is widely used to detect potential antidepressant effects of drugs [248].

If the results of an efficacy study were the same as bupropion or better some toxicity data would have to be generated. A rotarod test may be required to evaluate if the prodrug is having any toxic effects on the co-ordination and balance of the animals [249]. A seizure study might be required to show that the prodrug has less or same seizure threshold as bupropion. This would be performed by increasing doses of bupropion, prodrugs and metabolites to see the statistical likelihood of inducing seizures [17].

5.6.3 Evaluation of *N*-benzyl bupropion *in vivo* pharmacokinetics

The second potential prodrug which emerged from the project at a late stage was *N*-benzyl bupropion. The *in vitro* human metabolism in intestinal and liver microsomes was evaluated and shown that the prodrug was successfully debenzylated to bupropion. The rates of conversion of *N*-benzyl bupropion to bupropion and affinity to enzyme compared to *N*-methyl bupropion were improved. It would be a good idea to assess if this conversion also happens in guinea-pig by some *in vitro* metabolic work, then to take this prodrug forward to an *in vivo* model. A successful result is likely and following on from this an efficacy and toxicity study would be encouraged. *N*-benzyl bupropion is likely to be a good prodrug of bupropion with new active metabolites.

5.6.4 Stereo-selective pharmacological and pharmacokinetic analysis

Both *N*-methyl and *N*-benzyl bupropion are chiral compounds. The pharmacological activity of both the enantiomers of these prodrugs should be evaluated. One enantiomer may have pharmacological activity while the other may reduce or inhibit the others activity. This has been shown before with other chiral anti-depressants. For example; escitalopram is more effective an antidepressant than its mixed racemic version citalopram [250]. The R-enantiomer was shown to counteract the S-enantiomers effects in many cases [251-255].

The reduction of the prodrugs during metabolism also introduces another chiral centre, creating a diastomeric pair of enantiomers. Therefore, there are 4 potential aminoalcohol metabolites of the prodrugs. This reduction should be studied *in vitro* and *in vivo* to see if it is stereoselective for any particular diastereomer or enantiomer and then these stereoisomers should be evaluated as new drug entities with the potential of pharmacological activities relating to bupropion.

5.6.5 Evaluation of pharmacological activity of hydroxyimine of bupropion

During the evaluation of potential prodrugs of bupropion in Chapter 4, it was found that the oxadiazine of bupropion was *N*-dealkylated and subsequently deformed to the hydroxyimine of bupropion. The oxadiazine therefore was a potential prodrug of the hydroxyimine of bupropion. The hydroxyimine was shown to have a much improved stability profile over bupropion possibly due to intramolecular hydrogen bonding and therefore could be used in such drug delivery systems such as transdermal patches or sprays.

The hydroxyimine is likely to have similar and potentially better pharmacological activity than bupropion and this should be evaluated for the oxadiazine too. The hydroxyimine has similar mass, lipophilicity, and ionisation properties of bupropion so is likely to cross the blood brain barrier. There are also four isomers of the hydroxyimine of bupropion. It has one chiral centre and two isomers around the syn and anti-hydroxyimine group. All of these

isomers are potential pharmaceuticals and the oxadiazine is a novel prodrug delivery method for the hydroxyimine, at this time there is no literature on such bio-precursor prodrugs. Further characterisation of the stability of all four isomers of the hydroxyimine should be assessed both hydrolytically and enzymatically as one of these isomers could still be a potential prodrug of bupropion. The hydroxyimine of *N*-methyl or *N*-benzyl bupropion is likely to be susceptible to metabolic enzymes as the ability of the hydroxyimino group to intramolecularly hydrogen bond with the secondary amino group has been removed in these potential multistep prodrugs of bupropion (Figure 5.14).

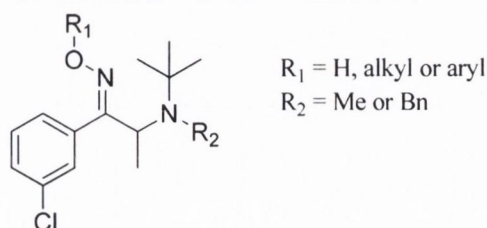


Figure 5.14 Potential multistep hydroxyimine-*N*-alkylated prodrugs of bupropion

5.6.6 Dialkylated prodrugs of bupropion

In chapter 4 it was shown that *N,O*-dimethylated bupropion was converted to *N*-methyl bupropion *in vitro*. Which means that this compound was *O*-demethylated. This compound should be assessed for its pharmacological activity and its induction/inhibition of CYP enzymes, especially CYP2B6. This could be a very interesting compound for two reasons It has to be *O*-demethylated before it can be reduced, so its prodrug form may inhibit the CYP2B6 or reductase enzymes leading to less unwanted metabolites, threohydrobupropion and hydroxybupropion. It also opens up a new prodrug functional group on bupropion, the enol ether group. This enol ether could be alkylated with a range of alkyl and aryl groups or even directly conjugated to another drug through an alkyl bond. The only drawback being that the amino group on bupropion will too have to also be alkylated in order to prevent the compound to tautomerize to the imine form which will occur if the secondary amino group is present. This stability problem was seen in chapter 3.

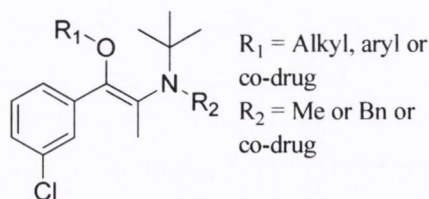


Figure 5.15 Potential *O*-alkylated double prodrugs and co-drugs of bupropion

5.6.7 Evaluation of SAR of *N*-alkylated analogues of bupropion

In concluding this chapter it was determined that prodrugs such as *N*-methyl and *N*-benzyl bupropion were *N*-dealkylated to bupropion. The nitrogen in the amino group of these prodrugs is therefore susceptible to oxidative *N*-dealkylation. It would be prudent now to alkylate this nitrogen with many different substituents, not only methyl but ethyl, propyl, butyl etc with growing chain length and branched alkyl groups to determine when sterically *N*-dealkylation will not occur by microsomes. Knowing the chain length that enzymes will stop de-alkylating will help to design co-drug alkyl chain linkers.

The benzyl substituent could also be varied with different substitutions to assess the effect this has on de-benylation. This data would be invaluable to the medicinal chemist as the kinetics of de-alkylation, physicochemical properties and enzyme induction/inhibition could be tailored for the drug delivery system and therapeutic setting. Each alkylated prodrug should be assessed for enzyme induction and inhibition as potentially one of these analogues will inhibit CYP2B6 leading to improvement in plasma profile as stated in 5.6.1.

It should also be noted that once the nitrogen in the amino group of these prodrugs is dealkylated, one of the resulting by-products is an aldehyde. These aldehydes are most likely quickly oxidized to the corresponding carboxylic acids by one of the many aldehyde oxidase enzyme systems. This can be used to our advantage by alkylating another drug to bupropion. This co-drug option only works for acidic type drugs. A purely proof of concept scheme is shown in Figure 5.16 by incorporating Nicotinic acid (AKA Niacin or vitamin B₃).

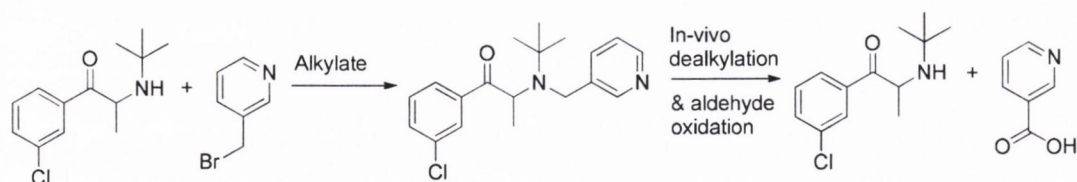


Figure 5.16 Alkylation and metabolism of an acidic co-drug (Niacin) to bupropion

5.6.8 Identification of new metabolites of *N*-alkylated analogues of bupropion

At every stage in the above processes during *in vitro* and *in vivo* work new metabolites of all these *N*-alkyl potential prodrugs are being generated. Each new metabolite should be identified and synthesized for full characterisation as each new metabolite is a potential pharmaceutical. The metabolic pathway can somewhat be predicted from the metabolites of bupropion, *N*-methyl bupropion, *N*-benzyl bupropion and the substituted cathinones such as diethylpropion. All these compounds are hydroxylated and reduced as the major basic metabolites of the secondary amino-ketones. The tertiary amino-ketones such as the *N*-alkylated prodrugs and substituted cathinones are de-alkylated. With this in mind a structure-

metabolism relationship can be drawn up theoretically for each *N*-alkylated prodrug and these metabolites can be synthesized and characterized as potential pharmacologically active products of each prodrug before the prodrug is synthesized.

5.6.9 Co-drugs for depression

Anti-depressants are frequently being co-administered. Combination therapies are prescribed regularly by GP's and the pharmaceutical companies have even developed combination anti-depressant formulations [256]. Triple reuptake inhibitors are the new developmental compounds for CNS therapies [257-266]. There are a number of SSRI type compounds that could be conjugated to bupropion via an alkyl or aryl bridge. These co-drugs when metabolised would give back bupropion and the SSRI's which means they functionally act as triple reuptake inhibitors. The increased lipophilicity of the co-drugs would enable them to cross the blood-brain barrier more efficiently where they can be metabolized to their precursor drugs *in situ* at the site of action.

The first example is bupropion-escitalopram, these two compounds are already formulated together [256] and could be linked by an alkyl bridge such as an ethyl group. Bupropion would be dealkylated at the amino group and escitalopram is also known to be dealkylated at its amino group to an active metabolite desmethylescitalopram.

Bupropion-paroxetine and bupropion-fluvoxamine too are possible co-drug TRI's. Paroxetine and fluvoxamine are also known to inhibit CYP2B6 [267] which may lead to reduced hydroxylation of bupropion. Bupropion-sertraline and bupropion-fluoxetine could be good candidate TRI co-drugs. Sertraline and fluoxetine are also known to inhibit CYP2B6 [267] and they are dealkylated to active metabolites at their amino groups, so particularly sensitive to oxidative *N*-dealkylation at the ethyl linker.

Bupropion-venlafaxine or bupropion-desmethylvenlafaxine have the potential to be TRI co-drugs. Venlafaxine does not inhibit CYP2B6, nor does its desmethyl metabolite. The advantages of using a bupropion-venlafaxine co-drug is they are both dosed individually at similar amounts and both compounds are susceptible to *N*-dealkylation.

There are advantages and disadvantages to using such co-drugs and there is really no way to determine the efficacy outcome until an animal model is tested with such co-drugs. Obviously the compounds are connected equimolarly and the dosages would have to be in similar range but a synergistic effect may be shown with these co-drugs and the equimolar dosage of the codrug could be reduced. Synthetic problems may arise too but at least one of these co-drugs could be attempted as a proof of concept. The chirality of bupropion and chirality of some of the SSRI's will increase the potential number of stereo-isomers but will lead to diastereomeric co-drugs. An example of the potential TRI co-drugs is demonstrated in Figure 5.17. The alkyl linker joining both bupropion to the SSRI is an ethyl bridge. The length and type of co-drug

linker would have to be optimized to enable metabolism of both precursor drugs at each end of the linker. Most amino groups in the SSRI's are susceptible to oxidative-dealkylation, as the majority of them have dealkylated active metabolites.

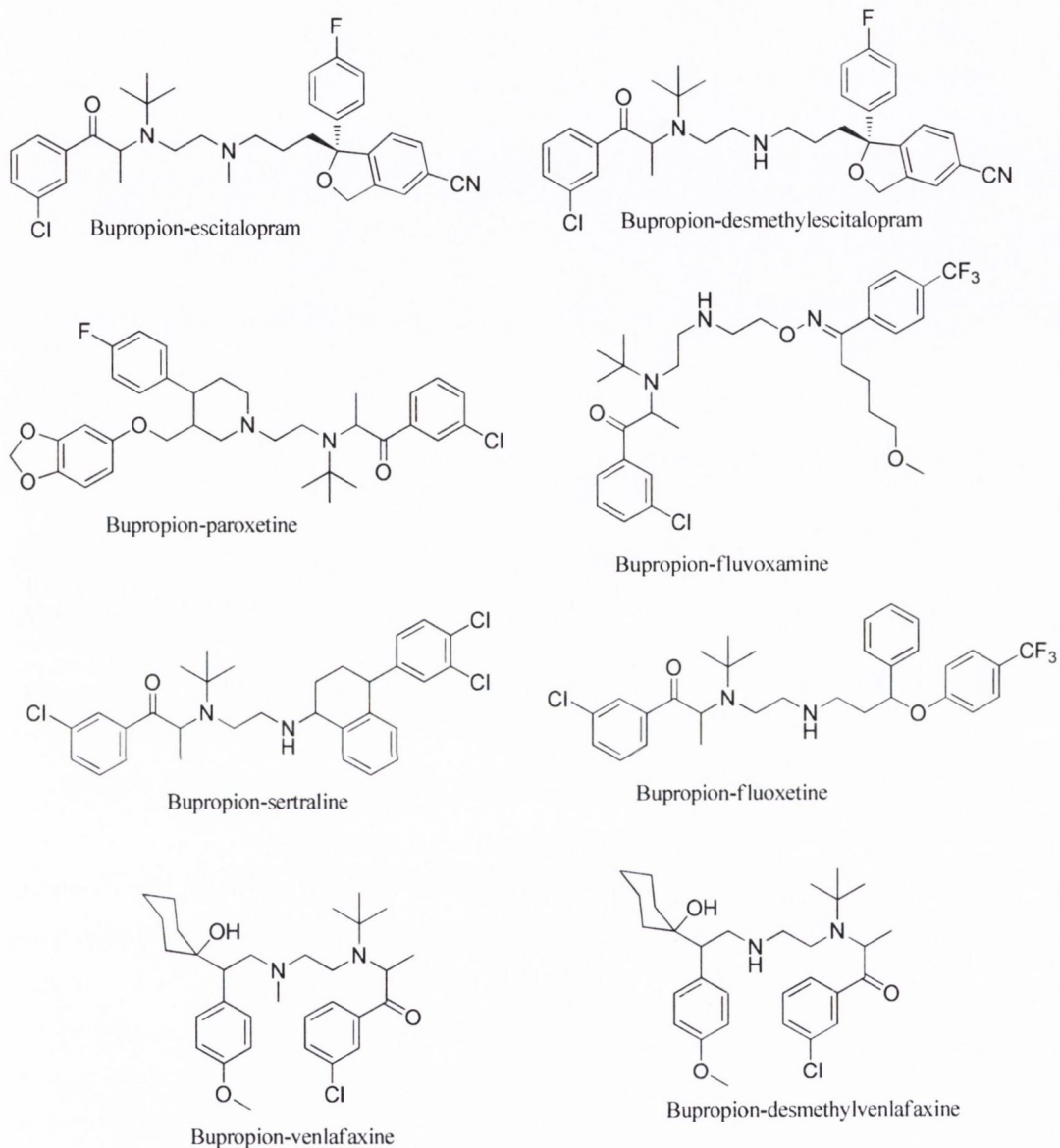


Figure 5.17 Potential triple reuptake inhibitor co-drugs of bupropion and SSRI's.

5.6.10 Prodrugs and co-drugs for Nicotine replacement therapy

Some antidepressant medications such as imipramine, doxepin, venlafaxine and fluoxetine have already been used in the past to encourage smoking cessation and some of these compounds are easily linked to bupropion via an alkyl bridge (See 5.6.9).

Varenicline is a nicotine receptor partial agonist. In this respect, it is similar to cytisine and different from the nicotine antagonist, bupropion, and nicotine replacement therapies (NRTs). As a partial agonist, it both reduces cravings for and decreases the pleasurable effects of cigarettes and other tobacco products, and through these mechanisms it can assist some patients to quit smoking. In combination, bupropion and varenicline have improved rates of smoking cessation [268]. These two compounds are easily linked via their amino groups.

The drug mecamylamine (a nicotine antagonist) was shown to improve abstinence rates in smoking cessation [269] and could be used in combination with bupropion [270] as an aid to smoking cessation. These potential co-drugs are shown in

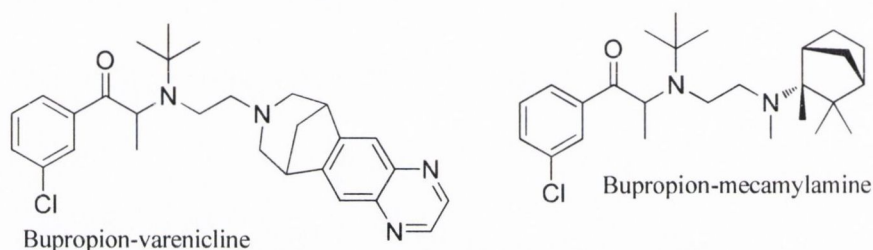


Figure 5.18 Potential co-drugs for Nicotine replacement therapy and smoking cessation

In chapter 4 we described the work carried out by Carroll *et al.* where they synthesized analogues of bupropion for potential pharmacotherapies for smoking cessation [124]. Since it has already been shown that bupropion prodrugs are susceptible to oxidative *N*-dealkylation and the known compounds diethylpropion and substituted cathinones are susceptible to *N*-dealkylation during metabolism, then it is likely that most of these cathinone type compounds can be developed into alkylated prodrugs. In Carroll *et al.*'s work, analogue (2x) with IC_{50} values of 31 and 180 nM for DA and NE, respectively, and with IC_{50} of 0.62 and 9.8 μ m for antagonism of $\alpha 3\beta 4$ and $\alpha 4\beta 2$ nAChRs had the best overall in vitro profile relative to bupropion. It can be assumed that the *N*-alkylated analogue of 2x could be a potential prodrug of 2x (Figure 5.19).

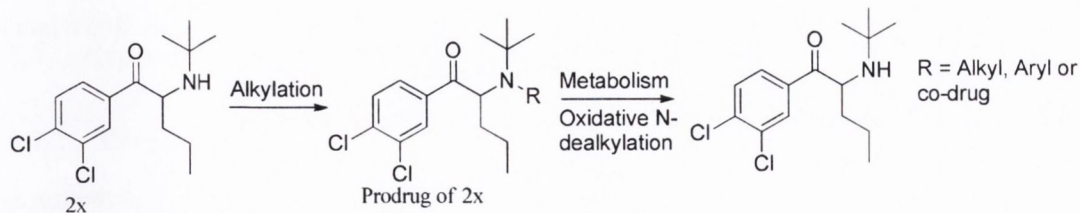


Figure 5.19 *N*-alkylated prodrugs of 2x

5.6.11 Co-drug for Crohn's disease (inflammatory bowel disease)

Bupropion has been shown to reduce symptoms and in some cases put into complete remission patients suffering from Crohn's disease [50, 52, 55, 271]. It has also been shown to slow chronic lymphocytic leukaemia [57]. 5-aminosalicylic acid is used clinically to treat ulcerative colitis and Crohn's disease [272-275]. Both these therapies can be combined using a co-drug strategy developed as a result of *N*-debenzylation of the *N*-benzyl prodrug of bupropion. Aldehyde oxidase is found almost ubiquitously throughout the body but in the gastrointestinal tract, its activity resides primarily in the small and large intestine [276, 277]. The beauty of this co-drug is it would be delivered directly to the site of action, cells of the intestine, then metabolized *in-situ* to a dual active combination therapy. The dealkylation of the co-drug will occur in the intestinal epithelia releasing bupropion and 5-aminosalicylic aldehyde where endogenous aldehyde oxidase will convert the aldehyde to the active 5-aminosalicylic acid. Successful prodrugs and co-drugs of 5-ASA have been attempted before [278-286] but never with bupropion.

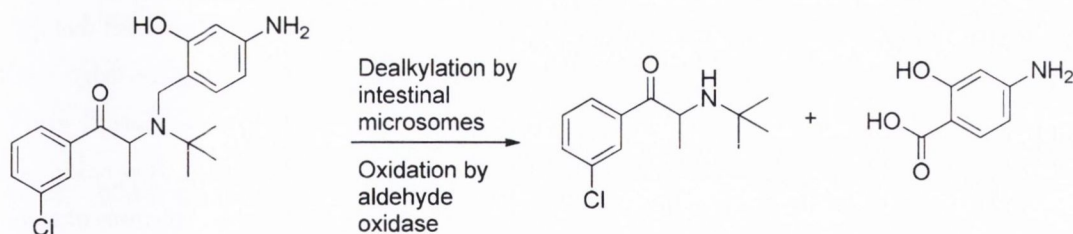


Figure 5.20 Potential co-drug of bupropion and 5-aminosalicylic acid

5.6.12 Pharmacotherapies for treating drugs of abuse addiction

Bupropion has recently been assessed as an anti-addiction remedy for drugs of abuse [123], smokeless tobacco [287] and even video games [288]. Its efficacy being related to its reuptake inhibition at NET and DAT. New analogues related to bupropion have been developed that have favourable *in vitro* efficacy and *in vivo* pharmacological profiles for indirect dopamine agonist pharmacotherapies for treating cocaine, methamphetamine, nicotine and other drugs of abuse addictions. The most favourable analogue developed by Carroll *et al.* [123], is a

secondary α -aminoketone related to bupropion which could easily be derivatized to a prodrug form by *N*-alkylation of the secondary amino group (Figure 5.21).

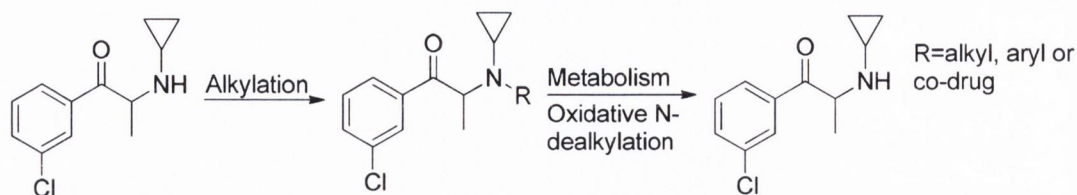


Figure 5.21 Potential *N*-alkylated analogue of bupropion for drugs of abuse addiction

5.6.13 Headshop type substituted cathinones

The substituted headshop type cathinones (Figure 5.22) are a diverse range of designer drugs that have recently become popular as replacement drugs of abuse due to their legality, price and ease of procurement through all of the many head-shops that have opened up over the last few years [289]. Many of the head-shop type compounds are directly related to the α -aminoketone cathinone and the derivatives thereof. The European Union has recently cracked down on the sale and distribution of any compound relating to these cathinones by imposing a change in law and scheduling any cathinone type compound. This has only served to drive these designer drugs underground and into the hands of the illicit drug market. Many users find themselves addicted and dependent on these cathinone designer drugs of which there is very little known due to their relative novelty. Bupropion is directly related to all these designer drugs yet doesn't have any abuse potential [290]. It is proposed here that bupropion and the prodrugs described in this chapter could be used as a safer replacement therapy to patients addicted to cathinone designer drugs. This area of abuse and the knowledge around these cathinones is at a very early stage but it is predicted to become much more relevant in the near future as newer designer drugs relating to these cathinones appear. Bupropion is the only compound excluded from the ban, therefore its chemistry, pharmacokinetics, pharmacology and stability are going to become much more important very rapidly as the structure activity relationships of these substituted cathinones are being understood.

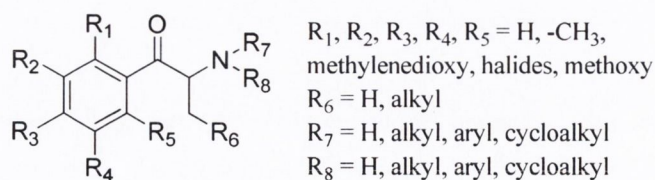


Figure 5.22 Substituted cathinones used as designer drugs

5.7 Experimental

5.7.1 Reagents and chemicals.

Ammonium hydroxide solution (30% as NH_3) HPLC grade, formic acid HPLC grade, MeOH, water and ACN all LC-MS grade were obtained from Fischer Scientific. Bupropion and metabolite standards were supplied as racemic mixtures from Toronto research chemicals. Human plasma donated by healthy fully consented TCD School of Pharmacy and Pharmaceutical Sciences postgraduate students.

5.7.2 Instrumentation

Chromatographic analysis was carried out on a Thermo Accela liquid chromatograph. The detector was a Thermo LTQ-XL-Orbitrap Discovery mass spectrometer. Centrifugation was carried out on an IEC Micromax centrifugator. Vortex mixing was carried out on a Velp Scientifica Rx3 vortex mixer. Standards were stored in a Thermo Forma -86°C ULT freezer. Brain samples were homogenized using an IKA T10 basic homogenizer.

5.7.3 Chromatographic conditions

The column used for chromatographic separation was a Waters Xbridge C18, 2.1 x 50 mm 2.5 μm at 30°C . Mobile phase A consisted of: 10:40:50, 1.0 % ammonium hydroxide solution in water, adjusted to pH 10.5 with formic acid: water: ACN. Mobile phase B consisted of: 10:90, 1.0 % ammonium hydroxide solution in water, adjusted to pH 10.5 with formic acid: ACN. The flow rate was 250 $\mu\text{L}/\text{min}$; injection volume 10 μL ; run time 10 min. The gradient was 100 % A held for 1 min, 0 % B to 100 % B over 4 min, hold 100 % B for 0.5 min, 0 % B at 5.51 min and equilibrate for 0.5 min.

5.7.4 Mass spectrometer conditions

The LTQ-XL ion trap mass spectrometer was coupled to the Accela LC system via an electrospray ionization (ESI) probe. The capillary temperature was maintained at 350°C , sheath gas flow rate 50 arbitrary units, auxiliary gas flow rate 5 arbitrary units, sweep gas flow rate 0 arbitrary units, source voltage 3.20 kV, source current 100 μA , capillary voltage 43.00 V and tube lens 100 V.

Compounds were detected in positive ion mode using selected ion monitoring (SIM). Hydroxybupropion was detected $(\text{M}+\text{H})^+ = 256.1099$, RT = 1.0 min, Rac-erythrohydrobupropion $(\text{M}+\text{H})^+ = 242.1306$, RT = 2.3 min, Rac-threo hydrobupropion $(\text{M}+\text{H})^+ = 242.1306$, RT 2.8 min, bupropion $(\text{M}+\text{H})^+ = 240.1150$, RT = 2.0 min, *N*-methyl bupropion $(\text{M}+\text{H})^+ = 254.1306$, RT = 4.9 min, Rac-*N*-methylerythrohydrobupropion $(\text{M}+\text{H})^+$

= 256.1463, RT = 4.1 min and Rac-*N*-methylthreohydrobupropion (M+H)⁺ = 256.1463, RT = 4.6 min. The optimum detector conditions were found by tuning the instrument to be most sensitive for bupropion's most abundant ion at 240 (m/z).

5.7.5 Guinea pig enzyme kinetics (Michaelis-Menten)

Guinea pig S9 liver fraction, NADPH regenerating solutions A and B were thawed rapidly to 37°C, then kept on wet ice until ready for use. A number of different concentration substrate solutions were prepared where the maximum concentration of DMSO was 1 %, and the concentration of guinea pig S9 liver fraction, NADP regenerating solution B and phosphate buffer was fixed. After incubation for 5 min, NADP regenerating solution A was added and the metabolism was initiated. Final volume was 100 µL. The tube was inverted twice and vortex mixed. The final concentrations in this solution was 50-1000 µM prodrug, 0.1 mg/mL guinea-pig S9 liver fraction, 1.3 mM NADP⁺, 0.4 U/mL glucose-6-phosphate dehydrogenase and 1.0 % DMSO. This solution was incubated for 20 min at 37°C. The reaction was quenched by addition of 100 µL of acetonitrile. The mixture was centrifuged at 10,000 x g for 10 min. The supernatant was analysed by LC-MS analysis.

5.7.6 Standard preparation

Stock standard solutions were prepared at 10 mg/ml the freebase in MeOH, for example 9.0 mg bupropion hydrochloride was dissolved in MeOH (779 µL). Stock standard solutions were prepared in duplicate and verified off each other at working standard level to ensure accurate preparation. Acceptable standard verification was 95-105 %. Working standard solutions were prepared by serial dilution of stock standards in 0.001 M HCl solution.

5.7.7 System suitability

System suitability of the LC-MS system was established on the day of use by repeat injection of a working standard solution. The % RSD of six replicate standard injections for retention time and area was not more than 3.0 %. This ensured that the system was stable, equilibrated and suitable for analysis. System suitability throughout the analysis run and at the end of the analysis run was also established by performing a quality control standard injection. This ensured system drift was kept to a minimum. The quality control sample was injected after every eight samples. The % RSD of the totalled quality control samples was less than 10%.

5.7.8 Analytical method validation

5.7.8.1 Selectivity

Selectivity solutions were evaluated by preparing all standards, blanks, plasma and brain homogenates separately. The solutions were prepared and diluted appropriately as per method and chromatographed. Minimum resolution, interference and carryover were evaluated.

5.7.8.2 Linearity

Stock standard solutions were prepared in methanol on the day of analysis. Standards were prepared by serial dilution of stock standard solutions using 60:40 0.001 M HCl:ACN as diluent. Standards were prepared in the concentration range of 0.1 ng/mL to 1000 ng/mL. The linear range was calculated by least squares linear regression analysis. All linear portions of each calibration curve had a correlation coefficient of > 0.995.

5.7.8.3 Accuracy/Precision

Human plasma was spiked with *N*-methyl bupropion, bupropion and metabolites at three concentrations, 100, 500 and 1000 ng/mL. Aliquots (6 × 50 μL) were transferred to 1.5 mL microcentrifuge tubes. ACN (200 μL) was added and the solution was vortex mixed. The remaining mixture was centrifuged at 10,000 rpm for 10 min. Supernatant (100 μL) was removed and added to 0.001 M HCl (100 μL). The solution was vortex mixed again and an aliquot (100 μL) was placed in a micro-insert for HPLC analysis. The final concentrations were 10, 50, 100 ng/mL.

5.7.8.4 Plasma LLOQ/precision

Human plasma was spiked with *N*-methyl bupropion, bupropion and metabolites at a concentration of 10 ng/mL. Aliquots (6 × 50 μL) were transferred to 1.5 mL microcentrifuge tubes. ACN (200 μL) was added and the solution was vortex mixed. The remaining mixture was centrifuged at 10,000 rpm for 10 min. An aliquot (100 μL) of supernatant was removed and added to 0.001 M HCl (100 μL). The solution was vortex mixed again and 100 μL was placed in a micro-insert for HPLC analysis. The final concentration was 1 ng/mL. All LLOQ solutions had an analyte peak signal to noise ratio greater than 10.

5.7.8.5 Plasma LOD

The limit of detection of the method was determined by injection of serially diluted standards from highest to lowest level. The limit of detection was determined as the lowest peak seen with a minimum signal to noise ratio of three.

5.7.8.6 Brain LLOQ Accuracy/Precision

Rat brain homogenate (165 mg brain per mL 0.01M HCl) was spiked with *N*-methyl bupropion, bupropion and metabolites at two concentrations, 250 and 2500 ng/mL. Aliquots (5 × 200 μL) were transferred to 1.5 mL microcentrifuge tubes. The mixture was centrifuged at 15,000 rpm for 10 min. Supernatant (100 μL) was transferred to 1.5 mL microcentrifuge

tubes. ACN (300 μ L) was added and the solution was vortex mixed. The remaining mixture was centrifuged at 15,000 rpm for 10min. 200 μ L of supernatant was removed and added to 800 μ L of water. The solution was vortex mixed again and analysed by HPLC. Final concentration 12.5, 125 ng/mL.

5.7.9 Pharmacokinetic study

5.7.9.1 Intraperitoneal animal handling (Charles Rivers Laboratories)

After acclimatization, male Hartley albino guinea-pigs, weighing 280 – 320 g (from Charles River Laboratories, 69592 L'Arbresle, France) were deprived of food for 16 h with free access to water (food withdrawal at 04:00 PM the day before). On the day of the experiment 5 guinea pigs per group were weighed then injected through the abdominal wall with bupropion given at 40 mg/kg intraperitoneum. A second group of 5 guinea pigs were weighed then injected through the abdominal wall with *N*-methyl bupropion given at 42 mg/Kg intraperitoneum.

Guinea pigs were placed under isoflurane anaesthesia and approximately 100 μ L of blood was collected using hematocrit capillaries or by cardiac puncture (terminal) into dry heparin/Li containing tubes before administration and then at 5 time points post-administration (0, 20, 40, 60, 120 and 180 min). After blood was collected, the tubes were inverted several times and placed on ice. The samples were centrifuged within 30 min maximum after sampling, at 2205g at 4 °C for 10 min. Plasma was transferred to polypropylene tubes (two aliquots of at least 100 μ l each) and frozen with minimal delay at approximately -70°C.

An additional group of guinea-pigs were used for brain collection at a single time point (20 min). The day of the experiment 4 guinea pigs per group were weighed then injected through the abdominal wall with bupropion given at 40 mg/kg IP and *N*-methyl bupropion given at 42 mg/Kg IP. At time 20 min post-injection, the animals were decapitated and the brain extracted and rinsed in cold physiological saline. The whole brain was fast frozen on dry ice and placed into pre-labelled vials and stored at approximately -70°C (deep frozen).

5.7.9.2 Oral study animal handling (MDS Pharma Services)

After acclimatization, male Hartley albino guinea-pigs, weighing 280 – 320 g (from Charles River Laboratories, 69592 L'Arbresle, France) were deprived of food for 16 h with free access to water (food withdrawal at 04:00 PM the day before). On the day of the experiment 5 guinea pigs per group were weighed then fed by oral gavage with bupropion given at 40 mg/kg intraperitoneum. A second group of 5 guinea pigs were weighed then fed by oral gavage with *N*-methyl bupropion given at 42 mg/Kg intraperitoneum.

Guinea pigs were placed under isoflurane anaesthesia and approximately 100 μ L of blood was collected using hematocrit capillaries or by cardiac puncture (terminal) into dry heparin/Li containing tubes before administration and then at 5 time points post-administration (0, 20, 40, 60, 120, 180, 240 and 360 min). After blood was collected, the tubes were inverted several times and placed on ice. The samples were centrifuged within 30 min maximum after sampling, at 2205g at 4 °C for 10 min. Plasma was transferred to polypropylene tubes (two aliquots of at least 100 μ l each) and frozen with minimal delay at approximately -70°C.

An additional group of guinea-pigs were used for brain collection at a single time point (20 min). The day of the experiment 4 guinea pigs per group were weighed then fed by oral gavage with bupropion given at 40 mg/kg IP and *N*-methyl bupropion given at 42 mg/Kg IP. At time 20 min post-injection, the animals were decapitated and the brain extracted and rinsed in cold physiological saline. The whole brain was fast frozen on dry ice and placed into pre-labelled vials and stored at approximately -70°C (deep frozen).

5.7.9.3 Plasma sample preparation

Guinea pig plasma was defrosted and centrifuged. 50 μ L of plasma was added to a 1.5 mL microcentrifuge tube. 200 μ L ACN was added and the mixture was vortex mixed. The resulting solution was centrifuged at 10,000 rpm for 10 min. 100 μ L of the supernatant was added to 100 μ L of 0.001 M HCl. The solution was vortex mixed and added to a 100 μ L micro-insert for LC-MS analysis.

5.7.9.4 Brain sample preparation

Guinea pig brain was defrosted. The whole brain was weighed into a beaker. 20 mL 0.01 M HCl was added and the mixture was homogenized for 3 min on level 6. The mixture was allowed to settle for 10 min. An aliquot of the resulting solution was centrifuged at 15,000 rpm for 10 min. 250 μ L of the supernatant was added to 750 μ L ACN. The mixture was centrifuged at 15,000 rpm for 10 min. 200 μ L of the supernatant was added to 800 μ L water. The clear solution was vortexed mixed and analysed by LC-MS.

6 Bibliography

- [1] N.B. Mehta, United States Patent 3819796, (1974).
- [2] GlaxoSmithKline, Research Triangle Park, NC, Prescribing Information, (2006).
- [3] N.B. Mehta, United states Patent US3885046, (1975).
- [4] J.W. Jefferson, J.F. Pradko, K.T. Muir, *Clinical Therapeutics*, 27 (2005) 1685-1695.
- [5] Y. Chen, H.F. Liu, L. Liu, K. Nguyen, E.B. Jones, A.J. Fretland, *Xenobiotica*, 40 (2010) 536-546.
- [6] S.R. Faucette, R.L. Hawke, E.L. Lecluyse, S.S. Shord, B. Yan, R.M. Laethem, C.M. Lindley, *Drug Metab Dispos*, 28 (2000) 1222-1230.
- [7] M.I. Damaj, F.I. Carroll, J.B. Eaton, H.A. Navarro, B.E. Blough, S. Mirza, R.J. Lukas, B.R. Martin, *Mol Pharmacol*, 66 (2004) 675-682.
- [8] U.C.T. Oppermann, E. Maser, *Toxicology*, 144 (2000) 71-81.
- [9] W.D. Horst, S.H. Preskorn, *Journal of Affective Disorders*, 51 (1998) 237-254.
- [10] S.M. Stahl, J.F. Pradko, B.R. Haight, J.G. Modell, C.B. Rockett, S. Learned-Coughlin, *Prim Care Companion J Clin Psychiatry*, 6 (2004) 159-166.
- [11] K.F. Foley, K.P. DeSanty, R.E. Kast, *Expert Rev Neurother*, 6 (2006) 1249-1265.
- [12] J.E. Slemmer, B.R. Martin, M.I. Damaj, *Journal of Pharmacology and Experimental Therapeutics*, 295 (2000) 321-327.
- [13] D. Brustolim, R. Ribeiro-dos-Santos, R.E. Kast, E.L. Altschuler, M.B. Soares, *Int Immunopharmacol*, 6 (2006) 903-907.
- [14] GlaxoSmithKline, Research Triangle Park, NC, Prescribing Information, (2006).
- [15] S.M. Stahl, *J Clin Psychiatry*, 59 Suppl 18 (1998) 23-29.
- [16] J. Davidson, *J Clin Psychiatry*, 50 (1989) 256-261.
- [17] P.H. Silverstone, R. Williams, L. McMahon, R. Fleming, S. Fogarty, *Ann Gen Psychiatry*, 7 (2008) 19.
- [18] R.J. Lukas, A.Z. Muresan, M.I. Damaj, B.E. Blough, X. Huang, H.A. Navarro, S.W. Mascarella, J.B. Eaton, S.K. Marxer-Miller, F.I. Carroll, *J Med Chem*, 53 (2010) 4731-4748.
- [19] B.R. Cooper, C.M. Wang, R.F. Cox, R. Norton, V. Shea, R.M. Ferris, *Neuropsychopharmacology*, 11 (1994) 133-141.
- [20] R.N. Golden, C.L. De Vane, S.C. Laizure, M.V. Rudorfer, M.A. Sherer, W.Z. Potter, *Arch Gen Psychiatry*, 45 (1988) 145-149.
- [21] M. Turpeinen, R. Nieminen, T. Juntunen, P. Taavitsainen, H. Raunio, O. Pelkonen, *Drug Metab Dispos*, 32 (2004) 626-631.
- [22] M.P. Kotlyar, L.H.P. Brauer, T.S.P. Tracy, D.K.P. Hatsukami, J.B.S. Harris, C.A.M.A. Bronars, D.E.M.D. Adson, *Journal of Clinical Psychopharmacology*, 25 (2005) 226-229.

- [23] D. Flockhart, in, Indiana University School of Medicine, 2007.
- [24] R.M. Hirschfeld, *J Clin Psychiatry*, 61 Suppl 6 (2000) 4-6.
- [25] M. Maes, *Prog Neuropsychopharmacol Biol Psychiatry*, 19 (1995) 11-38.
- [26] M. Maes, E. Bosmans, E. Suy, C. Vandervorst, C. De Jonckheere, J. Raus, *Neuropsychobiology*, 24 (1990) 115-120.
- [27] O.J. Schiepers, M.C. Wichers, M. Maes, *Prog Neuropsychopharmacol Biol Psychiatry*, 29 (2005) 201-217.
- [28] G. Irmisch, D. Schlaefke, J. Richter, *Neurochem Res*, 35 (2010) 1376-1383.
- [29] M. Maes, H.Y. Meltzer, S. Scharpe, W. Cooreman, W. Uyttenbroeck, E. Suy, C. Vandervorst, J. Calabrese, J. Raus, P. Cosyns, *Psychiatry Res*, 47 (1993) 229-241.
- [30] M. Maes, R. Yirmiya, J. Norberg, S. Brene, J. Hibbeln, G. Perini, M. Kubera, P. Bob, B. Lerer, M. Maj, *Metab Brain Dis*, 24 (2009) 27-53.
- [31] M. Fava, A.J. Rush, M.E. Thase, A. Clayton, S.M. Stahl, J.F. Pradko, J.A. Johnston, *Prim Care Companion J Clin Psychiatry*, 7 (2005) 106-113.
- [32] M.E. Thase, B.R. Haight, N. Richard, C.B. Rockett, M. Mitton, J.G. Modell, S. VanMeter, A.E. Harriett, Y. Wang, *J Clin Psychiatry*, 66 (2005) 974-981.
- [33] A.H. Clayton, H.A. Croft, J.P. Horrigan, D.S. Wightman, A. Krishen, N.E. Richard, J.G. Modell, *J Clin Psychiatry*, 67 (2006) 736-746.
- [34] M.E. Thase, A.H. Clayton, B.R. Haight, A.H. Thompson, J.G. Modell, J.A. Johnston, *J Clin Psychopharmacol*, 26 (2006) 482-488.
- [35] D.S. Baldwin, G.I. Papakostas, *J Clin Psychiatry*, 67 Suppl 6 (2006) 9-15.
- [36] S. Zisook, A.J. Rush, B.R. Haight, D.C. Clines, C.B. Rockett, *Biological Psychiatry*, 59 (2006) 203-210.
- [37] J. Jonas, A. Bose, J. Tsai, in, United States Patent 7569605 2009.
- [38] M.G. Dedhiya, A. Chhetry, N. Mani, in, United States Patent Application 20070112075, 2007.
- [39] S.A. Spier, *Depress Anxiety*, 7 (1998) 73-75.
- [40] J.A. Bodkin, R.A. Lasser, J.D. Wines, Jr., D.M. Gardner, R.J. Baldessarini, *J Clin Psychiatry*, 58 (1997) 137-145.
- [41] M.H. Trivedi, M. Fava, S.R. Wisniewski, M.E. Thase, F. Quitkin, D. Warden, L. Ritz, A.A. Nierenberg, B.D. Lebowitz, M.M. Biggs, J.F. Luther, K. Shores-Wilson, A.J. Rush, *N Engl J Med*, 354 (2006) 1243-1252.
- [42] A.J. Rush, M.H. Trivedi, S.R. Wisniewski, J.W. Stewart, A.A. Nierenberg, M.E. Thase, L. Ritz, M.M. Biggs, D. Warden, J.F. Luther, K. Shores-Wilson, G. Niederehe, M. Fava, *N Engl J Med*, 354 (2006) 1231-1242.
- [43] R. Edwards, *BMJ*, 328 (2004) 217-219.
- [44] K. Fagerstrom, *Drugs*, 62 Suppl 2 (2002) 1-9.

- [45] M.G. Goldstein, *J Clin Psychiatry*, 59 Suppl 4 (1998) 66-72.
- [46] R.D. Hurt, D.P. Sachs, E.D. Glover, K.P. Offord, J.A. Johnston, L.C. Dale, M.A. Khayrallah, D.R. Schroeder, P.N. Glover, C.R. Sullivan, I.T. Croghan, P.M. Sullivan, *N Engl J Med*, 337 (1997) 1195-1202.
- [47] K.E. Hayford, C.A. Patten, T.A. Rummans, D.R. Schroeder, K.P. Offord, I.T. Croghan, E.D. Glover, D.P. Sachs, R.D. Hurt, *Br J Psychiatry*, 174 (1999) 173-178.
- [48] E.L. Altschuler, R.E. Kast, *Psychosom Med*, 65 (2003) 719.
- [49] E.L. Altschuler, R.E. Kast, *Med Hypotheses*, 64 (2005) 118-119.
- [50] R.E. Kast, *Gen Hosp Psychiatry*, 25 (2003) 495-496.
- [51] R.E. Kast, *Leuk Res*, 29 (2005) 1459-1463.
- [52] R.E. Kast, E.L. Altschuler, *Gastroenterology*, 121 (2001) 1260-1261.
- [53] R.E. Kast, E.L. Altschuler, *J Hepatol*, 39 (2003) 131-133.
- [54] R.E. Kast, E.L. Altschuler, *Med Hypotheses*, 62 (2004) 817-818.
- [55] R.E. Kast, E.L. Altschuler, *Gut*, 53 (2004) 1056.
- [56] R.E. Kast, E.L. Altschuler, *Med Hypotheses*, 65 (2005) 374-376.
- [57] R.E. Kast, E.L. Altschuler, *Arch Immunol Ther Exp (Warsz)*, 53 (2005) 143-147.
- [58] E. Altschuler, R.E. Kast, in, United States Patent Application 20060173080, 2006.
- [59] J.G. Simeon, H.B. Ferguson, J. Van Wyck Fleet, *Can J Psychiatry*, 31 (1986) 581-585.
- [60] C.D. Casat, D.Z. Pleasants, D.H. Schroeder, D.W. Parler, *Psychopharmacol Bull*, 25 (1989) 198-201.
- [61] C.D. Casat, D.Z. Pleasants, J. Van Wyck Fleet, *Psychopharmacol Bull*, 23 (1987) 120-122.
- [62] C.K. Conners, C.D. Casat, C.T. Gualtieri, E. Weller, M. Reader, A. Reiss, R.A. Weller, M. Khayrallah, J. Ascher, *J Am Acad Child Adolesc Psychiatry*, 35 (1996) 1314-1321.
- [63] W. Oberegger, P. Maes, M.A. Saleh, G. Jackson, in, United States Patent 7645802, 2010.
- [64] S. Tardieu, Y. Poirier, J. Micallef, O. Blin, *Acta Psychiatr Scand*, 109 (2004) 75-77; discussion 77-78.
- [65] T.F. Newton, J.D. Roache, R. De La Garza, 2nd, T. Fong, C.L. Wallace, S.H. Li, A. Elkashef, N. Chiang, R. Kahn, *Neuropsychopharmacology*, 31 (2006) 1537-1544.
- [66] A. Ansari, *Harv Rev Psychiatry*, 7 (2000) 257-277.
- [67] J.R. Davidson, R.D. France, *J Clin Psychiatry*, 55 (1994) 362.
- [68] W. Pinsker, *Headache*, 38 (1998) 58.
- [69] M.R. Semenchuk, B. Davis, *Clin J Pain*, 16 (2000) 6-11.
- [70] M.R. Semenchuk, S. Sherman, B. Davis, *Neurology*, 57 (2001) 1583-1588.
- [71] J.R. McCullough, P.D. Rubin, in, United States Patent 6495605, 2002.
- [72] N. Harto-Truax, W.C. Stern, L.L. Miller, T.L. Sato, A.E. Cato, *J Clin Psychiatry*, 44 (1983) 183-186.

- [73] K.M. Gadde, C.B. Parker, L.G. Maner, H.R. Wagner, 2nd, E.J. Logue, M.K. Drezner, K.R. Krishnan, *Obes Res*, 9 (2001) 544-551.
- [74] J.W. Anderson, F.L. Greenway, K. Fujioka, K.M. Gadde, J. McKenney, P.M. O'Neil, *Obes Res*, 10 (2002) 633-641.
- [75] C.G. Goetz, C.M. Tanner, H.L. Klawans, *Neurology*, 34 (1984) 1092-1094.
- [76] J.W. Young, in, United States Patent 6277887, 2001.
- [77] M.R. Safarinejad, *J Psychopharmacol*, (2010).
- [78] M.R. Safarinejad, *BJU Int*, 106 (2010) 840-847.
- [79] M.R. Safarinejad, S.Y. Hosseini, M.A. Asgari, F. Dadkhah, A. Taghva, *BJU Int*, 106 (2010) 832-839.
- [80] W.C. Stern, in, United States Patent 4507323, 1985.
- [81] S.W. Kim, I.S. Shin, J.M. Kim, S.J. Yang, H.Y. Shin, J.S. Yoon, *Clin Neuropharmacol*, 28 (2005) 298-301.
- [82] J.J. Lee, J. Erdos, M.F. Wilkosz, R. LaPlante, B. Wagoner, *Ann Pharmacother*, 43 (2009) 370-374.
- [83] *FDA Consum*, 40 (2006) 7.
- [84] *Mayo Clin Womens Healthsource*, 10 (2006) 3.
- [85] S.C. Dilsaver, A.B. Qamar, V.J. Del Medico, *J Clin Psychiatry*, 53 (1992) 252-255.
- [86] J.G. Modell, N.E. Rosenthal, A.E. Harriett, A. Krishen, A. Asgharian, V.J. Foster, A. Metz, C.B. Rockett, D.S. Wightman, *Biol Psychiatry*, 58 (2005) 658-667.
- [87] M.E. Myles, A.M. Azcuy, N.T. Nguyen, E.R. Reisch, S.A. Barker, H.W. Thompson, J.M. Hill, *J Pharmacol Exp Ther*, 311 (2004) 640-644.
- [88] C.W. Reindler, in, United States Patent 6512011, 2003.
- [89] J.G. Modell, S. Boyce, E. Taylor, C. Katholi, *Psychosom Med*, 64 (2002) 835-840.
- [90] A.W. Peck, in, United States Patent 4393078, 1983.
- [91] A. Albert, *Nature*, 182 (1958) 421-422.
- [92] V. Wehner, *Angewandte Chemie*, 116 (2004) 550-551.
- [93] J. Rautio, H. Kumpulainen, T. Heimbach, R. Oliyai, D. Oh, T. Jarvinen, J. Savolainen, *Nat Rev Drug Discov*, 7 (2008) 255-270.
- [94] K.-M. Wu, *Pharmaceuticals*, 2 (2009) 77-81.
- [95] K.-M. Wu, J.G. Farrelly, *Toxicology*, 236 (2007) 1-6.
- [96] J. Rautio, K. Laine, M. Gynther, J. Savolainen, *AAPS J*, 10 (2008) 92-102.
- [97] J. Temsamani, J.M. Scherrmann, A.R. Rees, M. Kaczorek, *Pharm Sci Technolo Today*, 3 (2000) 155-162.
- [98] B. Pavan, A. Dalpiaz, N. Ciliberti, C. Biondi, S. Manfredini, S. Vertuani, *Molecules*, 13 (2008) 1035-1065.
- [99] A. Simplício, J. Clancy, J. Gilmer, *Molecules*, 13 (2008) 519-547.

- [100] A.J. Nazarali, G.B. Baker, R.T. Coutts, F.M. Pasutto, *Prog Neuropsychopharmacol Biol Psychiatry*, 7 (1983) 813-816.
- [101] D.S. Goldstein, *Cardiovascular Drug Reviews*, 24 (2006) 189-203.
- [102] A. Di Stefano, P. Sozio, L.S. Cerasa, *Molecules*, 13 (2008) 46-68.
- [103] G.B. Baker, R.T. Coutts, A.J. Nazarali, T.J. Danielson, M. Rubens, *Proc West Pharmacol Soc*, 27 (1984) 523-525.
- [104] R.B. Walker, L.D. Fitz, L.M. Williams, Y.M. McDaniel, *Gen Pharmacol*, 27 (1996) 109-111.
- [105] Y. Tsukamoto, Y. Kato, M. Ura, I. Horii, H. Ishitsuka, H. Kusuhara, Y. Sugiyama, *Pharm Res*, 18 (2001) 1190-1202.
- [106] H.G. Bray, S.P. James, J.W. Thorpe, M.R. Wasdell, *Biochem J*, 47 (1950) 294-299.
- [107] P.R. Chen, W.C. Dauterman, *Biochim Biophys Acta*, 250 (1971) 216-223.
- [108] H.K. Crewe, L.M. Notley, R.M. Wunsch, M.S. Lennard, E.M.J. Gillam, *Drug Metabolism and Disposition*, 30 (2002) 869-874.
- [109] H. Yu, R.B. Rothman, C.M. Dersch, J.S. Partilla, K.C. Rice, *Bioorganic & Medicinal Chemistry*, 8 (2000) 2689-2692.
- [110] I. Johno, B.T. Ludwick, R.H. Levy, *J Pharm Sci*, 71 (1982) 633-636.
- [111] D. Parmar, L.T. Burka, *Drug Metab Dispos*, 19 (1991) 1101-1107.
- [112] A. Mantyla, J. Rautio, T. Nevalainen, J. Vepsalainen, R. Juvonen, H. Kendrick, T. Garnier, S.L. Croft, T. Jarvinen, *Bioorg Med Chem*, 12 (2004) 3497-3502.
- [113] H. Kumpulainen, N. Mahonen, M.L. Laitinen, M. Jaurakkajarvi, H. Raunio, R.O. Juvonen, J. Vepsalainen, T. Jarvinen, J. Rautio, *J Med Chem*, 49 (2006) 1207-1211.
- [114] A.K. Cederstav, B.M. Novak, *Journal of the American Chemical Society*, 116 (1994) 4073-4074.
- [115] J.P. Patel, A.J. Repta, *International Journal of Pharmaceutics*, 5 (1980) 329-333.
- [116] J.P. Patel, A.J. Repta, *International Journal of Pharmaceutics*, 9 (1981) 29-47.
- [117] J.P. Burkhart, S. Mehdi, J.R. Koehl, M.R. Angelastro, P. Bey, N.P. Peet, *Bioorganic & Medicinal Chemistry Letters*, 8 (1998) 63-64.
- [118] P.K. Kiptoo, K.S. Paudel, D.C. Hammell, R.R. Pinninti, J. Chen, P.A. Crooks, A.L. Stinchcomb, *J Pharm Sci*, (2008).
- [119] M.O. Hamad, P.K. Kiptoo, A.L. Stinchcomb, P.A. Crooks, *Bioorganic & Medicinal Chemistry*, 14 (2006) 7051-7061.
- [120] A. Santamaria, H.R. Arias, *Behav Brain Res*, 211 (2010) 132-139.
- [121] M.R. Meyer, H.H. Maurer, *Curr Drug Metab*, 11 (2010) 468-482.
- [122] H.T. Kamata, N. Shima, K. Zaitso, T. Kamata, A. Miki, M. Nishikawa, M. Katagi, H. Tsuchihashi, *Xenobiotica*, 36 (2006) 709-723.

- [123] F.I. Carroll, B.E. Blough, P. Abraham, A.C. Mills, J.A. Holleman, S.A. Wolckenhauer, A.M. Decker, A. Landavazo, K.T. McElroy, H.A. Navarro, M.B. Gatch, M.J. Forster, *J Med Chem*, 52 (2009) 6768-6781.
- [124] F.I. Carroll, B.E. Blough, S.W. Mascarella, H.A. Navarro, J.B. Eaton, R.J. Lukas, M.I. Damaj, *J Med Chem*, 53 (2010) 2204-2214.
- [125] ICH Harmonised Tripartite Guideline, (2003).
- [126] M.D. Ruff, S.R. Kalidindi, J.E. Sutton Jr., United States Patent 5358970 (1994).
- [127] P.S. Kulkarni, B.B. Shah, A. Maitra, J.M. Devito, United States Patent 20010021721 (2001).
- [128] C. Arellano, C. Philibert, C. Vachoux, J. Woodley, G. Houin, *Journal of Chromatography B*, 829 (2005) 50-55.
- [129] R. Coles, E.D. Kharasch, *Pharm Res*, 25 (2008) 1405-1411.
- [130] M.W. Trumbore, R.V. Rariy, J.C. Hirsh, M. Hirsh, United States Patent 20080044462 (2008).
- [131] M. Chawla, R.S. Raghuvanshi, A. Rampal, United States Patent 20060165779 (2006).
- [132] S.K. Gidwani, P. Singnurkar, P.K. Tewari, United States Patent 6462237, (2002).
- [133] S. Chungi, K. Lin, United States Patent 6306436 (2001).
- [134] S.C. Laizure, C.L. DeVane, *Ther Drug Monit*, 7 (1985) 447-450.
- [135] R. Suma, H. Kosanam, P.K. Sai Prakash, *Rapid Commun Mass Spectrom*, 20 (2006) 1390-1394.
- [136] S.M. Walters, *J Pharm Sci*, 69 (1980) 1206-1209.
- [137] C.L. Stevens, R.D. Elliott, B.L. Winch, *Journal of the American Chemical Society*, 85 (1963) 1464-1470.
- [138] C.L. Stevens, R.D. Elliott, B.L. Winch, I.L. Klundt, *Journal of the American Chemical Society*, 84 (1962) 2272-2274.
- [139] P. Compain, J. Goré, J.-M. Vatèle, *Tetrahedron*, 52 (1996) 6647-6664.
- [140] G.M. Loudon, *Journal of Chemical Education*, 68 (1991) 973.
- [141] E.J.H. Bechara, F. Dutra, V.E.S. Cardoso, A. Sartori, K.P.K. Olympio, C.A.A. Penatti, A. Adhikari, N.A. Assunção, *Comparative Biochemistry and Physiology Part C: Toxicology & Pharmacology*, 146 88-110.
- [142] E.J. Bechara, *Braz J Med Biol Res*, 29 (1996) 841-851.
- [143] W.J. Baader, C. Bohne, G. Cilento, H.B. Dunford, *J Biol Chem*, 260 (1985) 10217-10225.
- [144] M.P. Kalapos, *Toxicol Lett*, 110 (1999) 145-175.
- [145] H.P. Monteiro, D.S. Abdalla, O. Augusto, E.J. Bechara, *Arch Biochem Biophys*, 271 (1989) 206-216.
- [146] T. Mashino, I. Fridovich, *Arch Biochem Biophys*, 254 (1987) 547-551.

- [147] H.L.T. Mobley, R.P. Hausinger, *Microbiological Reviews*, 53 (1989) 85-108.
- [148] H.L.T. Mobley, M.D. Island, R.P. Hausinger, *Microbiological Reviews*, 59 (1995) 451-480.
- [149] T. Tanaka, M. Kawase, S. Tani, *Bioorganic & Medicinal Chemistry*, 12 (2004) 501-505.
- [150] M.M. Dell'Anna, P. Mastroianni, C.F. Nobile, L. Lopez, *Journal of Molecular Catalysis A: Chemical*, 111 (1996) 33-36.
- [151] R.M. Welch, A.A. Lai, D.H. Schroeder, *Xenobiotica*, 17 (1987) 287-298.
- [152] M.M. Ames, C.D. Selassie, L.C. Woodson, J.A. Van Loon, C. Hansch, R.M. Weinshilboum, *Journal of Medicinal Chemistry*, 29 (1986) 354-358.
- [153] R.M. Wadkins, J.L. Hyatt, X. Wei, K.J.P. Yoon, M. Wierdl, C.C. Edwards, C.L. Morton, J.C. Obenauer, K. Damodaran, P. Beroza, M.K. Danks, P.M. Potter, *Journal of Medicinal Chemistry*, 48 (2005) 2906-2915.
- [154] P.M. O'Byrne, R. Williams, J.J. Walsh, J.F. Gilmer, *J Pharm Biomed Anal*, 53 (2010) 376-381.
- [155] D.M. Kalendra, B.R. Sickles, *J Org Chem*, 68 (2003) 1594-1596.
- [156] O.S. Gudmundsson, Case Study: Ximelagatran: A Double Prodrug of Melagatran, in: *Prodrugs*, 2007, pp. 1395-1402.
- [157] G. Fager, M. Cullberg, M. Eriksson-Lepkowska, L. Frison, U.G. Eriksson, *Eur J Clin Pharmacol*, 59 (2003) 283-289.
- [158] B. Clement, K. Lopian, *Drug Metabolism and Disposition*, 31 (2003) 645-651.
- [159] A. Ghosal, S. Gupta, R. Ramanathan, Y. Yuan, X. Lu, A.D. Su, N. Alvarez, S. Zbaida, S.K. Chowdhury, K.B. Alton, *Drug Metab Lett*, 3 (2009) 162-170.
- [160] Q. Meng, H. Luo, Y. Liu, W. Li, W. Zhang, Q. Yao, *Bioorg Med Chem Lett*, 19 (2009) 2808-2810.
- [161] Y.F. Zhang, X.Y. Chen, D.F. Zhong, Y.M. Dong, *Acta Pharmacol Sin*, 24 (2003) 715-718.
- [162] G.M.W. Peter, W.G. Theodora, Protection for the Amino Group, in: *Greene's Protective Groups in Organic Synthesis (Fourth Edition)*, 2006, pp. 696-926.
- [163] L. Mu, J.A. Qi, Q.D. Zhang, *Yao Xue Xue Bao*, 27 (1992) 336-344.
- [164] N. Shinsuke, Y. Masayoshi, Y. Isao, *Cardiovascular Drug Reviews*, 10 (1992) 101-116.
- [165] D.M. Gasparro, D.R.P. Almeida, L.F. Pisterzi, J.R. Juhasz, B. Viskolcz, B. Penke, I.G. Csizmadia, *Journal of Molecular Structure: THEOCHEM*, 666-667 (2003) 527-536.
- [166] T.S. Rao, G.B. Baker, R.T. Coutts, *Brain Research Bulletin*, 19 (1987) 47-55.
- [167] T.S. Rao, G.B. Baker, R.T. Coutts, *Naunyn Schmiedebergs Arch Pharmacol*, 336 (1987) 25-32.
- [168] G. Chelucci, M. Falorni, G. Giacomelli, *Synthesis*, 1990 (1990) 1121,1122.

- [169] W.S. Saari, W. Halczenko, D.W. Cochran, M.R. Dobrinska, W.C. Vincek, D.C. Titus, S.L. Gaul, C.S. Sweet, *J Med Chem*, 27 (1984) 713-717.
- [170] N. Bodor, A. Elkoussi, *Pharm Res*, 8 (1991) 1389-1395.
- [171] L. Prokai, W.M. Wu, G. Somogyi, N. Bodor, *J Med Chem*, 38 (1995) 2018-2020.
- [172] M. Krause, A. Rouleau, H. Stark, P. Luger, R. Lipp, M. Garbarg, J.C. Schwartz, W. Schunack, *J Med Chem*, 38 (1995) 4070-4079.
- [173] M. Krause, H. Stark, W. Schunack, *Curr Med Chem*, 8 (2001) 1329-1340.
- [174] C.A.G.N. Montalbetti, V. Falque, *Tetrahedron*, 61 (2005) 10827-10852.
- [175] R.J. Bergeron, J.S. McManis, *The Journal of Organic Chemistry*, 53 (1988) 3108-3111.
- [176] R. Baker, J.L. Castro, *Journal of the Chemical Society, Perkin Transactions 1*, (1990) 47-65.
- [177] D. Albanese, F. Corcella, D. Landini, A. Maia, M. Penso, *Journal of the Chemical Society, Perkin Transactions 1*, (1997) 247-250.
- [178] M. Imazawa, F. Eckstein, *The Journal of Organic Chemistry*, 44 (1979) 2039-2041.
- [179] F. Weygand, W. Swodenk, *Chemische Berichte*, 90 (1957) 639-645.
- [180] F. Weygand, E. Frauendorfer, *Chemische Berichte*, 103 (1970) 2437-2449.
- [181] S.B. King, B. Ganem, *Journal of the American Chemical Society*, 116 (1994) 562-570.
- [182] A.M. Calcagno, T.J. Siahaan, *Physiological, Biochemical, and Chemical Barriers to Oral Drug Delivery*, John Wiley & Sons, Inc., 2005.
- [183] N.W. McCracken, P.G. Blain, F.M. Williams, *Biochem Pharmacol*, 46 (1993) 1125-1129.
- [184] N.W. McCracken, P.G. Blain, F.M. Williams, *Chem Biol Interact*, 87 (1993) 183-185.
- [185] N.W. McCracken, P.G. Blain, F.M. Williams, *Biochem Pharmacol*, 45 (1993) 31-36.
- [186] T. Satoh, P. Taylor, W.F. Bosron, S.P. Sanghani, M. Hosokawa, B.N. La Du, *Drug Metab Dispos*, 30 (2002) 488-493.
- [187] P. Artursson, K. Palm, K. Luthman, *Advanced Drug Delivery Reviews*, 22 (1996) 67-84.
- [188] S. Rendic, *Drug Metab Rev*, 34 (2002) 83-448.
- [189] T. Shimada, H. Yamazaki, M. Mimura, Y. Inui, F.P. Guengerich, *J Pharmacol Exp Ther*, 270 (1994) 414-423.
- [190] F.P. Guengerich, *Chem Res Toxicol*, 14 (2001) 611-650.
- [191] C. Ju, J.P. Uetrecht, *Curr Drug Metab*, 3 (2002) 367-377.
- [192] G. Fricker, J. Drewe, *J Pept Sci*, 2 (1996) 195-211.
- [193] K. Sugano, M. Kansy, P. Artursson, A. Avdeef, S. Bendels, L. Di, G.F. Ecker, B. Faller, H. Fischer, G.g. Gerebtzoff, H. Lennernaes, F. Senner, *Nat Rev Drug Discov*, 9 (2010) 597-614.
- [194] J.T. Goodwin, R.A. Conradi, N.F. Ho, P.S. Burton, *J Med Chem*, 44 (2001) 3721-3729.

- [195] G.M. Pauletti, F.W. Okumu, R.T. Borchardt, *Pharm Res*, 14 (1997) 164-168.
- [196] N.J. Proctor, G.T. Tucker, A. Rostami-Hodjegan, *Xenobiotica*, 34 (2004) 151-178.
- [197] T.D. Bjornsson, J.T. Callaghan, H.J. Einolf, V. Fischer, L. Gan, S. Grimm, J. Kao, S.P. King, G. Miwa, L. Ni, G. Kumar, J. McLeod, R.S. Obach, S. Roberts, A. Roe, A. Shah, F. Snikeris, J.T. Sullivan, D. Tweedie, J.M. Vega, J. Walsh, S.A. Wrighton, *Drug Metab Dispos*, 31 (2003) 815-832.
- [198] T.D. Bjornsson, J.T. Callaghan, H.J. Einolf, V. Fischer, L. Gan, S. Grimm, J. Kao, S.P. King, G. Miwa, L. Ni, G. Kumar, J. McLeod, S.R. Obach, S. Roberts, A. Roe, A. Shah, F. Snikeris, J.T. Sullivan, D. Tweedie, J.M. Vega, J. Walsh, S.A. Wrighton, *J Clin Pharmacol*, 43 (2003) 443-469.
- [199] E.B. Nelson, P.P. Raj, K.J. Belfi, B.S. Masters, *J Pharmacol Exp Ther*, 178 (1971) 580-588.
- [200] A. Guillouzo, F. Morel, O. Fardel, B. Meunier, *Toxicology*, 82 (1993) 209-219.
- [201] S. Thohan, M.C. Zurich, H. Chung, M. Weiner, A.S. Kane, G.M. Rosen, *Drug Metabolism and Disposition*, 29 (2001) 1337-1342.
- [202] P. Wright, C. Chassaing, N. Cussans, D. Gibson, C. Green, M. Gleave, R. Jones, P. Macrae, K. Saunders, *Biomed Chromatogr*, 20 (2006) 585-596.
- [203] X. Li, G. Jiang, C. Luo, F. Xu, Y. Wang, L. Ding, C.-F. Ding, *Analytical Chemistry*, 81 (2009) 4840-4846.
- [204] A.C. Li, W.Z. Shou, T.T. Mai, X.y. Jiang, *Rapid Communications in Mass Spectrometry*, 21 (2007) 4001-4008.
- [205] S.A. Wring, I.S. Silver, C.J. Serabjit-Singh, *Methods Enzymol*, 357 (2002) 285-295.
- [206] A. Tolonen, M. Turpeinen, O. Pelkonen, *Drug Discov Today*, 14 (2009) 120-133.
- [207] H. Keski-Hynnily, M. Kurkela, E. Elovaara, L. Antonio, J. Magdalou, L. Luukkanen, J. Taskinen, R. Kostianen, *Anal Chem*, 74 (2002) 3449-3457.
- [208] K.C. Saunders, *Drug Discovery Today: Technologies*, 1 (2004) 373-380.
- [209] K.M. Jenkins, R. Angeles, M.T. Quintos, R. Xu, D.B. Kassel, R.A. Rourick, *Journal of Pharmaceutical and Biomedical Analysis*, 34 (2004) 989-1004.
- [210] R.R. Burgess, *Methods Enzymol*, 463 (2009) 331-342.
- [211] R.B. Walker, V.N. Dholakia, K.L. Brasfield, R. Bakhtiar, *Gen Pharmacol*, 30 (1998) 725-731.
- [212] R. Bakhtiar, R.B. Walker, V.N. Dholakia, *Rapid Commun Mass Spectrom*, 12 (1998) 1417-1418.
- [213] I.H. Pitman, *Medicinal Research Reviews*, 1 (1981) 189-214.
- [214] A.J. Repta, J.P. Patel, *International Journal of Pharmaceutics*, 10 (1982) 29-42.
- [215] A.J. Repta, M.J. Hageman, J.P. Patel, *International Journal of Pharmaceutics*, 10 (1982) 239-248.

- [216] G.E. Torres, R.R. Gainetdinov, M.G. Caron, *Nat Rev Neurosci*, 4 (2003) 13-25.
- [217] P. Artursson, J. Karlsson, *Biochemical and Biophysical Research Communications*, 175 (1991) 880-885.
- [218] I. Hubatsch, E.G. Ragnarsson, P. Artursson, *Nat Protoc*, 2 (2007) 2111-2119.
- [219] J.D. Irvine, L. Takahashi, K. Lockhart, J. Cheong, J.W. Tolan, H.E. Selick, J.R. Grove, *J Pharm Sci*, 88 (1999) 28-33.
- [220] P.K. Bhadra, G.A. Morris, J. Barber, *J Med Chem*, 48 (2005) 3878-3884.
- [221] A. Galli, L.J. DeFelice, B.J. Duke, K.R. Moore, R.D. Blakely, *J Exp Biol*, 198 (1995) 2197-2212.
- [222] B. Giros, M.G. Caron, *Trends Pharmacol Sci*, 14 (1993) 43-49.
- [223] H. Gu, S.C. Wall, G. Rudnick, *J Biol Chem*, 269 (1994) 7124-7130.
- [224] G.R. Luthin, B.B. Wolfe, *J Pharmacol Exp Ther*, 228 (1984) 648-655.
- [225] M.I. Davila-Garcia, J.L. Musachio, D.C. Perry, Y. Xiao, A. Horti, E.D. London, R.F. Dannals, K.J. Kellar, *J Pharmacol Exp Ther*, 282 (1997) 445-451.
- [226] P. Whiteaker, M. Jimenez, J.M. McIntosh, A.C. Collins, M.J. Marks, *Br J Pharmacol*, 131 (2000) 729-739.
- [227] L.P. Shearman, A.M. McReynolds, F.C. Zhou, J.S. Meyer, *Am J Physiol*, 275 (1998) C1621-1629.
- [228] W.A. Wolf, D.M. Kuhn, *J Biol Chem*, 267 (1992) 20820-20825.
- [229] A.R. Davies, D.J. Hardick, I.S. Blagbrough, B.V. Potter, A.J. Wolstenholme, S. Wonnacott, *Neuropharmacology*, 38 (1999) 679-690.
- [230] R.J. Lukas, *J Neurochem*, 46 (1986) 1936-1941.
- [231] S.M. Sine, *J Biol Chem*, 263 (1988) 18052-18062.
- [232] L.A. Pabreza, S. Dhawan, K.J. Kellar, *Mol Pharmacol*, 39 (1991) 9-12.
- [233] J.W. Jefferson, J.F. Pradko, K.T. Muir, *Clin Ther*, 27 (2005) 1685-1695.
- [234] A. Petsalo, M. Turpeinen, A. Tolonen, *Rapid Commun Mass Spectrom*, 21 (2007) 2547-2554.
- [235] K.K. Loboz, A.S. Gross, J. Ray, A.J. McLachlan, *Journal of Chromatography B*, 823 (2005) 115-121.
- [236] J.J. Stewart, H.J. Berkel, R.C. Parish, M.R. Simar, A. Syed, J.A. Bocchini, Jr., J.T. Wilson, J.E. Manno, *J Clin Pharmacol*, 41 (2001) 770-778.
- [237] V. Borges, E. Yang, J. Dunn, J. Henion, *Journal of Chromatography B*, 804 (2004) 277-287.
- [238] R. Coles, E.D. Kharasch, *Journal of Chromatography B*, 857 (2007) 67-75.
- [239] S. Giegold, M. Holzhauser, T. Kiffmeyer, J. Tuerk, T. Teutenberg, M. Rosenhagen, D. Hennies, T. Hoppe-Tichy, B. Wenclawiak, *Journal of Pharmaceutical and Biomedical Analysis*, 46 (2008) 625-630.

- [240] R.F. Suckow, T.M. Smith, A.S. Perumal, T.B. Cooper, *Drug Metab Dispos*, 14 (1986) 692-697.
- [241] P.K. Kiptoo, K.S. Paudel, D.C. Hammell, M.O. Hamad, P.A. Crooks, A.L. Stinchcomb, *Eur J Pharm Sci*, 33 (2008) 371-379.
- [242] P.K. Kiptoo, K.S. Paudel, D.C. Hammell, R.R. Pinninti, J. Chen, P.A. Crooks, A.L. Stinchcomb, *J Pharm Sci*, 98 (2009) 583-594.
- [243] T.B. Cooper, R.F. Suckow, A. Glassman, *J Pharm Sci*, 73 (1984) 1104-1107.
- [244] R. Ravichandran, *United States Pharmacopeia*, Current (2010).
- [245] R.F. Butz, D.H. Schroeder, R.M. Welch, N.B. Mehta, A.P. Phillips, J.W. Findlay, *J Pharmacol Exp Ther*, 217 (1981) 602-610.
- [246] R.F. Butz, R.M. Welch, J.W. Findlay, *J Pharmacol Exp Ther*, 221 (1982) 676-685.
- [247] Y. Kitada, T. Miyauchi, A. Satoh, S. Satoh, *Eur J Pharmacol*, 72 (1981) 145-152.
- [248] L. Steru, R. Chermat, B. Thierry, P. Simon, *Psychopharmacology (Berl)*, 85 (1985) 367-370.
- [249] K. Pritchett, G.B. Mulder, *Contemp Top Lab Anim Sci*, 42 (2003) 49.
- [250] S. Montgomery, T. Hansen, S. Kasper, *Int J Neuropsychopharmacol*, (2010) 1-8.
- [251] A. Mork, M. Kreilgaard, C. Sanchez, *Neuropharmacology*, 45 (2003) 167-173.
- [252] C. Sanchez, P. Gruca, E. Bien, M. Papp, *Pharmacol Biochem Behav*, 75 (2003) 903-907.
- [253] C. Sanchez, P. Gruca, M. Papp, *Behav Pharmacol*, 14 (2003) 465-470.
- [254] C. Sanchez, M. Kreilgaard, *Pharmacol Biochem Behav*, 77 (2004) 391-398.
- [255] S. Storustovu, C. Sanchez, P. Porzgen, L.T. Brennum, A.K. Larsen, M. Pulis, B. Ebert, *Br J Pharmacol*, 142 (2004) 172-180.
- [256] M.G.P. Dedhiya, NY, US), Chhettry, Anil (Holtsville, NY, US), Mani, Narasimhan (Morris Plains, NJ, US), in, *Forest Laboratories, Inc. (New York, NY, US), United States*, 2007.
- [257] B. Beer, J. Stark, P. Krieter, P. Czobor, G. Beer, A. Lippa, P. Skolnick, *J Clin Pharmacol*, 44 (2004) 1360-1367.
- [258] M.E. Breuer, J.S. Chan, R.S. Oosting, L. Groenink, S.M. Korte, U. Campbell, R. Schreiber, T. Hanania, E.M. Snoeren, M. Waldinger, B. Olivier, *Eur Neuropsychopharmacol*, 18 (2008) 908-916.
- [259] B.J. Caldarone, N.E. Paterson, J. Zhou, D. Brunner, A.P. Kozikowski, K.G. Westphal, G.A. Korte-Bouws, J. Prins, S.M. Korte, B. Olivier, A. Ghavami, *J Pharmacol Exp Ther*, (2010).
- [260] R.A. Hauser, L. Salin, N. Juhel, V.L. Konyago, *Mov Disord*, 22 (2007) 359-365.
- [261] Y. Liang, A.M. Shaw, M. Boules, S. Briody, J. Robinson, A. Oliveros, E. Blazar, K. Williams, Y. Zhang, P.R. Carlier, E. Richelson, *J Pharmacol Exp Ther*, 327 (2008) 573-583.

- [262] F. Micheli, P. Cavanni, D. Andreotti, R. Arban, R. Benedetti, B. Bertani, M. Bettati, L. Bettelini, G. Bonanomi, S. Braggio, R. Carletti, A. Checchia, M. Corsi, E. Fazzolari, S. Fontana, C. Marchioro, E. Merlo-Pich, M. Negri, B. Oliosi, E. Ratti, K.D. Read, M. Roscic, I. Sartori, S. Spada, G. Tedesco, L. Tarsi, S. Terreni, F. Visentini, A. Zocchi, L. Zonzini, R. Di Fabio, *J Med Chem*, 53 (2010) 4989-5001.
- [263] N.E. Paterson, F. Balci, U. Campbell, B.E. Olivier, T. Hanania, *J Psychopharmacol*, (2010).
- [264] J. Prins, D.A. Denys, K.G. Westphal, G.A. Korte-Bouws, M.S. Quinton, R. Schreiber, L. Groenink, B. Olivier, S.M. Korte, *Eur J Pharmacol*, 633 (2010) 55-61.
- [265] P. Skolnick, P. Krieter, J. Tizzano, A. Basile, P. Popik, P. Czobor, A. Lippa, *CNS Drug Rev*, 12 (2006) 123-134.
- [266] P. Skolnick, P. Popik, A. Janowsky, B. Beer, A.S. Lippa, *Eur J Pharmacol*, 461 (2003) 99-104.
- [267] L.M. Hesse, K. Venkatakrishnan, M.H. Court, L.L. von Moltke, S.X. Duan, R.I. Shader, D.J. Greenblatt, *Drug Metab Dispos*, 28 (2000) 1176-1183.
- [268] J.O. Ebbert, I.T. Croghan, A. Sood, D.R. Schroeder, J.T. Hays, R.D. Hurt, *Nicotine Tob Res*, 11 (2009) 234-239.
- [269] T. Lancaster, L.F. Stead, *Cochrane Database Syst Rev*, (2000) CD001009.
- [270] R.E. Vann, J.A. Rosecrans, J.R. James, S.D. Philibin, S.E. Robinson, *Brain Res*, 1117 (2006) 18-24.
- [271] S. Kane, E.L. Altschuler, R.E. Kast, *Gastroenterology*, 125 (2003) 1290.
- [272] E. Bayerdorffer, H. Bock, *Leber Magen Darm*, 18 (1988) 104-113.
- [273] W.E. Fleig, *Med Klin (Munich)*, 94 Suppl 1 (1999) 22-25.
- [274] W. Kruis, *Z Gastroenterol Verh*, 26 (1991) 154-156.
- [275] K. Otake, K. Uchida, M. Inoue, Y. Ohkita, T. Araki, C. Miki, M. Kusunoki, *J Pediatr Gastroenterol Nutr*, 44 (2007) 378-381.
- [276] Y. Moriwaki, T. Yamamoto, S. Takahashi, Z. Tsutsumi, T. Hada, *Histol Histopathol*, 16 (2001) 745-753.
- [277] D.C. Pryde, D. Dalvie, Q. Hu, P. Jones, R.S. Obach, T.-D. Tran, *Journal of Medicinal Chemistry*, (2010) null-null.
- [278] S.S. Dhaneshwar, N. Gairola, M. Kandpal, L. Bhatt, G. Vadnerkar, S.S. Kadam, *Bioorg Med Chem Lett*, 17 (2007) 1897-1902.
- [279] S.S. Dhaneshwar, N. Gairola, M. Kandpal, G. Vadnerkar, L. Bhatt, *Bioorg Med Chem*, 15 (2007) 4903-4909.
- [280] S.S. Dhaneshwar, M. Kandpal, G. Vadnerkar, B. Rathi, S.S. Kadam, *Eur J Med Chem*, 42 (2007) 885-890.

- [281] Y. Jung, H.H. Kim, H. Kim, H. Kong, B. Choi, Y. Yang, Y. Kim, *Eur J Pharm Sci*, 28 (2006) 26-33.
- [282] Y.J. Jung, H.H. Kim, H.S. Kong, Y.M. Kim, *Arch Pharm Res*, 26 (2003) 264-269.
- [283] Y.J. Jung, J.S. Lee, H.H. Kim, Y.T. Kim, Y.M. Kim, *Arch Pharm Res*, 21 (1998) 179-186.
- [284] Y.J. Jung, J.S. Lee, Y.M. Kim, *J Pharm Sci*, 89 (2000) 594-602.
- [285] H. Kim, J. Huh, H. Jeon, D. Choi, J. Han, Y. Kim, Y. Jung, *J Pharm Sci*, 98 (2009) 159-168.
- [286] T. Yamaguchi, K. Sasaki, Y. Kurosaki, T. Nakayama, T. Kimura, *J Drug Target*, 2 (1994) 123-131.
- [287] T.R. Berigan, E.A. Deagle, 3rd, *JAMA*, 281 (1999) 233.
- [288] D.H. Han, J.W. Hwang, P.F. Renshaw, *Exp Clin Psychopharmacol*, 18 (2010) 297-304.
- [289] S. McNamara, S. Stokes, N. Coleman, *Ir Med J*, 103 (2010) 134, 136-137.
- [290] J.D. Griffith, J. Carranza, C. Griffith, L.L. Miller, *J Clin Psychiatry*, 44 (1983) 206-208.

7 Appendices

7.1 *The aqueous stability of bupropion (Publication)*

7.2 *Isosorbide-based aspirin prodrugs: integration of nitric oxide releasing groups (Publication)*

7.3 *Bupropion pharmacology*

7.4 *N-methyl bupropion pharmacology*

7.5 *Bupropion and N-methyl bupropion pharmacology (nAChR subtypes)*



ELSEVIER

Contents lists available at ScienceDirect

Journal of Pharmaceutical and Biomedical Analysis

journal homepage: www.elsevier.com/locate/jpba

The aqueous stability of bupropion

Paul M. O'Byrne*, Robert Williams, John J. Walsh, John F. Gilmer

School of Pharmacy and Pharmaceutical Sciences, Trinity College, Dublin 2, Ireland

ARTICLE INFO

Article history:

Received 23 January 2010

Received in revised form 19 April 2010

Accepted 21 April 2010

Available online 4 May 2010

Keywords:

Bupropion

Aqueous

Stability

pH

Kinetics

Hydrolysis

ABSTRACT

In this study the aqueous stability of bupropion was determined and the pH-degradation profile was obtained. The effects of hydrogen ion, solvent and hydroxide ion concentration are discussed with particular emphasis on the kinetics of degradation of bupropion. Kinetics and degradation of bupropion were determined by HPLC-UV and LC-MS analysis both utilising high pH chromatographic methods. Degradation of bupropion in aqueous solutions follows first-order reaction kinetics. The pH-degradation profile was determined using non-linear regression analysis. The micro- and macro-reaction constants for degradation are presented. Bupropion was most stable in aqueous solutions below pH 5. Degradation was catalyzed by water but mainly by hydroxide ion on the unionised form of bupropion. The energy of activation for decomposition in aqueous solution pH 10.7 $I = 0.055$ was determined to be 53 kJ mol^{-1} with a frequency factor of $6.43 \times 10^{10} \text{ s}^{-1}$. The degradants of bupropion were positively identified and a mechanism of degradation is proposed. The inherent instability of bupropion above pH 5 has implications for its therapeutic use, formulation, pharmacokinetics and use during analysis and storage.

© 2010 Elsevier B.V. All rights reserved.

1. Introduction

Bupropion was first patented in 1974 [1] and released onto the world market in 1985. It was briefly withdrawn due to seizures incidence but reintroduced in 1989 after the daily recommended dose was reduced to lower seizure likelihood. Bupropion is a dopamine and norepinephrine reuptake inhibitor [2]. It is about twice as potent an inhibitor of dopamine reuptake than of norepinephrine reuptake.

Bupropion has numerous therapeutic indications including, depression [3], smoking cessation [4], sexual dysfunction [5], obesity [6], attention deficit hyperactivity disorder [7] and seasonal affective disorder [8]. It has recently been shown to have anti-inflammatory properties [9]. In 2007 it was the fourth-most prescribed antidepressant in the USA. While there has been little published in peer reviewed journals, it is widely acknowledged that bupropion presents serious stability problems in manufacturing, formulation and use. This is partly reflected in the numerous patents directed at methods to improve the stability of bupropion formulations.

Abbreviations: HPLC-UV, high performance liquid chromatography with ultra-violet spectrophotometric detection; LC-MS, liquid chromatography with mass spectrometric detection; pH, $\log[\text{H}^+]$; pK_a , $\log[K_a]$; K_a , acid dissociation constant; ESI, electrospray ionisation; SIM, selected ion monitoring; USP, United States pharmacopoeia; CE, carboxylesterase; TMPT, thiopurine methyltransferase; I , ionic strength; RSD, relative standard deviation.

* Corresponding author. Tel.: +353 1 896 2794; fax: +353 1 896 2793.

E-mail address: obyrne@tcd.ie (P.M. O'Byrne).

One method to improve the stability of bupropion in oral formulations involves addition of a stabilizer to the formulation, in this case cysteine or glycine hydrochloride which acts to buffer the formulation at a pH between 0.9 and 4.0 [10]. Other stabilizers used to improve the stability of bupropion in tablet formulations are organic acid [11], inorganic acids [12] and salts of organic bases [13].

Pharmaceutical compositions for transdermal administration containing fatty acid salts of bupropion free base and metabolites have also been developed [14]. The salt form of bupropion is more stable than the freebase.

The levels of moisture are evidently critical in controlling degradation during processing. Chawla et al. developed a dry granulation process for tableting of bupropion, avoiding the use of stabilizers [15]. Indeed, an inclusion complex of bupropion hydrochloride with beta-cyclodextrin that stabilizes bupropion hydrochloride against degradation has been developed by Gidwani et al. [16].

Other physical methods have been developed to trap bupropion inside a moisture barrier within an oral tablet formulation. These usually involve polymer coatings around the tablet or sometimes polymer microspheres within the tablet. These formulations create dry micro-environments within the tablet matrix limiting access between bupropion and its outside environment. Stabilized bupropion hydrochloride pharmaceutical compositions are described that are free of acid additives and provide for a sustained release of bupropion hydrochloride [17]. The particulate bupropion hydrochloride is coated with a polymer membrane coating.

Bupropion half-life in plasma stored at 22 and 37 °C was 54.2 and 11.4 h, respectively. It was only shown to be stable at pH 2.5 [18].

Another study on the chemical stability of bupropion in isotonic pH 7.4 at 32 °C over two weeks showed that its disappearance follows first-order kinetics [19].

The stability of bupropion in formalin has been studied and it was shown that at lower pH, bupropion is most stable; at higher pH, bupropion is converted into *N*-methyl bupropion [20]. Compounds with similar structure to bupropion, i.e. diethylpropion have shown similar degradation characteristics. Hydrolytic decomposition of diethylpropion in solution at 45 °C occurred at a very slow and constant rate at pH 3.5 and below but increased rapidly as the pH was raised above 3.5 [21].

The formulation, stabilisation and use of bupropion is therefore an active area of pharmaceutical research. There is currently no injectable delivery vehicle for bupropion in clinical use and its absolute oral bioavailability in humans has not been reported. Against this background and in the context of its expanding therapeutic uses this paper reports on the kinetics of degradation of bupropion in aqueous solution including routes of degradation and influence of parameters such as ionic strength and buffer identity.

2. Materials and methods

2.1. Chemicals

Methanol, acetonitrile and water were supplied by Fisher Scientific Ireland (LC–MS grade). Ammonium hydroxide solution (30% as NH₃), glacial acetic acid, formic acid, boric acid, citric acid monohydrate, sodium chloride and tripotassium phosphate were supplied by Sigma–Aldrich Ireland (reagent grade). Bupropion hydrobromide and related degradants were supplied as a gift from Biovail Technologies Ireland Ltd.

2.2. Instrumentation

A stability indicating HPLC–UV assay was used to monitor degradants of bupropion. The HPLC system consisted of a Waters Alliance 2695 separations module connected to a Waters 2996 Photodiode Array detector. The column was a Waters XBridge C18 250 mm × 4.6 mm, 5 μm fitted with a Waters XBridge C18 guard column heated at 50 °C. Mobile phase A was pH 10.0 ammonium acetate buffer (1.27 M)/water/acetonitrile, 10:80:10, mobile phase B was pH 10.0 ammonium acetate buffer (1.27 M)/water/acetonitrile, 10:20:70. Injection volume was 20 μL, flow rate 1.5 mL/min. Gradient; 0–42% B over 5 min, hold for 10 min, 42–100% B over 10 min, hold for 5 min and equilibrate to starting gradient. The retention time of bupropion standard was approximately 23 min. Detection wavelength 239 nm. This method was demonstrated to be linear over a working range of 0.01–0.50 mg/mL bupropion hydrobromide.

Degradation kinetics and mass spectrometric measurements were carried out on a Thermo Accela Liquid chromatograph. The detector was a Thermo LTQ–XL–Orbitrap Discovery mass spectrometer. The column used for chromatographic separation was a Waters Xbridge C18, 2.1 mm × 50 mm 2.5 μm at 20 °C. Mobile Phase A: 10:40:50, 0.5% Ammonium hydroxide solution in water, adjusted to pH 10.0 with formic acid; water: methanol. Mobile Phase B: 10:90, 0.5% Ammonium hydroxide solution in water, adjusted pH 10.0 with formic acid; methanol. Flow rate: 100 μL/min, Injection volume: 10 μL, run time: 15 min. Gradient, 0% B to 100% B over 8.00 min, hold until 12.00 min. 0% B at 12.01 min and equilibrate for 3 min. This method was validated as appropriate according to ICHQ2R and demonstrated to be linear over a working range of 1–250 ng/mL bupropion.

The LTQ–XL ion trap mass spectrometer was coupled to the Accela LC system via an electrospray ionization (ESI) probe. The

capillary temperature was maintained at 400 °C, sheath gas flow rate 50 arbitrary units, auxiliary gas flow rate 5 arbitrary unit sweep gas flow rate 0 arbitrary units, source voltage 3.20 kV, source current 100 μA, capillary voltage 43.00 V and tube lens 100 V.

Bupropion was detected in positive ion mode using selected ion monitoring (SIM). Bupropion SIM 184, (M+H)⁺ = 240, retention time = 9.4 min. The optimum detector conditions were found by tuning the instrument to the highest sensitivity for bupropion molecular ion at 184 (m/z).

2.3. Determination of rate constant

The observed first-order degradation rate constants, k_{obs} , were calculated from the slopes of the natural-logarithmic plots of the drug fraction remaining versus time in accordance with Eq. (1):

$$\ln\left(\frac{C_t}{C_0}\right) = -k_{obs}t \quad (1)$$

where C_0 was the initial concentration and C_t was the remaining concentration of bupropion at time t . Solutions were monitored for two weeks and stored protected from light.

2.4. pH-degradation profile

Bupropion solutions were prepared at a concentration of 250 ng/mL in aqueous buffers from a 1 mg/mL methanol stock solution. The final concentration of methanol in the buffered solution was approximately 1%. Buffers over the pH range of 2–13 were prepared by mixing two stock buffered solutions to give solution of different pH but equal ionic strength. This buffer system was adapted from a previously described universal buffer system by Carmody.

Stock buffer A: boric acid 0.2 M, citric acid 0.05 M, NaCl 0.594 M, $I = 0.6$. Stock buffer B: tripotassium phosphate 0.1 M, $I = 0.6$.

For example, to prepare a solution of pH ~ 7.2 with an $I = 0.05$, add 0.5 mL solution A and 0.5 mL solution B to 10 mL deionised H₂O. Buffered solutions at the lowest and highest pH were prepared with 0.055 M HCl pH 2.0 and 0.055 M NaOH pH 13.1. Solution pH was measured at room temperature 20 ± 1 °C using a Radiometer Copenhagen PHM61 laboratory pH meter. The pH meter was calibrated before use with standard buffers, 4.0, 7.0 and 10.0. Solutions were incubated either in a digital oven (for long term storage) or in the Accela LC system autosampler (for short term). Aliquots were taken at appropriate times depending on the decomposition rate and analyzed immediately for remaining bupropion. Buffer concentrations throughout the study were low. However the effect of buffer concentration on rate was evaluated at kinetically and mechanistically distinguishable phases of the resulting pH–rate profile. Dilution did not affect degradation rate using the universal buffer system and therefore we did not extrapolate to zero buffer.

2.5. Effects of temperature and buffer on the stability of bupropion

The effect of temperature on the rate of bupropion degradation was determined at pH 10.7. Bupropion solutions were prepared in the appropriate buffers as described in Section 2.4, and incubated at 40, 46, 54 and 60 °C. Aliquots were taken at appropriate time depending on the decomposition rate and analyzed immediately for bupropion. The observed first-order degradation rate constants, k_{obs} were calculated using Eq. (1). The Arrhenius factor A , and activation energy E_a for bupropion degradation were determined from a plot of $\ln(k_{obs})$ against $1/T$ (K) according to Eq. (2) using least

Table 1
Rate constants determined for the degradation of bupropion.

Temperature (K)	313	323	333
Ionic strength	0.055	0.12	0.055
pH _{RT}	<i>k</i> _{obs} (h ⁻¹)		
5.1	0.002	0.001	0.004
6.3	0.003	0.002	0.008
7.4	0.004	0.004	0.019
8.3	0.006	0.017	0.035
9.4	0.012	N/D	0.051
10.7	0.018	0.052	0.055
11.9	0.034	0.072	0.101
12.3	0.042	0.114	0.166
13.0	0.102	N/D	0.407

squares regression:

$$\ln k_{\text{obs}} = \ln A - \frac{E_a}{RT} \quad (2)$$

where *R* is the universal gas constant and *T* the absolute temperature (K).

Buffer catalysis was investigated by monitoring the amount of bupropion degradation in three different buffers pH 7.4 at 60 °C, ionic strength 0.055, 0.275 and 0.55 using the universal buffer system described in Table 1. From the slope of plots of $\ln[C_t/C_0]$ versus time, the rate constant was calculated. A plot of rate constants versus buffer concentration gave a straight line of which extrapolation back to zero gave the buffer-free rate constant.

The effects of different buffers were determined by monitoring the disappearance of bupropion at pH 7.4 at 60 °C in different buffer types with fixed ionic strength, 0.055. Four buffer systems were studied; citrate, phosphate, borate and a TRIS buffer system. Ionic strength was adjusted with NaCl. The slopes of plots of $\ln[C_t/C_0]$ versus time were determined to establish the effect of buffer anion on degradation of bupropion (Fig. 4).

2.6. Liquid chromatography with UV and mass spectrometric detection

Two HPLC systems were used in the study. The LCMS system as described in instrumentation section was used to assay bupropion and determine kinetic data. The HPLC-UV system was used to monitor and determine the degradation pathway of bupropion. The HPLC-UV system was a validated stability indicating assay for bupropion and its degradants. This system was better suited for assay of bupropion degradants as they had good UV absorbances but poor positive electrospray ionisation character. System suitability was determined on the day of use and throughout the analysis by repeat injection of a bupropion standard. The % RSD of area and retention time of repeat injections was not more than 5.0%. Degradant peaks were quantified off bupropion using relative response factors and relative retention times, which were generated during the validation of the stability indicating method using external standards.

3. Results and discussion

3.1. pH-rate profile of bupropion

The disappearance of bupropion in aqueous solution was monitored by HPLC-MS. The degradation in the pH range 2–13 followed apparent first-order rate kinetics. Rate constants from a matrix of different experiments are presented in Table 1, where the temperature, pH and ionic strength have been varied. Rate constants were estimated from the resulting slopes after a plot of $\ln[C_t/C_0]$ versus time (Fig. 1) and the resulting *k*_{obs} values (Table 1) plotted against

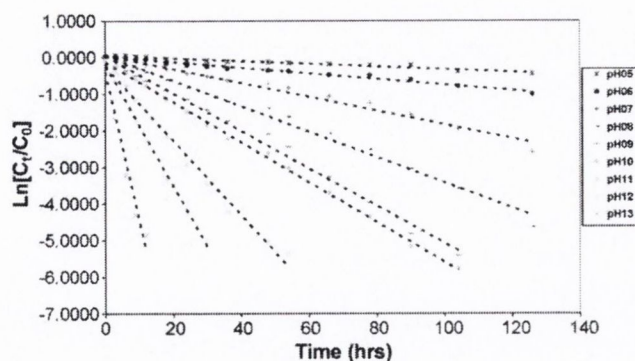


Fig. 1. First-order plots showing the degradation of bupropion at 60 °C in aqueous solution in the pH range 5–13.

pH. The pH-rate profile was fitted using a mechanistic interpretation of pH-rate profiles suggested by Loudon [22]. By analysing the shape of the pH-rate profile a mathematical equation that best describes the degradation can be formulated, Eq. (3):

$$k_{\text{obs}} = c_1[\text{H}^+] + \frac{c_2[\text{H}^+]}{K_a + [\text{H}^+]} + \frac{c_3K_a}{K_a + [\text{H}^+]} + \frac{c_4K_w}{[\text{H}^+]} \quad (3)$$

where *K*_a and *K*_w are the acid dissociation constant for bupropion and water respectively and *c*₁, *c*₂, *c*₃ and *c*₄ are the macro-reaction rate constants of the pH-rate profile. Constants *c*₁ and *c*₄ are kinetically distinguishable and are equal to the specific hydronium catalysed degradation on the protonated form and hydroxide catalysed degradation on the deprotonated form of bupropion respectively. Constants *c*₂ and *c*₃ contain contributions from kinetically indistinguishable micro-reaction rate constants. The macro-reaction rate constants were determined by fitting the *k*_{obs} values with the model and solving the rate equation using non-linear regression analysis. These rate constants are described in Table 2. Bupropion was shown to be stable over the course of the degradation study below pH 5, and therefore the specific hydronium catalysis rate constant *c*₁ is many orders of magnitude lower than *c*₂, *c*₃ and *c*₄. Therefore *c*₁ can be assumed to be zero and Eq. (3) simplifies to Eq. (4):

$$k_{\text{obs}} = \frac{c_2[\text{H}^+]}{K_a + [\text{H}^+]} + \frac{c_3K_a}{K_a + [\text{H}^+]} + \frac{c_4K_w}{[\text{H}^+]} \quad (4)$$

The macro-reaction rate constant *c*₂ combines two micro-reaction rate constants that are kinetically indistinguishable. Empirically these are the contribution of hydronium catalysed degradation on the deprotonated form of bupropion and solvent catalysed degradation on the protonated form of bupropion.

The macro-reaction rate constant *c*₃ combines two micro-reaction rate constants that are also kinetically indistinguishable. These are the contribution of hydroxide ion catalysis on the protonated form of bupropion and solvent catalysed degradation on the deprotonated form of bupropion. The magnitude of rate constants at 40, 50 and 60 °C follows *c*₄ > *c*₃ > *c*₂ > *c*₁, showing the rate of degradation is strongly influenced not only by hydroxide ion

Table 2

The macro-reaction constants determined by non-linear regression analysis.

	40 °C	60 °C
<i>c</i> ₁	0.0000	0.0000
<i>c</i> ₂	0.0000	0.0041
<i>c</i> ₃	0.0187	0.0596
<i>c</i> ₄	0.2914	0.2224
<i>K</i> _a	1.26 × 10 ⁻⁸	1.26 × 10 ⁻⁸
<i>K</i> _w	2.92 × 10 ⁻¹⁴	1.26 × 10 ⁻¹³

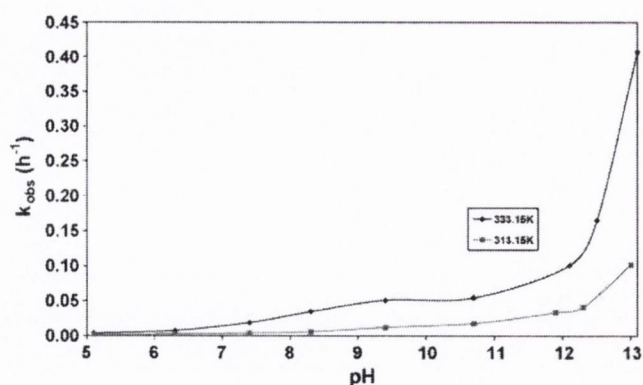


Fig. 2. pH-degradation profile of bupropion at 40 and 60 °C.

concentration but also from solvent catalysed degradation on the deprotonated form of bupropion. Bupropion degradation was not observed at $\text{pH} \leq 5.0$ at 60 °C when it is principally in its protonated form (pK_a 25 °C = 7.9).

Fig. 2 presents the pH-degradation rate profile of bupropion at 40 and 60 °C, ionic strength 0.055. The degradation rate exhibited a marked pH dependence. An inflection point at $\text{pH} 7.9$ corresponds to the bupropion pK_a . At $\text{pH} \geq 11$ there was a significant increase in the rate of disappearance. Degradation of bupropion was markedly hydroxide ion dependent. Non-linear regression analysis of the pH-degradation profile of bupropion is shown in Fig. 3.

3.2. Influence of temperature and buffer concentration on the stability of bupropion

The degradation of bupropion was monitored in the temperature range 40–60 °C at $\text{pH} 10.7$ and ionic strength, 0.055. This pH was chosen as degradation happened at a sufficiently fast rate to enable analysis over a 24 h period. The rate constant for each temperature was calculated from the slope of the first-order degradation profile. When $\ln k$ was plotted against $1/T$ the equation of the line was

$$\ln k = \frac{-6497}{R} \cdot \frac{1}{T} + \ln 16.69,$$

the activation energy E_a for the degradation of bupropion was calculated to be $52.85 \text{ kJ mol}^{-1}$, the frequency factor A , was found to be $1.78 \times 10^7 \text{ h}^{-1}$ or $6.43 \times 10^{10} \text{ s}^{-1}$.

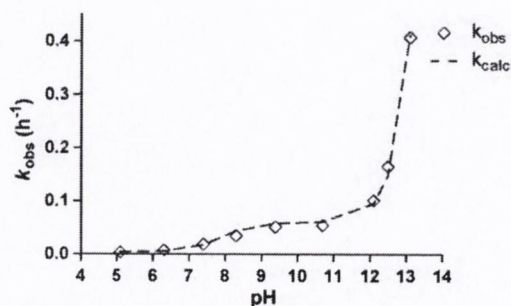


Fig. 3. The pH-degradation profile of bupropion at 60 °C, $I = 0.055$. Macro reaction constants have been calculated by non-linear regression analysis. The fitted line was constructed using Eq. (4) and the data appearing in Tables 1 and 2.

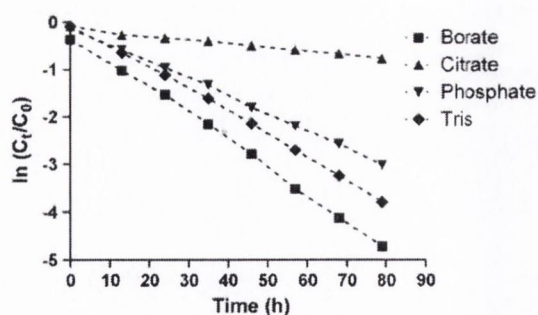


Fig. 4. The effect of different buffer systems on the rate of degradation of bupropion at $\text{pH} 7.4$ 60 °C, $I = 0.055$, adjusted with sodium chloride.

3.3. Identification of bupropion degradants and mechanistic proposal

Degradation products of bupropion were identified by matching the retention time and photo-diode array UV spectra of eluted peaks from degraded samples with those of external standards run under similar conditions (Fig. 6). Four main degradants were identified as **2**, **4**, **3** and **1** (Scheme 1). Bupropion related compounds **1** and **4** are poorly ionized by +ESI due to loss of the amino functionality. These degradants were all seen at $\text{pH} > 5$ but above $\text{pH} 10$ only *m*-chlorobenzoic acid **2** was seen at significant levels. Fig. 6 shows the concentration versus time profiles for bupropion and its degradants at different pH values.

A proposed degradation pathway of bupropion is presented in Scheme 1. The mathematical model that best described the mechanism of degradation follows consecutive and parallel reactions. Degradation of bupropion was strongly pH dependent, and below $\text{pH} 5$ bupropion was protonated and stable. Above $\text{pH} 5$ and approaching its pK_a bupropion becomes increasingly deprotonated and suffers from water catalysed and hydroxide catalysed degradation. This was evident from the pH-rate profile of bupropion. Under these conditions the proposed reaction (Scheme 1) is kinetically possible.

$$\frac{d[\text{bup}]}{dt} = -k_1[\text{bup}] \quad (5)$$

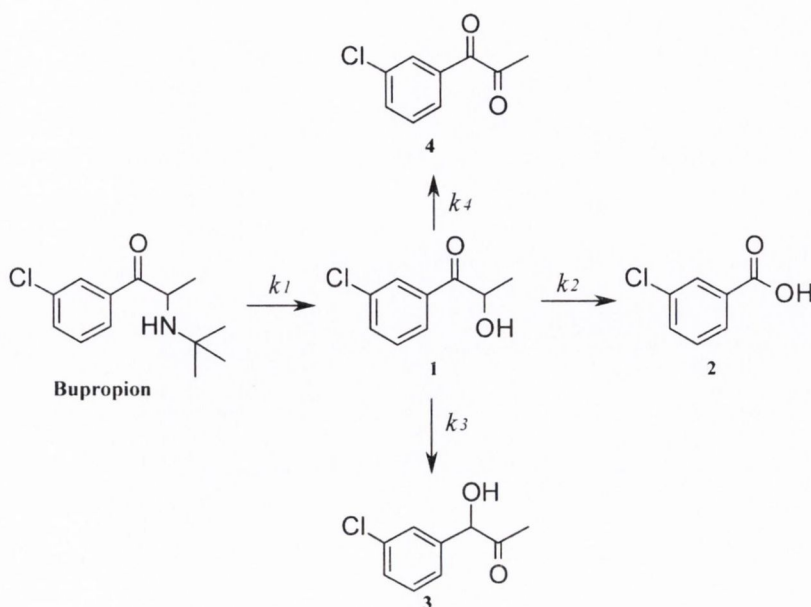
$$[\text{bupropion}] = [\text{bup}]_0 e^{-k_1 t} \quad (6)$$

Bupropion's rate constant of decomposition was calculated by fitting a first-order plot using non-linear regression analysis, Eq. (5). The first product of bupropion degradation at high pH is compound **1** formed from loss of the *t*-butylamine group during hydrolysis. The concentration of **1** during the course of the hydrolysis remains below 1% of the total degradation products of bupropion. The rate of decomposition of **1** was faster than the rate of formation of **1** and therefore can be assumed at steady state throughout the time course of the reaction. The hydrolysis and oxidation products of **1** are the major apparent degradation products of bupropion. These are the two oxidation products, **2** and **4** and the tautomeric pair **3** and **1**. Eqs. (7)–(9) were used to calculate the rate constants of these parallel reactions. The experimental data fitted with these equations using non-linear regression analysis allowed calculation of the rate constants.

$$[2] = [2]_0 + \frac{[\text{bup}]_0 k_2 (1 - e^{-k_1 t})}{k_1} \quad (7)$$

$$[3] = [3]_0 + \frac{[\text{bup}]_0 k_3 (1 - e^{-k_1 t})}{k_1} \quad (8)$$

$$[4] = [4]_0 + \frac{[\text{bup}]_0 k_4 (1 - e^{-k_1 t})}{k_1} \quad (9)$$



Scheme 1. Proposed pathway for base catalyzed degradation of bupropion in aqueous solution. **1** = 1-(3-chlorophenyl)-2-hydroxy-1-propanone, **2** = 3-chlorobenzoic acid, **3** = 1-(3-chlorophenyl)-1-hydroxy-2-propanone, **4** = 1-(3-chlorophenyl)-1,2-propanedione.

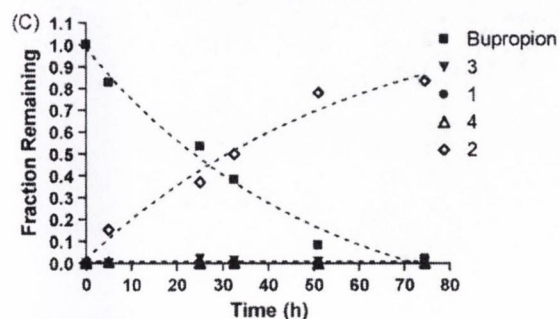
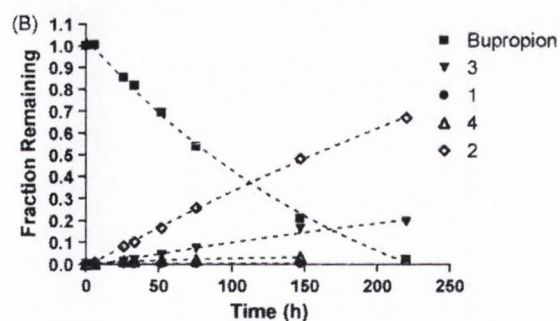
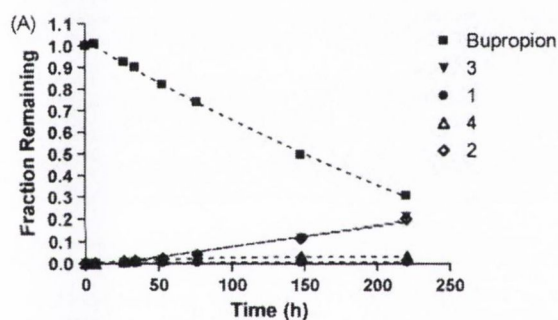


Fig. 5. The time course profile for degradation of bupropion at (A) pH 7.6, (B) pH 8.7 and (C) pH 10.9, 50 °C, $I=0.12$.

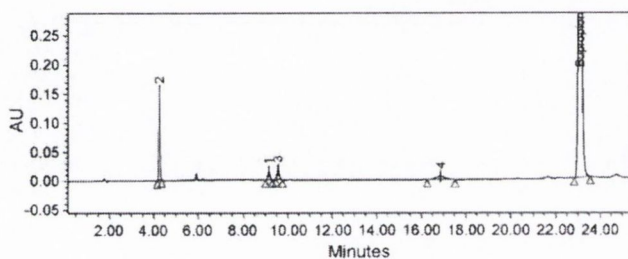


Fig. 6. A typical LC-UV chromatogram of bupropion hydrolysis at pH 8.7, 50 °C, $I=0.12$, $T=144$ h. **1** = 1-(3-chlorophenyl)-2-hydroxy-1-propanone, **2** = 3-chlorobenzoic acid, **3** = 1-(3-chlorophenyl)-1-hydroxy-2-propanone, **4** = 1-(3-chlorophenyl)-1,2-propanedione.

The rate constants calculated at pH 8.7, 50 °C, $I=0.12$ were 0.0050, 0.0045, 0.00138 and 0.00023 h^{-1} for k_1 , k_2 , k_3 and k_4 , respectively (Fig. 7).

The rate constants calculated at pH 7.6, 50 °C, $I=0.12$ were 0.0046, 0.0012, 0.0012 and 0.00028 h^{-1} for k_1 , k_2 , k_3 and k_4 , respectively.

The loss of the amino functionality during degradation is likely to render the degradants neuropharmacologically inactive. The

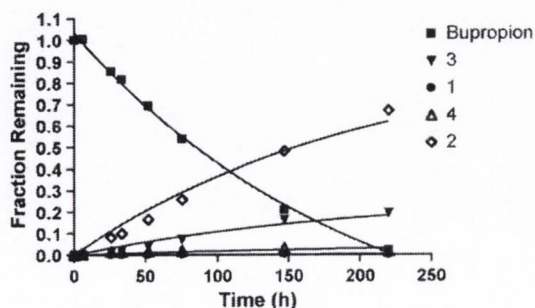


Fig. 7. Data at pH 8.7, 50 °C, $I=0.12$. The solid lines were constructed using Eqs. (5)–(9) with the calculated k_{obs} values.

most polar and prominent degradant **2**, is likely the least problematic as this compound is reported to be easily metabolized and excreted in the urine as *m*-chlorohippuric acid [23]. However, high levels of **2** have been reported to inhibit thiopurine methyltransferase (TMPT) [24]. TMPT is best known for its role in the metabolism of the thiopurine drugs such as azathioprine, 6-mercaptopurine and 6-thioguanine.

Toxicological and pharmacological data on degradants **1**, **3** and the diketone **4** is absent. The latter is likely to be chemically active towards formulation components and in vivo towards proteins such as carboxylesterases (CEs) [25]. CE's are involved in the detoxification of xenobiotics in both prokaryotes and eukaryotes. Bupropion is rapidly and extensively metabolised in vivo. Its metabolites contribute significantly to its pharmacological and toxicological profile. The rate data at pH 7.4 do not indicate that its chemical reactivity in vivo is likely to affect its profile.

4. Conclusion

Bupropion undergoes degradation in aqueous solution in a pH dependent manner. Its most prominent degradation pathway involves hydroxide ion catalysis of the free base form. Degradation involves loss of the *t*-butylamino group and the degradants are therefore likely to be neuropharmacologically inactive. The effect of ionic strength, buffer type and temperature on the kinetics was also characterised.

The poor stability profile of bupropion above pH 5 has implications for its formulation in drug delivery systems, its distribution in vivo and its analysis and storage in assay systems. The data shows that careful buffering below pH 5 during processing and formulation is needed in order to have the most stable product containing bupropion. There is also a need during sample preparation and storage to consider appropriate solvents and buffers which again keep the pH low.

Acknowledgement

The authors wish to acknowledge funding and support from Biovail Corporation.

References

- [1] N.B. Mehta, Meta chloro substituted- α -butylaminopropiophenones, United States Patent 3,819,796 (1974).
- [2] S.M. Stahl, J.F. Pradko, B.R. Haight, J.G. Modell, C.B. Rockett, S. Learned-Coughlin, A review of the neuropharmacology of bupropion, a dual norepinephrine and dopamine reuptake inhibitor, *Prim. Care Companion J. Clin. Psychiatry* 6 (2004) 159–166.
- [3] W.W. Zung, H.K. Brodie, L. Fabre, D. McLendon, D. Garver, Comparative efficacy and safety of bupropion and placebo in the treatment of depression, *Psychopharmacology (Berl.)* 79 (1983) 343–347.
- [4] H.I. Lief, Bupropion treatment of depression to assist smoking cessation, *Am. Psychiatry* 153 (1996) 442.
- [5] L.A. Labbate, J.B. Grimes, A. Hines, M.H. Pollack, Bupropion treatment of serotonin reuptake antidepressant-associated sexual dysfunction, *Ann. Clin. Psychiatry* 9 (1997) 241–245.
- [6] R.A. Plodkowski, Q. Nguyen, U. Sundaram, L. Nguyen, D.L. Chau, S. St Jeor, Bupropion and naltrexone: a review of their use individually and in combination for the treatment of obesity, *Expert Opin Pharmacother.* 10 (2009) 1069–1081.
- [7] D.P. Cantwell, ADHD through the life span: the role of bupropion in treatment, *J. Clin. Psychiatry* 59 (Suppl. 4) (1998) 92–94.
- [8] J.G. Modell, N.E. Rosenthal, A.E. Harriett, A. Krishen, A. Asgharian, V.J. Foster, J. Metz, C.B. Rockett, D.S. Wightman, Seasonal affective disorder and its prevention by anticipatory treatment with bupropion XL, *Biol. Psychiatry* 58 (2005) 658–667.
- [9] D. Brustolim, R. Ribeiro-dos-Santos, R.E. Kast, E.L. Altschuler, M.B. Soares, A new chapter opens in anti-inflammatory treatments: the antidepressant bupropion lowers production of tumor necrosis factor- α and interferon- γ in mice, *Int. Immunopharmacol.* 6 (2006) 903–907.
- [10] M.D. Ruff, S.R. Kalidindi, J.E. Sutton Jr., Pharmaceutical composition containing bupropion hydrochloride and a stabilizer, United States Patent 5,358,971 (1994).
- [11] P.S. Kulkarni, B.B. Shah, A. Maitra, J.M. Devito, Pharmaceutical composition containing bupropion hydrochloride and a stabilizer, United States Patent 20,010,021,721 (2001).
- [12] A. Maitra, P.S. Kulkarni, B.B. Shah, J.M. Devito, Pharmaceutical composition containing bupropion hydrochloride and an inorganic acid stabilizer, United States Patent 5,968,553 (1999).
- [13] C.-H. Han, G. Liaw, Stabilized pharmaceutical compositions containing bupropion hydrochloride, United States Patent 6,333,332 (2001).
- [14] M.W. Trumbore, R.V. Rariy, J.C. Hirsh, M. Hirsh, Stabilized transdermal bupropion formulations, United States Patent 20,080,044,462 (2008).
- [15] M. Chawla, R.S. Raghuvanshi, A. Rampal, Novel method stabilizing bupropion hydrochloride tablets, United States Patent 20,060,165,779 (2006).
- [16] S.K. Gidwani, P. Singnurkar, P.K. Tewari, Cyclodextrin stabilized pharmaceutical compositions of bupropion hydrochloride, United States Patent 6,462,233 (2002).
- [17] S. Chungi, K. Lin, Stabilized, acid-free formulation for sustained release of bupropion hydrochloride, United States Patent 6,306,436 (2001).
- [18] S.C. Laizure, C.L. DeVane, Stability of bupropion and its major metabolites in human plasma, *Ther. Drug Monit.* 7 (1985) 447–450.
- [19] P.K. Kiptoo, K.S. Paudel, D.C. Hammell, R.R. Pinninti, J. Chen, P.A. Crooks, A. Stinchcomb, Transdermal delivery of bupropion and its active metabolite, hydroxybupropion: a prodrug strategy as an alternative approach, *J. Pharm. Sci.* 98 (2009) 583–594.
- [20] R. Suma, H. Kosanam, P.K. Sai Prakash, Stability study of bupropion and olanzapine in formaldehyde solutions, *Rapid Commun. Mass Spectrom.* 20 (2006) 1390–1394.
- [21] S.M. Walters, Influence of pH on hydrolytic decomposition of diethylpropion hydrochloride: stability studies on drug substance and tablets using high performance liquid chromatography, *J. Pharm. Sci.* 69 (1980) 1206–1209.
- [22] G.M. Loudon, Mechanistic interpretation of pH-rate profiles, *J. Chem. Educ.* 68 (1991) 973–984.
- [23] R.M. Welch, A.A. Lai, D.H. Schroeder, Pharmacological significance of the species differences in bupropion metabolism, *Xenobiotica* 17 (1987) 287–298.
- [24] M.M. Ames, C.D. Selassie, L.C. Woodson, J.A. Van Loon, C. Hansch, R.M. Weirshilbom, Thiopurine methyltransferase: structure-activity relationships for benzoic acid inhibitors and thiophenol substrates, *J. Med. Chem.* 29 (1986) 354–358.
- [25] R.M. Wadkins, J.L. Hyatt, X. Wei, K.J.P. Yoon, M. Wierdl, C.C. Edwards, C. Morton, J.C. Obenauer, K. Damodaran, P. Beroza, M.K. Danks, P.M. Potte, Identification and characterization of novel benzil (diphenylethane-1,2-dione) analogues as inhibitors of mammalian carboxylesterases, *J. Med. Chem.* 48 (2005) 2906–2915.

Isosorbide-Based Aspirin Prodrugs: Integration of Nitric Oxide Releasing Groups

Michael Jones, Iwona Inkielewicz,[†] Carlos Medina, Maria Jose Santos-Martinez, Anna Radomski, Marek W. Radomski, Maeve N. Lally, Louise M. Moriarty, Joanne Gaynor, Ciaran G. Carolan, Denise Khan, Paul O'Byrne, Shona Harmon, Valerie Holland, John M. Clancy, and John F. Gilmer*

School of Pharmacy and Pharmaceutical Sciences, Trinity College, Dublin 2, Ireland. [†]Present address: Department of Toxicology, Medical University of Gdańsk, Hallera 107, 80-416 Gdańsk, Poland.

Received May 1, 2009

Aspirin prodrugs and related nitric oxide releasing compounds hold significant therapeutic promise, but they are hard to design because aspirin esterification renders its acetate group very susceptible to plasma esterase mediated hydrolysis. Isosorbide-2-aspirinate-5-salicylate is a true aspirin prodrug in human blood because it can be effectively hydrolyzed to aspirin upon interaction with plasma BuChE. We show that the identity of the remote 5-ester dictates whether aspirin is among the products of plasma-mediated hydrolysis. By observing the requirements for aspirin release from an initial panel of isosorbide-based esters, we were able to introduce nitroxymethyl groups at the 5-position while maintaining ability to release aspirin. Several of these compounds are potent inhibitors of platelet aggregation. The design of these compounds will allow better exploration of cross-talk between COX inhibition and nitric oxide release and potentially lead to the development of selective COX-1 acetylating drugs without gastric toxicity.

Introduction

Aspirin is the world's most widely used medicine. Some of its effects are due to its ability to trans-acetylate platelet cyclooxygenase-1 (COX-1¹), resulting in effective abolition of platelet derived thromboxane A₂ (TXA₂), leading to cardiovascular and cerebrovascular protection.¹ Other effects can be attributed to COX-2 inhibition and the shunting of arachidonic acid that occurs when COX-2 is acetylated.² Long-term aspirin use is associated with reduced lung cancer death as well as decreased incidence of colorectal cancer in patients with colon polyps.³ The pharmacological target here may be COX-2 or be COX-independent, and the dose requirement has yet to be resolved but it is likely to be higher than in antiplatelet therapy. Aspirin may have a role in attenuating drug-induced liver damage⁴ and in preventing Alzheimer's disease progression.⁵ COX acetylation is generally beneficial in preventing, curing, and ameliorating human disease.

Aspirin use carries a 2–3 fold increase in risk of a serious gastrointestinal bleed that is of particular importance in the elderly population.⁶ Given the widespread use of aspirin, this side effect is a matter of serious public concern. Furthermore,

aspirin-induced gastropathy prevents its full clinical exploitation because in an individual instance the risk of ulceration tends to exceed the perceived risk of a disease event.⁷ Ulceration is not reduced by pharmaceutical approaches such as enteric coating⁸ or buffering,⁹ its severity is dose-dependent, and, crucially, it may not be directly attributable to the mechanism of action or pharmacological target of the drug.^{10,11} Therefore, there is a need to separate COX-1 acetylation from aspirin's side effects.¹²

Nitric oxide releasing aspirin compounds (termed NO-aspirins) are a type of hybrid intended to be capable of liberating nitric oxide and aspirin.¹³ Nitric oxide is gastro-protective through multiple mechanisms.¹⁴ However, the combination of aspirin and nitric oxide release exhibits pharmacological effects in cardiovascular, cancer, and inflammatory models that hold significant therapeutic potential.¹⁵ The NO-aspirin **1** was tested in a number of clinical trials, and it has little or no gastric toxicity either because it releases NO or simply because it is an ester.¹³ Aspirin has been linked to a number of other nitric oxide pro-moieties (Figure 1), including furoxan (**2**) and diazeniumdiolate (**3**) groups.^{16,17} An interesting group of salicylates were recently reported with incorporation of a nitroxyl group on the acetyl moiety rather than at the carboxylate (**4**).¹⁸

While the concept holds rich promise, the design of true aspirin nitric oxide hybrids has hitherto proven difficult. Human blood plasma butyrylcholinesterase (BuChE, EC 3.1.1.7) tends to catalyze the hydrolysis of the acetyl group of aspirin esters before the pendant ester whether or not it bears a nitric oxide precursor (this is shown in the special case of isosorbide-based aspirin esters as pathway B in Figure 2).^{19,20} The design challenge in nitric oxide releasing aspirins is therefore similar to the design challenge with aspirin prodrugs generally—how to induce release of the group bearing the nitric oxide precursor before deacetylation (pathway A in Figure 2). None of the

*To whom correspondence should be addressed. Phone: +353-1-896 2795. Fax: +353-1-896 2793. E-mail: gilmerjf@tcd.ie

[†]Abbreviations: AChE, acetyl cholinesterase; ADP, adenosine diphosphate; BNPP, bis-*p*-nitrophenylphosphate; (hu)BuChE, (human) butyrylcholinesterase; BW254c51, 1:5-bis(4-allyl-dimethyl)ammonium-phenyl-pentan-3-one; CES, carboxylesterase; COX, cyclooxygenase; DCC, dicyclohexylcarbodiimide; DMAP, dimethylaminopyridine; EDTA, ethylenediaminetetraacetic acid; EtOAc, ethyl acetate; GIT, gastrointestinal tract; GSH, glutathione; Hex, *n*-hexane; ISAS, isosorbide-2-aspirinate-5-salicylate; ISDA, isosorbide-2,5-diaspirinate; ISMN, isosorbide mononitrate; ISMNA, isosorbide mononitrate aspirinate; iso-OMPA, tetraisopropylpyrophosphoramide; MeCN, acetonitrile; MeOH, methanol; NO, nitric oxide; ODQ, 1*H*-[1,2,4]oxadiazolo[4,3-*a*]quinoxalin-1-one; PMSF, phenylmethylsulfonyl fluoride; PRP, platelet rich plasma; RPHPLC, reverse-phase high performance liquid chromatography; SAR, structure–activity relationship; TXA₂, thromboxane A₂.

aspirin nitric oxide hybrids reported so far generate aspirin in blood. The overall aim of the work described in the present study was to design an aspirin ester capable of liberating aspirin and a nitric oxide precursor in human plasma.

We have recently reported on isosorbide-2-aspirinate-5-salicylate **5a** (Figure 2) which acts as a true aspirin prodrug because of an unusually productive interaction with BuChE.²¹ The 5-salicylate group in **5a** appeared to have a decisive effect on the specificity of processing in this compound because the isosorbide-2-aspirinate **5b** was not an aspirin prodrug [pathway B in Figure 2]. We had earlier reported the aspirin ester (**6**) of the clinically used nitrate isosorbide mononitrate (ISMN), a promising hybrid design as its two components are already approved for human medicine and in similar doses.²² This paper describes initially an evaluation of **6** as a potential human aspirin-nitrate hybrid prodrug. Following this we investigated the influence of the 5-ester group in **5** on the A/B hydrolysis ratio, leading eventually to successful incorporation of a nitrate group (**7**, Figure 2) while maintaining aspirin release characteristics in human plasma.

Evaluation of Aspirin Ester of Isosorbide-5-mononitrate. Isosorbide-5-mononitrate-2-aspirinate (**6**) was evaluated as an aspirin prodrug by incubating it in human plasma at 37 °C (10 and 50%) and monitoring its decay by RPHPLC. In human plasma solution (10%), compound **6** was hydrolyzed mainly along the salicylate pathway (B in Figure 2), producing <10% aspirin. The amount of aspirin evident under these conditions can be used to estimate the ratio of pathways A to B because aspirin hydrolysis is slow in dilute

plasma solution ($t_{1/2}$ for aspirin in 10% plasma is reported to be 9.8 h).¹⁹ Hydrolysis of **6** in 10% plasma solution was rapid, with an apparent first-order half-life of 52 s. This behavior is not unusual for aspirin esters, especially where deacetylation predominates, but the ISMN-salicylate product of the hydrolysis process was consumed with striking rapidity (Figure 3). Typically, the rate of plasma-mediated hydrolysis of salicylic acid esters is slow. For example, methyl salicylate hydrolyzes in 80% human plasma with a half-life of 17.6 h.²³ It would appear therefore that the ISMN group promotes rapid hydrolysis of the salicylate ester in human plasma solution. Indeed productive hydrolysis of the parent **6** almost competes with the unproductive acetyl group detachment. The isomeric isosorbide-2-nitrate-5-aspirinate²¹ (**6a**) was tested under the same conditions. It too disappeared rapidly ($t_{1/2} = 1.3$ min) but with the exclusive liberation of the isosorbide-2-mononitrate-5-salicylate, which was stable in plasma. Isosorbide-2-mononitrate has been used as a nitrovasodilator but it has significant side effects due to rapid nitric oxide release; the more slowly metabolized 5-mononitrate has a better clinical profile.²⁴ The progress curve for the hydrolysis of **6a** (Figure 3) illustrates how much faster hydrolysis of the 2-*exo*-ester is and how close **6** is to acting as a true nitro-aspirin prodrug in human plasma. The identity of BuChE in mediating aspirin release from **6** was confirmed by repeating the hydrolysis experiment in the presence of selective esterase inhibitors, eserine (cholinesterases), *iso*OMPA (BuChE), phenylmethylsulfonyl fluoride (PMSF; serine proteases, AChE), and dibucaine (BuChE-subtype) (Table 1).²⁵ The hydrolysis was also monitored in human plasma solution in the concentration range 2–30% (pH 7.4, 37 °C). The extent of aspirin production relative to salicylate was found to be invariant with plasma concentration, although the k_{obs} increased linearly with plasma concentration (Figure 3). Because **6** did not have desirable aspirin release characteristics in human plasma, we were forced to consider how to replace the 5-nitrate with a substituent that could promote hydrolysis to aspirin at position 2 while at the same time being itself amenable to nitrate substitution. To better define the requirements for isosorbide-aspirinate activation to aspirin, we prepared a number of isosorbide-aspirinate 5-esters (**5**). We focused on esters because these would ultimately be hydrolyzed to isosorbide, which is innocuous. This led to the design and synthesis of a second group of

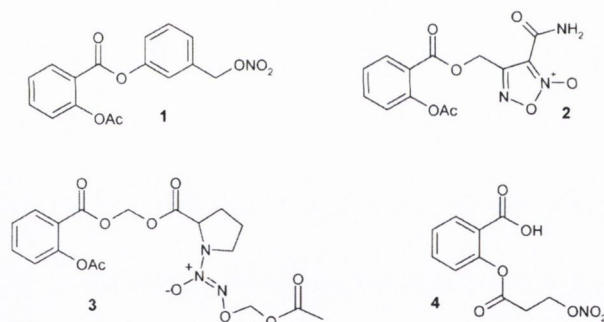


Figure 1. Aspirin-nitrate, **1**, furoxans **2**, diazeniumdiolates (NONOates) **3**, nitroxyacyl salicylates **4**.

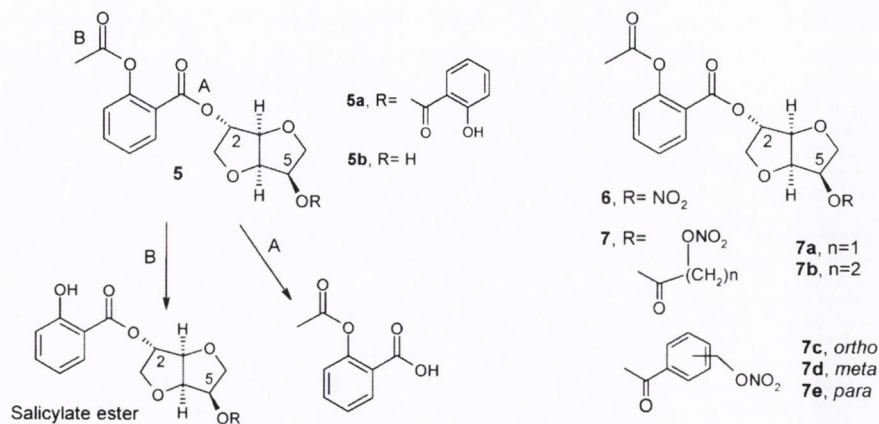


Figure 2. Hydrolysis pathways of aspirin prodrugs.

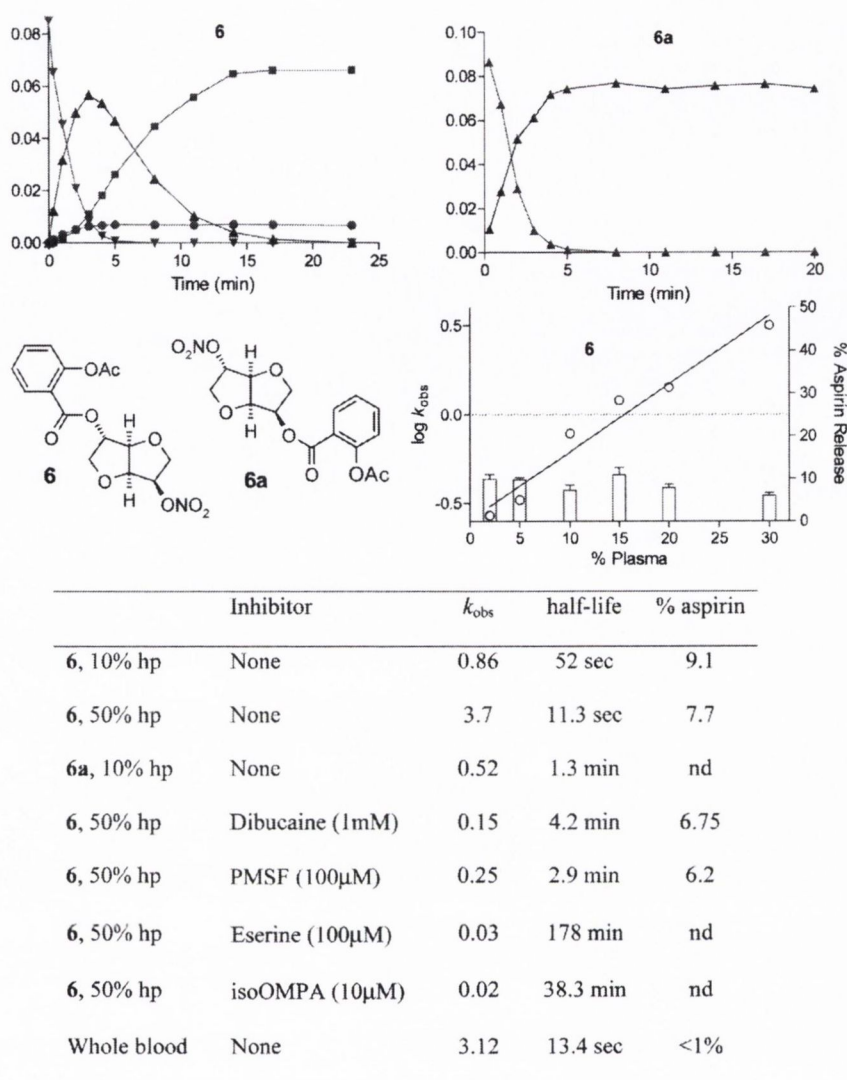


Figure 3. Progress curves for the disappearance of **6** and **6a** in 10% human plasma buffered at pH 7.4 (37 °C): **6** (downward-pointing solid green triangle), aspirin (solid red circle), isosorbide-2/5-salicylate-2/5-nitrate (upward-pointing solid blue triangle), salicylic acid (solid purple square). Plot showing the relationship between rate of hydrolysis and proportion of **7** undergoing hydrolysis to aspirin in the range 2–30% human plasma buffered at pH 7.4 and 37 °C. ($n = 3$).

compounds in which the 5-ester was elaborated with a nitrate group as a nitric oxide donor (**7**).

Chemistry

Compounds **5** were obtained by esterification of **5b** with the appropriate acid and DCC coupling procedures or by treatment with the corresponding acid chloride in the presence of Et_3N (Scheme 1). We were unable to obtain the 3- and 4-hydroxybenzoates (**5c**, **5d**) by direct coupling because of competition between the isosorbide-5-OH and phenolic -OH groups. In these cases, the benzylprotected hydroxybenzoic acids were coupled first to **5b** by DCC-mediated coupling, followed by reduction in the presence of H_2 over Pd/C. The synthesis of the alkyl nitrate esters **7a,b** is shown in Scheme 2. The intermediate nitroxyalkyl acids **10** were first prepared by treating the corresponding commercially available bromoacids **9** with AgNO_3 in MeCN. Nitroxyacids **10** were linked by esterification with DCC and DMAP to **5b** to yield the

isosorbide-2-aspirinate-nitroxyalkyl esters **7a,b**. The nitroxy-methylbenzoate compounds **7c–e** were prepared by treating **5b** with the appropriate chlorobenzoyl chloride (Scheme 3). The chloromethyl esters were carried through unpurified and the halide–nitrate exchange accomplished using AgNO_3 in MeCN. In the case of the *ortho*-chloromethyl benzoic acid was generated from phthalide in the presence of dichlorotriphenylphosphorane and used unpurified.²⁶ The final compounds were characterized by HRMS, CHN, NMR, and HPLC. Compounds **5a**, **5b**, **6**, and **6a** were obtained as described previously.^{21,22}

Evaluation of Isosorbide-Based Aspirinates. The panel of **5** esters was incubated in 10 and 50% plasma solution (pH 7.4, 37 °C) and the reaction progress monitored at intervals by RPHPLC. Ester consumption followed first-order kinetics with half-lives of 2–5 min in 10% human plasma and around 1 min in 50% human plasma (Table 1). The salicylates eluted after the parent aspirinates in each case and were quantitated using the response of the parent at 230 nm. The identity of the

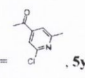
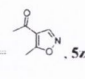
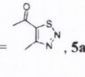
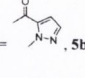
salicylates was confirmed using photodiode array (PDA) (λ_{max} , ~300 nm) and in some cases by LCMS. The extent of aspirin release was estimated from progress curves at maximum aspirin concentration relative to the extrapolated initial parent ester concentration (Table 1). The esters underwent hydrolysis with markedly different outcomes in rate and extent of aspirin release.

The four 5-alkyl esters **5e–h** were exclusively hydrolyzed to the corresponding salicylates (pathway B). The benzoate esters tended to be hydrolyzed along pathway A to some extent. The hydroxybenzoate ester compounds **5c,d**, which are isomers of **5a**, underwent typically rapid hydrolysis in human plasma. Isomer **5c** produced significant amounts of aspirin (29–44%), but the para isomer **5d** was hydrolyzed along the salicylate pathway (< 1% aspirin). The *ortho*- and *meta*-toluate esters **5j** (46–59%) and **5k** (38–54%) were excellent aspirin prodrugs, but the *para*-toluate (**5l**) was less effective (~15% aspirin release). Of the methoxybenzoates (**5m–o**) the meta isomer was most efficient (17–19%). The 5-biphenyl ester **5t** was not consumed over a period of one hour at either 10% or 50% plasma. Instead, the typical initially rapid hydrolysis tapered quickly and stopped abruptly following around 20% consumption of the parent compound ($n = 3$). No aspirin was produced. The interaction of the isosorbide-based compounds with the cholinesterases is not straightforward. Whereas isosorbide diesters (including those here) are in general extremely rapidly hydrolyzed by BuChE, some are micromolar inhibitors of the homologous enzyme AChE.²⁷ Therefore, the failure of **5t** to undergo significant consumption could be due to enzyme inhibition by the intact compound or one of its hydrolysis products. Overall, in the benzoate group, *ortho*-substitution and to a lesser extent *meta*-substitution conferred good aspirin release characteristics in human plasma solution. The *para*-substituted 5-benzoates tended not to act as aspirin prodrugs as evidenced by the behavior of **5d**, **5l**, **5o**, **5s**, and **5t**. Some heterocyclic substituted compounds (**5v–5bb**) were also prepared and evaluated, initially with the objective of improving water solubility. The nicotinate (**5v**) is an interesting compound because it produces substantial amounts of aspirin (40%) and is subsequently hydrolyzed to nicotinic acid and isosorbide. The water solubility of the two nicotinates (**5v,w**) was significantly better than the alkyl and carbocyclic aryl compounds, but the others, apart from thiazazole (**5aa**), were not sufficiently efficient as aspirin prodrugs to warrant further investigation.

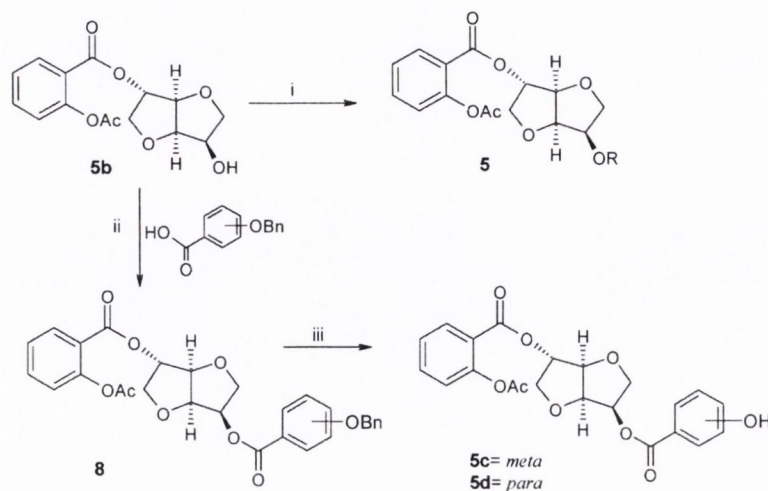
Having established the general requirements for productive hydrolysis in human plasma solution for the 2-aspirinate-5-esters, we next turned to the problem of integrating a potential nitric oxide releasing moiety (**7**, Table 2, Figure 4).

We had chosen to evaluate nitrate esters as potential NO delivery groups because nitrates are synthetically accessible, stable, lipophilic, and have a long history of clinical use. We were drawn toward nitroxymethylbenzoates because these corresponded most closely to the benzoates that were associated with good aspirin release characteristics in human plasma in series **5**. We evaluated two nitroxymethyl compounds for comparison. Nitroxy-substitution directly to the benzene ring was rejected because phenylnitrates are reported to spontaneously disproportionate to nitrophenols.²⁸ The 5-nitroxymethyl esters **7a,b** were hydrolyzed exclusively along the salicylate pathway in human plasma solution (10 and 50%) as observed for the unsubstituted analogs **5e–h**. The *ortho*- and *meta*-substituted compounds

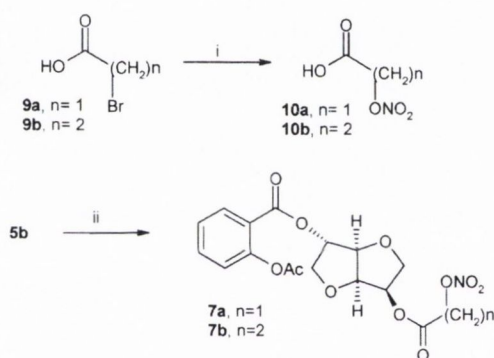
Table 1. Kinetic Data for the Hydrolysis of Compounds **5** and Extent of Aspirin Released Based on Initial Ester Concentration in Moles Measured at Peak Aspirin Production Following Addition of Candidate Esters to Buffered Human Plasma (10 or 50%) at 37 °C and pH 7.4 by HPLC

5	First-order rate constant (min ⁻¹) ^a , half-life (min) ^b						Sol ^c
	and mole % aspirin ^c released						
	^d Solubility in water (μg/mL)						
	10% plasma			50% plasma			
	a	b	c	a	b	c	
R=2-hydroxybenzoate, 5a	0.14	4.95	72	0.61	1.14	85	11.2
R=3-hydroxybenzoyl, 5c	0.63	1.10	44	0.77	0.90	29	
R=4-hydroxybenzoyl, 5d	0.58	1.19	1	0.58	1.19	0.5	
R=acetyl, 5e	0.19	3.65	1.2	1.22	0.57	1.3	18.8
R=propanoyl, 5f	0.19	3.65	6.8	1.05	0.66	7	57
R=pentanoyl, 5g	0.58	1.19	nd	0.99	0.70	<0.5	
R=cyclopropanoyl, 5h	0.36	1.93	2	0.77	0.90	<0.5	
R=benzoyl, 5i	0.21	3.30	19	1.08	0.64	29	1.2
R=2-methylbenzoyl, 5j	0.33	2.10	46	0.83	0.83	59	5.34
R=3-methylbenzoyl, 5k	0.07	9.90	38	0.57	1.22	54	0.6
R=4-methylbenzoyl, 5l	0.11	6.30	16	0.32	2.17	14.7	5.3
R=2-methoxybenzoyl, 5m	0.2	3.47	5	0.7	0.99	7	9.9
R=3-methoxybenzoyl, 5n	0.22	3.15	19	0.82	0.85	17	15.6
R=4-methoxybenzoyl, 5o	0.22	3.15	2.6	0.63	1.10	4	0.31
R=2-benzoyloxybenzoyl, 5p	0.03	23.10	28	0.16	4.33	19	0.51
R=4-nitrobenzoyl, 5q	0.25	2.77	13	0.51	1.36	22	1.72
R=4-cyanobenzoyl, 5r	0.13	5.33	19	0.17	4.08	<0.5	
R=4-phenylbenzoyl, 5s	na	>20	<0.5	na	>20	<0.5	
R=3,5-diethoxybenzoyl, 5t	nt	nt	nt	0.41	1.7	<0.5	
R=3-acetamidobenzoyl, 5u	nt	nt	nt	0.2	3.5	11	
R=nicotinoyl, 5v	0.5	1.39	41	1.87	0.37	32	87
R= <i>iso</i> -nicotinoyl, 5w	0.18	3.7	19	2.1	0.33	27	207.2
R=6-chloronicotinoyl, 5x	0.18	3.85	18	0.36	1.93	17	
R=  , 5y	0.6	1.16	24	0.6	1.16	14	
R=  , 5z	0.06	11.55	18	12	0.06	14	
R=  , 5aa	0.18	3.85	32	1.8	0.39	31	
R=  , 5bb	0.12	5.78	7	0.18	3.85	6	
R=H, 5b	0.21	3.30	<0.5	0.63	1.10	<0.5	

7c and **7d** were effective aspirin prodrugs generating ~30 ar ~50% aspirin respectively in human plasma solution. Compounds **7c** and **7d** were incubated in solutions of wild type BuChE purified from human plasma with similar A_v/hydrolysis ratio supporting the identity of BuChE in the

Scheme 1. Synthesis of Isosorbide-2-aspirinate-5-esters **5**

Conditions: (i) RCOOH, DCC, DMAP in DCM or RCOCl, Et₃N, DCM; (ii) DCC, DMAP, DCM; (iii) H₂, Pd/C, EtOAc/MeOH.

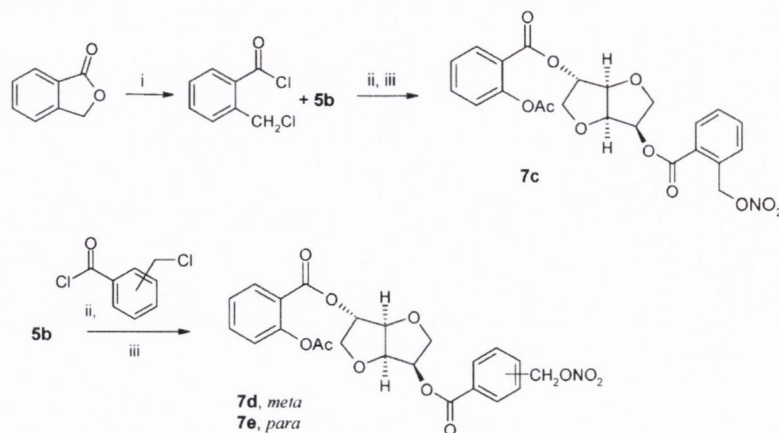
Scheme 2. Synthesis of Isosorbide Based Alkylnitrate Aspirinates **7a–b**

Conditions: (i) AgNO₃, MeCN; (ii) RCOOH, DCC, DMAP; (iii) Et₃N, DCM.

hydrolysis in plasma. The *para*-substituted compound **7e** did not act as an aspirin prodrug, consistent with the observations about *para*-substitution in series **5** (Table 3). The 50% plasma samples following incubation of **7d** were analyzed by LCMS to confirm the hydrolysis pathway evident by HPLC-UV and to look for evidence of nitrate hydrolysis/metabolism. All of the expected plasma esterase products were observed— aspirin, salicylic acid, the salicylate analogue of **7d**, isosorbide-5-*m*-nitroxymethyl benzoate, and *m*-nitroxymethyl benzoic acid. However there was no evidence of the hydroxymethyl products that would be expected following loss of NO/NO₂. Alkyl nitrates, including clinically used nitrates, degrade very slowly in plasma and buffer solution but produce pharmacologically effective amounts of nitric oxide in media containing cell types including smooth muscle cells and, to a lesser extent, platelets.^{24,29}

The remote control over the direction of hydrolysis by the 5-ester is peculiar. Isosorbide aspirinate diesters are V-shaped with the 2-substituent directed exo to the fused ring system and the 5-group endo. The exo group is predicted to be more reactive on purely steric grounds, but the high susceptibility of isosorbide-2-esters to BuChE processing is connected to their overall shape and topological complementarity with the

BuChE active site. Isosorbide-2,5-diester are in general rapidly and exclusively hydrolyzed at the 2-ester.³⁵ The rate of hydrolysis of the isosorbide-2-benzoate ester increases 20-fold across the series –5-OH, –5-nitrate, –5-benzoate with an accompanying depression of *K_M* values, indicating that the rate enhancement is substrate affinity driven.³⁰ We also reported recently on isosorbide-2-carbamate esters as low nM and selective inhibitors of BuChE over AChE (6 × 10⁴).³¹ These compounds were characterized as time-dependent pseudosubstrate competitive inhibitors. In that class, potency (and presumably affinity) significantly increased in the series –5-nitrate, –5-alkyl ester, –5-aryl ester. The general problem in aspirin prodrug chemistry is that the acetyl group is chemically and enzymatically susceptible to hydrolysis by plasma esterase for electronic, steric, and mechanistic reasons. It seems that in the isosorbide-aspirinate series, 5-aryl substitution can stabilize substrate orientations associated with hydrolysis along pathway A so that it can be competitive with acetate group hydrolysis. We decided to see if a modeling approach could be used to investigate why some benzoates might be better in this regard than others. In ester hydrolysis, we can assume that the transition state resembles the ensuing tetrahedral intermediate and it follows that differences in stability between competing transition states in parallel ester processing will be reflected in the relative energies and geometries of the respective tetrahedral intermediates. We therefore modeled the respective compounds **5a** and **5i** in BuChE using a docking approach in which the carbonyls were rehybridized and linked covalently to the active site serine (198 in HuBuChE; PDB code 1p0i).³² This approach has been used previously for carbamate interactions with the cholinesterases.^{31,33} It finds significant justification in the fact that the X-ray crystal structure of BuChE had a fragment at the active site that could be modeled as covalently bound butyrate with the anionic intermediate directed into the oxyanion hole.³² One of the virtues of the approach is that it limits the containment volume of the substrate and reduces the problem to a unimolecular one although rehybridization of the carbonyl carbon creates a new sp³ stereocenter. Docking runs were therefore performed using AUTODOCK 3 with full bond rotation for both stereoisomers of *E*-**5a** and *E*-**5i**.^{34,35} It was found that the only realistic poses for processing involving attack on the

Scheme 3. Synthesis of Isosorbide Based Alkylnitrate Aspirinates **7c–e**

Conditions: (i) PPh_3Cl_2 , 180°C , 4 h; (ii) Et_3N , DCM; (iii) AgNO_3 , MeCN.

Table 2. Kinetic Data for the Hydrolysis of Nitroxy-Substituted Compounds **6**, **7a–e**, and Extent of Aspirin Released Based on Initial Ester Concentration in Moles Measured at Peak Aspirin Production Following Addition of Candidate Esters to Buffered Human Plasma (10 and 50%) at 37°C and pH 7.4 by HPLC

	first-order rate constant (mol^{-1}) (a), half-life (min) (b), and mol % aspirin (c) released					
	10% plasma			50% plasma		
	a	b	c	a	b	c
R = (nitroxy)-acetyl, 7a	0.19	3.6	nd	0.77	0.9	nd
R = (nitroxy)-propanoyl, 7b	0.18	3.9	nd	0.53	1.3	nd
R = (2-nitroxymethyl)-benzoyl, 7c	0.26	2.7	32	0.21	3.2	34
R = (3-nitroxymethyl)-benzoyl, 7d	0.26	2.6	51	0.25	2.7	55
R = (4-nitroxymethyl)-benzoyl, 7e	0.11	6.0	< 5	0.29	2.4	< 1

benzoate ester were those in which the isosorbide-5-ester was orientated toward Trp82 (the cation- π site) and the aspirin phenyl group into the acyl pocket (Leu286/Val288). The 5-salicylate group in **5a** is predicted to interact with Trp82 via π - π attractions. There were also interactions between the salicylate -OH group and a H-bond network involving Asp70, Tyr332, Ser79, and Trp82 (Supporting Information (SI)). Figure 5 shows the 5-benzoate derivative **5i** in its most favorable pose following attack on the benzoate. The overall conformation is similar to that of **5a** apart from the H-bonding contacts to the salicylate -OH. There is a predicted energy difference between the docked poses of $2.4 \text{ kcal}\cdot\text{mol}^{-1}$ in favor of **5a**. Compound **5a** was then covalently docked to BChE such that the attack occurred at the acetate ester rather than the benzoic acid ester. While binding was predicted to be good, there were no specific interactions between the macromolecule and the OH group of the salicylate moiety (SI). The binding energy of the substrate in this orientation was predicted to be similar to that of the benzoate in Figure 5 ($11.25 \text{ kcal}\cdot\text{mol}^{-1}$ compared to $12.15 \text{ kcal}\cdot\text{mol}^{-1}$). It therefore appears that the -OH group of the salicylate ester in **5a** can form specific interactions

with the enzyme when it is being hydrolyzed at the phenyl ester (specifically with the residues of the peripheral site). For compounds lacking the hydroxyl group, there is a smaller energy difference between formation of the intermediate/transition states for hydrolysis at the acetyl and benzoate esters.

Inhibition of Platelet Aggregation in Vitro. Compounds **5a**, **7c–d**, and aspirin were evaluated as inhibitors of platelet aggregation in platelet rich plasma (PRP) in response to collagen ($5 \mu\text{g}/\text{mL}$) and ADP ($3 \mu\text{M}$). At these concentrations, platelet aggregation induced by collagen is highly dependent on the release of arachidonic acid and TXA_2 generation, while aggregation by ADP is less thromboxane-dependent. As shown in Figure 6, **5a** and the nitroaspirin hybrids **7c** and **7d** and aspirin in the range 10 – $300 \mu\text{M}$ caused concentration-dependent inhibition of collagen-induced platelet aggregation. **5a** ($20.6 \mu\text{M}$) and hybrid **7d** ($17.1 \mu\text{M}$) were significantly more potent than aspirin ($92.7 \mu\text{M}$), which was similar in potency to **7c** ($90.3 \mu\text{M}$), a moderate aspirin releasing compound that also bears a nitroxyl ester (Table 3). Hybrid **7e**, which does not liberate aspirin in human plasma, did not cause inhibition of collagen-induced

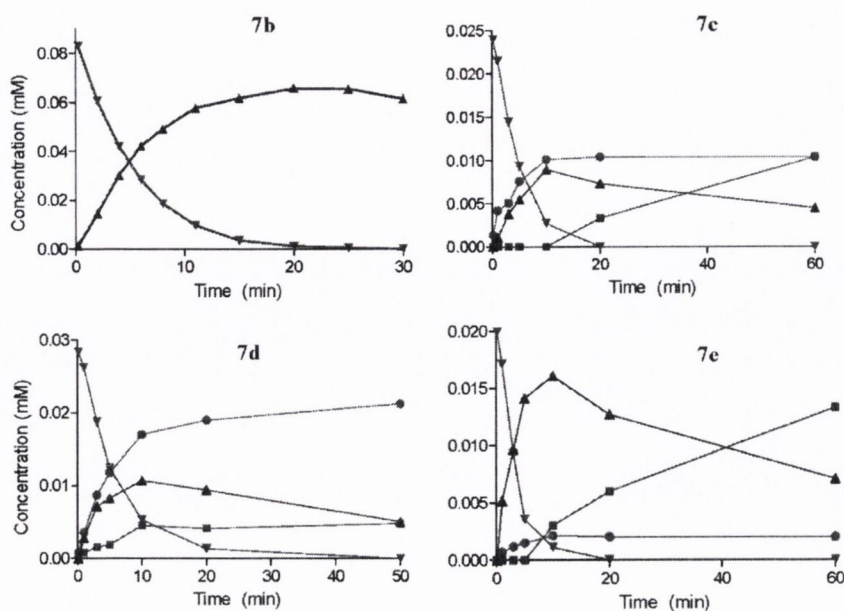


Figure 4. Progress curves for the disappearance of **7b** and the isomeric nitroxymethyl benzoates **7c–e** in 50% human plasma buffered at pH 7.4 (37 °C): prodrug (downward-pointing solid green triangle), aspirin (solid red circle), isosorbide-2-salicylate-5-ester (upward-pointing solid blue triangle), salicylic acid (solid purple square).

Table 3. Inhibition Data for Platelet Aggregation in Response to Collagen (5 µg/mL) in PRP

compd	<i>n</i>	IC ₅₀ (µM)	SE	CI	% aspirin
5a	3	20.6	1.6	17.2–23.9	80
7c (<i>ortho</i>)	5	90.3	5.3	79.5–100.1	34
7d (<i>meta</i>)	3	17.1	4.1	8.8–26.4	55
7e (<i>para</i>)	3	> 300			1
aspirin	3	92.7	3.6	84.9–100.4	100

aggregation at concentrations < 300 µM. Compounds **5a** and **7d** were also significantly more potent inhibitors of ADP (3 µM)-induced aggregation than aspirin. However, when the aggregation experiments were repeated using collagen or ADP in the presence of the cGMP inhibitor 1*H*-[1,2,4]-oxadiazolo[4,3-*a*]quinoxalin-1-one (ODQ), there was no attenuation of platelet inhibition by **7d**, indicating that in PRP in vitro, NO release from **7d** did not make a significant contribution to inhibition. In washed platelets suspension (WP), the addition of 1 mM glutathione (GSH), which promotes NO release from nitrates, enhanced the inhibitory effects of **7d** (Figure 6c). This subtle effect could be abolished by preincubating WP with ODQ. The data indicates that significant inhibition of aggregation by compounds **7** in PRP requires the presence of promoters of NO release. This is consistent with the potency of the non-nitrate **5a**, the lack of effect of the nonaspirin releasing **7e**, and the generally reported failure of platelets to release substantial amounts of nitric oxide from organic nitrates. The unexpected potency of **7d** in this context will be the subject of careful pharmacological studies in vitro, and in vivo where nitric oxide release from other cell types can be expected to contribute to effects.

Conclusion

We have shown that by taking account of the substrate preferences, human BuChE can be used as a vector for the release of aspirin and a nitric oxide precursor from aspirin

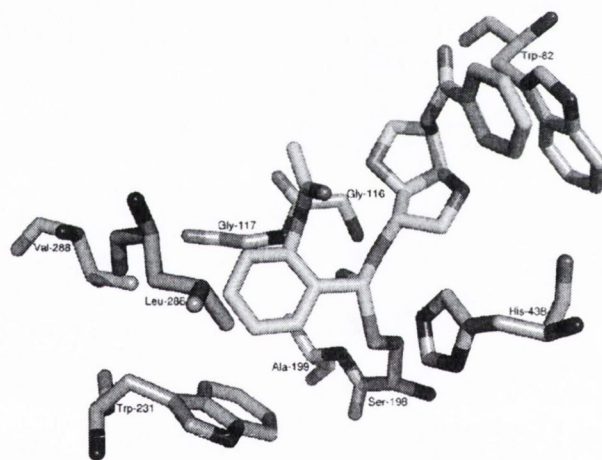


Figure 5. Predicted (and representative) lowest energy conformation for **5i** bound covalently to BChE at the phenyl ester as the tetrahedral intermediate using Autodock 3.

hybrid esters. Compounds **7c** and **7d** are the first compounds reported with the ability to generate aspirin and a potential nitric oxide releasing group under physiologically relevant conditions. They are potent inhibitors of ADP and collagen induced platelet aggregation. They will prove valuable in pharmacological studies on the interactions between nitric oxide and COX inhibition in vivo.

Experimental Section

Chemistry. ¹H and ¹³C spectra were recorded at 27 °C on a Bruker DPX 400 MHz FT NMR spectrometer (400.13 MHz ¹H, 100.61 MHz ¹³C) or a Bruker AV600 (600.13 MHz ¹H, 150.6 MHz ¹³C) in either CDCl₃ or (CD₃)₂CO with TMS as internal standard. In CDCl₃, ¹H spectra were assigned relative to the TMS peak at 0.0 ppm and ¹³C spectra were assigned relative to the middle CDCl₃ triplet at 77.00 ppm. In (CD₃)₂CO, ¹H spectra

Individual Tests Data Report Trinity College Dublin

Study Completed: April 27, 2009

Report Printed: April 27, 2009

MDSPTS PT#: 1116710

Alt. Code 1: Bup HBr

Alt. Code 2:

Alt. Code 3:

Sample(s): TRN-29

M.W.: 320.7

Objectives:

To evaluate, in Radioligand Binding assays, the activity of test compound Bup HBr (PT# 1116710).



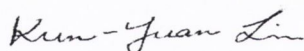
PT#: 1116710
CODE: TRN-29, Bup HBr

April 27, 2009 3:53 PM
Page 2 of 14

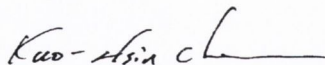
MDS Pharma Services Pharmacology Data Report On Compound TRN-29, Bup HBr For Trinity College Dublin

Work Order Number:	1-1035283-0	Services Being Reported:	Individual Tests
Study Number:	AA84831	Alternative Work Order No:	
Quote No:	13104-1	Purchase Order Number:	POB-636195
Compound Information:		Total # of Assays:	5
Compound Code:	TRN-29		
Alternative Code 1:	Bup HBr		
Alternative Code 2:			
Alternative Code 3:			
MDSPS Internal #:	1116710		
Molecular Weight:	320.7		
Sponsor:	Trinity College Dublin School of Pharmacy College Green Dublin 2, Ireland		
Undertaken at:	MDS Pharma Services - Taiwan Ltd. Pharmacology Laboratories 158 Li-Teh Road, Peitou Taipei, Taiwan 112 R. O. C.		
Date of Study:	April 20, 2009 - April 27, 2009		
Study Directors:	Kun-Yuan Lin, MDS Pharma Services - Taiwan Ltd. Kuo-Hsin Chen, MDS Pharma Services - Taiwan Ltd.		
Distribution:	Trinity College Dublin		

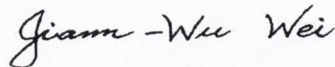
"This study was conducted according to the procedures described in this report. All data presented are authentic, accurate and correct to the best of our knowledge."



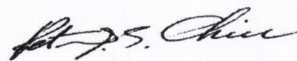
Kun-Yuan Lin
Study Director for Animal Assays



Kuo-Hsin Chen
Study Director for Biochemical Assays



Jiann-Wu Wei, Ph.D
Quality Control and Data Reviewer



Peter Chiu, Ph.D
Technical Director

PT #: 1116710
CODE: TRN-29, Bup HBr

April 27, 2009 3:53 PM
Page 3 of 14

TABLE OF CONTENTS

REPORT SECTION	PAGE
Summary	4
Summary of Significant Results	5
Experimental Results	7
Response Curves	8
Methods	11
Reference Compound Data	13
Literature References	14

SUMMARY

STUDY OBJECTIVE

To evaluate, in Radioligand Binding assays, the activity of compound Bup HBr (TRN-29, PT# 1116710).

METHODS

Methods employed in this study have been adapted from the scientific literature to maximize reliability and reproducibility. Reference standards were run as an integral part of each assay to ensure the validity of the results obtained. Assays were performed under conditions described in the accompanying "Methods" section of this report. The literature reference(s) for each assay are in the "Literature References" section. If either of these sections were not originally requested with the accompanying report, please contact us at the number below for a printout of either of these report sections.

Where presented, IC_{50} values were determined by a non-linear, least squares regression analysis using MathIQ™ (ID Business Solutions Ltd., UK). Where inhibition constants (K_i) are presented, the K_i values were calculated using the equation of Cheng and Prusoff (Cheng, Y., Prusoff, W.H., *Biochem. Pharmacol.* 22:3099-3108, 1973) using the observed IC_{50} of the tested compound, the concentration of radioligand employed in the assay, and the historical values for the K_D of the ligand (obtained experimentally at **MDS Pharma Services**). Where presented, the Hill coefficient (n_H), defining the slope of the competitive binding curve, was calculated using MathIQ™. Hill coefficients significantly different than 1.0, may suggest that the binding displacement does not follow the laws of mass action with a single binding site. Where IC_{50} , K_i , and/or n_H data are presented without Standard Error of the Mean (SEM), data are insufficient to be quantitative, and the values presented (K_i , IC_{50} , n_H) should be interpreted with caution.

RESULTS

A summary of results meeting the significance criteria is presented in the following sections. Complete results are presented under the section labeled "Experimental Results". Individual responses, if requested, are presented in the appendix to this report.

SUMMARY/CONCLUSION

Significant results are displayed in the following table(s) in rank order of potency for estimated IC_{50} and/or K_i values.

SUMMARY OF SIGNIFICANT PRIMARY RESULTS

Biochemical assay results are presented as the percent inhibition of specific binding or activity throughout the report. All other results are expressed in terms of that assay's quantitation method (see Methods section).

- For primary assays, only the lowest concentration with a significant response judged by the assays' criteria, is shown in this summary.
- Where applicable, either the secondary assay results with the lowest dose/concentration meeting the significance criteria or, if inactive, the highest dose/concentration that did not meet the significance criteria is shown.
- Unless otherwise requested, primary screening in duplicate with quantitative data (e.g., $IC_{50} \pm SEM$, $K_i \pm SEM$ and n_H) are shown where applicable for individual requested assays. In screening packages, primary screening in duplicate with semi-quantitative data (e.g., estimated IC_{50} , K_i and n_H) are shown where applicable (concentration range of 4 log units); available secondary functional assays are carried out (30 μM) and MEC or MIC determined only if active in primary assays >50% at 1 log unit below initial test concentration.
- Please see Experimental Results section for details of all responses.

Significant responses ($\geq 50\%$ inhibition or stimulation for Biochemical assays) were noted in the primary assays listed below:

PRIMARY TESTS

PRIMARY							
CAT. #	BIOCHEMICAL ASSAY	SPECIES	CONC.	% INH.	IC_{50} *	K_i	n_H
204410	Transporter, Norepinephrine (NET)	hum	100 μM	80	19.9 μM	19.8 μM	0.835
220320	Transporter, Dopamine (DAT)	hum	1 μM	58	< 1 μM		
254000	Muscarinic, Non-Selective, Central	rat	100 μM	55	86.5 μM	27 μM	1.42

‡ Partially soluble in *in vitro* test solvent.

* A standard error of the mean is presented where results are based on multiple, independent determinations.

hum=human

PT#: 1116710
CODE: TRN-29, Bup HBr

April 27, 2009 3:54 PM
Page 6 of 14

SUMMARY OF SIGNIFICANT PRIMARY RESULTS

ABOVE PRIMARY TESTS IN RANK ORDER OF POTENCY

PRIMARY							
CAT. #	RADIOLIGAND ASSAY	SPECIES	CONC.	% INH.	IC ₅₀ *	K _i	n _H
204410	Transporter, Norepinephrine (NET)	hum	100 µM	80	19.9 µM	19.8 µM	0.835
254000	Muscarinic, Non-Selective, Central	rat	100 µM	55	86.5 µM	27 µM	1.42
220320	Transporter, Dopamine (DAT)	hum	1 µM	58	< 1 µM		

‡ Partially soluble in *in vitro* test solvent.

* A standard error of the mean is presented where results are based on multiple, independent determinations.

hum=human

EXPERIMENTAL RESULTS - BIOCHEMICAL ASSAYS

Cat. #	TARGET	BATCH*	SPP.	n=	CONC.	†% INHIBITION					IC ₅₀	K _I	n _H	R
						%	-100	-50	0	50				
◆ 254000	Muscarinic, Non-Selective, Central	246310	rat	2	100 µM	55			█		86.5 µM	27 µM	1.42	
				2	10 µM	4								
				2	1 µM	9								
258590	Nicotinic Acetylcholine	246311	hum	2	100 µM	15			█		>100 µM			
				2	10 µM	4								
				2	1 µM	1								
◆ 220320	Transporter, Dopamine (DAT)	246308	hum	2	100 µM	98			█		<1 µM			
◆				2	10 µM	91			█					
◆				2	1 µM	58			█					
◆ 204410	Transporter, Norepinephrine (NET)	246369	hum	2	100 µM	80			█		19.9 µM	19.8 µM	0.835	
				2	10 µM	35			█					
				2	1 µM	9								
274030	Transporter, Serotonin (5-Hydroxytryptamine) (SERT)	246309	hum	2	100 µM	34			█		>100 µM			
				2	10 µM	14			█					
				2	1 µM	8								

* Batch: Represents compounds tested concurrently in the same assay(s). ‡ Partially soluble in *in vitro* test solvent.

◆ Denotes item meeting criteria for significance

† Results with ≥ 50% stimulation or inhibition are highlighted.

R=Additional Comments

hum=human

PT #: 1116710
CODE: TRN-29, Bup HBr

April 27, 2009 3:55 PM
Page 8 of 14

PHARMACOLOGY REPORT

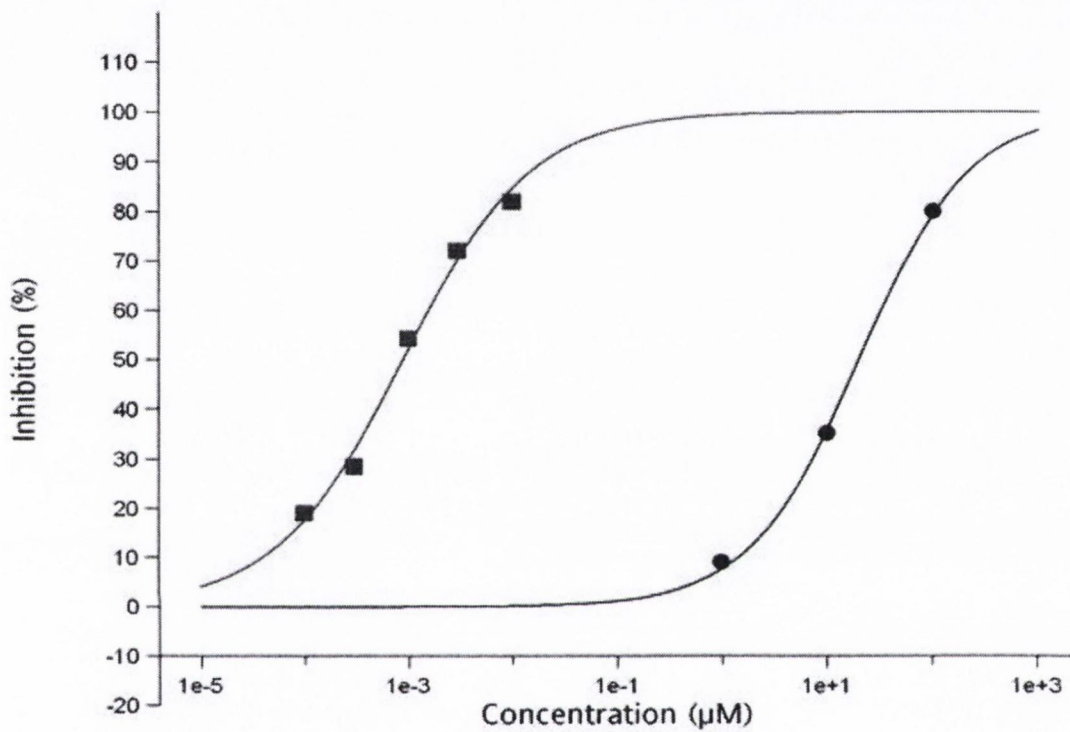
RESPONSE CURVES

PT #: 1116710
CODE: TRN-29, Bup HBr

April 27, 2009 3:55 PM
Page 9 of 14

RESPONSE CURVES

ASSAY: 204410 - 1 Transporter, Norepinephrine (NET)



Compound

IC₅₀

K_i

n_H

● Bup HBr (1116710)

19.9 µM

19.8 µM

0.835

■ Desipramine

0.890 nM

0.882 nM

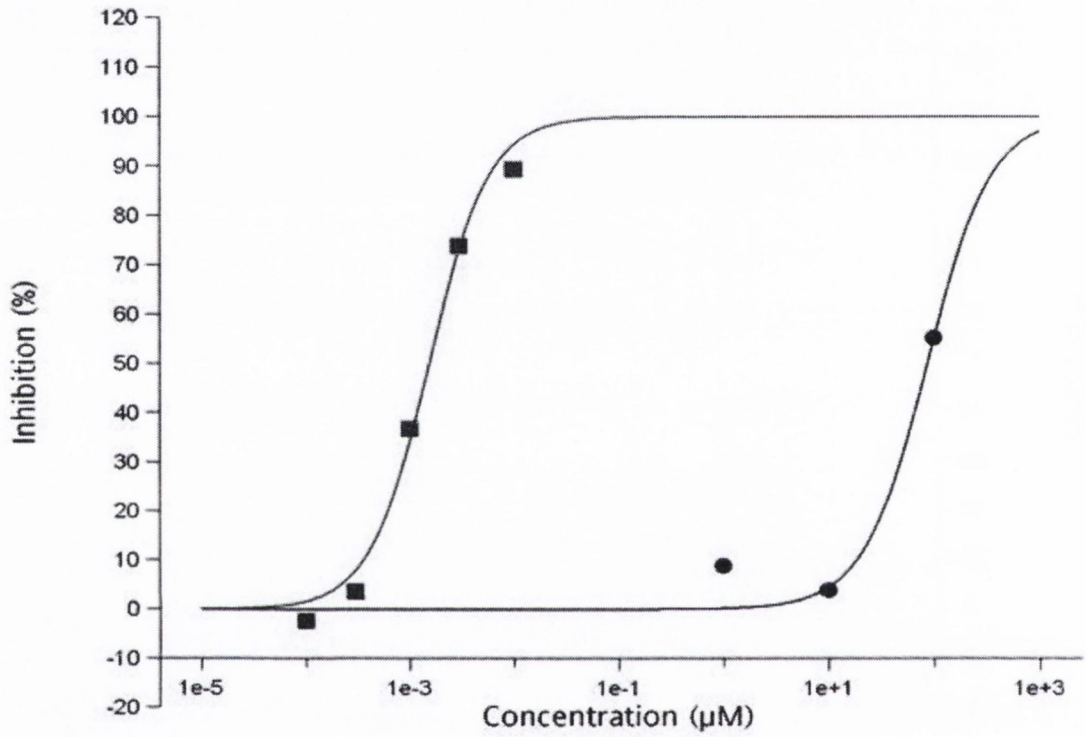
0.706

PT #: 1116710
CODE: TRN-29, Bup HBr

April 27, 2009 3:55 PM
Page 10 of 1

RESPONSE CURVES

ASSAY: 254000 - 1 Muscarinic, Non-Selective, Central



Compound	IC ₅₀	K _i	n _H
● Bup HBr (1116710)	86.5 µM	27 µM	1.42
■ Atropine	1.54 nM	0.480 nM	1.51

METHODS - RADIOLIGAND BINDING ASSAYS

■ 254000 Muscarinic, Non-Selective, Central

Source: Wistar Rat cerebral cortex
Ligand: 0.15 nM [³H] Quinuclidinyl benzilate
Vehicle: H₂O
Incubation Time/Temp: 60 minutes @ 25°C
Incubation Buffer: 50 mM Phosphate Buffer, pH 7.4
Non-Specific Ligand: 0.1 μM Atropine
K_D: 0.068 nM *
B_{MAX}: 1.4 pmole/mg Protein *
Specific Binding: 97% *
Quantitation Method: Radioligand Binding
Significance Criteria: ≥ 50% of max stimulation or inhibition

■ 258590 Nicotinic Acetylcholine

Source: Human IMR-32 cells
Ligand: 0.1 nM [¹²⁵I] Epibatidine
Vehicle: H₂O
Incubation Time/Temp: 60 minutes @ 25°C
Incubation Buffer: 20 mM HEPES, pH 7.5, 150 mM NaCl, 1.5 mM KCl, 2 mM CaCl₂, 1 mM MgSO₄.
Non-Specific Ligand: 300 μM (-)-Nicotine
K_D: 0.22 nM *
B_{MAX}: 0.46 pmole/mg Protein *
Specific Binding: 97% *
Quantitation Method: Radioligand Binding
Significance Criteria: ≥ 50% of max stimulation or inhibition

■ 220320 Transporter, Dopamine (DAT)

Source: Human recombinant CHO-K1 cells
Ligand: 0.15 nM [¹²⁵I] RTI-55
Vehicle: H₂O
Incubation Time/Temp: 3 hours @ 4°C
Incubation Buffer: 50 mM Tris-HCl, pH 7.4, 100 mM NaCl, 1 μM Leupeptin, 10 μM PMSF
Non-Specific Ligand: 10 μM Nomifensine
K_D: 0.58 nM *
B_{MAX}: 0.047 pmole/mg Protein *
Specific Binding: 90% *
Quantitation Method: Radioligand Binding
Significance Criteria: ≥ 50% of max stimulation or inhibition

■ 204410 Transporter, Norepinephrine (NET)

Source: Human recombinant MDCK cells
Ligand: 0.2 nM [¹²⁵I] RTI-55
Vehicle: H₂O
Incubation Time/Temp: 3 hours @ 4°C
Incubation Buffer: 50 mM Tris-HCl, pH 7.4, 100 mM NaCl, 1 μM Leupeptin, 10 μM PMSF
Non-Specific Ligand: 10 μM Desipramine
K_D: 0.024 μM *
B_{MAX}: 2.5 pmole/mg Protein *
Specific Binding: 75% *
Quantitation Method: Radioligand Binding
Significance Criteria: ≥ 50% of max stimulation or inhibition

* Historical Values

PT #: 1116710
CODE: TRN-29, Bup HBr

April 27, 2009 3:55
Page 12 of

METHODS - RADIOLIGAND BINDING ASSAYS

■ 274030 Transporter, Serotonin (5-Hydroxytryptamine) (SERT)

Source: Human recombinant HEK-293 cells
Ligand: 0.4 nM [³H] Paroxetine
Vehicle: H₂O
Incubation Time/Temp: 60 minutes @ 25°C
Incubation Buffer: 50 mM Tris-HCl, pH 7.4, 120 mM NaCl, 5 mM KCl
Non-Specific Ligand: 10 μM Imipramine
K_D: 0.078 nM *
B_{MAX}: 4.4 pmole/mg Protein *
Specific Binding: 95% *
Quantitation Method: Radioligand Binding
Significance Criteria: ≥ 50% of max stimulation or inhibition

* Historical Values

PT #: 1116710
CODE: TRN-29, Bup HBr

April 27, 2009 3:55 PM
Page 13 of 14

REFERENCE COMPOUND DATA - BIOCHEMICAL ASSAYS

CAT. #	ASSAY NAME	REFERENCE COMPOUND	HISTORICAL		CONCURRENT		
			IC ₅₀	K _i	n _H	BATCH *	IC ₅₀
254000	Muscarinic, Non-Selective, Central	Atropine	1.2 nM	0.37 nM	0.9	246310	1.54 nM
258590	Nicotinic Acetylcholine	Epibatidine	0.076 nM	0.052 nM	0.9	246311	0.123 nM
220320	Transporter, Dopamine (DAT)	GBR-12909	1.7 nM	1.3 nM	0.9	246308	1.16 nM
204410	Transporter, Norepinephrine (NET)	Desipramine	0.93 nM	0.92 nM	0.6	246369	0.890 nM
274030	Transporter, Serotonin (5-Hydroxytryptamine) (SERT)	Fluoxetine	8.6 nM	1.4 nM	0.9	246309	2.87 nM

* Batch: Represents compounds tested concurrently in the same assay(s). ‡ Partially soluble in *in vitro* test solvent.

LITERATURE REFERENCES

CAT. #	REFERENCE
204410	Galli A, De Felice L, Duke B-J, Moore K and Blakely R (1995) Sodium dependent norepinephrine induced currents in norepinephrine transporter transfected HEK293 cells blocked by cocaine and antidepressants. <i>J Exp Biol.</i> <u>198</u> :2197-2212.
220320	Giros B and Caron MG (1993) Molecular characterization of the dopamine transporter. <i>Trends Pharmacol Sci.</i> <u>14</u> : 43-49. Gu H, Wall S and Rudnick G (1994) Stable expression of biogenic amine transporters reveals differences in inhibitor sensitivity, kinetics, and ion dependence. <i>J Biol Chem.</i> <u>269</u> (10):7124-7130.
254000	Luthin GR and Wolfe BB. (1984) Comparison of [3H] pirenzepine and [3H] quinuclidinylbenzilate binding to muscarinic cholinergic receptors in rat brain. <i>J Pharmacol Exp Ther.</i> <u>228</u> :648-655.
258590	Davila-Garcia MI, Musachio JL, Perry DC, Xiao Y, Horti A, London ED, Dannals RF and Kellar KJ (1997) [¹²⁵ I]IPH, an epibatidine analog, binds with high affinity to neuronal nicotinic cholinergic receptors. <i>J Pharmacol Exp Ther.</i> <u>282</u> (1): 445-451. Whiteaker P, Jimenez M, McIntosh JM, Collins AC and Marks MJ (2000) Identification of a novel nicotinic binding site in mouse brain using [¹²⁵ I]-epibatidine. <i>Br J Pharmacol.</i> <u>131</u> (4): 729-739.
274030	Shearman LP, McReynolds AM, Zhou FC, Meyer JS. (1998) Relationship between [125I]RTI-55-labeled cocaine binding sites and the serotonin transporter in rat placenta. <i>Am J Physiol.</i> <u>275</u> (6 Pt 1): C1621-1629 Wolf WA and Kuhn DM. (1992) Role of essential sulfhydryl groups in drug interactions at the neuronal 5-HT transporter. Differences between amphetamines and 5-HT uptake inhibitors. <i>J Biol Chem.</i> <u>267</u> (29): 20820-20825.

Individual Tests Data Report Trinity College Dublin

Study Completed: April 27, 2009

Report Printed: April 27, 2009

MDSPTS PT#: 1116711

Alt. Code 1: POB147

Alt. Code 2:

Alt. Code 3:

Sample(s): TRN-30

M.W.: 290.2

Objectives:

To evaluate, in Radioligand Binding assays, the activity of test compound POB147 (PT# 1116711).



Pharma Services

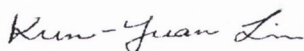
PT#: 1116711
CODE: TRN-30, POB147

April 27, 2009 3:53
Page 2 of 2

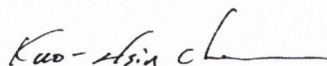
MDS Pharma Services Pharmacology Data Report On Compound TRN-30, POB147 For Trinity College Dublin

Work Order Number:	1-1035283-0	Services Being Reported:	Individual Tests
Study Number:	AA84831	Alternative Work Order No:	
Quote No:	13104-1	Purchase Order Number:	POB-636195
Compound Information:		Total # of Assays:	5
Compound Code:	TRN-30		
Alternative Code 1:	POB147		
Alternative Code 2:			
Alternative Code 3:			
MDSPS Internal #:	1116711		
Molecular Weight:	290.2		
Sponsor:	Trinity College Dublin School of Pharmacy College Green Dublin 2, Ireland		
Undertaken at:	MDS Pharma Services - Taiwan Ltd. Pharmacology Laboratories 158 Li-Teh Road, Peitou Taipei, Taiwan 112 R. O. C.		
Date of Study:	April 20, 2009 - April 27, 2009		
Study Directors:	Kun-Yuan Lin, MDS Pharma Services - Taiwan Ltd. Kuo-Hsin Chen, MDS Pharma Services - Taiwan Ltd.		
Distribution:	Trinity College Dublin		

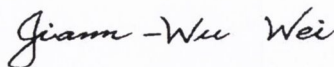
"This study was conducted according to the procedures described in this report. All data presented are authentic, accurate and correct to the best of our knowledge."



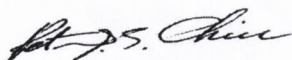
Kun-Yuan Lin
Study Director for Animal Assays



Kuo-Hsin Chen
Study Director for Biochemical Assays



Jiann-Wu Wei, Ph.D
Quality Control and Data Reviewer



Peter Chiu, Ph.D
Technical Director

TABLE OF CONTENTS

REPORT SECTION	PAGE
Summary	4
Summary of Significant Results	5
Experimental Results	7
Response Curves	8
Methods	13
Reference Compound Data	15
Literature References	16

SUMMARY

STUDY OBJECTIVE

To evaluate, in Radioligand Binding assays, the activity of compound POB147 (TRN-30, PT# 1116711).

METHODS

Methods employed in this study have been adapted from the scientific literature to maximize reliability and reproducibility. Reference standards were run as an integral part of each assay to ensure the validity of the results obtained. Assays were performed under conditions described in the accompanying "Methods" section of this report. The literature reference(s) for each assay are in the "Literature References" section. If either of these sections were not originally requested with the accompanying report, please contact us at the number below for a printout of either of these report sections.

Where presented, IC_{50} values were determined by a non-linear, least squares regression analysis using MathIQ™ (ID Business Solutions Ltd., UK). Where inhibition constants (K_i) are presented, the K_i values were calculated using the equation of Cheng and Prusoff (Cheng, Y., Prusoff, W.H., *Biochem. Pharmacol.* 22:3099-3108, 1973) using the observed IC_{50} of the tested compound, the concentration of radioligand employed in the assay, and the historical values for the K_D of the ligand (obtained experimentally at **MDS Pharma Services**). Where presented, the Hill coefficient (n_H), defining the slope of the competitive binding curve, was calculated using MathIQ™. Hill coefficients significantly different than 1.0, may suggest that the binding displacement does not follow the laws of mass action with a single binding site. Where IC_{50} , K_i , and/or n_H data are presented without Standard Error of the Mean (SEM), data are insufficient to be quantitative, and the values presented (K_i , IC_{50} , n_H) should be interpreted with caution.

RESULTS

A summary of results meeting the significance criteria is presented in the following sections. Complete results are presented under the section labeled "Experimental Results". Individual responses, if requested, are presented in the appendix to this report.

SUMMARY/CONCLUSION

Significant results are displayed in the following table(s) in rank order of potency for estimated IC_{50} and/or K_i values.

SUMMARY OF SIGNIFICANT PRIMARY RESULTS

Biochemical assay results are presented as the percent inhibition of specific binding or activity throughout the report. All other results are expressed in terms of that assay's quantitation method (see Methods section).

- For primary assays, only the lowest concentration with a significant response judged by the assays' criteria, is shown in this summary.
- Where applicable, either the secondary assay results with the lowest dose/concentration meeting the significance criteria or, if inactive, the highest dose/concentration that did not meet the significance criteria is shown.
- Unless otherwise requested, primary screening in duplicate with quantitative data (e.g., $IC_{50} \pm SEM$, $K_i \pm SEM$ and n_H) are shown where applicable for individual requested assays. In screening packages, primary screening in duplicate with semi-quantitative data (e.g., estimated IC_{50} , K_i and n_H) are shown where applicable (concentration range of 4 log units); available secondary functional assays are carried out (30 μM) and MEC or MIC determined only if active in primary assays >50% at 1 log unit below initial test concentration.
- Please see Experimental Results section for details of all responses.

Significant responses ($\geq 50\%$ inhibition or stimulation for Biochemical assays) were noted in the primary assays listed below:

PRIMARY TESTS

CAT. #	PRIMARY		SPECIES	CONC.	% INH.	IC ₅₀ *	K _i	n _H
	BIOCHEMICAL ASSAY							
204410	Transporter, Norepinephrine (NET)		hum	100 μM	61	57.9 μM	57.4 μM	0.764
220320	Transporter, Dopamine (DAT)		hum	10 μM	72	3.71 μM	2.95 μM	0.924
254000	Muscarinic, Non-Selective, Central		rat	100 μM	72	39.3 μM	12.3 μM	0.957
258590	Nicotinic Acetylcholine		hum	100 μM	57	71.6 μM	49.2 μM	0.836

‡ Partially soluble in *in vitro* test solvent.

* A standard error of the mean is presented where results are based on multiple, independent determinations.

hum=human

PT#: 1116711
CODE: TRN-30, POB147

April 27, 2009 3:54 PM
Page 6 of 16

SUMMARY OF SIGNIFICANT PRIMARY RESULTS

ABOVE PRIMARY TESTS IN RANK ORDER OF POTENCY

PRIMARY							
CAT. #	RADIOLIGAND ASSAY	SPECIES	CONC.	% INH.	IC ₅₀ *	K _i	n _H
220320	Transporter, Dopamine (DAT)	hum	10 µM	72	3.71 µM	2.95 µM	0.924
254000	Muscarinic, Non-Selective, Central	rat	100 µM	72	39.3 µM	12.3 µM	0.957
258590	Nicotinic Acetylcholine	hum	100 µM	57	71.6 µM	49.2 µM	0.836
204410	Transporter, Norepinephrine (NET)	hum	100 µM	61	57.9 µM	57.4 µM	0.764

‡ Partially soluble in *in vitro* test solvent.

* A standard error of the mean is presented where results are based on multiple, independent determinations.

hum=human

EXPERIMENTAL RESULTS - BIOCHEMICAL ASSAYS

Cat. #	TARGET	BATCH*	SPP.	n=	CONC.	‡% INHIBITION					IC ₅₀	K _i	n _H	R
						%	-100	-50	0	50				
◆ 254000	Muscarinic, Non-Selective, Central	246310	rat	2	100 µM	72						39.3 µM	12.3 µM	0.957
				2	10 µM	20								
				2	1 µM	7								
◆ 258590	Nicotinic Acetylcholine	246311	hum	2	100 µM	57						71.6 µM	49.2 µM	0.836
				2	10 µM	17								
				2	1 µM	0								
◆ 220320	Transporter, Dopamine (DAT)	246308	hum	2	100 µM	94						3.71 µM	2.95 µM	0.924
				2	10 µM	72								
				2	1 µM	23								
◆ 204410	Transporter, Norepinephrine (NET)	246369	hum	2	100 µM	61						57.9 µM	57.4 µM	0.764
				2	10 µM	19								
				2	1 µM	7								
274030	Transporter, Serotonin (5-Hydroxytryptamine) (SERT)	246309	hum	2	100 µM	-2						>100 µM		
				2	10 µM	9								
				2	1 µM	13								

* Batch: Represents compounds tested concurrently in the same assay(s). ‡ Partially soluble in *in vitro* test solvent.

◆ Denotes item meeting criteria for significance

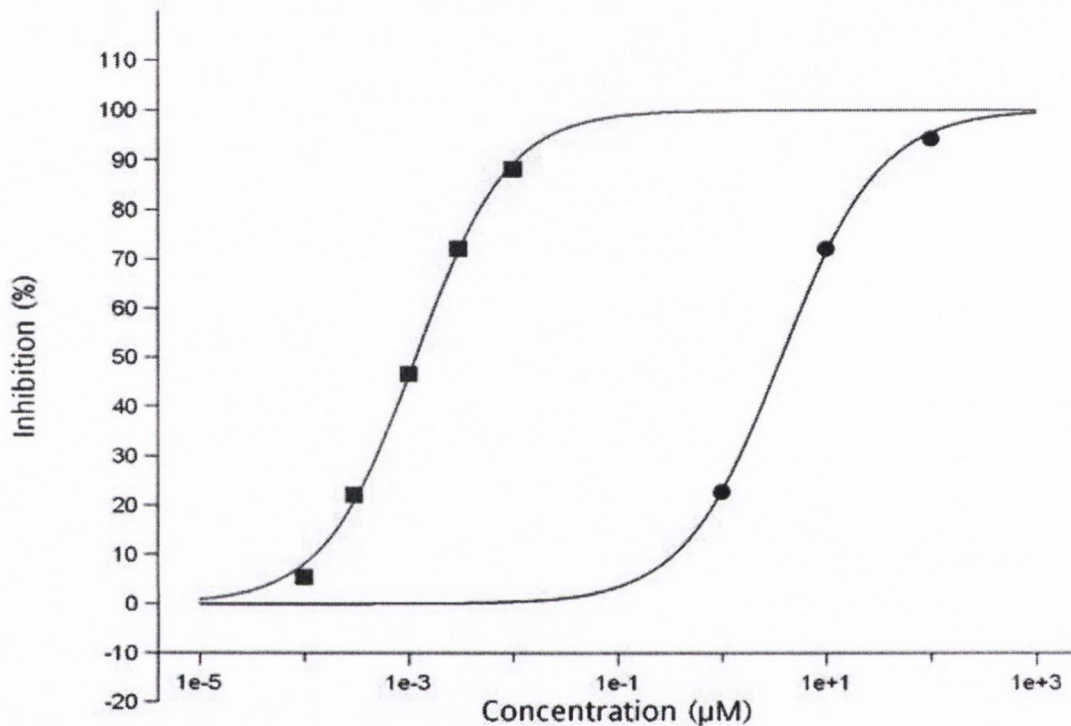
† Results with ≥ 50% stimulation or inhibition are highlighted.

R=Additional Comments

hum=human

RESPONSE CURVES

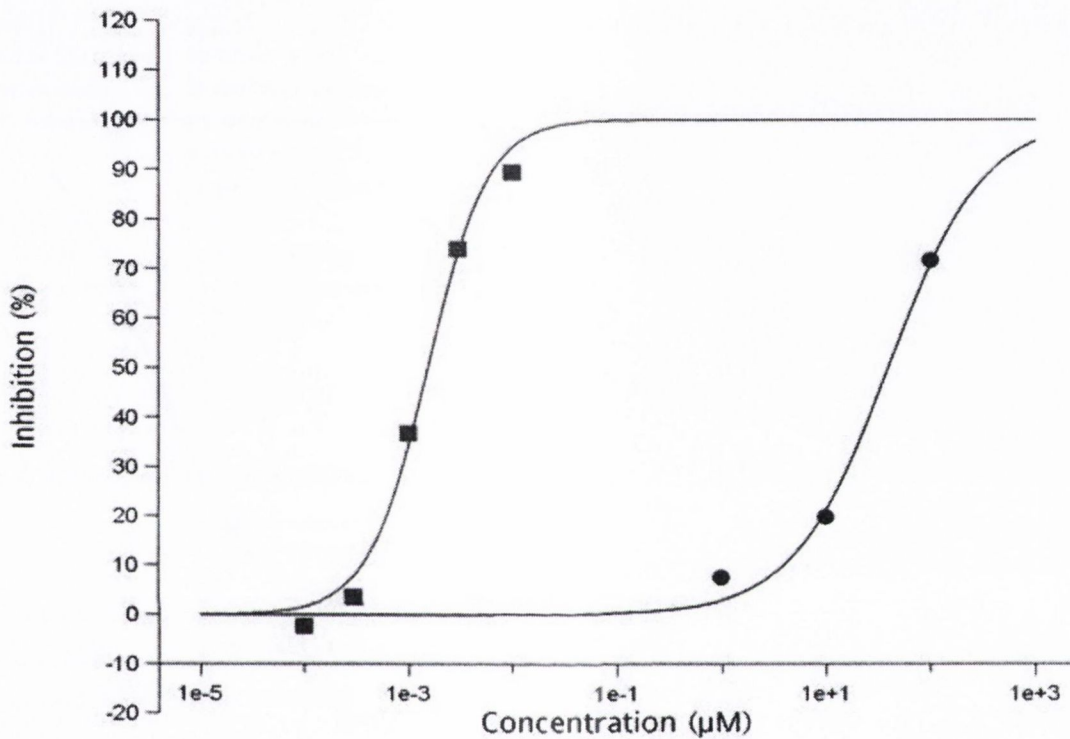
ASSAY: 220320 - 1 Transporter, Dopamine (DAT)



Compound	IC ₅₀	K _i	n _H
● POB147 (1116711)	3.71 µM	2.95 µM	0.924
■ GBR-12909	1.16 nM	0.925 nM	0.989

RESPONSE CURVES

ASSAY: 254000 - 1 Muscarinic, Non-Selective, Central



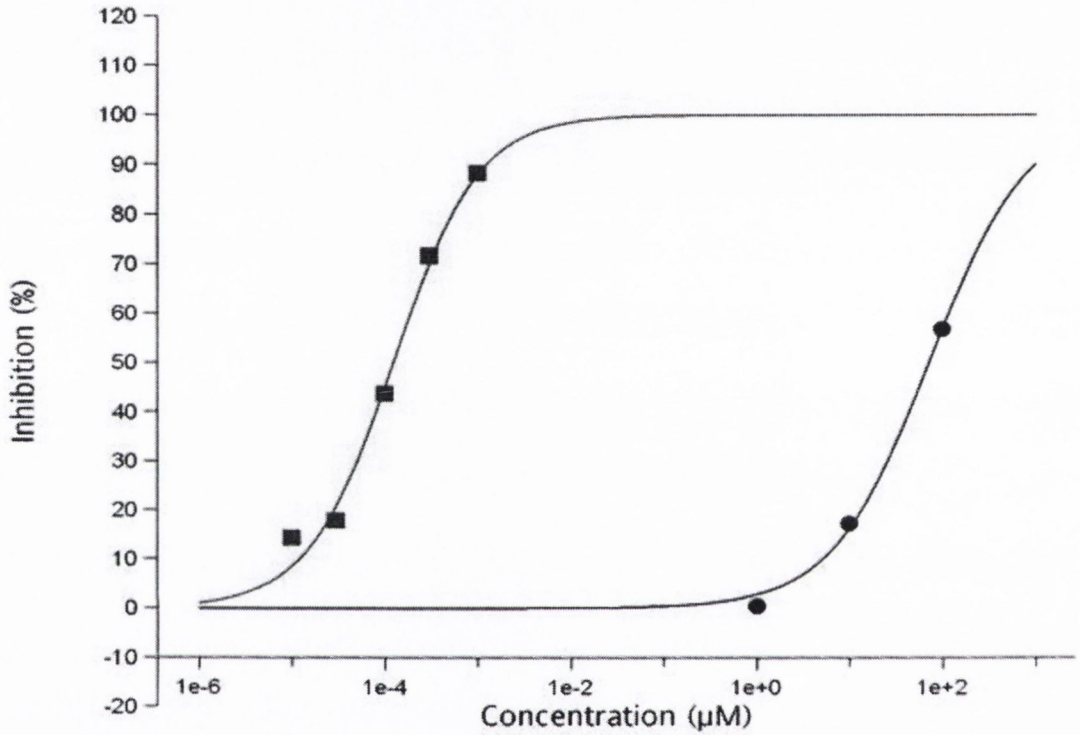
Compound	IC ₅₀	K _i	n _H
● POB147 (1116711)	39.3 µM	12.3 µM	0.957
■ Atropine	1.54 nM	0.480 nM	1.51

PT #: 1116711
CODE: TRN-30, POB147

April 27, 2019 3:55 PM
Page 12 of 16

RESPONSE CURVES

ASSAY: 258590 - 1 Nicotinic Acetylcholine



Compound	IC ₅₀	K _i	n _H
● POB147 (1116711)	71.6 µM	49.2 µM	0.836
■ Epibatidine	0.123 nM	0.0846 nM	0.950

METHODS - RADIOLIGAND BINDING ASSAYS

■ 254000 Muscarinic, Non-Selective, Central

Source: Wistar Rat cerebral cortex
Ligand: 0.15 nM [³H] Quinuclidinyl benzilate
Vehicle: H₂O
Incubation Time/Temp: 60 minutes @ 25°C
Incubation Buffer: 50 mM Phosphate Buffer, pH 7.4
Non-Specific Ligand: 0.1 μM Atropine
K_D: 0.068 nM *
B_{MAX}: 1.4 pmole/mg Protein *
Specific Binding: 97% *
Quantitation Method: Radioligand Binding
Significance Criteria: ≥ 50% of max stimulation or inhibition

■ 258590 Nicotinic Acetylcholine

Source: Human IMR-32 cells
Ligand: 0.1 nM [¹²⁵I] Epibatidine
Vehicle: H₂O
Incubation Time/Temp: 60 minutes @ 25°C
Incubation Buffer: 20 mM HEPES, pH 7.5, 150 mM NaCl, 1.5 mM KCl, 2 mM CaCl₂, 1 mM MgSO₄.
Non-Specific Ligand: 300 μM (-)-Nicotine
K_D: 0.22 nM *
B_{MAX}: 0.46 pmole/mg Protein *
Specific Binding: 97% *
Quantitation Method: Radioligand Binding
Significance Criteria: ≥ 50% of max stimulation or inhibition

■ 220320 Transporter, Dopamine (DAT)

Source: Human recombinant CHO-K1 cells
Ligand: 0.15 nM [¹²⁵I] RTI-55
Vehicle: H₂O
Incubation Time/Temp: 3 hours @ 4°C
Incubation Buffer: 50 mM Tris-HCl, pH 7.4, 100 mM NaCl, 1 μM Leupeptin, 10 μM PMSF
Non-Specific Ligand: 10 μM Nomifensine
K_D: 0.58 nM *
B_{MAX}: 0.047 pmole/mg Protein *
Specific Binding: 90% *
Quantitation Method: Radioligand Binding
Significance Criteria: ≥ 50% of max stimulation or inhibition

■ 204410 Transporter, Norepinephrine (NET)

Source: Human recombinant MDCK cells
Ligand: 0.2 nM [¹²⁵I] RTI-55
Vehicle: H₂O
Incubation Time/Temp: 3 hours @ 4°C
Incubation Buffer: 50 mM Tris-HCl, pH 7.4, 100 mM NaCl, 1 μM Leupeptin, 10 μM PMSF
Non-Specific Ligand: 10 μM Desipramine
K_D: 0.024 μM *
B_{MAX}: 2.5 pmole/mg Protein *
Specific Binding: 75% *
Quantitation Method: Radioligand Binding
Significance Criteria: ≥ 50% of max stimulation or inhibition

* Historical Values

PT #: 1116711
CODE: TRN-30, POB147

April 27, 2009 3:55 P
Page 14 of

METHODS - RADIOLIGAND BINDING ASSAYS

■ 274030 Transporter, Serotonin (5-Hydroxytryptamine) (SERT)

Source: Human recombinant HEK-293 cells
Ligand: 0.4 nM [³H] Paroxetine
Vehicle: H₂O
Incubation Time/Temp: 60 minutes @ 25°C
Incubation Buffer: 50 mM Tris-HCl, pH 7.4, 120 mM NaCl, 5 mM KCl
Non-Specific Ligand: 10 μM Imipramine
K_D: 0.078 nM *
B_{MAX}: 4.4 pmole/mg Protein *
Specific Binding: 95% *
Quantitation Method: Radioligand Binding
Significance Criteria: ≥ 50% of max stimulation or inhibition

* Historical Values

REFERENCE COMPOUND DATA - BIOCHEMICAL ASSAYS

CAT. #	ASSAY NAME	REFERENCE COMPOUND	HISTORICAL		CONCURRENT		
			IC ₅₀	K _i	n _H	BATCH *	IC ₅₀
154000	Muscarinic, Non-Selective, Central	Atropine	1.2 nM	0.37 nM	0.9	246310	1.54 nM
158590	Nicotinic Acetylcholine	Epibatidine	0.076 nM	0.052 nM	0.9	246311	0.123 nM
20320	Transporter, Dopamine (DAT)	GBR-12909	1.7 nM	1.3 nM	0.9	246308	1.16 nM
204410	Transporter, Norepinephrine (NET)	Desipramine	0.93 nM	0.92 nM	0.6	246369	0.890 nM
274030	Transporter, Serotonin (5-Hydroxytryptamine) (SERT)	Fluoxetine	8.6 nM	1.4 nM	0.9	246309	2.87 nM

* Batch: Represents compounds tested concurrently in the same assay(s). ‡ Partially soluble in *in vitro* test solvent.

LITERATURE REFERENCES

- | CAT. # | REFERENCE |
|--------|--|
| 204410 | Galli A, De Felice L, Duke B-J, Moore K and Blakely R (1995)
Sodium dependent norepinephrine induced currents in norepinephrine transporter transfected HEK293 cells blocked by cocaine and antidepressants. <i>J Exp Biol.</i> <u>198</u> :2197-2212. |
| 220320 | Giros B and Caron MG (1993)
Molecular characterization of the dopamine transporter. <i>Trends Pharmacol Sci.</i> <u>14</u> : 43-49.
Gu H, Wall S and Rudnick G (1994)
Stable expression of biogenic amine transporters reveals differences in inhibitor sensitivity, kinetics, and ion dependence. <i>J Biol Chem.</i> <u>269</u> (10):7124-7130. |
| 254000 | Luthin GR and Wolfe BB. (1984)
Comparison of [3H] pirenzepine and [3H] quinuclidinylbenzilate binding to muscarinic cholinergic receptors in rat brain. <i>J Pharmacol Exp Ther.</i> <u>228</u> :648-655. |
| 258590 | Davila-Garcia MI, Musachio JL, Perry DC, Xiao Y, Horti A, London ED, Dannals RF and Kellar KJ (1997)
[¹²⁵ I]IPH, an epibatidine analog, binds with high affinity to neuronal nicotinic cholinergic receptors. <i>J Pharmacol Exp Ther.</i> <u>282</u> (1) 445-451.
Whiteaker P, Jimenez M, McIntosh JM, Collins AC and Marks MJ (2000)
Identification of a novel nicotinic binding site in mouse brain using [¹²⁵ I]-epibatidine. <i>Br J Pharmacol.</i> <u>131</u> (4): 729-739. |
| 274030 | Shearman LP, McReynolds AM, Zhou FC, Meyer JS. (1998)
Relationship between [125I]RTI-55-labeled cocaine binding sites and the serotonin transporter in rat placenta. <i>Am J Physiol.</i> <u>275</u> (6 Pt 1): C1621-1629
Wolf WA and Kuhn DM. (1992)
Role of essential sulfhydryl groups in drug interactions at the neuronal 5-HT transporter. Differences between amphetamines and 5-HT uptake inhibitors. <i>J Biol Chem.</i> <u>267</u> (29): 20820-20825. |

Individual Tests Data Report

Trinity College Dublin

Study Completed: May 22, 2009

Report Printed: May 26, 2009

Work Order #: 1035513

MDSPTS PT #: 1116710
1116711



MDS Pharma Services Pharmacology Data Report

On Compounds TRN-29, Bup HBr To TRN-30, POB 147 For Trinity College Dublin

Work Order Number: 1-1035513-0
Purchase Order Number: N01107 **Quote No:** 13466-1 **Study No:** AA85495
Services Being Reported: Individual Tests
Total # of Assays: 3

Compound Information:

MDSPS Internal #:	Compound Code:	Alt. Code 1:	Alt. Code 2:	Alt. Code 3:	Molecular Weight:
1116710	TRN-29	Bup HBr			320.7
1116711	TRN-30	POB 147			290.2

Sponsor: Trinity College Dublin
 School of Pharmacy
 Dublin 2,
 Ireland

Undertaken at: MDS Pharma Services - Taiwan Ltd.
 Pharmacology Laboratories
 158 Li-Teh Road, Peitou
 Taipei, Taiwan 112
 R. O. C.

Date of Study: May 11, 2009 - May 22, 2009

Study Directors: Kun-Yuan Lin, MDS Pharma Services - Taiwan Ltd.
 Kuo-Hsin Chen, MDS Pharma Services - Taiwan Ltd.

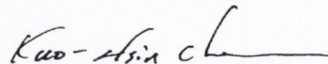
Objectives: To evaluate, in Radioligand Binding assays, the activity of test compound(s) listed above in work order 1-1035513-0.

Distribution: Trinity College Dublin

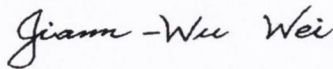
"This study was conducted according to the procedures described in this report. All data presented are authentic, accurate and correct to the best of our knowledge."



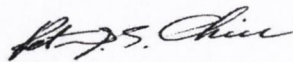
Kun-Yuan Lin
 Study Director for Animal Assays



Kuo-Hsin Chen
 Study Director for Biochemical Assays



Jiann-Wu Wei, Ph.D
 Quality Control and Data Reviewer



Peter Chiu, Ph.D
 Technical Director

TABLE OF CONTENTS

REPORT SECTION	PAGE
Summary	4
Summary of Significant Results	5
Experimental Results	6
Methods	7
Reference Compound Data	8
Literature References	9

EXPERIMENTAL RESULTS - BIOCHEMICAL ASSAYS

COMPOUND CODE	PT NUMBER	BATCH*	SPP.	n=	CONC.	‡% INHIBITION					IC ₅₀	K _i	n	R		
						-100	-50	0	50	100						
						%	↓	↓	↓	↓	↓					
258700	Nicotinic Acetylcholine α1, Bungarotoxin															
Bup HBr	1116710	247797	hum	2	100 μM	-6		█				>100 μM				
				2	10 μM	3										
				2	1 μM	-10		█								
POB 147	1116711	247797	hum	2	100 μM	7						>100 μM				
				2	10 μM	0										
				2	1 μM	-17		█								
258750	Nicotinic Acetylcholine α4β2, Cytisine															
Bup HBr	1116710	248063	rat	2	100 μM	0						>100 μM				
				2	10 μM	5										
				2	1 μM	-13		█								
POB 147	1116711	248063	rat	2	100 μM	-2						>100 μM				
				2	10 μM	-3										
				2	1 μM	-10		█								
258650	Nicotinic Acetylcholine α7, Methyllycaconitine															
Bup HBr	1116710	248062	rat	2	100 μM	18		█				>100 μM				
				2	10 μM	11		█								
				2	1 μM	-1										
POB 147	1116711	248062	rat	2	100 μM	35		█				>100 μM				
				2	10 μM	12		█								
				2	1 μM	9		█								

* Batch: Represents compounds tested concurrently in the same assay(s). ‡ Partially soluble in *in vitro* test solvent.

◆ Denotes item meeting criteria for significance

† Results with ≥ 50% stimulation or inhibition are highlighted.

R=Additional Comments

hum=human

METHODS - RADIOLIGAND BINDING ASSAYS■ 258700 Nicotinic Acetylcholine α 1, Bungarotoxin

Source: Human RD cells
Ligand: 0.6 nM [¹²⁵I] α -Bungarotoxin
Vehicle: H₂O
Incubation Time/Temp: 2 hours @ 25°C
Incubation Buffer: 150 mM NaCl, 4 mM KCl, 2.3 mM CaCl₂, pH 7.4
Non-Specific Ligand: 1 μ M α -Bungarotoxin
K_D: 1.1 nM *
B_{MAX}: 1 pmole/mg Protein *
Specific Binding: 85% *
Quantitation Method: Radioligand Binding
Significance Criteria: \geq 50% of max stimulation or inhibition

■ 258750 Nicotinic Acetylcholine α 4 β 2, Cytisine

Source: Rat brain
Ligand: 2 nM [³H] Cytisine
Vehicle: H₂O
Incubation Time/Temp: 2 hours @ 4°C
Incubation Buffer: 50 mM Tris-HCl, pH 7.4, 2 mM CaCl₂, 5 mM KCl, 1 mM MgCl₂, 120 mM NaCl
Non-Specific Ligand: 10 μ M (-)-Nicotine
K_D: 0.86 nM *
B_{MAX}: 0.039 pmole/mg Protein *
Specific Binding: 75% *
Quantitation Method: Radioligand Binding
Significance Criteria: \geq 50% of max stimulation or inhibition

■ 258650 Nicotinic Acetylcholine α 7, Methyllycaconitine

Source: Rat brain
Ligand: 2 nM [³H] Methyllycaconitine
Vehicle: H₂O
Incubation Time/Temp: 2 hours @ 25°C
Incubation Buffer: 50 mM Tris-HCl, pH 7.4, 0.1% BSA, 2 mM CaCl₂, 5 mM KCl, 1 mM MgCl₂, 120 mM NaCl
Non-Specific Ligand: 10 μ M Methyllycaconitine
K_D: 1.6 nM *
B_{MAX}: 0.015 pmole/mg Protein *
Specific Binding: 55% *
Quantitation Method: Radioligand Binding
Significance Criteria: \geq 50% of max stimulation or inhibition

* Historical Values